

# LIPID MAPS MASS SPECTROMETRY METHODS CHAPTERS

DISCLAIMER: These chapters were written for the sole purpose of guiding qualified, professional scientists in the indicated laboratory procedures. Some of the procedures involve the use of chemicals or equipment that may be dangerous, particularly if improperly performed or if carried out by personnel that are not appropriately trained in laboratory procedures. The authors, editors, institutions, publisher, and associated companies have no responsibility whatsoever for any injuries, harm, damage to property or any monetary losses associated with the use of the procedures described in these chapters. The end user accepts all responsibility for use of the procedures described in these chapters. This work is provided on the LIPID MAPS website with the written permission of the Publisher and the entire volume may be viewed from the website <http://www.sciencedirect.com/science/bookseries/00766879>.

# CONTENTS

<i>Contributors</i>	<i>xi</i>
<i>Preface</i>	<i>xvii</i>
<i>Volumes in Series</i>	<i>xix</i>

**1. Qualitative Analysis and Quantitative Assessment of Changes in Neutral Glycerol Lipid Molecular Species Within Cells** **1**

Jessica Krank, Robert C. Murphy, Robert M. Barkley, Eva Duchoslav, and Andrew McAnoy

1. Introduction	2
2. Reagents	3
3. Methods	4
4. Results	7
5. Conclusions	19
Acknowledgments	19
References	19

**2. Glycerophospholipid Identification and Quantitation by Electrospray Ionization Mass Spectrometry** **21**

Pavlina T. Ivanova, Stephen B. Milne, Mark O. Byrne, Yun Xiang, and H. Alex Brown

1. Introduction	22
2. Nomenclature	25
3. Mass Spectrometry	26
4. General Strategy for Phospholipid Isolation and Mass Spectral Analysis	27
5. Extraction and Mass Spectral Analysis of Global Glycerophospholipids	28
6. Polyphosphoinositide Extraction and Mass Spectral Analysis	35
7. Computational Analysis of Mass Spectral Data	41
Acknowledgments	54
References	54

<b>3. Detection and Quantitation of Eicosanoids via High Performance Liquid Chromatography-Electrospray Ionization-Mass Spectrometry</b>	<b>59</b>
Raymond Deems, Matthew W. Buczynski, Rebecca Bowers-Gentry, Richard Harkewicz, and Edward A. Dennis	
1. Introduction	60
2. Methods	62
3. Results and Discussion	74
Acknowledgments	80
References	81
<b>4. Structure-Specific, Quantitative Methods for Analysis of Sphingolipids by Liquid Chromatography-Tandem Mass Spectrometry: "Inside-Out" Sphingolipidomics</b>	<b>83</b>
M. Cameron Sullards, Jeremy C. Allegood, Samuel Kelly, Elaine Wang, Christopher A. Haynes, Hyejung Park, Yanfeng Chen, and Alfred H. Merrill, Jr.	
1. Introduction: An Overview of Sphingolipid Structures and Nomenclature	86
2. Analysis of Sphingolipids by Mass Spectrometry	89
3. Analysis of Sphingolipids by "OMIC" Approaches	92
4. Materials and Methods	95
5. Materials	98
6. Extraction	98
7. Identification of the Molecular Species by Tandem Mass Spectrometry	100
8. Quantitation by LC-ESI-MS/MS Using Multireaction Monitoring	101
9. Analysis of (Dihydro)Ceramides, (Dihydro)Sphingomyelins, and (Dihydro)Monohexosyl-Ceramides in Positive Ion Mode	104
10. Other Methods	109
Acknowledgments	111
References	112
<b>5. Analysis of Ubiquinones, Dolichols, and Dolichol Diphosphate-Oligosaccharides by Liquid Chromatography-Electrospray Ionization-Mass Spectrometry</b>	<b>117</b>
Teresa A. Garrett, Ziqiang Guan, and Christian R. H. Raetz	
1. Introduction	118
2. Materials	121
3. Liquid Chromatography-Mass Spectrometry	122
4. Preparation of Lipid Extracts	122
5. LC-MS Detection and Quantification of Coenzyme Q	123
6. LC-MS Detection and Quantification of Dolichol	130

---

7. LC-MS and LC-MS/MS Characterization of Dolichol Diphosphate-Linked Oligosaccharides	136
Acknowledgment	140
References	140
<b>6. Extraction and Analysis of Sterols in Biological Matrices by High Performance Liquid Chromatography Electrospray Ionization Mass Spectrometry</b>	<b>145</b>
Jeffrey G. McDonald, Bonne M. Thompson, Erin C. McCrum, and David W. Russell	
1. Introduction	146
2. Supplies and Reagents	148
3. Extraction of Lipids from Cultured Cells and Tissues	149
4. Saponification of Lipid Extracts	151
5. Solid-Phase Extraction	152
6. Analysis by HPLC-ESI-MS	153
7. Quantitation	156
8. Data	157
9. Discussion, Nuances, Caveats, and Pitfalls	162
Acknowledgments	168
References	169
<b>7. The Lipid Maps Initiative in Lipidomics</b>	<b>171</b>
Kara Schmelzer, Eoin Fahy, Shankar Subramaniam, and Edward A. Dennis	
1. Introduction	172
2. Building Infrastructure in Lipidomics	173
3. Classification, Nomenclature, and Structural Representation of Lipids	174
4. Mass Spectrometry as a Platform for Lipid Molecular Species	177
5. Future Plans	180
Acknowledgments	182
References	182

---

<b>11. Bioinformatics for Lipidomics</b>	<b>247</b>
Eoin Fahy, Dawn Cotter, Robert Byrnes, Manish Sud, Andrea Maer, Joshua Li, David Nadeau, Yihua Zhou, and Shankar Subramaniam	
1. Introduction	248
2. Lipid Structure Databases	249
3. Lipid-Associated Protein/Gene Databases	254
4. Tools for Lipidomics	256
5. Lipid Pathways	268
6. Challenges for Future Lipid Informatics	270
Acknowledgments	272
References	272

---

<b>14. Quantitation and Standardization of Lipid Internal Standards for Mass Spectroscopy</b>	<b>351</b>
Jeff D. Moore, William V. Caufield, and Walter A. Shaw	
1. Introduction	352
2. Lipid Handling Guidelines	352
3. Chemical Characterization of Lipid Stocks	353
4. Preparation of Working Lipid Standards	355
5. Packaging of Lipid Standards	359
6. Quality Control and Stability Testing	361
7. Discussion	364
References	366
<i>Author Index</i>	369
<i>Subject Index</i>	381

# QUALITATIVE ANALYSIS AND QUANTITATIVE ASSESSMENT OF CHANGES IN NEUTRAL GLYCEROL LIPID MOLECULAR SPECIES WITHIN CELLS

Jessica Krank,<sup>\*</sup> Robert C. Murphy,<sup>\*</sup> Robert M. Barkley,<sup>\*</sup>  
Eva Duchoslav,<sup>†</sup> and Andrew McAnoy<sup>\*</sup>

---

## Contents

1. Introduction	2
2. Reagents	3
2.1. Cell culture	3
2.2. Standards	3
2.3. Extraction and purification	3
3. Methods	4
3.1. Cell culture	4
4. Results	7
4.1. Qualitative analysis	7
4.2. Quantitative analysis	11
5. Conclusions	19
Acknowledgments	19
References	19

## Abstract

Triacylglycerols (TAGs) and diacylglycerols (DAGs) are present in cells as a complex mixture of molecular species that differ in the nature of the fatty acyl groups esterified to the glycerol backbone. In some cases, the molecular weights of these species are identical, confounding assignments of identity and quantity by molecular weight. Electrospray ionization results in the formation of  $[M+NH_4]^+$  ions that can be collisionally activated to yield an abundant product ion corresponding to the loss of ammonia plus one of the fatty acyl groups as a free carboxylic acid. A method was developed using tandem mass

<sup>\*</sup> Department of Pharmacology, University of Colorado at Denver and Health Sciences Center, Aurora, Colorado

<sup>†</sup> Applied Research Group, MDS Sciex, Concord, Ontario, Canada

spectrometry (MS) and neutral loss scanning to analyze the complex mixture of TAGs and DAGs present in cells and to quantitatively determine changes in TAGs and DAGs molecular species containing identical fatty acyl groups in an experimental series. Eighteen different deuterium-labeled internal standards were synthesized to serve to normalize the ion signal for each neutral loss scan. An example of the application of this method was in the quantitative analysis of TAG and DAG molecular species present in RAW 264.7 cells treated with a Toll-4 receptor ligand, Kdo<sub>2</sub>-lipid A, in a time course study.

## 1. INTRODUCTION

Diacylglycerols and triacylglycerols represent major classes of glyceryl lipids that are present in all mammalian cells. Class analysis of these compounds has largely centered around total DAG or TAG content based upon a spectrophotometric-linked enzymatic assay; however, it is possible to determine individual molecular species of both of these classes of glyceryl lipids by MS. The major challenge in analysis of DAGs and TAGs is the total number of molecular species present within a cell, which results in multiple components appearing at the same molecular weight or truly isobaric compounds. Thus, the measurement of only the molecular ion species by MS, either the ammonium adduct ion or the alkali attachment ion (Han and Gross, 2001; McAnoy *et al.*, 2005), would be insufficient to uniquely identifying each component. Qualitative analysis can be carried out even when faced with complex mixtures of these neutral lipids if one employs tandem MS in three steps (MS<sup>3</sup>) (McAnoy *et al.*, 2005). However, quantitative analysis is confounded by the isobaric nature of multiple species, and several strategies have been developed through which changes in molecular species can be assessed. The method described here employs a series of experiments using deuterium-labeled internal standards where the deuterium atoms are placed in the glycerol backbone, and the abundance of each glyceryl lipid is compared to the signal for the internal standard. Alternative methods are available to assess TAG and DAG molecular species based upon chromatographic separation of individual molecular species (Phillips *et al.*, 1984) and analysis by gas chromatographs–mass spectrometers (GC–MS) (Myher *et al.*, 1988) or liquid chromatographs–mass spectrometers (LC–MS) using electrospray ionization (ESI) or atmospheric pressure chemical ionization (Byrdwell *et al.*, 1996; Hsu and Turk, 1999). The application of the method presented here will be exemplified by glyceryl lipid analysis in the RAW 264.7 cell line. These macrophage-like cells were originally derived from tumors induced in male BALB/c mice by the Abelson murine leukemia virus and respond to the Toll-4 receptor agonist Kdo<sub>2</sub>-lipid A (Raetz *et al.*, 2006).

## 2. REAGENTS

### 2.1. Cell culture

RAW 264.7 cells were obtained from American Type Culture Collection (Manassas, VA). Tissue culture reagents included high-glucose Dulbecco's Modified Eagle's Medium (DMEM) (Cellgro, Herndon, VA), fetal calf serum (Hyclone, Logan, UT), Dulbecco's Phosphate-Buffered Saline (D-PBS; Cellgro, Herndon, VA), and penicillin/streptomycin (Cellgro, Herndon, VA). The cells were carried in culture in either 150-cm<sup>2</sup> tissue culture flasks with filter caps or 100-mm<sup>2</sup> tissue culture dishes (Fisher Scientific, Fair Lawn, NJ).

### 2.2. Standards

All deuterium-labeled glycerol lipids were [1,1,2,3,3]-d<sub>5</sub> in the glycerol backbone. The following lipids were obtained from Avanti Polar Lipids (Alabaster, AL): Kdo<sub>2</sub>-lipid A; d<sub>5</sub>-DAG mixture containing d<sub>5</sub>-14:0/14:0 DAG, d<sub>5</sub>-15:0/15:0 DAG, d<sub>5</sub>-16:0/16:0 DAG, d<sub>5</sub>-17:0/17:0 DAG, d<sub>5</sub>-19:0/19:0 DAG, d<sub>5</sub>-20:0/20:0 DAG, d<sub>5</sub>-20:2/20:2 DAG, d<sub>5</sub>-20:4/20:4 DAG, and d<sub>5</sub>-20:5/20:5 DAG; d<sub>5</sub>-TAG mixture containing d<sub>5</sub>-14:0/16:1/14:0 TAG, d<sub>5</sub>-15:0/18:1/15:0 TAG, d<sub>5</sub>-16:0/18:0/16:0 TAG, d<sub>5</sub>-17:0/17:1/17:0 TAG, d<sub>5</sub>-19:0/12:0/19:0 TAG, d<sub>5</sub>-20:0/20:1/20:0 TAG, d<sub>5</sub>-20:2/18:3/20:2 TAG, d<sub>5</sub>-20:4/18:2/20:4 TAG, and d<sub>5</sub>-20:5/22:6/20:5 TAG.

### 2.3. Extraction and purification

High performance liquid chromatography (HPLC)-grade ammonium acetate (NH<sub>4</sub>OAc), chloroform (CHCl<sub>3</sub>), ethyl acetate, hexanes, isooctane, isopropanol, methanol, and methylene chloride (CH<sub>2</sub>Cl<sub>2</sub>) were obtained from Fisher Scientific (Fair Lawn, NJ). Optima-grade toluene and water also were obtained from Fisher Scientific (Fair Lawn, NJ). Discovery DSC-Si silica, and Discovery DSC-NH<sub>2</sub> amino propyl solid phase extraction cartridges, and the vacuum manifold were obtained from Supelco (Bellefonte, PA). Other equipment included a benchtop vortexer (Vortex Genie 2, VWR Scientific, West Chester, PA), Fluoropore 0.2-μm FG membrane filters (Millipore, Billerica, MA), 96-well polypropylene plates (Eppendorf, Westbury, NY), and Quant-iT DNA analysis kit (Molecular Probes, Eugene, OR).



## 3. METHODS

### 3.1. Cell culture

RAW 264.7 cells were grown in T-150 flasks containing 30 ml of complete growth medium consisting of 500 ml of high-glucose DMEM supplemented with 10% FBS and 1% penicillin/streptomycin. The cells were maintained in a humidified incubator at 37° with a 5% CO<sub>2</sub> atmosphere. They were split such that  $2 \times 10^6$  cells were seeded in a new flask each time the cells reached 80% confluency. Briefly, when the cells reached this confluency (approximately every 2 to 3 days), the old growth medium was removed, and 10 ml of fresh medium, which had been previously warmed to 37°, was added. The cells were then scraped from the flask using a large disposable cell scraper. A 10- $\mu$ l aliquot was counted using a hemocytometer. The volume of media determined to contain  $2 \times 10^6$  cells was then added to a new T-150 flask, and the volume was adjusted to 30 ml with complete growth medium. The flasks were then placed back into the incubator.

For quantitative analysis, three additional T-150 flasks were seeded and allowed to grow until they were approximately 80% confluent. Once confluent, the medium was removed, 10 ml of fresh medium was added to each flask, and the cells were scraped as before. The scraped cells from the three flasks were then combined, and a 10  $\mu$ l aliquot was removed and counted. Cells ( $5 \times 10^6$ ) were then added to each of the 15 100-mm<sup>2</sup> tissue culture dishes. The volume of media in the dishes was adjusted to 5 ml with complete growth media. The dishes were then placed in the incubator and allowed to grow for 30 hr.

#### 3.1.1. Kdo<sub>2</sub>-lipid A preparation

A working solution of Kdo<sub>2</sub>-lipid A, the active component of bacterial endotoxin (Rietz, 1990), was prepared at a concentration of 100  $\mu$ g/ml in DPBS. This solution was sonicated for 5 min before each experiment to achieve a uniformly opalescent suspension.

#### 3.1.2. Stimulation and harvesting

RAW 264.7 cells were treated with Kdo<sub>2</sub>-lipid A to examine the changes in the neutral glyceryl lipids upon activation of the Toll-4 receptor. Cells were stimulated by the addition of 5  $\mu$ l of the Kdo<sub>2</sub>-lipid A working solution for a final concentration of 100 ng/ml. They were then incubated for 0.5, 1, 2, 4, 8, 12, and 24 hr. The same volume of DPBS was added to the corresponding control plates. At each time point, a 0.5 ml aliquot of the growth media was removed from each dish and reserved for tumor necrosis factor alfa (TNF- $\alpha$ ) analysis. The dishes containing the control and Kdo<sub>2</sub>-lipid A-treated cells were washed twice with ice-cold DPBS and then scraped into fresh DPBS at

a concentration of approximately  $16 \times 10^6$  cells per ml of buffer. A 50- $\mu$ l aliquot was reserved for DNA analysis using a fluorescence assay (Ahn *et al.*, 1996).

### 3.1.3. Quantitation of DNA

The total amount of DNA in each time course sample was determined using the Quant-iT kit. A standard curve was constructed using the included standards and was linear from 0 to 100 ng. A portion (10  $\mu$ l) of each reserved sample aliquot and each standard was added to the black 96-well plates. The working solution was prepared as a 1:200 dilution of reagent into the included buffer. An aliquot (190  $\mu$ l) of this solution was added to each well. Samples were then read on a fluorometer with an excitation wavelength maxima of 510 nm and an emission wavelength maxima of 527 nm. The fluorescence of the samples was compared to a calibration curve generated from the fluorescence of the standards to determine the amount of DNA in each sample.

### 3.1.4. Extraction of total lipids

Total lipids were extracted from the cell suspension (Bligh and Dyer, 1959). Ice-cold methanol (2.5 ml) was added to each 1 ml of DPBS containing the scraped cell suspension. A volume containing 600 pmol of each of the 18  $d_5$ -labeled DAG and TAG internal standards in toluene/methanol (1:1) was added to this suspension for samples being analyzed quantitatively. A monophasic solution was formed by the addition of 1.25 ml of  $CH_2Cl_2$  per ml of cell suspension. This solution was vortexed for 30 s using a benchtop vortexer. After the addition of water (1.0 ml) and  $CH_2Cl_2$  (1.25 ml), the sample was vortexed for an additional 30 s. The phases were then separated by centrifugation at 1000 rpm for 5 min. The lower organic phase was removed to a clean tube using a glass transfer pipette. The upper aqueous phase was reextracted with an additional 2 ml of  $CH_2Cl_2$ . This solution was vortexed and centrifuged as before. The lower organic layer was then combined with that obtained in the first extraction. The total lipid extract was taken to dryness under a gentle stream of nitrogen.

### 3.1.5. Solid-phase extraction of lipid classes

Total lipids from samples obtained for qualitative analysis were fractionated using Discovery-NH<sub>2</sub> solid-phase extraction cartridges following a previously published method (Kaluzny *et al.*, 1985). Cartridges containing 500 mg of solid phase were conditioned with 9 ml of hexane. The total lipid extract from  $100 \times 10^6$  RAW 264.7 cells was loaded in 200  $\mu$ l of  $CHCl_3$ . Glyceryl lipids were eluted with 6 ml of  $CHCl_3$ /IPA (2:1). This fraction was dried under a gentle stream of nitrogen. The samples were dissolved in 1 ml of  $CHCl_3$ . A 100- $\mu$ l aliquot of this sample was diluted into 900  $\mu$ l of  $CHCl_3$ /MeOH (1:1) to which 20  $\mu$ l of 0.1 M of  $NH_4OAc$  was

added for a final concentration of 5 mM. These samples were used for qualitative studies.

Glycerol lipids for quantitative analysis were obtained from the total lipid extract of approximately  $8 \times 10^6$  RAW 264.7 cells by solid-phase extraction using silica cartridges following a previously published method (Ingalls *et al.*, 1993). Cartridges of 100 mg of material were conditioned with 4 ml of isooctane/ethyl acetate (80:1). The samples were redissolved in 1 ml of isooctane/ethyl acetate (75:25), sonicated for 30 s, and loaded onto the cartridges using a vacuum manifold with the flow-through collected in a clean tube. The neutral lipid fraction was eluted into the same tube with 4 ml of isooctane/ethyl acetate (75:25). This fraction contained the TAGs and DAGs as well as cholesterol and cholesteryl esters, while nonesterified fatty acids, monoacylglycerols, and phospholipids were retained on the cartridge. The samples were then taken to dryness under a gentle stream of nitrogen. The samples were dissolved in 200  $\mu$ l of toluene/methanol (1:1) with 1 mM  $\text{NH}_4\text{OAc}$  for MS analysis using an API 4000 Q TRAP (Applied Biosystems, Foster City, CA).

### 3.1.6. Mass spectrometry

Qualitative analyses were performed on an LTQ, linear ion trap mass spectrometer (Thermo-Finnigan, San Jose, CA). Samples were introduced into the electrospray source using a drawn microcapillary at a flow rate of 1  $\mu$ l/min. The mass spectrometer was operated in positive ion mode with a spray voltage of 2.4 kV, a capillary temperature of 250°, a capillary voltage of 29.0 V, a 1.5-u ion isolation window, and a 100-ms maximum inject time. Scans (typically 50) were averaged for the MS spectra, and approximately 100 scans were averaged for the  $\text{MS}^2$  and  $\text{MS}^3$  spectra.

Neutral loss survey experiments were performed on an API 4000 Q TRAP equipped with a NanoMate nanoelectrospray ionization source (Advion Biosciences, Ithaca, NY). The NanoMate was operated in positive ion mode with a spray voltage of 1.35 kV, vented headspace, and pressure of 0.30 psi, which resulted in a flow rate of approximately 250 nl/min. The mass spectrometer was operated with a step size of 0.10 u, a curtain gas setting of 10, a collision gas setting of medium, a declustering potential of 120, an entrance potential of 10, collision energy of 37, and collision cell exit potential of 6.

The mass-to-charge ( $m/z$ ) range from  $m/z$  500 to 1200 was scanned over 6 s, giving a total of 30 scans for each neutral loss period. These scans were averaged before submission to the Lipid Profiler software (Ejsing *et al.*, 2006) for integration and subsequent analysis. This Applied Biosystems program was modified specifically to process this data format.

## 4. RESULTS

### 4.1. Qualitative analysis

Mass spectrometric analysis of the neutral lipid extract from RAW cells yielded a very complex spectrum. From  $m/z$  700 to 1000, peaks corresponded to ammoniated TAG species at nearly every even mass (Fig. 1.1). Each of these  $m/z$  values could be assigned a total number of carbon atoms and double bonds based on the mass; however, this designation did not indicate individual molecular species. Multiple isobaric species could exist, differing in the exact individual fatty acyl groups present, positional distribution of fatty acyl groups, double bond location, and geometry. These species could also be straight chained or branched fatty acyl groups. In order to improve the characterization of molecular species to individual fatty acyl groups present (total fatty acyl carbons and total number of double bonds in each fatty acyl group),  $MS^3$  was employed.

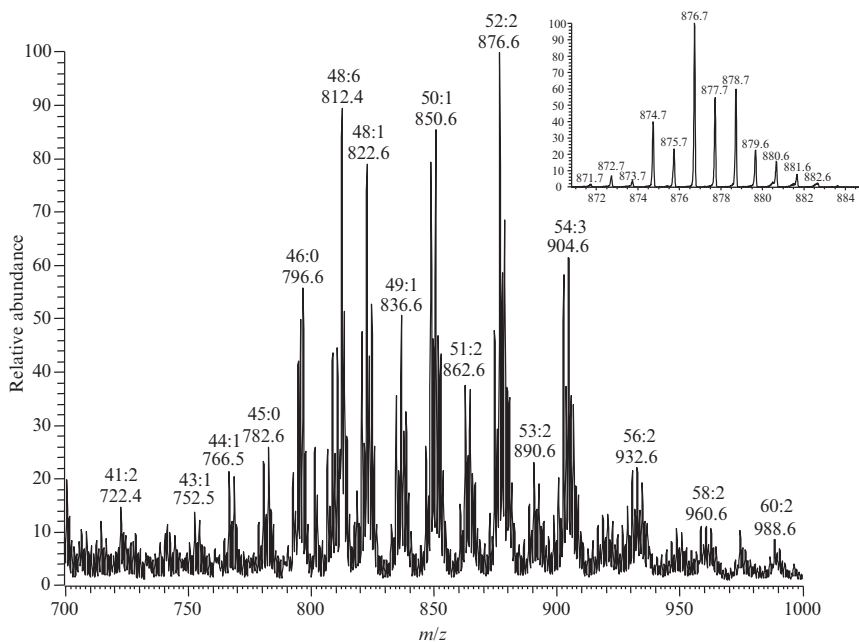


**Figure 1.1** Full-scan mass spectrum of the neutral lipid extract from RAW 264.7 cells showing several envelopes of molecular ions corresponding to triacylglycerols. The envelope corresponding to the series of triacylglycerols containing 52 carbon atoms is shown at high resolution (inset).

For example, the signal at  $m/z$  876 (Fig. 1.1) would correspond to many isobaric combinations of fatty acyl chains with a total of 52 carbons and 2 double bonds or a total of 53 carbons and 9 double bonds within the three esterified fatty acyl groups. To identify all of the isobaric species present, this strategy used both MS<sup>2</sup> and MS<sup>3</sup> experiments. For the MS<sup>2</sup> case, the TAG [M+NH<sub>4</sub>]<sup>+</sup> parent ion ( $m/z$  876) was selected to undergo collision-induced dissociation (CID) (Fig. 1.2). In general, when [M+NH<sub>4</sub>]<sup>+</sup> ions are activated, these ions undergo the neutral loss of a fatty acyl group and ammonia, yielding a corresponding DAG fragment ion (Byrdwell and Neff, 2002; Cheng *et al.*, 1998). The CID of  $m/z$  876 yielded several peaks ( $m/z$  549, 575, 577, 603, 605, 619, 631, and 647), each of which corresponded to the loss of a unique fatty acid from one of the isobaric TAG species present at this  $m/z$  ratio. The most abundant product ions corresponded to the neutral losses of 18:1 ( $m/z$  577), 16:0 ( $m/z$  603), and 18:0 ( $m/z$  575). The difference in the mass of the [M+NH<sub>4</sub>]<sup>+</sup> precursor ion and the product ion was used to identify the fatty acyl group lost from the total number of carbon atoms and double bonds. The neutral loss masses for several common fatty acyl groups are shown in Table 1.1; however, this neutral loss does not provide

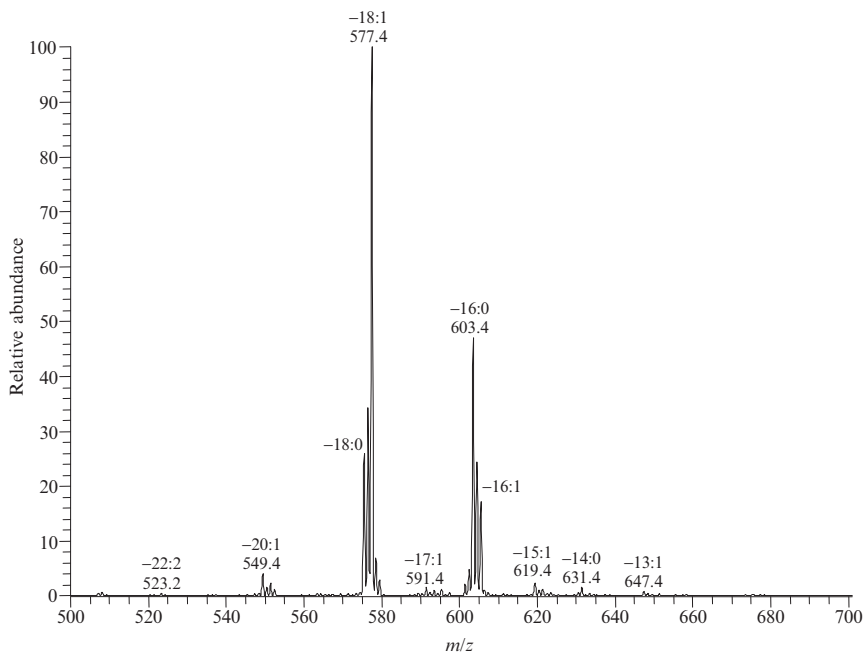


**Figure 1.2** Product ion spectrum from the collision-induced dissociation of the triacylglycerol ion at  $m/z$  876 from the full scan at a collision energy of 30 V. The ion at  $m/z$  876 undergoes loss of several fatty acyl groups as indicated, with the loss of 16:0 (palmitic acid) and 18:1 (oleic acid) being the most abundant.

information to assign double bond or alkyl branching in the lost fatty acyl group, nor does it indicate to which glycerol carbon atom it was esterified.

From the MS<sup>2</sup> spectrum, a product ion can be selected for further fragmentation in the linear ion trap. Collision-induced dissociation of the DAG product ions yielded information about both of the remaining fatty

**Table 1.1** Neutral loss mass corresponding to common fatty acyl groups esterified to triacylglycerol and diacylglycerol molecular species after collisional activation and observed by tandem mass spectrometry (MS/MS)

Fatty acyl substituent <sup>a</sup>	Neutral loss (u) <sup>b</sup> RCOOH+NH <sub>3</sub>
14:0 <sup>a</sup>	245
15:0	259
16:1	271
16:0	273
17:0	287
18:4	293
18:3	295
18:2	297
18:1	299
18:0	301
19:1	313
19:0	315
20:5	319
20:4	321
20:3	323
20:2	325
20:1	327
20:0	329
21:0	343
22:6	345
22:5	347
22:4	349
22:3	351
22:2	353
22:1	355
22:0	357
24:1	383
24:0	385

<sup>a</sup> Designation of total carbon atoms in the fatty acyl group: total number of double bonds.

<sup>b</sup> Neutral loss in daltons (u) as RCOOH+NH<sub>3</sub>, which corresponds to the mass of the fatty acyl group as a free carboxylic acid plus the mass of ammonia.

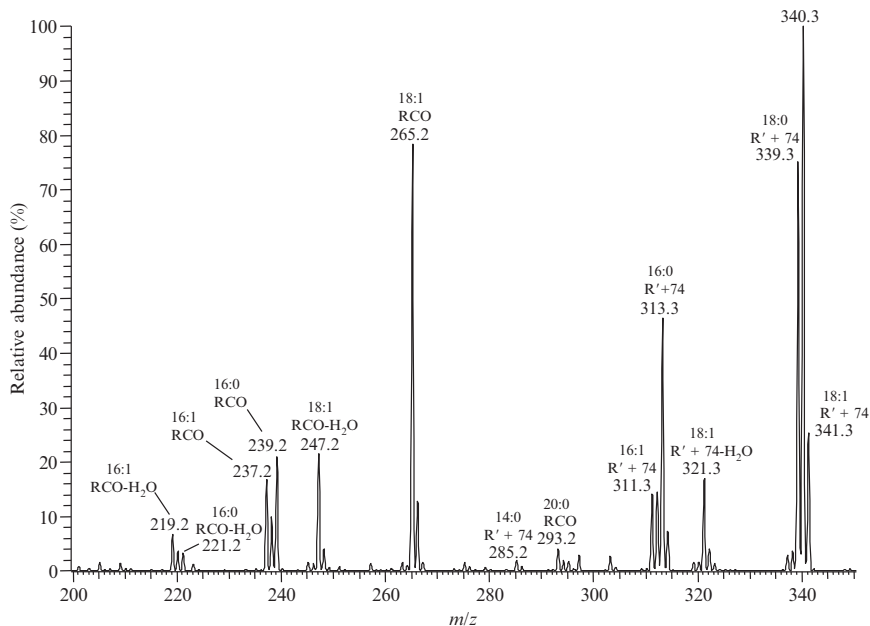


**Figure 1.3** MS/MS/MS spectrum of the diacyl product ion at  $m/z$  577 resulting from the collision-induced dissociation of the ion at  $m/z$  876 in the mass spectrum. The ion at  $m/z$  577 was selected in the linear ion trap to undergo collision-induced dissociation to determine the nature of the final fatty acyl species present in the isobaric molecules. Both acylium ions ( $[RCO]^+$ ) and ions retaining the glycerol backbone ( $[R'+74]^+$ ) are present in this spectrum.

acyl substituents. The mass of the  $MS^3$  product ions related directly to the final esterified acyl chain, and the difference in mass between the  $MS^2$  precursor and  $MS^3$  product ion gave information about the fatty acyl chain that was lost as a neutral species. As shown for the initial  $MS^2$  product ion at  $m/z$  577 (Fig. 1.3), collision-induced dissociation led to a number of  $MS^3$  product ions corresponding to the remaining fatty acyl chains as acylium ions ( $[RCO]^+$ ) and as fatty acids esterified to the glycerol backbone ( $[R'+74]^+$ ) with their associated losses of water. For example, the presence of an 18:1 fatty acyl component in the  $MS^2$  product ion  $m/z$  577 was revealed by the abundant  $MS^3$  product ion at  $m/z$  265 that corresponds to  $C_{17}H_{33}C=O^+$ , while the presence of 16:0 was revealed by the  $MS^3$  product ion at  $m/z$  239 ( $C_{15}H_{31}C=O^+$ ) and 313 ( $[C_{15}H_{31}COO-CH_2CH_2CHO] + H^+$ ). The mechanism for the formation of these ions had been described previously from labeling studies in which the hydrogen atoms on the glycerol backbone were replaced with deuterium atoms (McAnoy *et al.*, 2005).

From the information obtained from the  $MS^2$  and  $MS^3$  spectra, a table containing all of the isobaric species identified for a specific  $m/z$  value was

generated. As shown in Table 1.2, for the three most abundant fragment ions observed in the MS<sup>2</sup> spectrum of the ion at  $m/z$  876 ( $m/z$  577, 603, and 575), the DAG ions, subjected to MS<sup>3</sup>, yielded product ions with unique structural information. From a single  $[M+NH_4]^+$  ion, the identity of approximately 100 distinct molecular species (not counting stereoisomers and double-bond isomers) could be determined. Some species such as 16:0/18:1/18:1 or 16:0/18:0/18:2 would be predicted by the total carbons and double bonds present in the species and the relatively common nature of the fatty acids; however, the presence of these molecular species is directly supported by product ions from several MS<sup>3</sup> spectra. Other species were seen that would not be expected without mass spectral evidence. These included 17:1/18:1/17:0, which was observed in the MS<sup>3</sup> spectra of  $m/z$  577 (loss of 18:1) and 591 (loss of 17:1), and 16:1/14:0/22:1, which was observed in the MS<sup>3</sup> spectra of  $m/z$  605 (loss of 16:1) and 631 (loss of 14:0). Each of the molecular species in Table 1.2 was confirmed by ions in multiple spectra. Some species were repeated in Table 1.2 because their presence was suggested by ions in more than one MS<sup>3</sup> spectrum; however, species corresponding to 53:9 could not be found.

## 4.2. Quantitative analysis

A quantitative method for accurate determination of changes in molecular species components in the complex mixture of neutral lipids containing a number of isobaric species was developed utilizing the characteristic fragmentation pathways. Deuterium-labeled internal standards, whose masses fell into regions of the spectrum that did not contain ions corresponding to ammoniated DAG and TAG molecular species, afforded a means for normalization of neutral loss data for 18 different fatty acyl groups.

Neutral loss experiments were performed to follow changes in Kdo<sub>2</sub>-lipid A-treated cells in terms of DAG and TAG molecular species that contained at least one of the 18 different fatty acyl groups present in the deuterium-labeled internal standards. Each neutral loss corresponding to one of the 18 fatty acyl groups in the deuterated internal standards (Table 1.3) was monitored for a period of 3 min, yielding a characteristic total ion current (Fig. 1.4). For each period in the experiment, a unique neutral loss spectrum was obtained, which revealed all of the  $[M+NH_4]^+$  ions in the complex mixture that contained a single fatty acyl group as well as some indication of the abundance of this  $[M+NH_4]^+$  ion relative to a deuterium-labeled internal standard (Fig. 1.5). For example, the presence of 18:1 esterified to DAG molecular species gave abundant ions at  $m/z$  612, 638, and 668. The ion at  $m/z$  612 would correspond to an 18:1/16:0 DAG,  $m/z$  638 an 18:1/18:1 DAG, and  $m/z$  668 an 18:1/20:0 DAG molecular species (Fig. 1.5A). The abundance of these molecular species compared to the internal standard at  $m/z$  827.8 was monitored in a series of experiments



**Table 1.2** Triacylglycerol molecular species identified from the MS/MS/MS (MS<sup>3</sup>) analysis of the three most abundant diacylglycerol product ions observed in the tandem mass spectrometry (MS/MS) (MS<sup>2</sup>) spectrum of the [M+NH<sub>4</sub>]<sup>+</sup> triacylglycerol observed at *m/z* 876 in the full mass spectrum of RAW 264.7 cells

MS <sup>2</sup> product ion <sup>a</sup>	Triacylglycerol <sup>b</sup>	MS <sup>3</sup> ion type	MS <sup>2</sup> product ion <sup>a</sup>	Triacylglycerol <sup>b</sup>	MS <sup>3</sup> ion type	MS <sup>2</sup> product ion <sup>a</sup>	Triacylglycerol <sup>b</sup>	MS <sup>3</sup> ion type
577 (-18:1)	18:1/18:1/16:0	RCO	603 (-16:0)	16:0/18:1/18:1	RCO	575 (-18:0)	18:0/18:1/16:1	R'+74
	18:1/14:1/20:0	R'+74- H <sub>2</sub> O		16:0/14:1/22:1	R'+74- H <sub>2</sub> O		18:0/18:1/16:1	RCO
	18:1/18:1/16:0	R'+74		16:0/18:1/18:1	R'+74		18:0/14:1/20:1	R'+74- H <sub>2</sub> O
	18:1/18:0/16:1	R'+74		16:0/18:1/18:1	RCO- H <sub>2</sub> O		18:0/16:1/18:1	R'+74
	18:1/18:1/16:0	RCO- H <sub>2</sub> O		16:0/18:1/18:1	R'+74- H <sub>2</sub> O		18:0/16:1/18:1	RCO
	18:1/16:0/18:1	RCO		16:0/20:1/16:1	R'+74		18:0/12:1/22:1	R'+74- H <sub>2</sub> O
	18:1/12:0/22:1	R'+74- H <sub>2</sub> O		16:0/16:0/20:2	R'+74		18:0/16:0/18:2	R'+74
	18:1/22:1/12:0	RCO		16:0/18:2/18:0	R'+74- H <sub>2</sub> O		18:0/16:1/18:1	RCO- H <sub>2</sub> O
	18:1/17:3/18:5	R'+74		16:0/18:0/18:2	R'+74		18:0/18:1/16:1	RCO- H <sub>2</sub> O
	18:1/18:1/16:0	R'+74- H <sub>2</sub> O		16:0/18:2/18:0	R'+74		18:0/18:1/16:1	R'+74- H <sub>2</sub> O
	18:1/16:1/18:0	RCO		16:0/19:0/17:2	R'+74- H <sub>2</sub> O		18:0/22:1/12:1	RCO
	18:1/12:1/22:0	R'+74- H <sub>2</sub> O		16:0/17:2/19:0	R'+74		18:0/18:2/16:0	R'+74
	18:1/16:1/18:0	R'+74		16:0/18:0/18:2	R'+74- H <sub>2</sub> O		18:0/19:0/15:2	R'+74- H <sub>2</sub> O
	18:1/16:1/18:0			16:0/20:2/16:0			18:0/20:1/14:1	RCO

18:1/20:1/14:0	RCO- H <sub>2</sub> O RCO	16:0/18:2/18:0	R'+74- H <sub>2</sub> O RCO	18:0/16:1/18:1	R'+74- H <sub>2</sub> O
18:1/16:1/18:0	R'+74- H <sub>2</sub> O	16:0/19:0/17:2	RCO- H <sub>2</sub> O	18:0/18:2/16:0	R'+74- H <sub>2</sub> O
18:1/19:0/15:1	R'+74- H <sub>2</sub> O	16:0/18:2/18:0	RCO- H <sub>2</sub> O	18:0/22:2/12:0	RCO
18:1/22:1/12:0	RCO- H <sub>2</sub> O	16:0/20:1/16:1	RCO	18:0/18:2/16:0	RCO- H <sub>2</sub> O
18:1/16:0/18:1	RCO- H <sub>2</sub> O	16:0/16:1/20:1	R'+74- H <sub>2</sub> O	18:0/18:2/16:0	RCO
18:1/15:1/19:0	R'+74	16:0/20:2/16:0	R'+74	18:0/19:0/15:2	RCO- H <sub>2</sub> O
18:1/14:0/20:1	R'+74	16:0/21:0/15:2	R'+74- H <sub>2</sub> O	18:0/14:2/20:0	R'+74- H <sub>2</sub> O
18:1/18:0/16:1	RCO	16:0/20:2/16:0	RCO	18:0/14:0/20:2	R'+74
18:1/14:0/20:1	R'+74- H <sub>2</sub> O	16:0/21:0/15:2	RCO- H <sub>2</sub> O	18:0/22:1/12:1	RCO- H <sub>2</sub> O
18:1/20:0/14:1	RCO	16:0/16:2/20:0	R'+74- H <sub>2</sub> O		
18:1/16:0/18:1	R'+74- H <sub>2</sub> O	16:0/16:1/20:1	RCO		
18:1/22:0/12:1	RCO	16:0/16:1/20:1	R'+74		
18:1/18:0/16:1	R'+74- H <sub>2</sub> O	16:0/20:2/16:0	RCO- H <sub>2</sub> O		
18:1/23:0/11:1	RCO- H <sub>2</sub> O	16:0/14:0/22:2	R'+74		
18:1/15:1/19:0	RCO- H <sub>2</sub> O	16:0/15:1/21:1	RCO- H <sub>2</sub> O		
18:1/20:1/14:0		16:0/20:1/16:1			

(continued)

**Table 1.2** (continued)

MS <sup>2</sup> product ion <sup>a</sup>	Triacylglycerol <sup>b</sup>	MS <sup>3</sup> ion type	MS <sup>2</sup> product ion <sup>a</sup>	Triacylglycerol <sup>b</sup>	MS <sup>3</sup> ion type	MS <sup>2</sup> product ion <sup>a</sup>	Triacylglycerol <sup>b</sup>	MS <sup>3</sup> ion type
		RCO- H <sub>2</sub> O			RCO- H <sub>2</sub> O			
	18:1/19:0/15:1	RCO- H <sub>2</sub> O		16:0/16:1/20:1	RCO- H <sub>2</sub> O			
	18:1/14:1/20:0	RCO		16:0/15:1/21:1	RCO			
	18:1/15:1/19:0	RCO		16:0/20:1/16:1	R'+74- H <sub>2</sub> O			
	18:1/12:0/22:1	R'+74		16:0/21:1/15:1	RCO- H <sub>2</sub> O			
	18:1/13:1/21:0	RCO		16:0/19:1/17:1	RCO			
	18:1/17:1/17:0	RCO		16:0/15:1/21:1	R'+74- H <sub>2</sub> O			
	18:1/15:1/19:0	R'+74- H <sub>2</sub> O		16:0/13:0/23:2	R'+74			
	18:1/14:0/20:1	RCO- H <sub>2</sub> O		16:0/17:1/19:1	RCO			
	18:1/18:0/16:1	RCO- H <sub>2</sub> O						

<sup>a</sup> The neutral loss from  $m/z$  876 to the MS<sup>2</sup> product ion revealed one of the fatty acyl groups in this [M+NH<sub>4</sub>]<sup>+</sup> species in parentheses under the mass of the MS<sup>2</sup> product ion.

<sup>b</sup> Each TAG column has the first entry in the TAG molecular species abbreviation, by default, as the species that was lost as a neutral in MS<sup>2</sup>. The second entry in the abbreviation is the acyl group indicated by the presence of the specified ion type in the MS<sup>3</sup> spectrum (column 3) and the third entry of the abbreviation was calculated from the mass difference of the two.

**Table 1.3** [1,1,2,3,3-d<sub>5</sub>] Glycerol-labeled glycerol lipids used as internal standards for neutral loss mass spectrometric analysis

Triacylglycerol fatty acyl composition	$m/z$ [M+NH <sub>4</sub> ] <sup>+</sup>	Diacylglycerol fatty acyl composition	$m/z$ [M+NH <sub>4</sub> ] <sup>+</sup>
19:0/12:0/19:0 <sup>a</sup>	857.83	19:0/19:0	675.66
14:0/16:1/14:0	771.73	20:0/20:0	703.70
15:0/18:1/15:0	771.73	14:0/14:0	535.51
16:0/18:0/16:0	857.83	15:0/15:0	563.54
17:0/17:1/17:0	869.83	16:0/16:0	591.57
20:4/18:2/20:4	949.80	17:0/17:0	619.57
20:0/20:1/20:0	995.97	20:2/20:2	695.60
20:2/18:3/20:2	955.84	20:4/20:4	687.54
20:5/22:6/20:5	993.77	20:5/20:5	683.51

<sup>a</sup> The acyl order as indicated: sn-1/sn-2/sn-3.

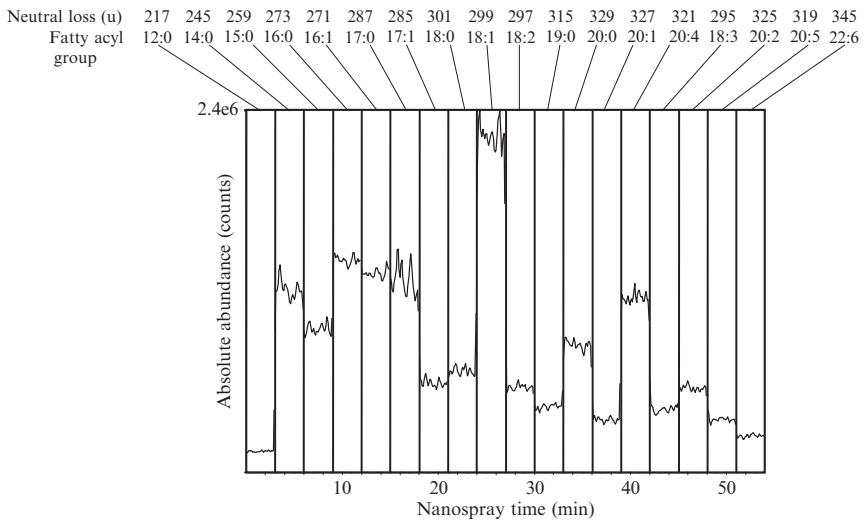


**Figure 1.4** Total ion current from a neutral loss survey in the time course of glycerol lipid changes upon activation of the Toll-4 receptor in RAW 264.7 cells. Each column represents a 3-min period in which the neutral loss of a different fatty acyl moiety from the diacylglycerol and triacylglycerol species was monitored.

covering the course of Kdo<sub>2</sub>-lipid A stimulation, revealing changes in each DAG species taking place. However, it would not be possible to state relative abundance of 18:1/18:1 DAG and 18:1/16:0 DAG to each other because of the difference in neutral loss behavior due to structural features such as esterification position on the glycerol backbone (Li and Evans, 2006).

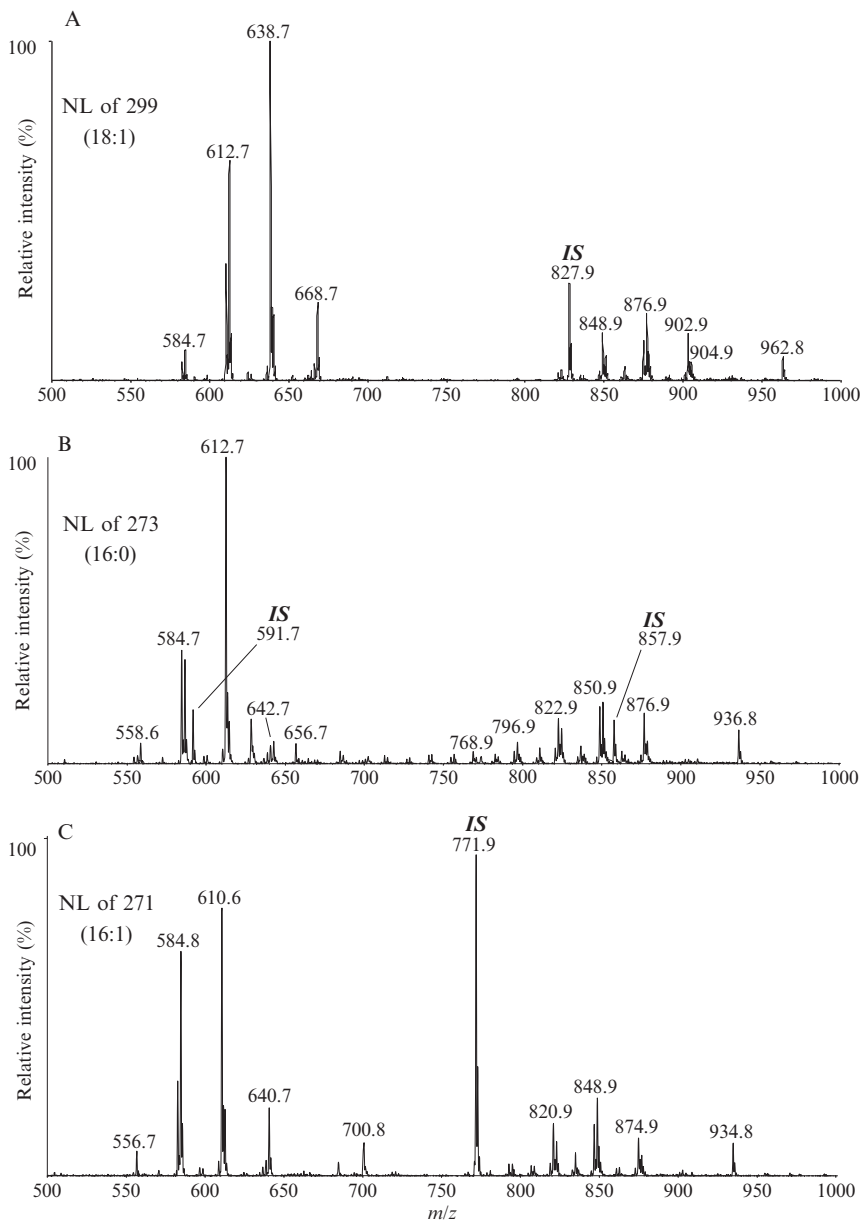


**Figure 1.5** Spectra showing the  $[M+NH_4]^+$  ions detected by the neutral loss of an 18:1, 16:0 or 16:1 fatty acyl group upon collisional activation. In this case, the diacylglycerol species can be uniquely identified, but the triacylglycerol molecular species can only be partially elucidated.

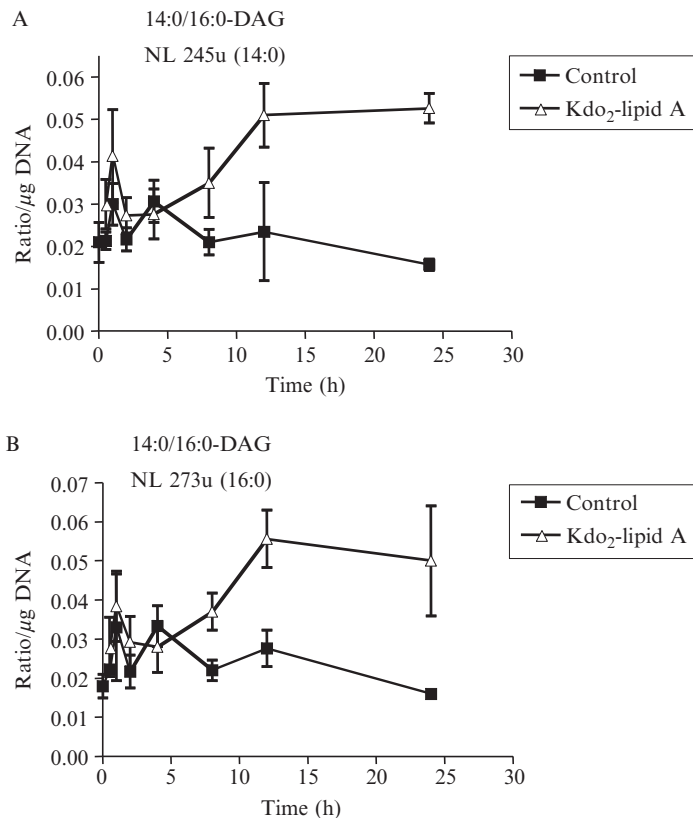


**Figure 1.6** (A) Quantitative analysis showing the increase in abundance of the 14:0/16:0 diacylglycerol over time in Kdo<sub>2</sub>-lipid A-treated cells compared to control measured from the neutral loss of 14:0. (B) Quantitative analysis showing the increase in abundance of the 14:0/16:0 diacylglycerol over time in Kdo<sub>2</sub>-lipid A-treated cells compared to control measured from the neutral loss of 16:0.

Each neutral loss experiment revealed common and new molecular species, such as species containing 16:0 (Fig. 1.5B) and 16:1 (Fig. 1.5C). Thus, these spectra gave unique identification of DAG species, but only partial characterization of TAG species.

The Lipid Profiler software package was used to integrate the ion abundance for each  $m/z$ , to correct abundances due to <sup>13</sup>C isotopes, and to identify DAG and TAG ions and the internal standards in the averaged spectra from each period in the neutral loss survey. The corrected DAG and TAG abundances were normalized to the abundance of the internal standards.

Changes in the abundance of specific species compared to the internal standard over time in the control and Kdo<sub>2</sub>-lipid A-treated cells were thereby assessed in a quantitative way (Fig. 1.6). This quantitative approach

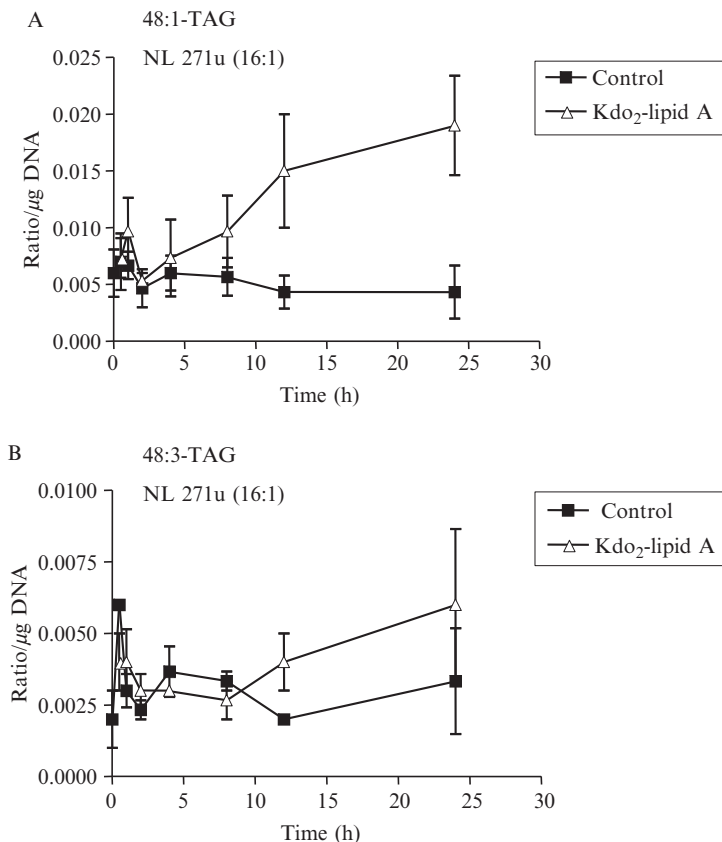


**Figure 1.7** (A) Quantitative analysis of the changes in the 48:1 triacylglycerol molecular species which contains a 16:1 fatty acyl group. The abundance of this species changes in Kdo<sub>2</sub>-lipid A-treated cells compared to controls. (B) Quantitative analysis of the changes in the 48:3 triacylglycerol molecular species that contains a 16:1 fatty acyl group. The abundance of this species in Kdo<sub>2</sub>-lipid A-treated cells does not change compared to control.

revealed time-dependent changes in the 14:0/16:0 DAG molecular species in Kdo<sub>2</sub>-lipid A-treated RAW cells, as measured by the neutral loss of 14:0 (Fig. 1.6A) or 16:0 (Fig. 1.6B). The abundance of 14:0/16:0 DAG in Kdo<sub>2</sub>-lipid A-treated cells was greater than that in control samples, with very similar time dependence, regardless of which neutral loss was monitored.

The neutral loss of 16:1 was common to several TAG molecular species; however, in some cases, a significant increase was observed between the ratios of abundances for molecular species in treated and control samples at 24 hr, as is the case for the 48:1 TAG molecular species that contain 16:1 (Fig. 1.7A). For the 48:3 TAG containing 16:1 (Fig. 1.7B), though, the relative abundance was constant for treated cells compared to controls at 24 h.

## 5. CONCLUSIONS

The analysis of glyceryl lipids present within mammalian cells is very challenging. However, the power of combining MS<sup>2</sup> and MS<sup>3</sup> can be used to uniquely identify TAGs and DAGs and to quantitate molecular species with a specific total of fatty acyl carbon atoms and double bonds and containing a specific fatty acyl group from a very complex biological sample in the neutral lipid extract of RAW 264.7 macrophages. This approach can be used to precisely assess changes within populations of molecular species that cannot be determined by measurement of molecular ion species such as [M+H]<sup>+</sup>, [M+Li]<sup>+</sup>, or [M+NH<sub>4</sub>]<sup>+</sup> abundances alone. However, these stable isotope-controlled MS<sup>2</sup> and MS<sup>3</sup> experiments do not provide molar concentration data and, in the case of TAG molecules, do not analyze the complex mixture to the extent of providing molecular species information, stereochemistry, or even positional analysis.

## ACKNOWLEDGMENTS

This work was supported in part by the LIPID MAPS Large Scale Collaborative Grant from the National Institutes of Health (GM069338).

## REFERENCES

- Ahn, S. J., Costa, J., and Emanuel, J. R. (1996). PicoGreen quantitation of DNA: Effective evaluation of samples pre- or post-PCR. *Nucleic Acids Res.* **24**, 2623–2625.
- Bligh, E. G., and Dyer, W. J. (1959). A rapid method of total lipid extraction and purification. *Can. J. Biochem. Physiol.* **37**, 911–917.
- Byrdwell, W. C., Emken, E. A., Neff, W. E., and Adlof, R. O. (1996). Quantitative analysis of triglycerides using atmospheric pressure chemical ionization–mass spectrometry. *Lipids* **31**, 919–935.
- Byrdwell, W. C., and Neff, W. E. (2002). Dual parallel electrospray ionization and atmospheric pressure chemical ionization mass spectrometry (MS), MS/MS, and MS/MS/MS for the analysis of triacylglycerols and triacylglycerol oxidation products. *Rapid Commun. Mass Spectrom.* **16**, 300–319.
- Cheng, C., Gross, M. L., and Pittenauer, E. (1998). Complete structural elucidation of triacylglycerols by tandem sector mass spectrometry. *Anal. Chem.* **70**, 4417–4426.
- Ejsing, C. S., Duchoslav, E., Sampaio, J., Simons, K., Bonner, R., Thiele, C., Ekroos, K., and Shevchenko, A. (2006). Automated identification and quantification of glycerophospholipid molecular species by multiple precursor ion scanning. *Anal. Chem.* **78**, 6202–6214.
- Han, X., and Gross, R. W. (2001). Quantitative analysis and molecular species fingerprinting of triacylglyceride molecular species directly from lipid extracts of biological samples by electrospray ionization tandem mass spectrometry. *Anal. Biochem.* **295**, 88–100.
- Hsu, F. F., and Turk, J. (1999). Structural characterization of triacylglycerols as lithiated adducts by electrospray ionization mass spectrometry using low-energy collisionally



- induced dissociation on a triple stage quadrupole instrument. *J. Am. Soc. Mass Spectrom.* **10**, 587–599.
- Ingalls, S. T., Kriaris, M. S., Xu, Y., DeWulf, D. W., Tserng, K. Y., and Hoppel, C. L. (1993). Method for isolation of non-esterified fatty acids and several other classes of plasma lipids by column chromatography on silica gel. *J. Chromatogr.* **619**, 9–19.
- Kaluzny, M. A., Duncan, L. A., Merritt, M. V., and Epps, D. E. (1985). Rapid separation and purification of lipid classes in high yield and purity using bonded phase columns. *J. Lipid Res.* **26**, 135–140.
- Li, X., Collins, E. J., and Evans, J. J. (2006). Examining the collision-induced decomposition spectra of ammoniated triglycerides as a function of fatty acid chain length and degree of unsaturation. II. The PXP/YPY series. *Rapid Commun. Mass Spectrom.* **20**, 171–177.
- McAnoy, A. M., Wu, C. C., and Murphy, R. C. (2005). Direct qualitative analysis of triacylglycerols by electrospray mass spectrometry using a linear ion trap. *J. Am. Soc. Mass Spectrom.* **16**, 1498–1509.
- Myher, J. J., Kuksis, A., Marai, L., and Sandra, P. (1988). Identification of the more complex triacylglycerols in bovine milk fat by gas chromatography-mass spectrometry using polar capillary columns. *J. Chromatogr.* **452**, 93–118.
- Phillips, F. C., Erdahl, W. L., Schmidt, J. A., and Privett, O. S. (1984). Quantitative analysis of triglyceride species of vegetable oils by high performance liquid chromatography via a flame ionization detector. *Lipids* **19**, 880–887.
- Raetz, C. R. H. (1990). Biochemistry of endotoxins. *Ann. Rev. Biochem.* **59**, 129–170.
- Raetz, C. R., Garrett, T. A., Reynolds, C. M., Shaw, W. A., Moore, J. D., Smith, D. C., Jr, Ribeiro, A. A., Murphy, R. C., Ulevitch, R. J., Fearn, C., Reichart, D., Glass, C. K., *et al.* (2006). Kdo<sub>2</sub>-Lipid A of *Escherichia coli*, a defined endotoxin that activates macrophages via TLR-4. *J. Lipid Res.* **47**, 1097–1111.

# GLYCEROPHOSPHOLIPID IDENTIFICATION AND QUANTITATION BY ELECTROSPRAY IONIZATION MASS SPECTROMETRY

Pavlina T. Ivanova, Stephen B. Milne, Mark O. Byrne, Yun Xiang,  
and H. Alex Brown

## Contents

1. Introduction	22
2. Nomenclature	25
3. Mass Spectrometry	26
4. General Strategy for Phospholipid Isolation and Mass Spectral Analysis	27
5. Extraction and Mass Spectral Analysis of Global Glycerophospholipids	28
5.1. Phospholipid extraction from cultured cells	29
5.2. Phospholipid extraction from tissue	30
5.3. Direct infusion mass spectrometry of phospholipid extracts	30
5.4. LC-MS analysis (quantitation) of phospholipid extracts	33
6. Polyphosphoinositide Extraction and Mass Spectral Analysis	35
6.1. Extraction of polyphosphoinositides from cultured cells	37
6.2. Extraction of polyphosphoinositides from tissue	37
6.3. Direct-infusion mass spectral analysis of polyphosphoinositides	38
6.4. Deacylation of GPIsPn lipids	39
6.5. LC-MS analysis of deacylated GPIsPn compounds	39
7. Computational Analysis of Mass Spectral Data	41
7.1. Direct infusion (intra-source separation)	43
7.2. LC-MS data analysis	47
Acknowledgments	54
References	54

Departments of Pharmacology and Chemistry, Vanderbilt University School of Medicine,  
Nashville, Tennessee

## Abstract

Glycerophospholipids are the structural building blocks of the cellular membrane. In addition to creating a protective barrier around the cell, lipids are precursors of intracellular signaling molecules that modulate membrane trafficking and are involved in transmembrane signal transduction. Phospholipids are also increasingly recognized as important participants in the regulation and control of cellular function and disease. Analysis and characterization of lipid species by mass spectrometry (MS) have evolved and advanced with improvements in instrumentation and technology. Key advances, including the development of “soft” ionization techniques for MS such as electrospray ionization (ESI), matrix-assisted laser desorption/ionization (MALDI), and tandem mass spectrometry (MS/MS), have facilitated the analysis of complex lipid mixtures by overcoming the earlier limitations. ESI-MS has become the technique of choice for the analysis of multi-component mixtures of lipids from biological samples due to its exceptional sensitivity and capacity for high throughput.

This chapter covers qualitative and quantitative MS methods used for the elucidation of glycerophospholipid identity and quantity in cell or tissue extracts. Sections are included on the extraction, MS analysis, and data analysis of glycerophospholipids and polyphosphoinositides.

## 1. INTRODUCTION

Lipids are defined as a wide variety of biological molecules demonstrating different structure and function. It is commonly accepted that lipids are molecules highly soluble in organic solvents; however, many classes (such as the highly polar polyphosphoinositides and molecules with large hydrophilic domains like lipopolysaccharide) exist that are not soluble in these solvents (Dowhan, 1997; Dowhan and Bogdanov, 2002). Their primary role has been thought of as a central component of a semipermeable membrane. Multiple functions and adaptability of cellular membranes require a wide spectrum of lipids to support the necessary environment. The physical and chemical properties of the membranes directly affect the cellular processes, making the role of the lipids dynamic rather than just a simple inert barrier. Additionally, phospholipids are linked to important physiological processes such as bioenergetics, signal transduction across the cell membrane, and cellular recognition. Upon activation of a number of enzymes (i.e., phospholipases, kinases, and phosphatases), membrane phospholipids generate signaling lipids. Their formation is generally initialized by a ligand binding to a cell surface receptor leading to activation of phospholipases or kinases. The synthesized lipid second messengers act on specific proteins to manipulate cell function. Signaling lipids are quickly metabolized to limit the response or to initiate another signaling cascade.

The major lipid constituents of most membranes are phosphate-containing glycerol-based lipids generally referred to as glycerophospholipids. Phospholipids are grouped into classes depending on the “headgroup” identity. The major classes (Fig. 2.1) of phospholipids found in a mammalian cell membrane include glycerophosphatidic acid (GPA), glycerophosphocholine (GPCho), glycerophosphoethanolamine (GPEtn), glycerophosphoinositol (GPIIns), glycerophosphoglycerol (GPGro), and glycerophosphoserine (GPSer). A multitude of molecular species exist within each class containing different combinations of fatty acids in the *sn*-1 and *sn*-2 position of the glycerol backbone. In addition, fatty acids at *sn*-1 position can be substituted for ether or vinyl ether moiety (plasmanyl and plasmeryl glycerophospholipids, respectively) in some of the classes.

Comprehensive analysis of phospholipid molecular species has been challenging owing to their large number and diversity, complicating their separation and identification. A liquid–liquid extraction of cellular material results in heterogeneous mixtures of phospholipids, which can be further separated by selective use of organic solvents. Class separation generally involves thin-layer chromatography (TLC), high-performance liquid chromatography (HPLC), and gas chromatography (GC), any of which utilizes known standards and sometimes requires prior derivatization. With the advent of gas chromatography and gas chromatography-MS (GC-MS), class separation by TLC followed by hydrolysis and derivatization made possible the identification of individual fatty acid species. The conventional method is not only time consuming but also requires large amounts of lipids. The analysis of intact polar phospholipids became possible only after development of fast atom bombardment mass spectrometry (FAB-MS). More recently, the introduction of “soft” ESI-MS has greatly simplified the procedure for lipid analysis. This ionization process results in decreased molecular ion decomposition, better reproducibility, and lower detection limits compared to FAB-MS. The great potential of ESI-MS for characterization of phospholipids and other polar lipids has been described in other publications (Brügger *et al.*, 1997; Fridriksson *et al.*, 1999; Han and Gross, 1994). We have expanded the use of direct infusion ESI-MS for identification of over 600 phospholipid species from an unprocessed total lipid extract. Changes in the cellular concentration of diverse lipids can be determined by analysis of the mass spectra via statistical algorithms. The generated lipid arrays represent a qualitative map of molecular species changes after challenge with a biological stimulant (Ivanova *et al.*, 2004). The quantitative analysis of the myriad of phospholipid species belonging to different phospholipid classes involves a chromatographic separation by class to avoid the possible mass overlap occurring during direct infusion analysis. Thus, a class separation by liquid chromatography (LC) followed by MS detection for species identification is very important in the analysis of glycerophospholipids extracted from a complex biological matrix (DeLong

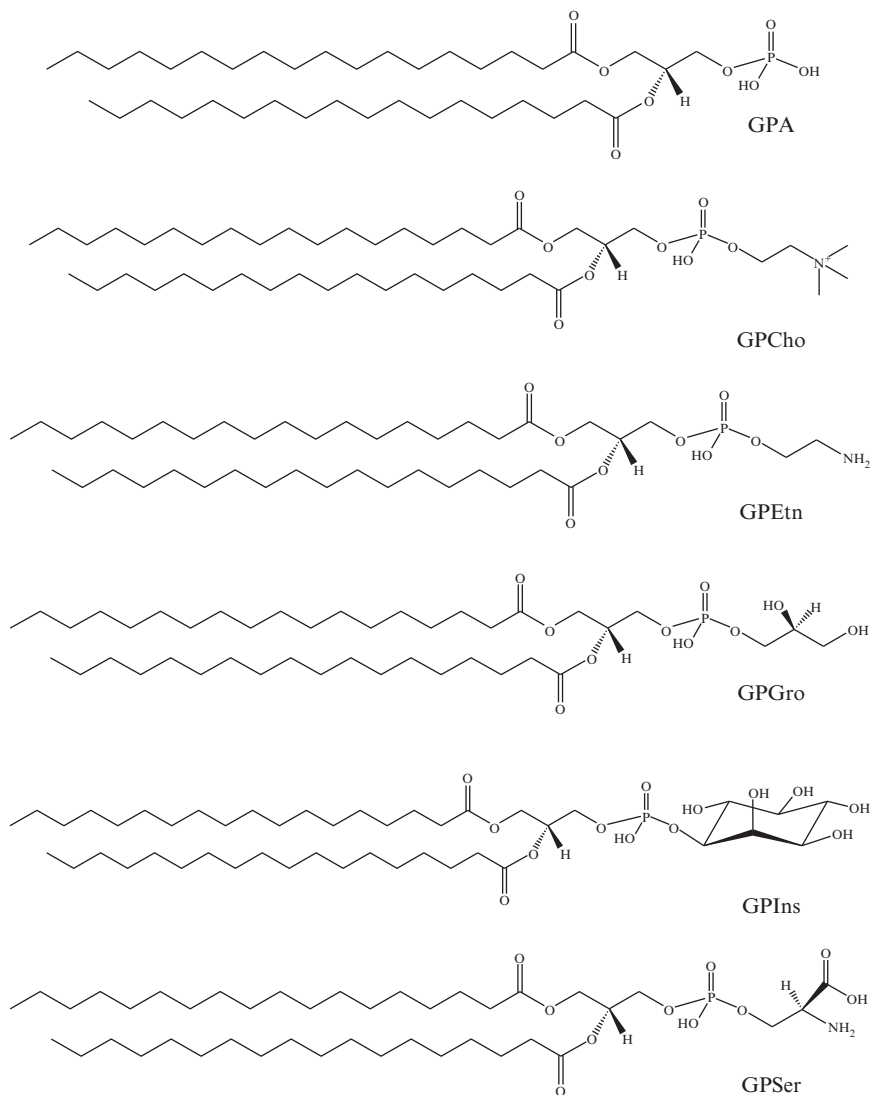


**Figure 2.1** Major glycerophospholipid classes. Phospholipids consist of a glycerol backbone, two acyl moieties, and a phosphodiester headgroup. The variety in length and degree of unsaturation of the acyl chains creates a wide spectrum of species within each class. Ethers or vinyl ethers can substitute the *sn*-1 position and generate plasmalogen species in some classes.

*et al.*, 2001; Lesnefsky *et al.*, 2000; Taguchi *et al.*, 2000; Wang *et al.*, 2004). The importance of phospholipids in cell signaling and organ physiology as well as their association with many diseases that implicate lipid metabolic pathways and enzyme disruption requires novel methodological approaches

and development of new technology for their analysis. Analyzing the complex lipid extracts from biological sources and obtaining a lipid profile will give information on the changes in lipid species composition as a result of the biological condition (stimulation by receptor activation; progress of a disease or comparison between normal and transformed cells).

In this chapter, we present a description of the lipidomics technology and its application for identification and quantitation of the major glycerophospholipid classes. Consistent with the spirit of *Methods in Enzymology* volumes, this chapter was designed for readers who may not have extensive experience with MS.

## 2. NOMENCLATURE

Classification of lipids has been difficult to define due to their diverse structures. Although they are derived from similar biological precursors and have similar physical and chemical properties, lipid classes diverge based on the chemical entities they possess. A categorization of a large spectrum of biologically relevant lipids has been proposed recently by [Fahy et al. \(2005\)](#). The simplest class of lipids is the fatty acids. Oxidation of long-chain fatty acids is one of the main sources of energy for mammals. Another group of biologically active lipids used as fuels and in many metabolic processes are the sterols (steroid hormones, vitamins, bile acids). Three other groups are closely related chemically and include neutral lipids (glycerolipids), glycerophospholipids, and sphingolipids. Glycerophospholipids are defined by the presence of a phosphate group esterified to one of the glycerol hydroxyl groups. Naming of the glycerophospholipids involves a stereo-specific numbering (*sn*) ([Hirschmann, 1960](#); [IUPAC-IUB CBN, 1967](#)), and the glycerol backbone is typically acylated or alkylated at the *sn*-1 and/or *sn*-2 position ([Fig. 2.2](#)). These substituents are generally expressed with the term “radyl.” The double bond geometry of the radyl moieties is described with E/Z designation (instead of *trans/cis*), and the lack of one radyl group is denoted as “lyso” glycerophospholipid.

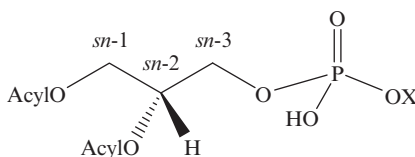


**Figure 2.2** Stereo-specific number system for glycerophospholipids (X is the headgroup).

### 3. MASS SPECTROMETRY

Mass spectrometry is a unique analytical technique, relying on the separation of ions according to both their electrical charge and their total atomic mass by magnetic and electrical fields. A mass spectrometer typically consists of four important components: inlet (for sample introduction), ion source, mass analyzer, and ion detector. The analyte solution is sprayed through a very thin capillary, and the application of a strong electric field generates highly charged droplets. They pass through a heated inert gas in the mass analyzer and separate according to their mass-to-charge ratio ( $m/z$ ), at which point they are recorded by a detection system. The very high vacuum in the instrument ( $10^{-5}$  to  $10^{-7}$  Torr) increases the free path of the ions and ensures mostly monomolecular reactions, which can disclose structural information of the analyzed compound. MS data are largely dependent on the sample introduction and method of ionization, while the type of mass analyzer does not usually alter the observed chemical reactions.

Despite the fact that lipid analysis was one of the first applications of the mass spectrograph after the founding studies by Sir J. J. Thompson and F. W. Aston, the routine analysis of lipids was hindered by their tendency to undergo fragmentation during the process (Fenwick, 1983). The development of FAB-MS allowed the analysis of natural phospholipids; however, along with the generated abundant molecular (i.e., unfragmented) ions, fragment ions were observed, providing some structural information and revealing the great potential of MS/MS (i.e., analysis of molecular and fragment ions generated thereof) for the structural characterization of lipids (Murphy and Harrison, 1994). Thus, the highly attractive MS analysis of phospholipids was rarely used until the introduction of “soft” ionization methods such as MALDI and ESI. “Soft” ionization does not cause extensive fragmentation, meaning that comprehensive detection of an entire range of phospholipids within a complex mixture can be correlated to experimental conditions or disease states. Various ESI-MS methods have been developed for analysis of different classes, subclasses, and individual lipid species from biological extracts. Comprehensive reviews of the methods and their application have recently been published (Murphy *et al.*, 2001; Pulfer and Murphy, 2003; Watson, 2006; Wenk, 2005). The major advantages of ESI-MS are high accuracy, sensitivity, reproducibility, and the applicability of the technique to complex phospholipid solutions without prior derivatization.

ESI-MS was initially developed by Fenn *et al.* (1989) for analysis of biomolecules. It depends on the formation of gaseous ions from polar, thermally labile, and mostly nonvolatile molecules, and thus is completely suitable for phospholipids. The principle of ionization involves a sample in solution that is passed through a very thin capillary or needle at a slow

rate (1–300  $\mu\text{l}/\text{min}$ ). The application of a strong electric field generates significant charge at the end of the capillary that produces a fine spray of highly charged droplets. These droplets then pass through a heated inert gas for desolvation prior to MS analysis of individual ionic species.

Electrospray ion sources can be combined with various mass analyzers such as ion trap (IT), quadrupole, time of flight (TOF), and Fourier transform ion cyclotron (FT-ICR). They all differ in their mass accuracy (the error in the exact mass determination compared to theoretical value) and resolution (the value of mass  $m$  divided by the mass difference  $\Delta m$  between two ion profiles with a small mass difference). Today, the most widely used mass spectrometers with ESI sources are triple quadrupole (TQ), quadrupole ion trap (QIT), IT, and quadrupole TOF (Q-TOF) instruments.

The “soft” ESI causes little or no fragmentation, and virtually all phospholipid species are detected as molecular ion species. The identification and structural information about a certain peak is acquired by fragmentation (MS/MS). The ion of interest is subjected to collision-induced dissociation by interaction with a collision gas. In tandem mass instruments, the first mass analyzer (Q1) is used for the selection of the ion of interest, which is then fragmented in the collision cell (Q2), and the second mass analyzer (Q3) is used to separate the fragment ions on the basis of their  $m/z$  values, thus creating a product or “daughter” spectrum that provides structural information.

#### 4. GENERAL STRATEGY FOR PHOSPHOLIPID ISOLATION AND MASS SPECTRAL ANALYSIS

The analysis and structural identification of glycerophospholipids from cell extracts or tissue biopsies is outlined in Fig. 2.3. Global (GPA, GPCho, GPEtn, GPGro, GPIns, and GPSer) glycerophospholipids are extracted by a modified Bligh and Dyer extraction. The samples are subjected to direct infusion MS, where qualitative changes in lipid species are documented by the construction of lipidomic arrays (Forrester *et al.*, 2004), as well as “ratiomics analysis”—comparison of peak intensities of various species in the same class (Rouzer *et al.*, 2006). Direct infusion is also used in MS/MS for species identification and structural confirmation (acyl chain and headgroup information). Another part of the obtained glycerophospholipid extract is put through LC-ESI-MS analysis, which results in a class separation and quantification of the individual glycerophospholipid species.

Polyphosphoinositides are extracted by a different procedure tailored to separate them from the other phospholipids. The species identification and acyl chain composition of the GPI<sub>n</sub>P<sub>n</sub> is achieved again by direct infusion and MS/MS, while the phosphate headgroup stereochemistry and quantification



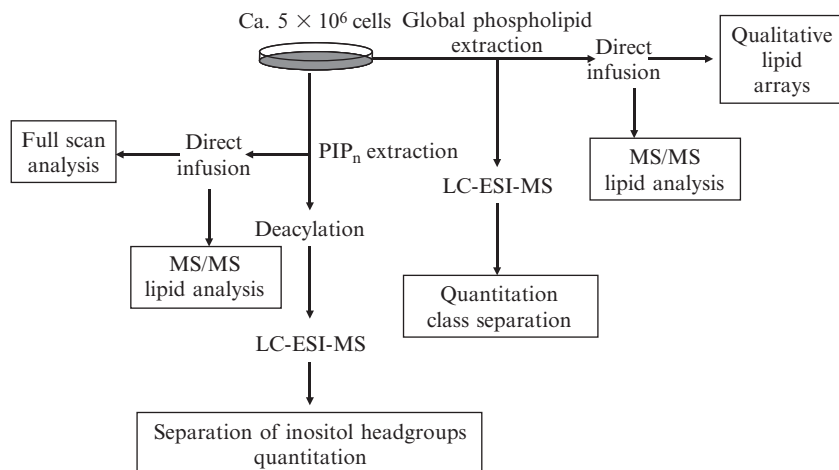


**Figure 2.3** General strategy for the extraction and analysis of glycerophospholipids from cell cultures or tissue. Glycerophospholipids or polyphosphoinositides are extracted according to respective procedures and subjected to direct infusion and tandem mass spectrometry analysis for species identification and qualitative lipid arrays construction for lipid changes evaluation between different conditions. Part or all of the same extract is analyzed by liquid chromatography–electrospray ionization–mass spectrometry glycerophospholipid analysis, which results in class separation and quantification. The quantitative analysis of polyphosphoinositides involves deacylation and liquid chromatography–electrospray ionization–mass spectrometry analysis of the glycerophosphoinositides for headgroup regioisomer identification.

can be evaluated by deacylation and LC–ESI–MS analysis of the resulting glycerophosphoinositides. Both LC–ESI–MS analyses utilize chemically defined standards and HPLC grade or higher solvents.

## 5. EXTRACTION AND MASS SPECTRAL ANALYSIS OF GLOBAL GLYCEROPHOSPHOLIPIDS

Phospholipid analysis begins with their isolation from cell culture or tissues. The use of organic solvents for extraction facilitates the removal of nonlipid components. By use of different organic solvents, the extractions can be modified and tailored for a specific class of lipids (e.g., phospholipids, sphingolipids, lysophospholipids, and polyphosphoinositides) (Christie, 2003). Special precautions should be taken to ensure the deactivation of enzymes and the completeness of lipid recovery. The nonlipid contaminants can be eliminated by washing the lipid-containing layer after phase separation. It is very important to minimize the risk of oxidation of the polyunsaturated fatty acids or lipid hydrolysis during the process of isolation.

Therefore, the extraction of lipids is always rapidly undertaken at low temperature (4°) as soon as possible after removal of the tissue from the living organism or from a cell culture, after the reactions have stopped.

Two structural features of phospholipids are the nonpolar hydrocarbon chains of the fatty acids and the polar phosphate-containing headgroups. The combination of polar and nonpolar groups within the molecule affects the solubility in organic solvent and, thus, their extraction. Hence, the use of a single organic solvent is not suitable for all species. The ability of phospholipids to swell in water and the likely interaction between lipids and proteins indicate that water is an important participant in the extraction process.

Historically, the most widely used extraction solvents were ethanol, as in diethyl ether (3:1) at 55 to 60° for several hours according to the method described by Bloor (1928). However, the solvent led to lipid peroxidation in animal samples and increased the enzymatic reactions on phospholipids during plant extraction. Considering the disadvantages of this solvent system, ethanol-diethyl ether mixtures have been substituted by more efficient solvents. The chemistry of the phospholipid molecules requires the presence of a more polar solvent, such as alcohol, and ultimately a nonpolar solvent, such as chloroform, for a complete extraction. The mixture of chloroform and methanol in various ratios is the most efficient extraction mixture for phospholipids. This approach was developed in the late 1950s by Folch *et al.* (1951) and uses chloroform:methanol in ratio 2:1 and large volumes of water for washing out the nonlipid components. Although the extraction procedure was very efficient, rapid, and conducted at room temperature (or lower), the formation of emulsions was a major drawback. Despite the modification Folch *et al.* made later by including salt in the media, this procedure has been replaced by the most widely adapted method for lipid extraction still in use today. The method of Bligh and Dyer (1959) was originally designed for the extraction of lipids from fish muscle. This method was advantageous for tissues containing a high percentage of water. The method is a variation of Folch's extraction, and calculates the amount of water present in the sample so that the final composition of chloroform:methanol:water is 1:2:0.8, creating a single extraction phase. The whole extraction is very rapid and most efficient. After addition of equal volumes of water and chloroform, the lipids are recovered in the chloroform-rich lower phase, which is separated and rinsed with water/methanol.

### 5.1. Phospholipid extraction from cultured cells

As an example of our lipidomics approach for phospholipid analysis by ESI-MS, we use RAW 264.7 cells. Phospholipids were extracted using a modified Bligh and Dyer procedure. The method is suitable for extraction from cell culture plates (100 mm) after aspirating the medium and washing

the adhered cells twice with 5 ml of ice-cold 1X phosphate-buffered saline (PBS). Approximately  $1 \times 10^7$  cells are then scraped using 800  $\mu\text{l}$  of cold 0.1 N HCl:CH<sub>3</sub>OH (1:1) and transferred into cold 1.5-ml microfuge tubes (# L292351, Laboratory Product Sales, Rochester, NY). Other tubes can be used, but should be checked with pure solvent prior to usage to ensure that impurities (plastic stabilizers, etc.) are not extracted from the plastic. After addition of 400  $\mu\text{l}$  of cold CHCl<sub>3</sub>, the extraction proceeds with vortexing (1 min) and centrifugation (5 min, 4°, 18,000 $\times g$ ). The lower organic phase is then isolated and solvent evaporated (Labconco Centrivap Concentrator, Kansas City, MO). The resulting lipid film is rapidly reconstituted in 80  $\mu\text{l}$  CH<sub>3</sub>OH:CHCl<sub>3</sub> (9:1). Prior to analysis, 1  $\mu\text{l}$  of NH<sub>4</sub>OH (18M) is added to each sample to ensure protonation of lipid species.

This method is also appropriate for extraction of phospholipids from previously isolated cell pellets while observing the restrictions for working fast and on ice at all times. After washing the adhered cells (from a 100-mm plate) twice with 5-ml, ice-cold 1X PBS, cells are scraped in 1 ml of 1X PBS, centrifuged (600 $\times g$ , 4°, 5 min), and, after aspirating off the PBS, quickly frozen in liquid nitrogen in the event of transportation or extraction. The extraction of cell pellets follows the same procedure as described above by vortexing the pellet with 800  $\mu\text{l}$  of cold 0.1 N HCl:CH<sub>3</sub>OH (1:1) and adding 400  $\mu\text{l}$  of CHCl<sub>3</sub> for phospholipid extraction.

## 5.2. Phospholipid extraction from tissue

Samples from tissue biopsies (20 to 50 mg) can also be extracted by this method. In this instance, the samples are quickly frozen by immersion in liquid nitrogen (stored at -80°, if not extracted immediately). The frozen samples are then placed in a tight-fit glass homogenizer (Kimble/Kontes Glass Co, Vineland, NJ), 800  $\mu\text{l}$  of cold 0.1 N HCl:CH<sub>3</sub>OH (1:1) is added, and the sample is homogenized for about 1 min while working on ice. The suspension is transferred to a cold microfuge tube, 400  $\mu\text{l}$  of ice-cold CHCl<sub>3</sub> is added, and the extraction proceeds as previously described. Care should be taken in using individual (or cleaned in between) homogenizers to prevent sample cross-contamination.

## 5.3. Direct infusion mass spectrometry of phospholipid extracts

The characterization of phospholipids from an unprocessed total lipid extract (i.e., extract whose compounds have not been derivatized) by ESI-MS is based on the ability of each lipid class to acquire positive or negative charges when in solution during ESI. Thus, under suitable conditions of sample preparation, all molecular species that exist among cellular lipid classes can be detected in a single run of a total lipid extract. A single

molecular ion with an  $m/z$  characteristic for the monoisotopic molecular weight is present for each molecular species. Collision-induced dissociation of the peaks of interest yields fragmentation patterns, which are used to unambiguously identify the lipid(s) present at a particular  $m/z$  value. A decade of dedicated research has been accomplished by a number of groups showing the potential of ESI-MS of lipids as a direct method to evaluate alterations in the cellular lipome (Ekroos *et al.*, 2002; Han and Gross, 1994, 2003; Kerwin *et al.*, 1994; Milne *et al.*, 2006; Murphy *et al.*, 2001; Ramanadham *et al.*, 1998; Schwudke *et al.*, 2006).

Typically, cellular lipid profiles under two experimental conditions (basal and stimulated, or wild type and mutant) can be monitored over a given time course, and the samples analyzed in both positive and negative ionization mode.

Three major lipid classes can be detected in positive ESI mode: GPCho, GPSer, and GPEtn (Ivanova *et al.*, 2001; Milne *et al.*, 2003). Fragmentation of the choline-containing GPCho results in a characteristic  $m/z$  184 phosphocholine headgroup peak and a  $[M+H-59]^+$  peak corresponding to the neutral loss of  $(CH_3)_3N$ . Relatively small peaks corresponding to the loss of one of the fatty acyl substituents as a ketene  $[M-R_2CH=C=O]^+$  (or so-called lyso GPCho) and lyso GPCho- $H_2O$  are also detected. In addition to the diacyl GPCho compounds, a large number of plasmanyl and plasmenyl phosphocholines can also be identified. All together, over 100 phosphatidylcholine lipids have been identified in RAW 264.7 cell extracts. GPSer fragmentation in positive mode produces ions resulting from the neutral loss of the polar headgroup phosphoserine ( $[M+H-185]$ ). Fragmentation of phosphatidylethanolamines and lyso phosphatidylethanolamines in positive mode normally yields one peak, a  $[M+H-141]^+$  ion from the neutral loss of the phosphoethanolamine headgroup. Again, plasmanyl and plasmenyl lipids were a large portion of the over 130 GPEtn species identified to date.

Six major lipid classes can be detected in negative ESI mode: GPIIns, GPSer, GPGro, GPA, GPEtn, and chloride adducts of GPCho (note that chloride is from decomposition of  $CHCl_3$ ). Additionally, the lyso variants for six of these phospholipids can also be detected in this mode. Negative mode fragmentation of these species yielded a wealth of structural information (Table 2.1). In each case, head group fragmentation, lyso-lipid formation, and fatty acid fragments aided in the lipid identification process (Hsu and Turk, 2000a,b). Phosphatidylinositol fragmentation can generate a wide variety of product ("daughter") ions (Hsu and Turk, 2000c). Four types of lyso-phosphatidic acid and lyso phosphatidylinositols and five characteristic head group fragments can routinely be used in identifying the observed GPIIns and lyso GPIIns species. In a similar fashion, GPSer and lyso GPSer compounds can be identified from their phosphatidic ( $[M-H-Y]^-$ ) and lyso phosphatidic ( $[M-H-Y-RCH=C=O]^-$ ) fragments (Han and Gross, 1995; Larsen *et al.*, 2001; Smith *et al.*, 1995). The product ion spectra of

**Table 2.1** Negative product (“daughter”) ions routinely observed from fragmentation of glycerophospholipids

	GPA	GPCho (Cl)	GPEtn	GPGro	GPIns	GPSer
[M-H] <sup>-</sup>	X		X	X	X	X
[M-H-RCO≡C≡O] <sup>-</sup>	X		X	X	X	
[M-H-RCOOH] <sup>-</sup>	X		X	X	X	
[M-H-RCOOH] <sup>-</sup>				X	X	X
[M-H-headgroup] <sup>-</sup>			X		X	X
[M-H-headgroup-RCH≡C≡O] <sup>-</sup>			X	X	X	X
[M-H-headgroup-RCOOH] <sup>-</sup>			X		X	
[M-H-RCHCO] <sup>-</sup>			X	X	X	
[M-H-RCHCO-2H <sub>2</sub> O] <sup>-</sup>				X	X	
[RCOO] <sup>-</sup>	X	X	X	X	X	X
Head-group-specific ion	135		140, 196	171	241, 223	
[GP-H <sub>2</sub> O-H] <sup>-</sup> (153)	X	X	X	X	X	X
[H <sub>2</sub> PO <sub>4</sub> ] <sup>-</sup>	X	X	X	X	X	X
[PO <sub>3</sub> ] <sup>-</sup>	X	X	X	X	X	X
[M+35] <sup>-</sup> [M+3] <sup>-</sup> (M+Cl)		X				
[M+CL-CH <sub>3</sub> ] <sup>-</sup> (M-50) (M-52)		X				

PGro also contain an ion formed by the loss of *sn*-2 substituent  $R_2COOH$  from its phosphatidic acid ion  $[M-74]$  (Hsu and Turk, 2001). Fully annotated MS/MS spectra for examples from all six major glycerophospholipid classes are available on the LIPID MAPS public website <http://www.lipidmaps.org/data/standards/standards.php?lipidclass=LMGP>.

Mass spectral analysis was performed on a Finnigan TSQ Quantum triple quadrupole mass spectrometer (ThermoFinnigan, San Jose, CA) equipped with a Harvard Apparatus syringe pump (Harvard Apparatus, Holliston, MA) and an electrospray source. Samples were analyzed at an infusion rate of 10  $\mu\text{l}/\text{min}$  in both positive and negative ionization modes over the range of  $m/z$  400 to 1200. Instrument parameters were optimized with 1, 2-dioctanoyl-*sn*-Glycero-3-phosphoethanolamine (16:0 GPEtn) prior to analysis. Examples of full-scan spectra in negative and positive instrument modes are shown in Fig. 2.4. Data were collected with the Xcalibur software package (ThermoFinnigan) and analyzed by a software program developed in our research group (see “Computational Analysis of Mass Spectral Data” section for a detailed description of data analysis).

#### 5.4. LC-MS analysis (quantitation) of phospholipid extracts

Quantification of glycerophospholipids is achieved by the use of a LC-MS technique employing synthetic (non-naturally occurring) diacyl (Table 2.2) and lysophospholipid standards (Table 2.3). Typically, 200 ng of each odd-carbon standard is added per  $10^7$  cells. The extraction of lipids from cell culture or tissue biopsies is the same as described previously for the direct infusion MS analysis (see “Extraction of Glycerophospholipids” section). After solvent evaporation, the resulting lipid film is dissolved in 100  $\mu\text{l}$  of Isopropanol (IPA):Hexane:100 mM  $\text{NH}_4\text{CO}_2\text{H}_{(\text{aq})}$  58:40:2 (mobile phase A). For our examples, we utilized an Applied Biosystems/MDS SCIEX 4000 Q TRAP hybrid triple quadrupole/linear ion trap mass spectrometer (Applied Biosystems, Foster City, CA). Coupled to this instrument were a Shimadzu (Shimadzu Scientific Instruments, Inc., Columbia, MD) HPLC system consisting of a SCL 10 AVP controller, two LC 10 ADVP pumps and a CTC HTC PAL autosampler (Leap Technologies, Carrboro, NC). All samples were separated on a Phenomenex (Phenomenex, Torrance, CA) Luna Silica column ( $2 \times 250$  mm, 5- $\mu$  particle size) using a 20- $\mu\text{l}$  sample injection. Lipids were separated using a binary gradient program consisting of IPA:Hexane:100 mM  $\text{NH}_4\text{CO}_2\text{H}_{(\text{aq})}$  58:40:2 (mobile phase A) and IPA:Hexane:100 mM  $\text{NH}_4\text{CO}_2\text{H}_{(\text{aq})}$  50:40:10 (mobile phase B). The following LC gradient was used: 0 to 5 min, B = 50%; 5 to 30 min, B = 50 to 100%; 30 to 40 min, B = 100%; 40 to 41 min, B = 100 to 50%; and 41 to 50 min, B = 50%. The mobile phase was delivered at a flow rate of 0.3 ml/min. The MS spectra were acquired in negative instrument mode using a turbo spray source operated at 450° with an ion voltage of -3500 V, and nitrogen as

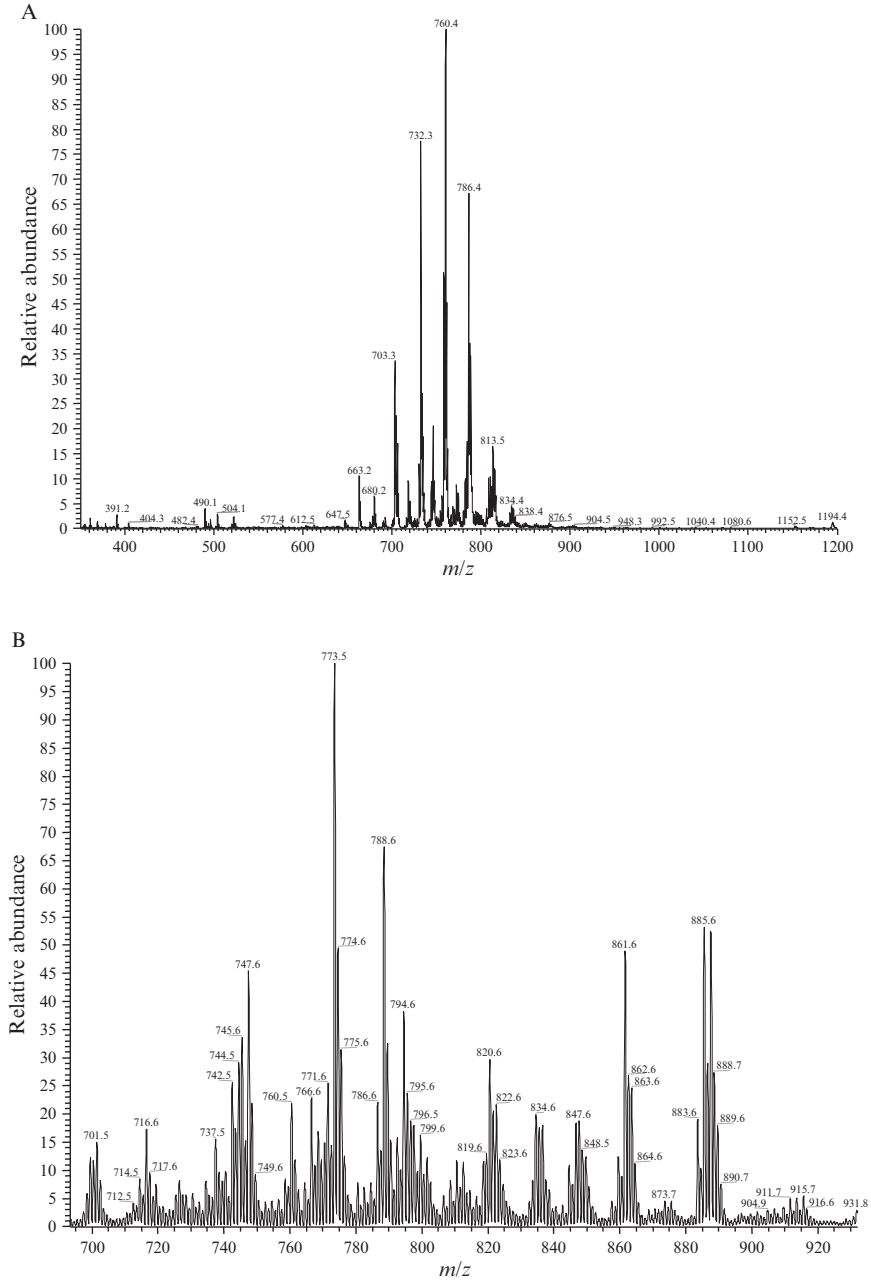


**Figure 2.4** Examples of glycerophospholipid direct infusion spectra. (A) Positive instrument mode spectra showing GPCho, GPEtn, and GPSer lipids. (B) Negative instrument mode showing GPA, GPCho (Cl adducts), GPEtn, GPGro, GPIns, and GPSer lipid species.

**Table 2.2** Odd-carbon standards for liquid chromatography-mass spectrometry analysis of phospholipids: Twenty-four odd-carbon diacyl standards

	12:0/ 13:0	17:0/14:1 (9Z)	17:0/20:4 (5Z,8Z,11Z,14Z)	21:0/22:6 (4Z,7Z,10Z,13Z,16Z,19Z)
GPA	25:0	31:1	37:4	43:6
GPCho	25:0	31:1	37:4	43:6
GPEtn	25:0	31:1	37:4	43:6
GPGro	25:0	31:1	37:4	43:6
GPIns	25:0	31:1	37:4	43:6
GPSer	25:0	31:1	37:4	43:6

**Table 2.3** Odd-carbon standards for liquid chromatography-mass spectrometry analysis of phospholipids: Four lysolipid standards

13:0/0:0	17:1 (9Z)/0:0
13:0 LysoGPA	17:1 LysoGPA
13:0 LysoGPCho	17:1 LysoGPCho

curtain and nebulizer gas. The curtain gas (CUR) was 30 l/hr, and ion source gas 1 and 2 were both 50 l/hr. The declustering potential (DP) was  $-110$  V, and the collision energy (CE) was  $-5$  V. Scan type: EMS, unit resolution for Q1; scan rate: 1000 amu/s; scan range from  $m/z$  350 to 1200, with the ion trap set for dynamic fill time. As an example of this technique, extracted ion chromatograms (XICs) of the four GPGro odd-carbon standards in a RAW 264.7 cell background are shown in Fig. 2.5. The creation of standard curves and quantitation of data will be described in the “LC-MS Data Analysis” section at the end of this chapter.

## 6. POLYPHOSPHOINOSITIDE EXTRACTION AND MASS SPECTRAL ANALYSIS

Polyphosphoinositides are low-abundance phospholipids in eukaryotic cell membranes that are involved in regulation of distinct cellular processes. In order to minimize the interference of other phospholipids during analysis, a selective two-step extraction is employed. First, the cell material is extracted with neutral solvents and the resulting pellet is extracted with acidified solvents for quantitative recovery of polyphosphoinositides. The majority of noninositol phospholipids are extracted with neutral solvents, and no GPIns<sub>2</sub> or GPIns<sub>3</sub> species are detected in this extract. The acyl composition of



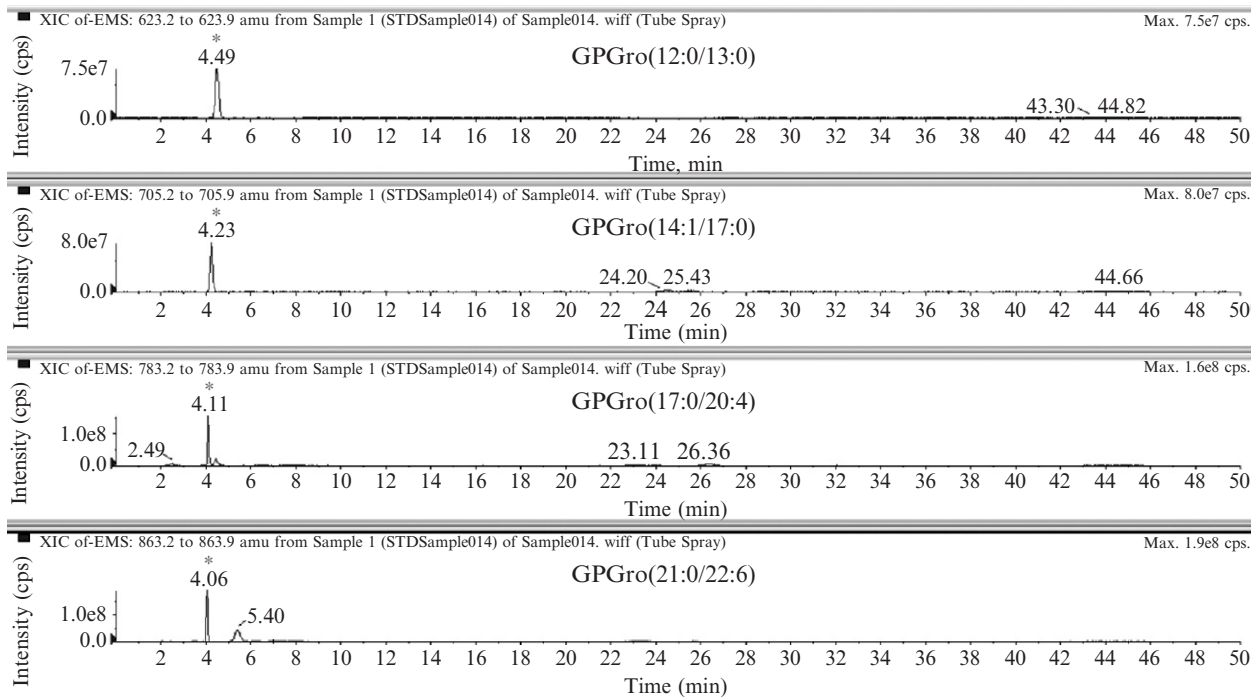


**Figure 2.5** Extracted ion chromatograms of the four GPGro odd-carbon internal standards.

polyphosphoinositides is determined by direct infusion and fragmentation MS. The quantification and analysis of headgroup regioisomers is accomplished by LC-MS analysis after deacylation.

### 6.1. Extraction of polyphosphoinositides from cultured cells

Cells for polyphosphoinositide analysis must be between 60 to 70% confluency at the time of harvesting, unless the experiment specifically requires otherwise. Systematic effects of confluence have been previously observed in our laboratory. Cells from 100 to 150 mm culture plates are washed with 2 ml of ice-cold 1X PBS after aspirating the culture medium. Then, 1.5 ml of 1X PBS is added, and cells are scraped and transferred into a cold 1.5-ml microfuge tube. Cell pellets are collected after centrifugation at  $4000\times g$  for 5 min at  $4^\circ$ . The procedures are performed on ice, and all solutions and sample tubes are kept on ice at all times. Each pellet is given  $400\ \mu\text{l}$  of ice-cold 1:1  $\text{CHCl}_3$ : $\text{CH}_3\text{OH}$  and vortexed for 1 min, or until thoroughly mixed. Samples are centrifuged at  $7500\times g$  for 5 min at  $4^\circ$ , supernatant decanted, and discarded. To the remainder of the cell pellet,  $200\ \mu\text{l}$  of 2:1  $\text{CHCl}_3$ : $\text{CH}_3\text{OH}$  containing 0.25% 12 N HCl are added. Samples are vortexed for 5 min and then pulse spun. The supernatant is then given  $40\ \mu\text{l}$  of 1 N HCl and vortexed for 15 s. The resulting two phases are separated by centrifugation (pulse at  $18,000\times g$ ). The solvent from the collected lower layer is evaporated in a vacuum centrifuge (Labconco CentriVap Concentrator, Kansas City, MO). The resulting lipid film is rapidly redissolved in  $55\ \mu\text{l}$  of 1:1:0.3  $\text{CHCl}_3$ : $\text{CH}_3\text{OH}$ : $\text{H}_2\text{O}$ . Before analysis,  $5\ \mu\text{l}$  of 300 mM piperidine (Lytle *et al.*, 2000) is added as an ionization enhancer, and the sample is vortexed and pulse spun.

### 6.2. Extraction of polyphosphoinositides from tissue

Biopsy samples (20 to 50 mg) are quickly frozen by immersion in liquid nitrogen. Samples can be stored at  $-80^\circ$ , if not immediately extracted. The frozen samples are homogenized using  $500\ \mu\text{l}$  of  $\text{CH}_3\text{OH}$  in a Dounce tissue grinder (Kimble/Kontes Co., Vineland, NJ) for about 1 min working on ice. The suspension is then transferred to a cold 1.5-ml microfuge tube, and  $500\ \mu\text{l}$  of cold  $\text{CHCl}_3$  are added. After vortexing for 1 min at  $4^\circ$ , samples are centrifuged at  $7500\times g$  for 5 min at  $4^\circ$ . Supernatant is decanted and discarded. The retained pellet is then given  $200\ \mu\text{l}$  of 2:1  $\text{CHCl}_3$ : $\text{CH}_3\text{OH}$  containing 0.25% 12 N HCl. Samples are vortexed for 5 min and then pulse spun. Supernatant is transferred to a new cold microfuge tube and, after addition of  $40\ \mu\text{l}$  of 1 N HCl, the samples are vortexed for 15 s. The resulting two phases are separated by centrifugation (pulse at  $18,000\times g$ ). The solvent from the collected lower layer is evaporated in a vacuum centrifuge. The resulting lipid film is rapidly redissolved in  $55\ \mu\text{l}$  of 1:1:0.3  $\text{CHCl}_3$ : $\text{CH}_3\text{OH}$ : $\text{H}_2\text{O}$ . Before analysis,  $5\ \mu\text{l}$  of

300-mM piperidine (Lytle *et al.*, 2000) is added as an ionization aid, and the sample is vortexed and pulse spun.

### 6.3. Direct-infusion mass spectral analysis of phosphoinositides

Mass spectral analysis was performed on an Applied Biosystems/MDS SCIEX 4000 Q TRAP hybrid, triple-quadrupole, linear ion trap MS (Applied Biosystems, Foster City, CA). The instrument was equipped with a Harvard Apparatus syringe pump and an ESI source. Samples were analyzed at an infusion rate of 10  $\mu\text{l}/\text{min}$  in negative ionization mode over the range of  $m/z$  400 to 1200. GPIIns $P$  and GPIIns $P_2$  were analyzed by full scan analysis and normalized to 16:0 GPIIns $P_2$  internal standard (Avanti Polar Lipids, Alabaster, AL). Utilizing this method, approximately 30 GPIIns $P$  and GPIIns $P_2$  species can be detected. A typical RAW 264.7 full-scan spectra highlighting the GPIIns $P$  and GPIIns $P_2$  spectral region is shown in Fig. 2.6. Due to their very low abundance and detection only after stimulation, GPIIns $P_3$  species cannot be identified by full or precursor ion scan ( $m/z$  481). Instead, identification of the individual phosphatidylinositol phosphates present in the total lipid extracts was accomplished by ESI-MS/MS with a collision energy of 50 eV (Milne *et al.*, 2005). Peaks corresponding to known GPIIns $P_3$  compounds were fragmented and manually inspected for the presence of the identification peaks (examples of GPIIns $P$ , GPIIns $P_2$ , and

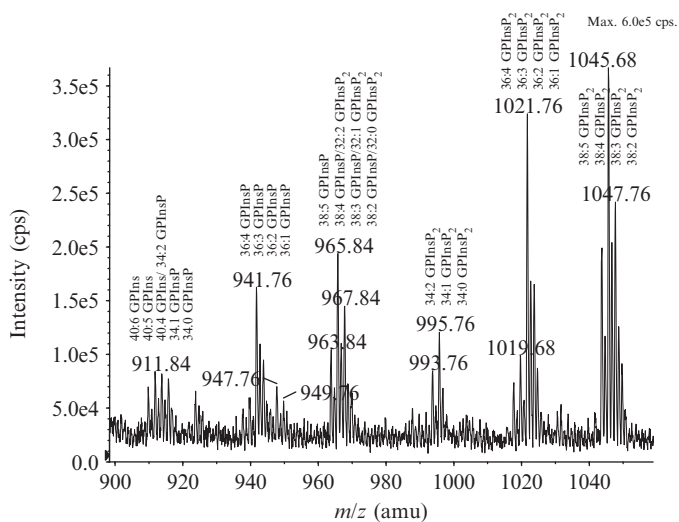


**Figure 2.6** GPIIns $P$  and GPIIns $P_2$  spectral region of a RAW 264.7 cell extract. Approximately 30 chemically distinct GPIIns $P$  and GPIIns $P_2$  species can be identified by tandem mass spectrometry fragmentation in a typical spectrum.

GPIIns $P_3$  fragmentation patterns can be found on the LIPID MAPS public website: <http://www.lipidmaps.org/data/standards/standards.php?lipidclass=LMGP>). A confirmed identification was achieved when key fragmentation peaks were larger than three times the signal-to-noise ratio (S/N). The limit of detection using this method was found to be less than 9 pmol/ml for 38:4 GPIIns $P_3$  (Avanti Polar Lipids, Alabaster, AL). Data were collected with the Analyst software package (Applied Biosystems).

#### 6.4. Deacylation of GPIIns $P_n$ lipids

The quantitative analysis of headgroup isomeric GPIIns $P_2$  and GPIIns $P_3$  is achieved by LC-MS analysis of the deacylated polyphosphoinositides and the use of cytidine-5'-monophosphate (CMP; Sigma-Aldrich, St. Louis, MO) as an internal standard. The lower layer of the last step of the extraction protocol that yields separation of phosphoinositides from the rest of the phospholipids is subjected to deacylation as described by others (Clarke and Dawson, 1981; Cunningham *et al.*, 1990). The organic phase (lower layer) is transferred into a glass screw-cap vial and solvent-evaporated under nitrogen. Afterward, 500  $\mu\text{l}$  of freshly prepared methylamine reagent (1-butanol, methanol, 40% aq. methylamine, 1:4:4, v/v) was added to the glass vial and heated at 53° in a heating block (water bath) for 1 hr. After cooling to room temperature, the content is transferred into a microfuge tube and solvent-evaporated in a vacuum centrifuge (Labconco CentriVap Concentrator, Kansas City, MO). The resulting film is resuspended in 500  $\mu\text{l}$  of distilled H $_2$ O, vortexed briefly, and centrifugated for 2 min at 18,000 $\times g$ . Supernatant is transferred to a new microfuge tube. GroGPIIns $P_n$  are extracted with 500  $\mu\text{l}$  of 1-butanol/petroleum ether/ethyl formate (20:4:1, v/v) to remove the undeacylated lipids and free fatty acids. After mixing (by vortex) for 30 s and centrifugation (18,000 $\times g$ , 2 min), the lower (aqueous) layer is collected. The extraction is repeated, and the upper phase is discarded. Combined aqueous phases are dried in a vacuum centrifuge (or lyophilized). The samples are resuspended in 36  $\mu\text{l}$  of methanol:water (1:1), mixed with 40  $\mu\text{l}$  of 100- $\mu\text{M}$  CMP and 4  $\mu\text{l}$  of 300-mM piperidine, and analyzed by LC-MS.

The phosphoinositides standards were deacylated likewise with methylamine and dissolved in methanol:water (1:1) containing 10% 300-mM piperidine to produce the stock solution with concentration of 200  $\mu\text{M}$ . The stock solution was further serially diluted to obtain working solution over the range 20 to 200  $\mu\text{M}$ .

#### 6.5. LC-MS analysis of deacylated GPIIns $P_n$ compounds

Phosphoinositides are precursors in intracellular signaling cascades as well as ligands for membrane-associated proteins that are involved in trafficking and cytoskeletal dynamics (Downes *et al.*, 2005; Michell *et al.*, 2006). Since the

mid-1980s, the understanding of inositol-containing glycerophospholipids has elevated from quantitatively minor membrane constituents to very important players in cellular functioning and responses. Seven phosphoinositides have been identified, and glycerophosphoinositol and its phosphorylated derivatives were demonstrated to be important in modulating cell proliferation and G-protein-dependent activities (Berrie *et al.*, 1999; Corda *et al.*, 2002). The detection, identification, and quantification of phosphatidylinositol phosphates (GPIIns $P$ ) and phosphatidylinositol bisphosphates (GPIIns $P_2$ ) with different fatty acid composition can be achieved by ESI-MS/MS (Milne *et al.*, 2005; Wenk *et al.*, 2003). However, the determination of the isomeric head-groups remains a challenge. For many years, glycerophosphoinositols have been traditionally analyzed by anion-exchange HPLC using gradients of aqueous mobile phases with high concentrations of buffer solutions and employing radiolabeling techniques as detection and quantitation systems (Alter and Wolf, 1995; Lips *et al.*, 1989; Morris *et al.*, 2000).

This technique has the main disadvantage of being a multi-step procedure that only measures the true levels of these compounds if the radiolabeling is taken to isotopic equilibrium, which is often difficult to achieve. Since no radioactive glycerophosphoinositide standards are commercially available, they are usually synthesized by radiolabeling of cell extracts and deacylation (Hama *et al.*, 2000). This process introduces impurities as well as some practical considerations, since the radiolabeling is not always feasible as in analysis of glycerophosphoinositides from tissues and organs.

Some nonradioactive methods have been used to analyze phosphatidylinositides. GPIIns $4P$  and GPIIns $4,5P_2$  were well resolved from each other and from other phospholipids using normal-phase HPLC and evaporative light-scattering detection (Gunnarsson *et al.*, 1997). The three regioisomers of GPIIns $P_2$  were separated by anion-exchange HPLC with NaOH gradients after deacylation, followed by suppressed conductivity detection (Nasuhoglu *et al.*, 2002). Recently, a new method for analysis of intact phosphoinositides by LC-MS using a microbore silica column was reported (Pettitt *et al.*, 2006).

The  $\beta$ -cyclodextrin-bonded column has been successfully employed for the analysis of phosphorylated carbohydrates, allowing the separation of both enantiomeric and positional isomers (Feurle *et al.*, 1998). It has also been used for analysis of glycerophosphoinositol (Dragani *et al.*, 2004). This stationary phase can be operated under water/organic conditions with the use of volatile modifiers at low concentrations, which is suitable for ESI-MS.

Here we describe an LC-MS method for separation, identification and quantification of the four GroPIIns $P_2$  and GroPIIns $P_3$  lipid species from cell extracts by using  $\beta$ -cyclodextrin-bonded column with on-line negative ESI-MS detection and internal standard calibration.

The HPLC system consisted of two Shimadzu (Shimadzu Scientific Instruments, Inc., Columbia, MD) LC-10 ADVP binary pumps and an SCL-10AVP system controller. A 20- $\mu$ l sample was injected via a CTC

HTC PAL autosampler (Leap Technologies, Carrboro, NC). The separation was performed on a Nucleodex  $\beta$ -OH column, 5  $\mu\text{m}$  (200  $\times$  4.0 mm i.d.) from Macherey-Nagel (Düren, Germany). The mobile phase included 50-mM ammonium formate aqueous solution (solvent A) and acetonitrile (solvent B). The following gradient was used: 0 to 1 min, B = 80%; 1 to 15 min, B = 80 to 70%; 15 to 30 min, B = 70 to 66%; 30 to 70 min, B = 66 to 61%; 70 to 75 min, B = 61 to 60%; 75 to 76 min, B = 60 to 80%; and 76 to 90, B = 80%. The mobile phase was delivered at a flow rate of 0.3 ml/min.

The MS spectrum was acquired in negative mode on a 4000 Q-Trap LC-MS/MS system, fitted with turbo spray ion source from Applied Biosystems (Foster City, CA). The turbo spray source was operated at 200° with an ion voltage of  $-4500$  V, and nitrogen as CUR and nebulizer gas. The CUR was 10 l/hr. The flow rate of ion source gas 1 and gas 2 was 20 and 40 l/hr, respectively. The declustering potential (DP) was  $-110$  V, and the collision energy (CE) was  $-5$  V. Settings include channel electron multiplier (CEM): 2200 V; scan type: enhanced MS (EMS), unit resolution for Q1; scan rate: 1000 amu/s; scan range from  $m/z$  300 to 590; duration: 90 min; step size: 0.08 amu; Q3 entry barrier: 8 V; and pause between mass ranges: 5.007 ms. A representative extracted ion current (XIC) is shown on Fig. 2.7 depicting the separation of the three GroPIns $P_2$  and GroPIns $P_3$  isomers.

Calibration curves were constructed by mixing deacylated GPIIns $P_n$  standards working solutions with equal volume of 100- $\mu\text{M}$  CMP. They were then analyzed by LC-MS. Calibration curves for deacylated GPIIns $4,5P_2$  and GPIIns $3,5P_2$  are shown on Fig. 2.8A and B. They are created by using the relationship between “peak area of GroPIns $P_n$ /peak area of CMP” and “amount of GroPIns $P_n$ /amount of CMP.” As an example, the method was applied to the analysis of RAW 264.7 cell extracts after stimulation with platelet activating factor (PAF) for 15 min. The extracts were deacylated and analyzed by LC-MS using CMP as an internal standard. The XIC traces from this analysis are shown on Fig. 2.9A and B.

## 7. COMPUTATIONAL ANALYSIS OF MASS SPECTRAL DATA

Complex mixtures of phospholipids from biological extracts generate mass spectra with hundreds to thousands of peaks associated with the molecular ions present in the sample, which includes any molecules that acquire a charge in the desired instrument mode over the applicable  $m/z$  range. In lipid extracts, these ions include phospholipids, solvent contaminants, fragments of larger macromolecules, and multiply charged ions, among other components. In addition, in the absence of chromatographic separation, any

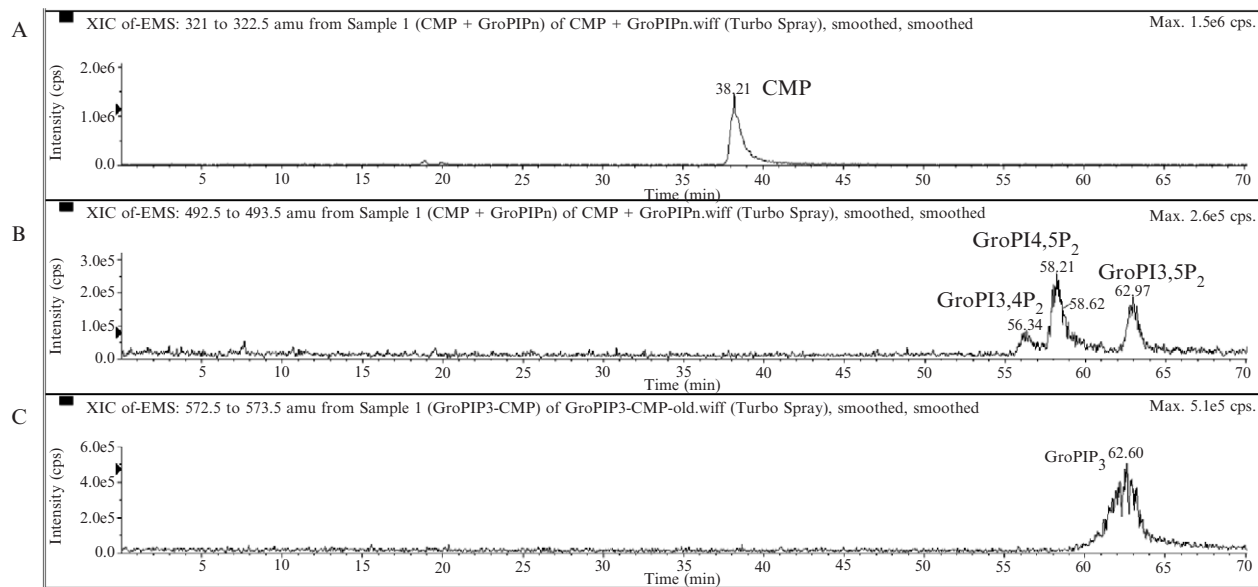


**Figure 2.7** Liquid chromatography-mass spectrometry spectra of GroPIns $P_2$  and GroPIns $P_3$  standards with internal standard cytidine-5'-monophosphate (CMP). (A) Extracted ion chromatograms (XICs) of cytidine-5'-monophosphate ( $m/z$  322); (B) Extracted ion chromatograms of GroPIns $P_2$  ( $m/z$  493). (C) Extracted ion chromatograms of GroPIns $P_3$  ( $m/z$  573).

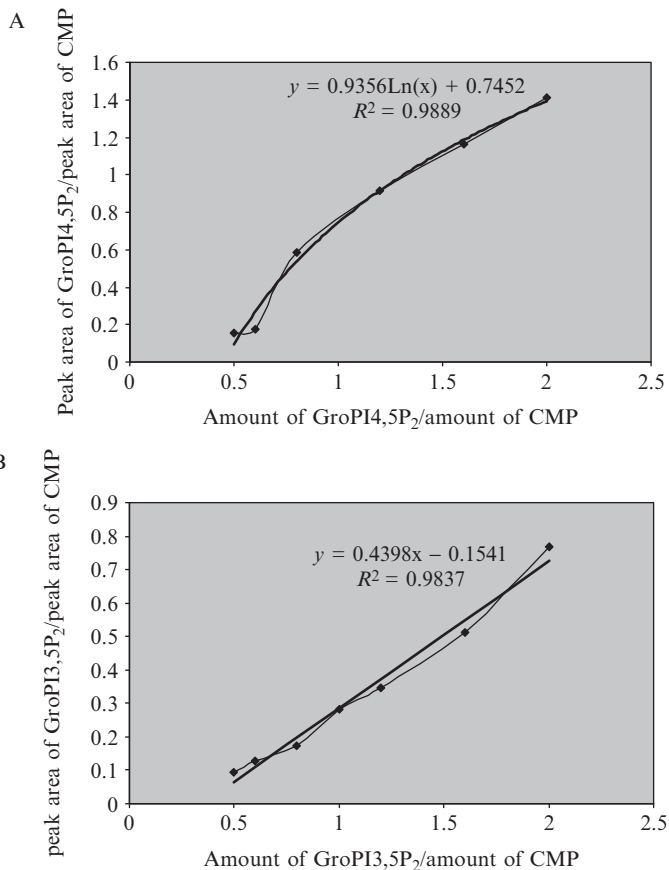


**Figure 2.8** Calibration curves for (A) GroPIIns4,5P<sub>2</sub> and (B) GroPIIns3,5P<sub>2</sub>.

particular  $m/z$  peak may contain ions from several different isobaric phospholipids or isotopic ions from molecular ions at  $m/z - 1$ ,  $m/z - 2$ , which may be appropriately corrected for isotopic distribution if the molecular composition is known.

## 7.1. Direct infusion (intra-source separation)

For direct infusion of samples in the MS, an initial qualitative screen to identify particular  $m/z$  values whose peak ions are consistently different between two conditions is readily developed. For direct infusion, we have created code to find all the peaks in each MS scan and to statistically compare these peaks across conditions (Forrester *et al.*, 2004). For direct infusion phospholipid spectra, alignment of the same peaks across different samples is



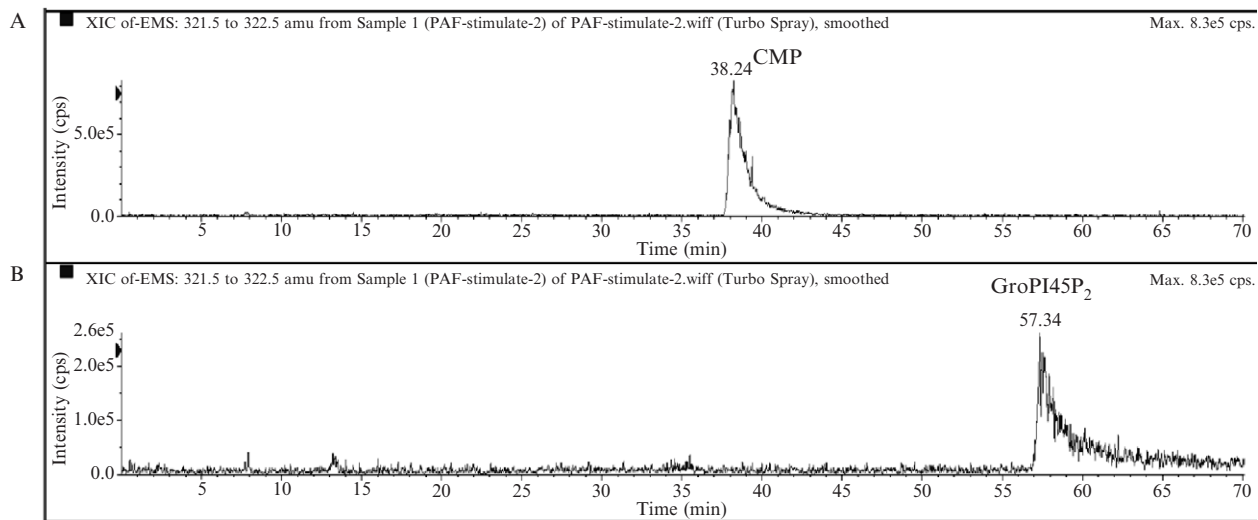


**Figure 2.9** Extracted ion chromatograms (XIC) of GroPIns $P_n$  from platelet activating factor (PAF)-stimulated RAW 264.7 cell extracts. (A) Extracted ion chromatograms of cytidine-5'-monophosphate (CMP) ( $m/z$  322). (B) Extracted ion chromatograms of GroPIns $P_2$  ( $m/z$  493).

relatively simple because there is usually only one peak per unit  $m/z$ , so that peak intensities from the same nominal  $m/z$  are directly comparable across samples. The comparison of peak ion intensities (or areas) may be done in several ways, with a desired normalization and using standard statistical tests. The visualization of these changes is relevant for interpretation and useful for suggesting specific  $m/z$  peak values which were different under the condition(s) being compared. Addition of internal standards to uniform background cell extracts can be used to validate this method, and titrations may be used to confirm the monotonic behavior of the peak ion intensity on molecular concentration (i.e., increasing concentration of a molecule generates an increase in peak intensity at the relevant  $m/z$ ). Due to nonlinearities (e.g., ion competition), however, the potential for false changes must be recognized as a true increase, or decrease in a molecule may consistently affect the ionization of other molecules during the infusion process. Note that this is true whether or not one normalizes to single or multiple internal standards. A general rule is that direct infusion spectra should only be compared (peak by peak) if the total spectra are sufficiently similar. Similarity can be defined both by the pattern the spectra create and by the total ion count (or mean ion count). A correlation coefficient can be used to quantitatively assess global similarity of spectra and a filter applied to limit the comparison of spectra to those with a sufficient number of peaks above the noise. If this is the case, one may then be reasonably confident that those isolated specific peaks, which differ in a statistically significant manner due to the condition, reflect true changes in molecular abundance of contributing ions at that  $m/z$ . Since a set of “control” spectra are generally used for any comparison, only those changes associated with the condition should repeatedly and reliably be indicated by statistical testing. This implies that the protocol for the control and condition should be identical (same “random” error sources from biological variability, experimenter, instrumentation, extraction methods, etc.) except for the effect of the condition. Any effects that are systematically different between the controls and condition will likely be reflected in the spectra. Randomizing the infusion of samples (between condition and controls) and any other protocol steps are suggested to minimize systematic influences except for the condition being tested. Since the comparison is the same for every  $m/z$ , the qualitative screen can be used to assess changes in peak ions at every  $m/z$ .

A single typical direct infusion spectra is binned in 0.07  $m/z$  units and spans a range of  $m/z$  350 to 1200 (12,142 bins). Each sample is scanned once per second for approximately 60 s (user-defined) so that a single spectrum actually consists of 60 scans. The vendor-supplied software typically time-averages these scans for graphical display. The ASCII data for each MS file can be obtained from the vendor files (.Raw files) by using XConvert.exe located in the \bin folder of Xcalibur. This program allows batch processing of a large number of .Raw files. The format of these ASCII files

(~60 MB) is cumbersome and contains mostly redundant text so that it is useful to write a parsing program to store the relevant time- $m/z$ -ion intensity information in separate files. We wrote a program in Fortran (G77) to batch process large numbers of these ASCII files. We have implemented a filter on the 60 scans (for each bin), which eliminates aberrant scans (infusion problems) by rank-ordering the ion counts and removing a user-defined percentile (e.g., the upper and lower tenth percentile) prior to time-averaging. This tends to have little effect on maxima, but creates well-defined minima in the spectra. Following time-averaging, a peak finding (or maxima) algorithm may then be applied to each file. It is also possible to forgo this step and directly compare all  $m/z$  binned intensity values (12,142) from each spectrum. For the phospholipid spectra, we currently determine the maximum for each nominal  $m/z$  by finding the maximum between adjacent minima. For example, for nominal  $m/z$  885, the code searches for a minimum intensity between 884.5 and 885.0 and another minimum between 885.5 and 886.0. An exclusion limit on the minima spacing (e.g., 0.3  $m/z$  units) can prevent erroneous assignments. The maximum intensity and  $m/z$  value between these two minima are then stored (e.g., peak  $m/z$  885.5, peak intensity  $6.37 \times 10^7$ ). For more complex spectra, one can smooth the time-averaged spectra and use a low-high-low pattern to determine peaks. We currently find the maxima for every nominal  $m/z$  (850 maxima for  $m/z$  350–1199) and use a characteristic noise level from the spectra to filter appropriately by S/N level when necessary. However, it is generally useful to compare all  $m/z$  values since, in some comparisons, the maximum intensity for a particular  $m/z$  could be at the noise level, but the condition may generate a sizable peak (or vice versa). In this formulation, each unique mass spectra corresponds to a vector of intensity values (e.g., 850) associated with each unit  $m/z$  value. The subsequent normalization and statistical comparison of these intensities across spectra are then relatively transparent; we wrote algorithms in a statistical package (SPlus) to batch-import these  $m/z$ -peak data files, to perform the relevant statistical tests, and to output the results comparing the appropriate conditions. In practice, this method provides a reliable way to qualitatively screen for potential phospholipid changes due to some perturbation or condition, and we created “arrays” to highlight the  $m/z$  values that appear to show statistically significant increasing or decreasing peak intensities due to the condition. Unlike gene expression arrays, the magnitude of peak intensity changes due to signaling events. For example, in mass spectra for phospholipids are not generally dramatic (a two “fold” peak change is quite large), since many structural lipids are already present in the control populations, and the cell likely does not tolerate very large changes in most species molecular abundance. To confirm direct infusion results, to minimize ion competition, to separate molecular classes of lipids,

and to quantify the phospholipid molecular species in extracts, LC-MS is employed.

## 7.2. LC-MS data analysis

The batch processing of full-scan LC-MS data requires significantly more computational processing than the direct infusion data, primarily due to the (typically) 60 min runs per sample, with approximately one scan per second. The MS data are contained in the vendor (Analyst, Applied Biosystems) .wiff files and must be converted into ASCII prior to further processing. We use a converter *mzStar.exe* from the Institute for Systems Biology (ISB), which converts the .wiff files into *mzXML* format (Pedrioli *et al.*, 2004). We convert the *mzXML* files to .mgf (Mascot Generic Format, ASCII files) and header files (ASCII) using *mzXML2other.exe* (ISB), which requires compilation on a cygwin, X-Windows terminal emulating a Unix shell. Each step is batchable (processes multiple files without user input), and the .mgf sample files are approximately 100 MB ASCII each. The .mgf files contain sequentially ordered scans (the retention time of each scan is located in the header file) and the  $m/z$  bins and their associated ion intensity values. We wrote code in Fortran (G77) to batch process these .mgf files creating two forms of output: (1) smoothed (time-averaged in  $\sim 10$ -s increments) XICs of retention time/intensity values for every nominal  $m/z$  value, and (2) integrated, aligned (by  $m/z$  and retention time) peaks across the samples. The former (1) is used to graphically check selected XICs across multiple samples for correct peak identification, integration windows selection, and peak alignment. The method of analysis is certainly not unique; however, we have also experimented with using three-dimensional (3D;  $m/z$ -retention time-intensity space) kernel smoothing and peak finding, but found that computational time and appropriate alignment checking across many samples ( $\sim 30$ ) was far more difficult to implement. By generating XICs for each  $m/z$ , the problem of 3D peak finding and integration is reduced to the more tractable two-dimensional (2D) problem in retention time-intensity space. Specifically, to create an XIC, a selected  $m/z$  window must be chosen (e.g.,  $m/z$  809.5 to 810.5) and the ion counts summed (or averaged) in this window to represent the ion counts for that particular retention time ( $\sim 10$  s time window). Recall that the short time-averaging (user-selectable in the code) is essentially a smoother and natural compression of the data. This time-averaging interval should be less than the retention time “width” of any peaks. Otherwise, temporal resolution is lost. Therefore, for any particular nominal  $m/z$ , the XICs from  $n$  samples are readily compared graphically across samples (intensity as a function of retention time). We currently have a user-selectable range in  $m/z$  for creating the XIC and usually select ranges ( $m/z -0.5$ ,  $m/z +0.5$ ) looping

over the range of  $m/z$  values (e.g., 350.5 to 1199.5) whose range is dynamically obtained from the spectra files. Since the 3D peak maxima about a nominal  $m/z$  (e.g.,  $m/z$  419.9 at 23.3 min) may not be symmetric about the XIC window selected, the XICs will indicate ion contributions in nominal  $m/z$  419.5 and nominal  $m/z$  420.5 with peaks  $\sim$ 23.3 minutes in both cases. This can be ameliorated by smoothing, finding the 3D peak max, and dynamically defining the  $m/z$  intervals (e.g., by slicing into 2D segments and cutting off the integration in  $m/z$  when the maxima falls below some predefined threshold relative to the global 3D maximum); alternatively, the internal standards for the lipid class should have a similar 3D peak  $m/z$  location, will be similarly subject to the same asymmetry in the chosen XIC selection range, and should therefore be valid for quantitatively normalizing by area. In Fig. 2.10 we indicate pseudo-code for the LC-MS analysis program. Briefly, the code first loops over all the MS files of interest ( $\sim$ 3 GB for 30 files), reading in the header files, which contain the

Pseudo-code for LC-MS processing:

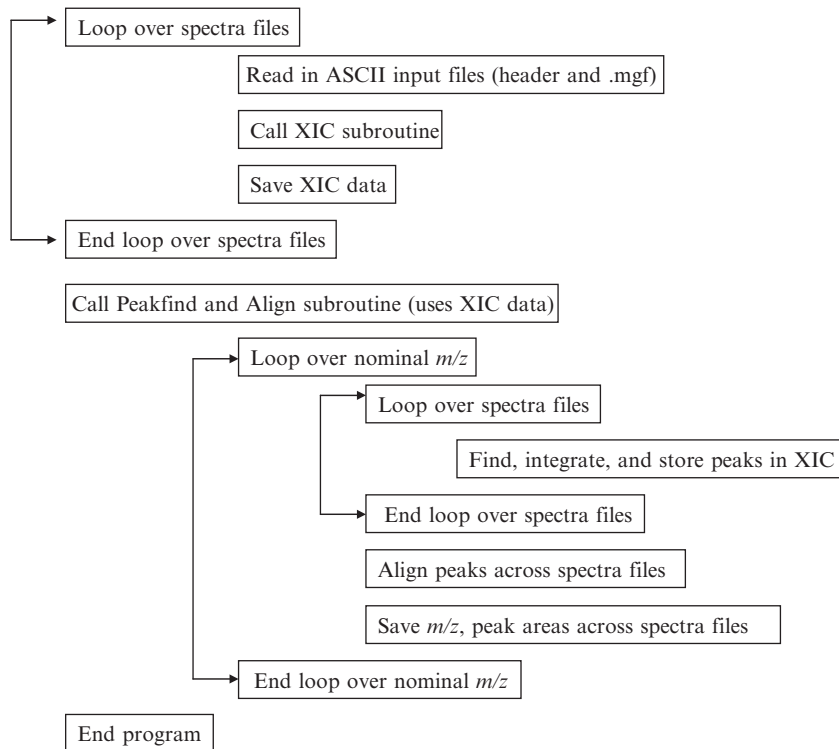


**Figure 2.10** Outline of liquid chromatography–mass spectrometry code for batch processing full-scan *wiff* spectra.

number of scans and retention times of each, and the data fields, which contain the scan number, followed by a list of  $m/z$  and corresponding ion intensity data. For each file, a subroutine is called, which loops over all the  $m/z$  values and stores an equivalent XIC for each  $m/z$ , as previously described. Given a list of XICs for each spectra file for every  $m/z$ , a peak finding and alignment subroutine are called, which take the saved XIC data as input. The subroutine chooses an  $m/z$  and examines the XICs for that  $m/z$  across each of the files. Looping over each file (XIC here), candidate peaks are identified using a median filter (user-selectable) and low-high-low pattern. Candidate peaks are integrated taking binned incremental steps (in retention time) away from the maxima (left and right) and applying a slope (user-selectable) and relative magnitude (user-selectable) filter to determine the endpoints of integration. Since the XICs can be noisy “near” the peak, it is advisable to either smooth or have exception handling for using the slope-filter to determine integration endpoints. We typically continue searching for integration endpoints even if the slope filter fails, as long as the ion intensity remains an appreciable fraction of the peak intensity (e.g., >60%, user-selectable). However, one must be careful because this selection becomes relevant for peaks that are not well separated in retention time (“just” resolved). In most cases, it is useful to check graphically the XICs for the  $m/z$  to confirm that the peak of interest is well separated, and the integration window determined by the code is appropriate (Fig. 2.11). The set of candidate peaks (amplitudes and areas) need to be aligned across the files so that they can be reliably compared. Experimentally, large retention time shifts (larger than 5 min) are possible across separate spectra files, and it is sometimes useful to prealign the spectra (e.g., optimizing a correlation coefficient between files and a chosen XIC or “average” XIC). Whether or not pre-alignment of XICs across files is used, we decided to align peaks by counting the number of peaks IDd in a retention time window (for that fixed nominal  $m/z$ ) across the files. If this number is above a threshold (user-selectable) based on the percent of the spectra files, then the candidate peak is considered a “true” peak centered at that relevant retention time (“true” peak time). For example, using a nominal  $m/z$  723.5 from 30 spectra files, 23 files could indicate a peak (or peaks) between 9 and 10 min, 4 files between 10 and 11 min, and 3 files between 8 and 9 min. The “true” time would be the average (e.g., 9.8 min). Then, for each file, the maximum peak intensity that occurs in some retention time window (e.g.,  $\pm 2$  min, user-selectable) about this “true” time is used to define the “true” peak for that file, and the integrated intensity (and peak amplitude) is saved. If no peak is identified for a particular file in this window, and then a zero is reported for that file. The more spectra files one has to compare, the lower the median threshold one can use for peak identification, since “random” candidate peaks (by low-high-low identification) are unlikely to repeat in the same retention time window across a

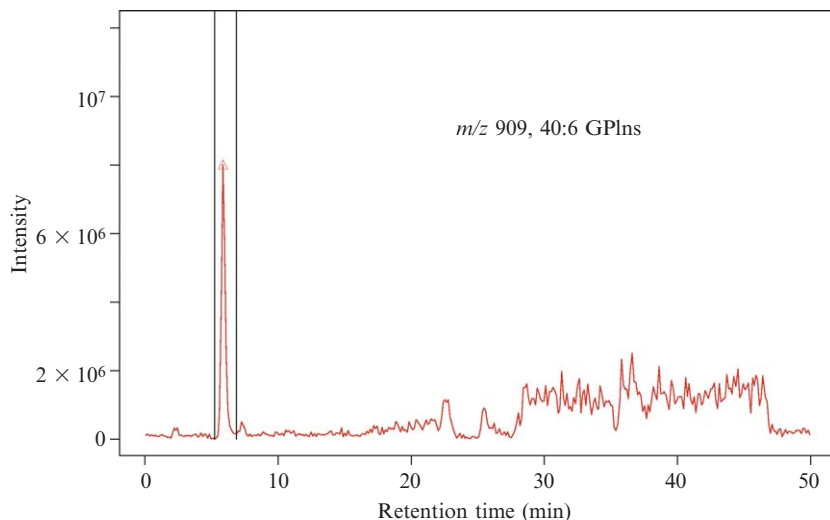


**Figure 2.11** Generation of extracted ion chromatograms (XIC;  $m/z$  909.06 to 909.96) from Fortran code as described in the text. The horizontal axis is retention time, and the vertical axis ion intensity. The vertical black lines indicate the region of integration dynamically selected by the code. The red triangle indicates the peak(s) automatically identified by the algorithms described in the text.

significant percent of the files. Once again, it is useful to graphically display the XICs across files and visually see the repeated peaks and their retention time fluctuations across files (Fig. 2.12). This is especially the case if one computed a large change in a molecular species due to a condition and would like to verify that large retention time shift across files were not erroneously picking up another, different peak in the XIC (at the same  $m/z$ ). If pre-alignment of XICs is used and the corrected correlation coefficients are near 1, then the retention time windows selected for assigning peaks may be of shorter duration ( $\sim 30$  s to 1 min). For identification and a quantitative assessment of individual phospholipids, multiple chemically defined internal standards per class identify typical retention times, peak profiles (widths), and retention time locations. Using multiple internal standards also allows for the examination of the variation in peak retention time as a function of  $m/z$  in addition to differential ionization across the lipid class. In practice, the molecular species in a phospholipid class are readily identified from full-scan data by  $m/z$  retention time information in comparison to similar peak profiles and retention times relative to the internal standards. Fragmentation of the peak ions at the relevant  $m/z$  retention time provides confirmation of the molecular species whose ions are contributing to the peak in the XIC.

Following the generation of integrated, aligned peak areas across multiple spectra files, accurate quantification of molecular species requires

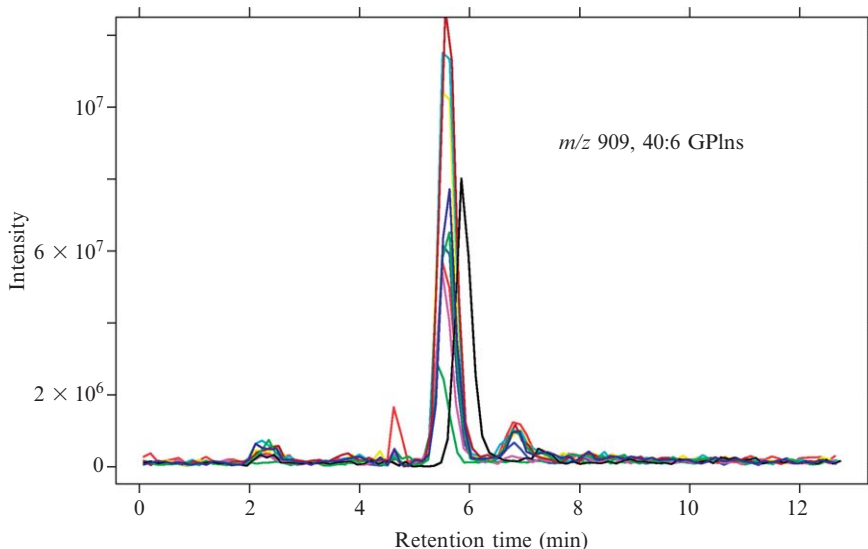


**Figure 2.12** A zoomed-in section including the extracted ion chromatogram (XIC) from Fig. 2.11 ( $m/z$  909.06 to 909.96), which also includes extracted ion chromatograms generated from nine other full-scan spectra files, indicative of the variation in amplitude and peak location across these files. Peak areas from the 10 files are automatically aligned as described and output in ASCII format for further analysis (normalization and quantification). Many mass-to-charge ( $m/z$ ) values in glycerophospholipid (GPL) full-scan spectra contain extracted ion chromatograms with multiple peaks at different retention times.

titrations of internal standards for individual species of phospholipids over the presumed physiological range of variation in abundance. To generate standard curves, we proceed as follows: (1) add fixed quantities of multiple fixed odd-chain internal standards (per glycerophospholipid [GPL] class) to every sample; (2) add varying amounts of even-carbon standards (e.g., 10, 50, 100, 500 ng) in triplicate; (3) normalize the peak areas of the even-carbon standards to the average of the fixed odd-carbon areas (per GPL class); and (4) repeat the process several times to estimate experiment to experiment variability in the slopes and intercepts (assuming linearity). An example of standard curves for the GPA class using experimental protocol and code described above is given in Fig. 2.13, and the variation in slope values and intercepts across independent experiments for the even-carbon internal standards are listed in Table 2.4.

For LC-MS with the protocol as described, we have found that the variation in slopes across GPLs within a class is nonlinear (and class-dependent) and has no obvious dependence on double bonds or carbon number. This is unfortunate since only rough slope and intercept estimates are possible for



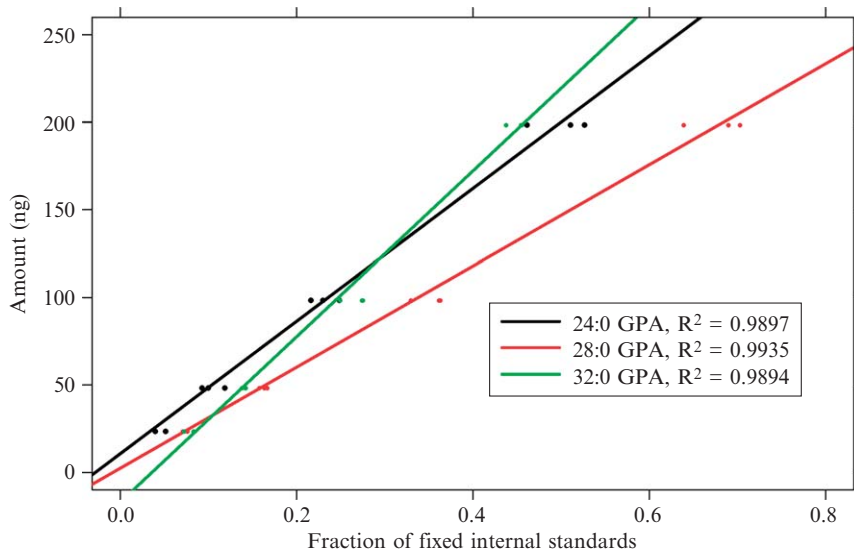


**Figure 2.13** Three standard curves for 24:0, 28:0, and 32:0 glycerophosphatidic acid (GPA) (black, green, and red, respectively) generated as described in the text using the automated code. The horizontal axis refers to peak areas normalized to the mean of four fixed odd-carbon internal standards, and the vertical axis is the amount added in nanograms (ng).

**Table 2.4** Variation in glycerophosphatidic acid (GPA) slopes across independent experiments

GPA	Experiment		
	1 <sup>a</sup>	2 <sup>a</sup>	3 <sup>a</sup>
24:0	254	289	X
28:0	189	184	X
32:0	238	267	266
34:1	172	244	204
34:2	147	179	145
36:0	192	352	330
36:1	206	247	202
36:2	195	288	194
38:4	253	218	230
38:6	299	388	337
40:6	437	403	384

<sup>a</sup> Standard deviations in slope values for individual experiments are approximately 5%.

**Table 2.5** Approximate amounts (ng) of individual GPSer molecular species in RAW 264.7 cells ( $5 \times 10^6$  cells)

GPSer <sup>a</sup>	Estimated amount (ng)	
32:1	52	40
32:0	30	24
34:3	41	18
34:2	62	54
34:1	393	441
34:0	163	172
36:4	20	23
36:3	30	30
36:2	249	314
36:1	1119	1319
36:0	464	510
38:6	21	25
38:5	60	70
38:4	188	326
38:3	293	340
38:2	144	12
38:1	60	65
38:0	9	26
40:7	37	47
40:6	575	692
40:5	770	895
40:4	451	538
40:3	200	260
40:2	78	87
40:0	33	41

<sup>a</sup> Shown are duplicate control (unstimulated) samples for a 2-h KDO2 Lipid A stimulation using a 10% serum LIPID MAPS protocol ([www.lipidmaps.org](http://www.lipidmaps.org)).

molecular species for which internal standards are not available. These estimated slopes for molecular species that lack titrations are based on the variation in slopes for other members of the same GPL class. One may use the range of slopes or regression estimates (e.g., in  $m/z$ ) across the GPL class to estimate the unknown slopes with appropriately large errors in the quantification of these molecular species. In Table 2.5, we list estimated amounts of different GPSer in RAW 264.7 cells following the LC-MS protocol described in the previous section. Once the molecular identity at a nominal  $m/z$  and retention time is known, isotopic corrections for  $m/z + 2$  contributions from the molecular species at a nominal  $m/z$  are readily computed, and normalized peak areas may be appropriately corrected and quantified within a GPL class. External normalization (e.g., cell counts, DNA) is useful for comparing across samples as

the fluctuation in individual GPLs may be significant due to extrinsic factors. Addition of internal standards prior to extraction may be used to estimate extraction efficiency per class and potential differential extraction efficiencies within a GPL class.

## ACKNOWLEDGMENTS

This work was supported in part by the NIH Large Scale Collaborative Initiative LIPID MAPS (U54 GM069338). The authors thank Andrew Goodman and Michelle Armstrong for excellent technical assistance with various aspects of this work. Dr. Brown is the Ingram Associate Professor of Cancer Research in Pharmacology.

## REFERENCES

- Alter, C. A., and Wolf, B. A. (1995). Identification of phosphatidylinositol 3,4,5-trisphosphate in pancreatic islets and insulin-secreting  $\beta$ -cells. *Biochem. Biophys. Res. Commun.* **208**, 190–197.
- Berrie, C. P., Iurisci, C., and Corda, D. (1999). Membrane transport and *in vitro* metabolism of the Ras cascade messenger, glycerophosphoinositol-4-phosphate. *Eur. J. Biochem.* **266**, 413–419.
- Bligh, E. G., and Dyer, W. J. (1959). A rapid method of total lipid extraction and purification. *Can. J. Biochem. Physiol.* **37**, 911–917.
- Bloor, W. R. (1928). The determination of small amounts of lipid in blood plasma. *J. Biol. Chem.* **77**, 53–73.
- Brügger, B., Erben, G., Sandhoff, R., Wieland, F. T., and Lehmann, W. D. (1997). Quantitative analysis of biological membrane lipids at the low picomole level by nano-electrospray ionization tandem mass spectrometry. *Proc. Natl. Acad. Sci. USA* **94**, 2339–2344.
- Christie, W. W. (2003). “Lipid analysis: Isolation, separation, identification, and structural analysis of lipids.” Oily Press, Bridgewater England.
- Clarke, N. G., and Dawson, R. M. C. (1981). Alkaline *O* leads to N-transacylation. *Biochem. J.* **195**, 301–306.
- Corda, D., Iurisci, C., and Berrie, C. P. (2002). Biological activities and metabolism of the lysophosphoinositides and glycerophosphoinositols. *Biochim. Biophys. Acta* **1582**, 52–69.
- Cunningham, T. W., Lips, D. L., Bansal, V. S., Caldwell, K. K., Mitchell, C. A., and Majerus, P. W. (1990). Pathway for the formation of D-3 phosphate containing inositol phospholipids in intact human platelets. *J. Biol. Chem.* **265**, 21676–21683.
- DeLong, C. J., Baker, P. R. S., Samuel, M., Cui, Z., and Thomas, M. J. (2001). Molecular species composition of rat liver phospholipids by ESI-MS/MS: The effect of chromatography. *J. Lipid Res.* **42**, 1959–1968.
- Dowhan, W. (1997). Molecular basis for membrane phospholipid diversity: Why are there so many lipids? *Annu. Rev. Biochem.* **66**, 199–232.
- Dowhan, W., and Bogdanov, M. (2002). Functional roles of lipids in membranes. In “New Comprehensive Biochemistry, Biochemistry of Lipids, Lipoproteins, and Membranes” (D. E. Vance and J. E. Vance, eds.), Vol. 36, pp. 1–35. Elsevier Science B.V., Amsterdam.
- Downes, C. P., Gray, A., and Lucocq, J. M. (2005). Probing phosphoinositide functions in signaling and membrane trafficking. *Trends Cell. Biol.* **15**, 259–268.

- Dragani, L. K., Berrie, C. P., Corda, D., and Rotilio, D. (2004). Analysis of glycerophosphoinositol by liquid chromatography–electrospray ionization tandem mass spectrometry using a  $\beta$ -cyclodextrin-bonded column. *J. Chromatogr. B Analyt. Technol. Biomed. Life Sci.* **802**, 283–289.
- Ekroos, K., Chernushevich, I. V., Simons, K., and Schevchenko, A. (2002). Quantitative profiling of phospholipids by multiple precursor ion scanning on a hybrid quadrupole time-of-flight mass spectrometer. *Anal. Chem.* **74**, 941–949.
- Fahy, E., Subramaniam, S., Brown, H. A., Glass, C. K., Merrill, A. H., Jr., Murphy, R. C., Raetz, C. R. H., Russell, D. W., Seyama, Y., Shaw, W., Shimizu, T., Spener, F., *et al.* (2005). A comprehensive classification system for lipids. *J. Lipid Res.* **46**, 839–862.
- Fenn, J. B., Mann, M., Meng, C. K., Wong, S. F., and Whitehouse, C. M. (1989). Electrospray ionization for mass spectrometry of large molecules. *Science* **246**, 64–71.
- Fenwick, G. R., Eagles, J., and Self, R. (1983). Fast atom bombardment mass spectrometry of intact phospholipids and related compounds. *Biomed. Mass Spectrom.* **10**, 382–386.
- Feurle, J., Jomaa, H., Wilhelm, M., Gutsche, B., and Herderich, M. (1998). Analysis of phosphorylated carbohydrates by high-performance liquid chromatography–electrospray ionization tandem mass spectrometry utilizing a  $\beta$ -cyclodextrin bonded stationary phase. *J. Chromatogr. A* **803**, 111–119.
- Folch, J., Ascoli, I., Lees, M., Meath, J. A., and LeBaron, F. N. (1951). Preparation of lipid extracts from brain tissue. *J. Biol. Chem.* **191**, 833–841.
- Forrester, J. S., Milne, S. B., Ivanova, P. T., and Brown, H. A. (2004). Computational lipidomics: A multiplexed analysis of dynamic changes in membrane lipid composition during signal transduction. *Mol. Pharm.* **65**, 813–821.
- Fridriksson, E. K., Shipkova, P. A., Sheets, E. D., Holowka, D., Baird, B., and McLafferty, F. W. (1999). Quantitative analysis of phospholipids in functionally important membrane domains from RBL-2H3 mast cells using tandem high-resolution mass spectrometry. *Biochemistry* **38**, 8056–8063.
- Gunnarsson, T., Ekblad, L., Karlsson, A., Michelsen, P., Odham, G., and Jergil, B. (1997). Separation of polyphosphoinositides using normal-phase high-performance liquid chromatography and evaporative light scattering detection or electrospray mass spectrometry. *Anal. Biochem.* **254**, 293–296.
- Hama, H., Takemoto, J. Y., and DeWald, D. B. (2000). Analysis of phosphoinositides in protein trafficking. *Methods* **20**, 465–473.
- Han, X., and Gross, R. W. (1994). Electrospray ionization mass spectroscopic analysis of human erythrocyte plasma membrane phospholipids. *Proc. Natl. Acad. Sci. USA* **91**, 10635–10639.
- Han, X., and Gross, R. W. (1995). Structural determination of picomole amounts of phospholipids via electrospray ionization tandem mass spectrometry. *J. Am. Soc. Mass Spectrom.* **6**, 1202–1210.
- Han, X., and Gross, R. W. (2003). Global analyses of cellular lipidomes directly from crude extracts of biological samples by ESI mass spectrometry: A bridge to lipidomics. *J. Lipid Res.* **44**, 1071–1079.
- Hirschmann, H. (1960). The nature of substrate asymmetry in stereoselective reactions. *J. Biol. Chem.* **235**, 2762–2767.
- Hsu, F. F., and Turk, J. (2000a). Charge-driven fragmentation processes in diacyl glycerophosphatidic acids upon low-energy collisional activation: A mechanistic proposal. *J. Am. Soc. Mass Spectrom.* **11**, 797–803.
- Hsu, F. F., and Turk, J. (2000b). Charge-remote and charge-driven fragmentation processes in diacyl glycerophosphoethanolamine upon low-energy collisional activation: A mechanistic proposal. *J. Am. Soc. Mass Spectrom.* **11**, 892–899.

- Hsu, F. F., and Turk, J. (2000c). Characterization of phosphatidylinositol, phosphatidylinositol-4-phosphate, and phosphatidylinositol-4, 5-bisphosphate by electrospray ionization tandem mass spectrometry: A mechanistic study. *J. Am. Soc. Mass Spectrom.* **11**, 986–999.
- Hsu, F. F., and Turk, J. (2001). Studies on phosphatidylglycerol with triple quadrupole tandem mass spectrometry with electrospray ionization: Fragmentation processes and structural characterization. *J. Am. Soc. Mass Spectrom.* **12**, 1036–1043.
- IUPAC-IUB Commission on Biochemical Nomenclature (CBN) (1967). The nomenclature of lipids. *Eur. J. Biochem.* **2**, 127–131.
- Ivanova, P. T., Milne, S. B., Forrester, J. S., and Brown, H. A. (2004). Lipid arrays: New tools in the understanding of membrane dynamics and lipid signaling. *Mol. Interv.* **4**, 84–94.
- Ivanova, P. T., Cerda, B. A., Horn, D. M., Cohen, J. S., McLafferty, F. W., and Brown, H. A. (2001). Electrospray ionization mass spectrometry analysis of changes in phospholipids in RBL-2H3 mastocytoma cells during degranulation. *Proc. Natl. Acad. Sci. USA* **98**, 7152–7157.
- Kerwin, J. L., Tuininga, A. R., and Ericsson, L. H. (1994). Identification of molecular species of glycerophospholipids and sphingomyelin using electrospray mass spectrometry. *J. Lipid Res.* **35**, 1102–1114.
- Larsen, A., Uran, S., Jacobsen, P. B., and Skotland, T. (2001). Collision-induced dissociation of glycerophospholipids using electrospray ion-trap mass spectrometry. *Rapid Commun. Mass Spectrom.* **15**, 2393–2398.
- Lesnfsky, E. J., Stoll, M. S. K., Minkler, P. E., and Hoppel, C. L. (2000). Separation and quantitation of phospholipids and lysophospholipids by high-performance liquid chromatography. *Anal. Biochem.* **285**, 246–254.
- Lips, D. L., Majerus, P. W., Gorga, F. R., Young, A. T., and Benjamin, T. L. (1989). Phosphatidylinositol 3-phosphate is present in normal and transformed fibroblasts and is resistant to hydrolysis by bovine brain phospholipase C II. *J. Biol. Chem.* **264**, 8759–8763.
- Lytle, C. A., Gan, Y. D., and White, D. C. (2000). Electrospray ionization/mass spectrometry compatible reversed-phase separation of phospholipids: Piperidine as a post column modifier for negative ion detection. *J. Microbiol. Methods* **41**, 227–234.
- Michell, R. H., Heath, V. L., Lemmon, M. A., and Dove, S. K. (2006). Phosphatidylinositol 3,5-bisphosphate: Metabolism and cellular functions. *Trends Biochem. Sci.* **31**, 52–63.
- Milne, S. B., Ivanova, P. T., Forrester, J. S., and Brown, H. A. (2006). LIPIDOMICS: An analysis of cellular lipids by ESI-MS. *Methods* **39**, 92–103.
- Milne, S. B., Forrester, J. S., Ivanova, P. T., Armstrong, M. D., and Brown, H. A. (2003). Multiplexed lipid arrays of anti-immunoglobulin M-induced changes in the glycerophospholipid composition of WEHI-231 cells. *AfCS Res. Reports* **1**, 1–11. Accessible at [www.signaling-gateway.org/reports/v1/DA0011/DA0011.htm](http://www.signaling-gateway.org/reports/v1/DA0011/DA0011.htm).
- Milne, S. B., Ivanova, P. T., DeCamp, D., Hsueh, R. C., and Brown, H. A. (2005). A targeted mass spectrometric analysis of phosphatidylinositol phosphate species. *J. Lipid Res.* **46**, 1796–1802.
- Morris, J. B., Hinchliffe, K.A., Ciruela, A., Letcher, A. J., and Irvine, R. F. (2000). Thrombin stimulation of platelets causes an increase in phosphatidylinositol 5-phosphate revealed by mass assay. *FEBS Lett.* **475**, 57–60.
- Murphy, R. C., and Harrison, K. A. (1994). Fast atom bombardment mass spectrometry of phospholipids. *Mass Spectrom. Rev.* **13**, 57–75.
- Murphy, R. C., Fiedler, J., and Hevko, J. (2001). Analysis of nonvolatile lipids by mass spectrometry. *Chem. Rev.* **101**, 479–526.
- Nasuhoglu, C., Feng, S., Mao, J., Yamamoto, M., Yin, H. L., Earnest, S., Barylko, B., Albanesi, J. P., and Hilgemann, D. W. (2002). Nonradioactive analysis of phosphatidylinositides and other anionic phospholipids by anion-exchange high-performance liquid chromatography with suppressed conductivity detection. *Anal. Biochem.* **301**, 243–254.

- Pedrioli, P. G., Eng, J. K., Hubley, R., Vogelzang, M., Deutsch, E. W., Raught, B., Pratt, B., Nilsson, E., Angeletti, R. H., Apweiler, R., Cheung, K., Costello, C. E., *et al.* (2004). A common open representation of mass spectrometry data and its application to proteomics research. *Nat. Biotechnol.* **22**, 1459–1466.
- Pettitt, T. R., Dove, S. K., Lubben, A., Calaminus, S. D. J., and Wakelam, M. J. O. (2006). Analysis of intact phosphoinositides in biological samples. *J. Lipid Res.* **47**, 1588–1596.
- Pulfer, M., and Murphy, R. C. (2003). Electrospray mass spectrometry of phospholipids. *Mass Spectrom. Rev.* **22**, 332–364.
- Ramanadham, S., Hsu, F. F., Bohrer, A., Nowatzke, W., Ma, Z., and Turk, J. (1998). Electrospray ionization mass spectrometric analyses of phospholipids from rat and human pancreatic islets and subcellular membranes: Comparison to other tissues and implications for membrane fusion in insulin exocytosis. *Biochemistry* **37**, 4553–4567.
- Rouzer, C. A., Ivanova, P. T., Byrne, M. O., Milne, S. B., Marnett, L. J., and Brown, H. A. (2006). Lipid profiling reveals arachidonate deficiency in RAW 264.7 cells: Structural and functional implications. *Biochemistry* **45**, 14795–14808.
- Schwudke, D., Oegema, J., Burton, L., Entchev, E., Hannich, J. T., Ejsing, C. S., Kurzchalia, T., and Schevchenko, A. (2006). Lipid profiling by multiple precursor and neutral loss scanning driven by the data-dependent acquisition. *Anal. Chem.* **78**, 585–595.
- Smith, P. B. W., Snyder, A. P., and Harden, C. S. (1995). Characterization of bacterial phospholipids by electrospray ionization tandem mass spectrometry. *Anal. Chem.* **67**, 1824–1830.
- Taguchi, R., Hayakawa, J., Takeuchi, Y., and Ishida, M. (2000). Two-dimensional analysis of phospholipids by capillary liquid chromatography/electrospray ionization mass spectrometry. *J. Mass Spectrom.* **35**, 953–966.
- Wang, C., Xie, S., Yang, J., Yang, Q., and Xu, G. (2004). Structural identification of human blood phospholipids using liquid chromatography/quadrupole-linear ion trap mass spectrometry. *Anal. Chim. Acta* **525**, 1–10.
- Watson, A. D. (2006). Lipidomics—a global approach to lipid analysis in biological systems. *J. Lipid Res.* **47**, 2101–2111.
- Wenk, M. R. (2005). The emerging field of lipidomics. *Nat. Rev. Drug Discov.* **4**, 594–610.
- Wenk, M. R., Lucast, L., DiPaolo, G., Romanelli, A. J., Suchy, S. F., Nussbaum, R. L., Cline, G. W., Shulman, G. I., McMurray, W., and DeCamilli, P. (2003). Phosphoinositide profiling in complex lipid mixtures using electrospray ionization mass spectrometry. *Nat. Biotechnol.* **21**, 813–817.

# DETECTION AND QUANTITATION OF EICOSANOIDS VIA HIGH PERFORMANCE LIQUID CHROMATOGRAPHY-ELECTROSPRAY IONIZATION-MASS SPECTROMETRY

Raymond Deems, Matthew W. Buczynski, Rebecca Bowers-Gentry,  
Richard Harkewicz, and Edward A. Dennis

## Contents

1. Introduction	60
2. Methods	62
2.1. Sample collection	62
2.2. Eicosanoid isolation	62
2.3. Reverse-phase liquid chromatography	62
2.4. Chiral chromatography	63
2.5. Mass spectrometry	63
2.6. Quantitation	63
3. Results and Discussion	74
3.1. MRM transition selection	74
3.2. Stereoisomer detection	77
3.3. Lower limit of detection	78
3.4. Recoveries	79
3.5. Miscellany	79
3.6. Summary	80
Acknowledgments	80
References	81

## Abstract

Eicosanoids constitute a large class of biologically active arachidonic acid (AA) metabolites that play important roles in numerous physiological processes. Eicosanoids are produced by several distinct routes, including the cyclooxygenase, lipoxygenase, and P450 enzymatic pathways, as well as by nonenzymatic processes. In order to completely understand the eicosanoid response of a cell

Departments of Chemistry, Biochemistry, and Pharmacology, University of California, San Diego, La Jolla, California

*Methods in Enzymology*, Volume 432  
ISSN 0076-6879, DOI: 10.1016/S0076-6879(07)32003-X

© 2007 Elsevier Inc.  
All rights reserved.

or tissue to a given stimulus, measuring the complete profile of eicosanoids produced is important. Since the eicosanoids are products of a single species, AA, and represent, for the most part, the addition of various oxygen species, the hundreds of eicosanoids have very similar structures, chemistries, and physical properties. The identification and quantitation of all eicosanoids in a single biological sample are a challenging task, one that high-performance liquid chromatography-mass spectrometry (LC-MS) is well suited to handle. We have developed a LC-MS/MS procedure for isolating, identifying, and quantitating a broad spectrum of eicosanoids in a single biological sample. We currently can measure over 60 eicosanoids in a 16-min LC-MS/MS analysis. Our method employs stable isotope dilution internal standards to quantitate these specific eicosanoids. In the course of setting up the LC-MS system, we have established a library that includes relative chromatographic retention times and tandem mass spectrometry data for the most common eicosanoids. This library is available to the scientific community on the website [www.lipidmaps.org](http://www.lipidmaps.org).

## 1. INTRODUCTION

The eicosanoids comprise a broad class of AA metabolites that mediate a wide variety of important physiological functions. Most of the AA found in cells is esterified to the *sn*-2 position of neutral lipids or phospholipids (Schaloske and Dennis, 2006; Six and Dennis, 2000). Upon activation, phospholipase A<sub>2</sub>s release the AA from cellular phospholipids. The free AA can then be converted by a score of enzymes in three distinct oxidation pathways (cyclooxygenase [Simmons *et al.*, 2004; Smith *et al.*, 2000], lipoxygenase [Funk, 2001; Peters-Golden and Brock, 2003; Spokas *et al.*, 1999], and cytochrome P450 [Sacerdoti *et al.*, 2003]) into hundreds of bioactive species. These pathways exhibit a fair amount of redundancy, as some eicosanoid species can be produced by more than one enzyme. Likewise, some enzymes are capable of producing more than one eicosanoid product. In addition to these reactions, AA and its metabolites can also undergo nonenzymatic oxidation and dehydration reactions to produce many of these same compounds as well as other metabolic species, including stereoisomers of the enzymatic products. Thus, eicosanoid biosynthesis is a complex network of interacting pathways and interconnected metabolites. It is quite possible that perturbing one arm of this system could produce changes and compensations in the other arms. In order to fully understand how a given cell or tissue responds to a stimulus or how a drug targeted for one eicosanoid might affect the distribution of the other eicosanoids, one must determine the entire eicosanoid spectrum.

Enzyme-linked immunosorbent assays have long been the primary means of quantitating eicosanoids (Reinke, 1992; Shono *et al.*, 1988). This method requires specific antibodies for each eicosanoid to be quantitated; however,



relatively few eicosanoids have commercially available antibodies. This significantly limits the number of eicosanoids that can be detected and quantitated. This technique is also expensive and inefficient in that only a single eicosanoid can be determined with each assay. Thus, it is not amenable to analyzing a large number of different eicosanoids. Gas chromatography-MS (GC-MS) methods were developed that greatly improved upon these limitations (Baranowski and Pacha, 2002) and allowed the simultaneous analysis of multiple eicosanoids. To volatilize the eicosanoids for GC, they must first be chemically derivatized. A wide variety of derivatization methods are available; however, a single derivatization method is not suitable for all eicosanoids. Furthermore, Murphy *et al.* (2005) have found that some eicosanoids are not suited for GC-MS analysis. These volatilization issues were overcome with the development of electrospray ionization (ESI), which allows the eicosanoids to be analyzed by MS directly from an aqueous sample. The eicosanoid carboxylate moiety readily ionizes in the ESI source.

The similarities in eicosanoid structure and chemical characteristics requires that both high performance LC and collision-induced decomposition (CID) be employed, in conjunction with ESI-MS, to isolate and unambiguously identify the individual eicosanoid species. LC isolates the eicosanoids based on their chemical and physical characteristics, while CID produces characteristic precursor/product transitions that can be employed in multi-reaction monitoring (MRM) mode on the MS. ESI-MRM was first employed in this field by Margalit *et al.* (1996) to quantitate 14 eicosanoids directly from a biological sample. In 2002, the resolving power of LC was coupled with the sensitivity of ESI-MRM to study five eicosanoids from LPS (lipopolysaccharide)-stimulated synovial cells (Takabatake *et al.*, 2002). Recently, Kita *et al.* (2005) developed a high-throughput method for the detection of 18 different eicosanoids from biological samples.

We present here a protocol for identifying and quantitating a large number of eicosanoids in a single ESI-based LC-MS/MS run without requiring derivitization. This technique employs a solid-phase extraction procedure to isolate eicosanoids, an LC method to separate species, and a MS-CID technique to unambiguously identify a large number of eicosanoids. To accurately quantitate eicosanoids using these procedures, we have employed the well-established stable isotope dilution method (Hall and Murphy, 1998). We have included deuterated eicosanoids as internal standards to track and measure losses during sample preparation and to account for the various response issues associated with mass spectral analysis.

We currently can identify over 60 discrete chemical species of eicosanoid in a single 16-min run and can quantitate a significant fraction of them (Buczynski *et al.*, 2007; Harkewicz *et al.*, 2007). We present the methods for the extraction and analysis of eicosanoids from media and cells produced during cell culture. We then describe the protocols for these methods and conclude with a discussion of some characteristics of this procedure.

## 2. METHODS

### 2.1. Sample collection

The following procedure was developed for the isolation of eicosanoids from six-well cell culture plates containing 2.0 ml of media. We have also adapted this method to other sample types and sample volumes by scaling our procedure as needed. The media was removed and 100  $\mu\text{l}$  of a mixture of internal standards (containing 10 ng/100  $\mu\text{l}$  of each standard in EtOH) was added followed by 100  $\mu\text{l}$  of EtOH to bring the total concentration of EtOH to 10% by volume. Samples were centrifuged for 5 min at 3000 rpm to remove cellular debris. The eicosanoids were then isolated via solid-phase extraction.

When intracellular eicosanoids were analyzed, adherent cells were scraped into 500  $\mu\text{l}$  of MeOH, and then 1000  $\mu\text{l}$  of phosphate-buffered saline (PBS) and 100  $\mu\text{l}$  of internal standards were added. Scraping cells in aqueous solutions was shown to activate eicosanoid production, whereas doing so in MeOH effectively stopped the reactions and lysed the cells. These samples were then processed the same as the media.

### 2.2. Eicosanoid isolation

Eicosanoids were extracted using Strata<sup>®</sup> X SPE columns (Phenomenex, Torrance, CA). Columns were washed with 2 ml of MeOH followed by 2 ml of H<sub>2</sub>O. After applying the sample, the columns were washed with 1 ml of 10% MeOH, and the eicosanoids were then eluted with 1 ml of MeOH. The eluant was dried under vacuum and redissolved in 100  $\mu\text{l}$  of solvent A (water-acetonitrile-formic acid [63:37:0.02; v/v/v]) for LC-MS/MS analysis.

### 2.3. Reverse-phase liquid chromatography

The analysis of eicosanoids was performed by LC-MS/MS. Eicosanoids were separated by reverse-phase LC on a C18 column (2.1  $\times$  250 mm; Grace-Vydac, Deerfield, IL) at a flow rate of 300  $\mu\text{l}/\text{min}$  at 25°. All samples were loaded via a Pal auto-sampler (Leap Technologies, Carrboro, NC) that maintained the samples at 4° to minimize degradation of eicosanoids while queued for analysis. The column was equilibrated in Solvent A, and samples (dissolved in Solvent A) were injected using a 50- $\mu\text{l}$  injection loop and eluted with a linear gradient from 0 to 20% solvent B (acetonitrile-isopropyl alcohol [50:50; v/v]) between 0 and 6 min; solvent B was increased to 55% from 6 to 6.5 min and held until 10 min; solvent B was increased to 100% from 10 to 12 min and held until 13 min; and then, solvent B was dropped to 0% by 13.5 min and held until 16 min.

## 2.4. Chiral chromatography

When it was required to isolate isomeric eicosanoids, normal-phase chiral liquid chromatography was carried out using the same pumping system described above for reverse-phase chromatography. Separation was carried out on a  $4.6 \times 250$  mm Chiral Technologies (West Chester, PA) derivatized amylose column (Chiralpak<sup>®</sup> AD-H) equipped with a guard column (Chiralpak<sup>®</sup> AD-H guard column) held at  $35^\circ$ . Buffer A was hexane/anhydrous ethanol/water/formic acid: 96/4/0.08/0.02, v/v; buffer B was 100% anhydrous ethanol. This small amount of water in buffer A is miscible in the hexane/anhydrous ethanol mix and was found to be vital for satisfactory chiral separation and peak shape. Gradient elution was achieved using 100/0:A/B at 0 min; linearly ramped to 90/10:A/B by 13 min; linearly ramped to 75/25:A/B by 15 min and held until 25 min; and then linearly ramped back to 100/0:A/B by 27 min and held there until 42 min to achieve column re-equilibration. The chiral chromatography effluent was coupled to a mass spectrometer for further analysis.

## 2.5. Mass spectrometry

All MS analyses were performed using an Applied Biosystems (Foster City, CA) 4000 QTRAP hybrid, triple-quadrupole, linear ion trap mass spectrometer equipped with a Turbo V ion source and operated in MRM mode. For all experiments, the Turbo V ion source was operated in negative electrospray mode (chiral chromatography utilized the ion source in chemical ionization mode, as shown later) and the QTRAP was set as follows: CUR = 10 psi, GS1 = 30 psi, GS2 = 30 psi, IS =  $-4500$  V, CAD = HIGH, TEM =  $525^\circ$ , ihe = ON, EP =  $-10$  V, and CXP =  $-10$  V. The voltage used for CID ( $-15$  to  $-35$  V) and the declustering potentials ( $-30$  to  $-100$  V) varied according to molecular species and were maximized for each eicosanoid.

The Turbo V ion source was operated in atmospheric pressure chemical ionization (APCI) mode when employing chiral chromatography using the following settings: CUR = 10 psi, GS1 = 45 psi, GS2 = 60 psi, NC =  $-3.0 \mu\text{A}$ , CAD = HIGH, TEM =  $400^\circ$ , ihe = ON, DP =  $-60$  V, EP =  $-15$  V, and CXP =  $-10$  V.

## 2.6. Quantitation

Eicosanoid quantitation was performed by the stable isotope dilution method previously described by Hall and Murphy (Hall and Murphy, 1998). For each eicosanoid to be quantitated, an internal standard was selected that had a different precursor ion mass than the target analyte, but was chemically and structurally as similar to the target analyte as possible. This is ideally achieved by using a deuterated analog of the analyte.

We employed these standards whenever they were commercially available. In other cases, we employed a deuterated analog that was the closest to the desired analog in characteristics. For example, 15d- $\Delta^{12,14}$  PGJ<sub>2</sub> (d4) was employed as the internal standard for PGJ<sub>2</sub>, 15d- $\Delta^{12,14}$  PGJ<sub>2</sub>, and 15d- $\Delta^{12,14}$  PGD<sub>2</sub>. Table 3.1 lists the internal standards that we are currently employing (boxes in gray) and indicates which internal standard is used with which analyte. Presently, eight deuterated internal standards are used to quantify 16 eicosanoids. An aliquot of the internal standard (10 ng std/100  $\mu$ l of ethanol) was added to either the media or cell extracts immediately following its isolation. The samples were then processed as previously detailed.

The primary standards contained an accurately known amount of each eicosanoid (non-deuterated) to be quantitated and an accurate aliquot of the internal standards. The concentration of the primary standards must be known with high accuracy. This can be accomplished in one of several ways. In some cases, they are commercially available. Cayman Chemicals, for example, offers a “Quanta-PAK” version of many eicosanoids that contains a deuterated internal standard and a vial containing an accurately determined amount of the non-deuterated primary standard. Some of the eicosanoids (e.g., some HETEs and leukotrienes) have significant ultraviolet (UV) absorption that can be employed to determine the concentration of the standard. The amount of standard can also be determined gravimetrically if a microbalance is available.

The set of primary standards was then prepared by adding accurately determined amounts of the given analyte (non-deuterated) to 100  $\mu$ l of the same internal standard used to spike the samples. (Note: the concentration of the internal standard does not need to be accurate, but it is crucial that an accurately known volume of the exact same internal standard is added to the sample and to the primary standards.) A typical standard curve consisted of 0.3, 1, 3, 10, 30, and 100 ng of primary standard per 100  $\mu$ l of internal standard containing 10 ng of each internal standard. The internal standard and the primary standard samples were run before and after each set of unknown samples, and 10  $\mu$ l of each was loaded onto the column.

A linear standard curve was generated where the ratio of analyte standard peak area to internal standard peak area in the primary standards was plotted versus the amount of primary standard (ng). Figure 3.1 shows examples of three typical standard curves. Linear regression analysis was used to calculate the slope and intercept of the standard curves that were then used to calculate the unknowns. R<sup>2</sup> values for these curves of greater than 0.99 were routinely obtained. The ratio of the unknown analyte peak area to internal standard peak area in the sample was then compared to the appropriate standard curve to calculate the amount of analyte in the sample. Since, in some cases, the deuterated standards contained a small percent of non-deuterated analyte, the LC-MS/MS of the internal standard was analyzed to determine the amount of non-deuterated analyte present. In this case, the

**Table 3.1** Eicosanoid library

Eicosanoid <sup>a</sup>	Systematic name	[M-H] ( <i>m/z</i> )	Production ( <i>m/z</i> )	LC retention time <sup>b</sup> (min)	Internal standard	Recovery <sup>c</sup>	Limit of detection (pg on column)
AA	5Z,8Z,11Z,14Z- eicosatetraenoic acid	303	259	12.4	AA-d <sub>8</sub>	E	50
AA-d <sub>8</sub>	5Z,8Z,11Z,14Z- eicosatetraenoic acid (5,6,8,9,11,12,14,15-d <sub>8</sub> )	311	267	12.4		ND	ND
AA-EA	N-(5Z,8Z,11Z,14Z- eicosatetraenoyl)- ethanolamine	346	259	10.6		E	10
5(S)6(R)DiHETE	5S,6R-dihydroxy- 7E,9E,11Z,14Z- eicosatetraenoic acid	335	163	9.0		M	5
5(S)6(S)DiHETE	5S,6S-dihydroxy- 7E,9E,11E,14Z- eicosatetraenoic acid	335	163	9.0		E	1
5(S)15(S)DiHETE	5S,15S-dihydroxy- 6E,8Z,11Z,13E- eicosatetraenoic acid	335	201	7.8		E	5
8(S)15(S)DiHETE	8S,15S-dihydroxy- 5Z,9E,11Z,13E- eicosatetraenoic acid	335		ND <sup>d</sup>		ND	ND
±5,6-DiHETrE	5,6-dihydroxy-8Z,11Z,14Z- eicosatrienoic acid	337	145	9.0		E	1
±8,9-DiHETrE	8,9-dihydroxy-5Z,11Z,14Z- eicosatrienoic acid	337	127	8.8		E	1

(continued)

Table 3.1 (continued)

Eicosanoid <sup>a</sup>	Systematic name	[M-H] ( <i>m/z</i> )	Production ( <i>m/z</i> )	LC retention time <sup>b</sup> (min)	Internal standard	Recovery <sup>c</sup>	Limit of detection (pg on column)
±11,12-DiHETrE	11,12-dihydroxy-5Z,8Z,14Z- eicosatrienoic acid	337	167	8.7		E	1
±14,15-DiHETrE	14,15-dihydroxy-5Z,8Z,11Z- eicosatrienoic acid	337	207	8.6		E	1
±5,6-EpETrE	5,6-epoxy-8Z,11Z,14Z- eicosatrienoic acid	319	191	10.1		E	5
±8,9-EpETrE	8,9-epoxy-5Z,11Z,14Z- eicosatrienoic acid	319	127	10.0		E	5
±11,12-EpETrE	11,12-epoxy-5Z,8Z,14Z- eicosatrienoic acid	319	167	9.8		E	10
±14,15-EpETrE	14,15-epoxy-5Z,8Z,11Z- eicosatrienoic acid	319	139	9.7		E	50
5(R)HETE	5R-hydroxy-6E,8Z,11Z,14Z- eicosatetraenoic acid	319	115	9.64	5(S)HETE-d <sub>8</sub>	ND	ND
5(S)HETE	5S-hydroxy-6E,8Z,11Z,14Z- eicosatetraenoic acid	319	115	9.64	5(S)HETE-d <sub>8</sub>	E	1
5(S)HETE-d <sub>8</sub>	5S-hydroxy-6E,8Z,11Z,14Z eicosatetraenoic acid (5,6,8,9,11,12,14,15-d8)	327	116	9.60		ND	ND
8(R)HETE	8R-hydroxy-5Z,9E,11Z,14Z- eicosatetraenoic acid	319	155	9.43		ND	ND
8(S)HETE	8S-hydroxy-5Z,9E,11Z,14Z- eicosatetraenoic acid	319	155	9.43		E	1
9-HETE	9-hydroxy-5Z,7E,11Z,14Z- eicosatetraenoic acid	319	151	9.49		E	1
11(R)HETE	11R-hydroxy-5Z,8Z,12E,14Z- eicosatetraenoic acid	319	167	9.31	5(S)HETE-d <sub>8</sub>	ND	ND
11(S)HETE	11S-hydroxy-5Z,8Z,12E,14Z- eicosatetraenoic acid	319	167	9.31	5(S)HETE-d <sub>8</sub>	E	1

12(R)HETE	12R-hydroxy-5Z,8Z,10E,14Z- eicosatetraenoic acid	319	179	9.38		ND	ND
12(S)HETE	12S-hydroxy-5Z,8Z,10E,14Z- eicosatetraenoic acid	319	179	9.38		E	1
15(R)HETE	15R-hydroxy-5Z,8Z,11Z,13E- eicosatetraenoic acid	319	175	9.19	5(S)HETE-d <sub>8</sub>	ND	ND
15(S)HETE	15S-hydroxy-5Z,8Z,11Z,13E- eicosatetraenoic acid	319	175	9.19	5(S)HETE-d <sub>8</sub>	E	1
20-HETE	20-hydroxy-5Z,8Z,11Z,14Z- eicosatetraenoic acid	319	245	8.98		E	1
12(S)HHTrE	12S-hydroxy-5Z,8E,10E- heptadecatrienoic acid	279	163	8.7		E	50
5(S)HpETE	5S-hydroperoxy- 6E,8Z,11Z,14Z- eicosatetraenoic acid	335	155	9.7		E	5
12(S)HpETE	12S-hydroperoxy- 5Z,8Z,10E,14Z- eicosatetraenoic acid	335	153	9.4		E	1
15(S)HpETE	15S-hydroperoxy- 5Z,8Z,11Z,13E- eicosatetraenoic acid	335	113	9.2		E	1
LTB <sub>4</sub>	5S,12R-dihydroxy- 6Z,8E,10E,14Z- eicosatetraenoic acid	335	195	8.2		M	5
6 trans LTB <sub>4</sub>	5S,12R-dihydroxy- 6E,8E,10E,14Z- eicosatetraenoic acid	335	195	7.8		E	1
6 trans 12 epi LTB <sub>4</sub>	5S,12S-dihydroxy- 6E,8E,10E,14Z- eicosatetraenoic acid	335	195	8.0		E	5

Table 3.1 (continued)

Eicosanoid <sup>a</sup>	Systematic name	[M-H] ( <i>m/z</i> )	Production ( <i>m/z</i> )	LC retention time <sup>b</sup> (min)	Internal standard	Recovery <sup>c</sup>	Limit of detection (pg on column)
LTC <sub>4</sub>	5S-hydroxy,6R-(S-glutathionyl), 7E,9E,11Z,14Z- eicosatetraenoic acid	624	272	8.8		P	1
11-trans LTC <sub>4</sub>	5S-hydroxy,6R-(S-glutathionyl), 7E,9E,11E,14Z- eicosatetraenoic acid	624	272	9.2		M	1
LTE <sub>4</sub>	5S-hydroxy,6R-(S-cysteinyl),7E,9E,11Z,14Z- eicosatetraenoic acid	438	235	10.1		M	5
11-trans LTE <sub>4</sub>	5S-hydroxy,6R-(S-cysteinyl),7E,9E,11E,14Z- eicosatetraenoic acid	438	235	10.4		M	1
5(S)6(R)15(S) LXA <sub>4</sub>	5S,6R,15S-trihydroxy- 7E,9E,11Z,13E- eicosatetraenoic acid	351	115	5.2		M	1
5(S)6(S)15(S) LXA <sub>4</sub>	5S,6S,15S-trihydroxy- 7E,9E,11Z,13E- eicosatetraenoic acid	351		ND <sup>d</sup>		ND	ND
5(S)14(R)15(S) LXB <sub>4</sub>	5S,14R,15S-trihydroxy- 6E,8Z,10E,12E- eicosatetraenoic acid	351		ND <sup>d</sup>		ND	ND
5-OxoETE	5-oxo 6E,8Z,11Z,14Z- eicosatetraenoic acid	317	203	9.8		E	5
12-OxoETE	12-oxo-5Z,8Z,10E,14Z- eicosatetraenoic acid	317	153	9.4		E	1
15-OxoETE	15-oxo-5Z,8Z,11Z,13E- eicosatetraenoic acid	317		ND <sup>d</sup>		ND	ND



PGA <sub>2</sub>	9-oxo-15S-hydroxy-5Z,10Z,13E-prostatrienoic acid	333		ND <sup>d</sup>		ND	ND
dhk-PGA <sub>2</sub>	9,15-dioxo-5Z,10-prostadienoic acid	333		ND <sup>d</sup>		ND	ND
PGB <sub>2</sub>	15S-hydroxy-9-oxo-5Z,8(12),13E-prostatrienoic acid	333	175	6.6		E	5
PGD <sub>2</sub>	9S,15S-dihydroxy-11-oxo-5Z,13E-prostadienoic acid	351	189	4.6	PGD <sub>2</sub> -d <sub>4</sub>	M	5
PGD <sub>2</sub> -d <sub>4</sub>	9S,15S-dihydroxy-11-oxo-5Z,13E-prostadienoic acid (3,3,4,4-d <sub>4</sub> )	355	193	4.6		ND	ND
PGD <sub>2</sub> -EA	N-(9S,15S-dihydroxy-11-oxo-5Z,13E-prostadienoyl)-ethanolamine	394	271	3.3		E	10
15d-Δ <sup>12,14</sup> PGD <sub>2</sub>	9S-hydroxy-11-oxo-5Z,12E,14E-prostatrienoic acid	333	271	8.2	15d-Δ <sup>12,14</sup> PGJ <sub>2</sub> -d <sub>4</sub>	E	1
dhk-PGD <sub>2</sub>	11,15-dioxo-9S-hydroxy-5Z-prostenoic acid	351	207	5.9	dhk-PGD <sub>2</sub> -d <sub>4</sub>	P	1
dhk-PGD <sub>2</sub> -d <sub>4</sub>	11,15-dioxo-9S-hydroxy-5Z-prostenoic acid (3,3,4,4-d <sub>4</sub> )	355	211	5.9		ND	ND
6-keto PGE <sub>1</sub>	6,9-dioxo-11R,15S-dihydroxy-13E-prostenoic acid	367	143	3.1		P	5
PGE <sub>2</sub>	9-oxo-11R,15S-dihydroxy-5Z,13E-prostadienoic acid	351	189	4.3	PGE <sub>2</sub> -d <sub>4</sub>	M	10
PGE <sub>2</sub> -d <sub>4</sub>	11R,15S-dihydroxy-9-oxo-5Z,13E-prostadienoic acid (3,3,4,4-d <sub>4</sub> )	355	193	4.3		ND	ND
PGE <sub>2</sub> -EA	N-(11R,15S-dihydroxy-9-oxo-5Z,13E-prostadienoyl)-ethanolamine	394	203	3.0		M	10000

(continued)

Table 3.1 (continued)

Eicosanoid <sup>a</sup>	Systematic name	[M-H] ( <i>m/z</i> )	Production ( <i>m/z</i> )	LC retention time <sup>b</sup> (min)	Internal standard	Recovery <sup>c</sup>	Limit of detection (pg on column)
bicyclo-PGE <sub>2</sub>	9,15-dioxo-5Z-prostaenoic acid-cyclo[11S,16]	333	175	7.4		E	5
dhk-PGE <sub>2</sub>	9,15-dioxo-11R-hydroxy-5Z-prostenoic acid	351	207	5.3	dhk-PGD <sub>2</sub> -d4	M	1
19(R)-hydroxy PGE <sub>2</sub>	9-oxo-11R,15S,19R-trihydroxy-5Z,13E-prostadienoic acid	367	287	2.4		M	1
20-hydroxy PGE <sub>2</sub>	9-oxo-11R,15S,20-trihydroxy-5Z,13E-prostadienoic acid	367	287	2.4		M	5
15-keto PGE <sub>2</sub>	9,15-dioxo-11R-hydroxy-5Z,13E-prostadienoic acid	349	161	4.7		M	1
tetranor PGEM	11R-hydroxy-9,15-dioxo-2,3,4,5-tetranor-prostan-1,20 dioic acid	327	291	2.3		P <sup>e</sup>	50
6,15-diketo 13,14-dihydro PGF <sub>1α</sub>	6,15-dioxo-9S,11R-dihydroxy-13E-prostenoic acid	369	267	3.6		P	50
6-keto PGF <sub>1α</sub>	6-oxo-9S,11R,15S-trihydroxy-13E-prostenoic acid	369	207	2.9	6-keto PGF <sub>1α</sub> -d4	E	10
6-keto PGF <sub>1α</sub> -d4	6-oxo-9S,11R,15S-trihydroxy-13E-prostenoic acid (3,3,4,4-d4)	373	211	2.9		ND	ND
PGF <sub>2α</sub>	9S,11R,15S-trihydroxy-5Z,13E-prostadienoic acid	353	193	4.0	PGF <sub>2α</sub> -d4	M	10
PGF <sub>2α</sub> -d4	9S,11R,15S-trihydroxy-5Z,13E-prostadienoic acid (3,3,4,4-d4)	357	197	4.0		ND	ND
PGF <sub>2α</sub> -EA	N-(9S,11R,15S-trihydroxy-5Z,13E-prostadienoyl)-ethanolamine	396	334	3.0		M	10

11 $\beta$ -PGF <sub>2<math>\alpha</math></sub>	9S,11S,15S-trihydroxy-5Z,13E-prostadienoic acid	353	193	3.7		M	1
dhk-PGF <sub>2<math>\alpha</math></sub>	9S,11S-dihydroxy-15-oxo-5Z-prostenoic acid	353	209	5.2	dhk-PGF <sub>2<math>\alpha</math></sub> -d4	M	5
dhk-PGF <sub>2<math>\alpha</math></sub> -d4	9S,11S-dihydroxy-15-oxo-5Z-prostenoic acid (3,3,4,4-d4)	357	213	5.2		ND	ND
2,3 dinor-11 $\beta$ PGF <sub>2<math>\alpha</math></sub>	9S,11S,13S-trihydroxy-2,3-dinor-5Z,13E-prostadienoic acid	325	145	3.0		M	1
20-hydroxy PGF <sub>2<math>\alpha</math></sub>	9S,11S,15S,20-tetrahydroxy-5Z,13E-prostadienoic acid	369	193	2.3		M	50
15-keto PGF <sub>2<math>\alpha</math></sub>	9S,11R-dihydroxy-15-oxo-5Z,13E-prostadienoic acid	351	217	4.5		M	1
PGF <sub>2<math>\beta</math></sub>	9R,11R,15S-trihydroxy-5Z,13E-prostadienoic acid	353		ND <sup>d</sup>		ND	ND
tetranor PGFM	9S,11R-dihydroxy-15-oxo-2,3,4,5-tetranor-prostan-1,20-dioic acid	329	293	2.1		P <sup>e</sup>	10
PGG <sub>2</sub>	9S,11R-epidioxy-15S-hydroperoxy-5Z,13E-prostadienoic acid	367		ND <sup>d</sup>		ND	ND
PGH <sub>2</sub>	9S,11R-epidioxy-15S-hydroxy-5Z,13E-prostadienoic acid	351		ND <sup>d</sup>		ND	ND
PGJ <sub>2</sub>	11-oxo-15S-hydroxy-5Z,9Z,13E-prostatrienoic acid	333	189	6.5	15d- $\Delta^{12,14}$ PGJ <sub>2</sub> -d4	E	1
$\Delta^{12}$ PGJ <sub>2</sub>	11-oxo-15S-hydroxy-5Z,9Z,12E-prostatrienoic acid	333		ND <sup>d</sup>		ND	ND
15d- $\Delta^{12,14}$ PGJ <sub>2</sub>	11-oxo-5Z,9Z,12E,14Z-prostatetraenoic acid	315	271	8.8	15d- $\Delta^{12,14}$ PGJ <sub>2</sub> -d4	E	5

**Table 3.1** (continued)

Eicosanoid <sup>a</sup>	Systematic name	[M-H] ( <i>m/z</i> )	Production ( <i>m/z</i> )	LC retention time <sup>b</sup> (min)	Internal standard	Recovery <sup>c</sup>	Limit of detection (pg on column)
15d-Δ <sup>12,14</sup> PGJ <sub>2</sub> - d4	11-oxo-5Z,9Z,12E,14Z- prostatetraenoic acid (3,3,4,4- d4)	319	275	8.8		ND	ND
PGK <sub>2</sub>	9,11-dioxo-15S-hydroxy- 5Z,13E-prostadienoic acid	349	205	4.4		ND	ND
TXB <sub>2</sub>	9S,11,15S-trihydroxy- thromboxa-5Z,13E-dien-1- oic acid	369	169	3.6	TXB <sub>2</sub> -d4	M	10
TXB <sub>2</sub> -d4	9S,11,15S-trihydroxy- thromboxa-5Z,13E-dien-1- oic acid (3,3,4,4-d4)	373	173	3.6		ND	ND
11-dehydro TXB <sub>2</sub>	9S,15S-dihydroxy-11-oxo- thromboxa-5Z,13E-dien-1- oic acid	367		ND <sup>d</sup>		ND	ND
2,3-dinor TXB <sub>2</sub>	9S,11,15S-trihydroxy-2,3- dinor-thromboxa-5Z,13E- dien-1-oic acid	341		ND <sup>d</sup>		ND	ND

<sup>a</sup> Gray boxes indicate internal standards.

<sup>b</sup> The retention times are given to indicate the relative elution position of the compounds with the understanding that the absolute values are not significant.

<sup>c</sup> Recoveries were grouped as P for poor (<25%), M for moderate (25–75%), E for excellent (>76%), and ND for not determined.

<sup>d</sup> These compounds were not analyzed quantitatively for this table, but the MS/MS spectra and LC retention times are available in the LIPID MAPS Eicosanoid Library at [www.lipidmaps.org](http://www.lipidmaps.org) or in [Harkewicz et al., 2007](#).

<sup>e</sup> Tetranor PGFM and tetranor PGEM did not bind to the Strata-X SPE column and thus could not be detected by this method.

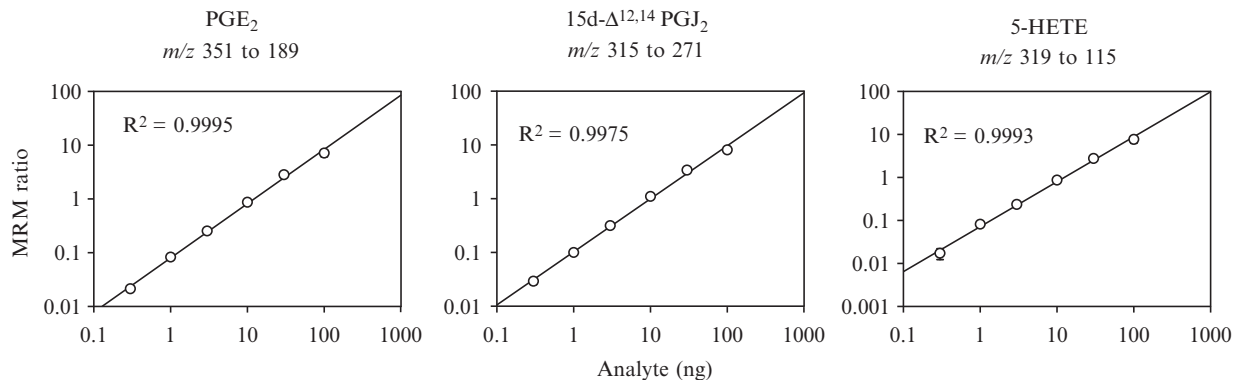


**Figure 3.1** Eicosanoid standard curves. Three typical standard curves are shown. The standard solutions are prepared as described in the “Methods” section. The solutions contained 10 ng of an internal standard for each analyte and 0.3 to 100 ng of the analyte in 140  $\mu$ l of which 10  $\mu$ l were analyzed. The multi-reaction monitoring (MRM) transitions employed to monitor the analytes are listed in the figure. The internal standards and transitions were: PGE<sub>2</sub> (d4)  $m/z$  355–193, 15d- $\Delta^{12,14}$  PGJ<sub>2</sub> (d4)  $m/z$  319–275, and 5-HETEs (d8)  $m/z$  327–116. The data were presented in log scale, but the linear regression analysis to determine parameters was done on the original non-log data.

non-deuterated contaminant was subtracted from each analysis. The dynamic range that can be covered is limited on the low end by the amount of non-deuterated analyte in the internal standards and the sensitivity of the mass spectrometer. The upper limit is restricted by ion suppression and detector saturation issues.

## 3. RESULTS AND DISCUSSION

### 3.1. MRM transition selection

To date, we have compiled a library of over 60 eicosanoids that we can detect and quantitate with these methods. These compounds are listed in [Table 3.1](#) with the precursor and product ions used in the MRM analysis. We have also included in this table several compounds for which we have MS/MS spectra but for which we have not selected MRM transitions. We have not included any recovery or limit of detection data for these compounds.

We have compiled the MS/MS spectra of each of these compounds. We have published these data ([Harkewicz \*et al.\*, 2007](#)). These data also can be accessed on the LIPID MAPS web page at <http://www.lipidmaps.org>. In addition to MS/MS spectra, the web visitor can obtain chemical structures for standards in both GIF and ChemDraw<sup>®</sup> formats, specific details regarding LC and MS parameters employed in our analysis, structures of dominant fragment ions (including literature references, when available, for fragment assignments), and retention times for a stated set of chromatographic conditions. Lastly, a web link to Cayman Chemical provides useful information and references on specific eicosanoids.

The product ions employed here for the MRM detection were selected to yield the best discrimination from other eicosanoids that co-elute in the vicinity of the analyte and to yield the highest signal. By balancing LC retention time and product ion selection, we were able to successfully distinguish the large majority of the eicosanoids listed. Various product ions can be selected to obtain greater sensitivity if conflicting eicosanoids are not present in a given set of samples.

The MS/MS spectra of most eicosanoids show numerous product ions. While a similar eicosanoid may have the same product ions, their relative intensities usually vary. The ratio of intensities of these product ions can be used to distinguish these species. In this case, multiple MRM transitions can then be analyzed, and the ratio of product ions found in the unknown can be compared with either an MS/MS library spectra or a pure standard run under the same conditions. This would aid in confirming the identity of a chromatographic peak.

Figure 3.2 shows the chromatograms of a few selected eicosanoids to illustrate several points about this procedure. All of the panels in Fig. 3.2 were generated by overlaying the individual MRM chromatograms for the various MRM pairs onto a single plot.

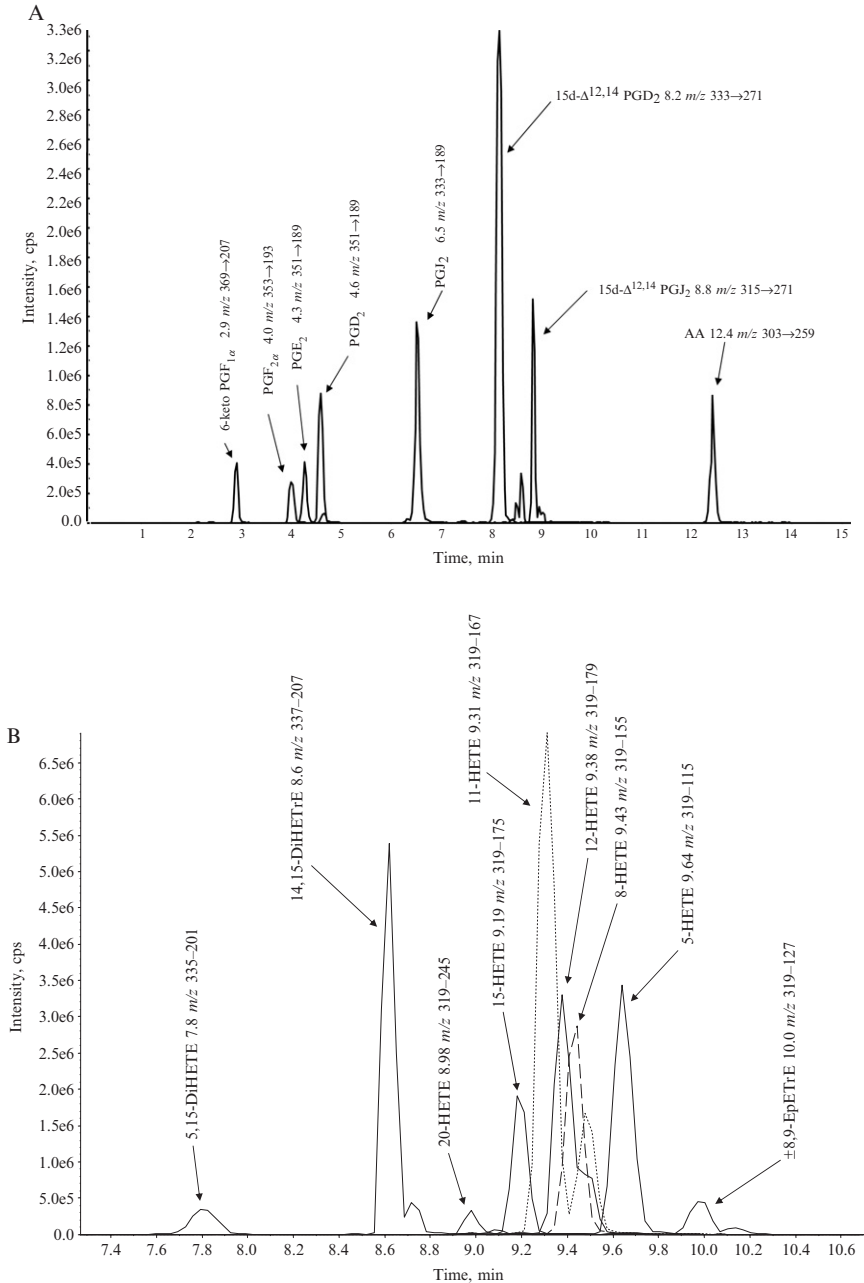
The sharpest peaks have a width at half height of 6 s and the baseline peak width on the order of 18 s. The Applied Biosystems 4000 QTrap can handle over 100 MRM pairs in a single scan. The dwell time employed when we are scanning 60 to 70 analytes is 25 ms. This produces a cycle time of 2 s per scan. This translates to at least nine data points per peak for the narrowest peaks, which is sufficient to accurately define the peak shape for quantitation. The Applied Biosystems 4000 QTrap software allows the user to break the MRM pairs into sets, and these sets can be run in series during the course of a single analysis so that only a fraction of the MRM pairs are being scanned during any time period. Running fewer MRM pairs in each scan allows the dwell time to be increased. Although this would not increase the absolute intensity of the peaks, it would increase the time averaging for each data point, thus decreasing the noise levels and increasing the signal-to-noise (S/N) ratio.

Figure 3.2A displays the retention times of several typical prostaglandins. Most of the prostaglandins show baseline separation from all other prostaglandins, and the analysis and identification of the peaks is fairly clear cut.

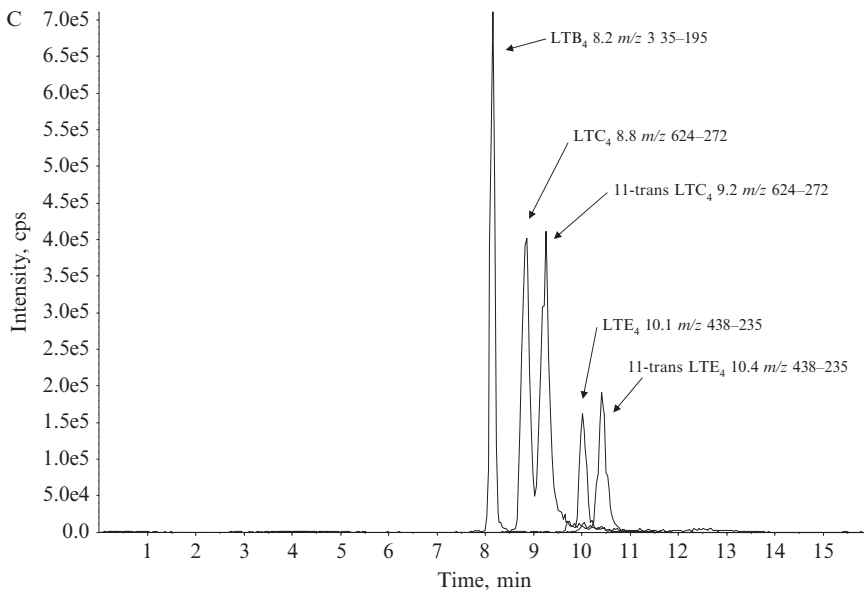
Figure 3.2B displays the region of the chromatogram that contains the HETEs, DiHETEs, EpETrEs, and DiHETrEs. Some prostaglandins and the leukotrienes also elute in this region; however, their molecular ions  $m/z$  are different from the hydroxy eicosanoids so that they do not appear in these scans. Even so, Fig. 3.2B clearly indicates that significant care must be taken when assigning the peaks in this region to the correct eicosanoid. While the differences in the retention times of the HETEs are reproducible, for the HETEs that elute between 8- and 12-HETE, they are not very large. The absolute value of the retention time for a given eicosanoid fluctuates due to batch variability in the LC solvents, and these shifts can be larger than the differences between the retention times of two neighboring eicosanoids. For this reason, a complete set of standards should be run both before and after each set of unknowns to accurately determine eicosanoid retention times, especially when assigning peak identities. If these HETEs are present in the samples, the gradient in this region of the chromatogram can be altered to spread out this region and improve the resolution.

Figure 3.2C shows the chromatograms of LTB<sub>4</sub>, LTC<sub>4</sub>, 11-trans LTC<sub>4</sub>, LTE<sub>4</sub>, and 11-trans LTE<sub>4</sub>. This panel also demonstrates one of the significant powers of the MRM method. Examination of Fig. 3.2A and B shows that the region from 8 to 11 min is very crowded, and that a significant number of eicosanoids elute in this region. Yet, when the MRM transitions are different, the chromatograms are very clean, and the assignments are easily made. This panel also highlights an important precaution that must be considered with the MRM method. While the chromatogram of a

particular analyte may appear to be very clean because no other compounds exhibit the same MRM transition, a tremendous amount of material may be eluting in the same place, but with different MRM transitions.







**Figure 3.2** High performance liquid chromatography (HPLC) eicosanoid chromatography on reverse-phase C18. The chromatography profiles of selected eicosanoid standards run on reverse-phase C18 HPLC (see “Methods” section). In each panel, the individual chromatograms produced by a given multi-reaction monitoring (MRM) pair have been overlaid. Each label lists the eicosanoid, retention time, and multi-reaction monitoring transition that produced a given chromatogram. (A) Representative sample of prostaglandins and arachidonic acid (AA). (B) Representative sample of the hydroxy-eicosanoids, including examples of HETEs, diHETEs, diHETrEs, and EpETrEs. (C) Representative sample of leukotrienes.

This material can still cause significant ion suppression of the analyte being examined. For example, we have found that  $PGE_2$  and  $PGD_2$  appear to co-elute with material co-extracted from Dulbecco’s Modification of Eagle’s Medium (DMEM) cell culture media, significantly diminishing the MS sensitivity of these eicosanoids (see “Recoveries” section). The proper use of internal standards can compensate for some of these issues during quantitation.

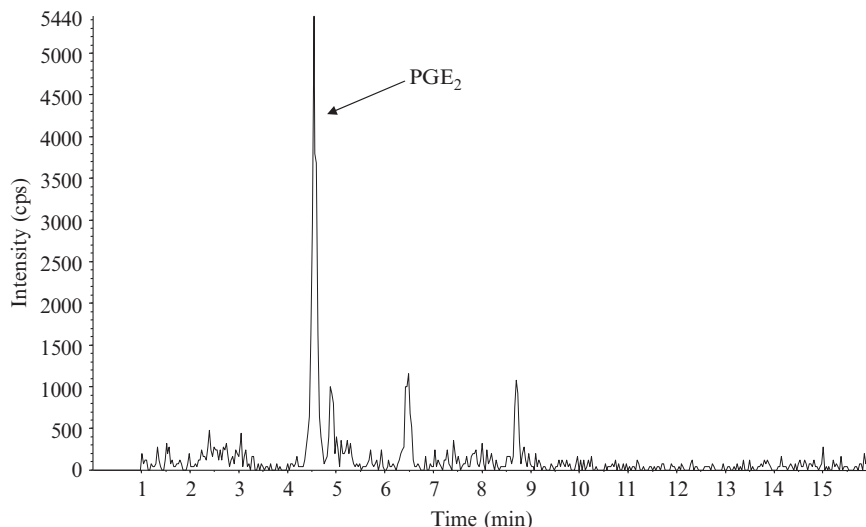
### 3.2. Stereoisomer detection

Table 3.1 contains eight pairs of isomers that have identical retention time and MS/MS spectra, and thus cannot be distinguished with the C18 column. To identify and quantitate these isomers normal phase chiral chromatography is required.

### 3.3. Lower limit of detection

Table 3.1 also contains an estimate of the lower limit of detection (LOD) for the eicosanoid when employing our standard procedures. A set of standards was made and then serially diluted to produce a set of standards such that 1 to 5000 pg would be loaded onto the column. A signal was judged to be significant if the signal area was three times the noise at the three-standard-deviation level. Most limits were between 1 and 50 pg loaded onto the column. Only PGE<sub>2</sub>-EA had an LOD greater than 50 ng. The detection limits that we obtained were achieved with a 2.1 × 250 mm Grace-Vydac reverse-phase C18 column with 5 μm particle size. Decreasing the column diameter, the particle size, and the flow rate can increase sensitivity, as can changing the column packing. We have analyzed only one isomer of any isomeric analytes and only non-deuterated analytes. Therefore, we have listed the LOD and recovery values for the other isomers and for the deuterated standards as not determined (ND) in Table 3.1. However, their recoveries and LODs should be very similar to the corresponding isomer that was analyzed or the equivalent non-deuterated analyte.

Figure 3.3 shows an example of the analysis of a sample that was close to our lower limit of detection. It is the chromatogram showing the analysis of PGE<sub>2</sub> and PGD<sub>2</sub> in a sample of spinal fluid from a rat that had been



**Figure 3.3** PGE<sub>2</sub> analysis of rat spinal fluid. Spinal fluid was collected from a rat whose paw had been injected with carrageenan to induce an inflammatory pain state. A sample of spinal fluid was removed (42 μl), processed as described in the “Methods” section and analyzed by liquid chromatography–mass spectrometry–mass spectrometry. Eighty percent of the sample was analyzed. The PGE<sub>2</sub> peak corresponds to 52 pg of PGE<sub>2</sub> being loaded onto the column. The signal-to-noise (S/N) ratio was 16-fold over a three-standard-deviation noise level.

subjected to the carrageenan model of inflammatory pain. This represents 52 pg of PGE<sub>2</sub> load onto the column and correlates with 150 pg of PGE<sub>2</sub> present in the original 42- $\mu$ l spinal fluid sample.

### 3.4. Recoveries

Our primary goal was to analyze as many eicosanoids in a single run as possible. We chose to focus on maximizing the recovery of AA, prostaglandins, and HETEs. Table 3.1 shows the recoveries that this system achieved for most of the analytes that we detect. These recoveries were determined by adding a known amount of each analyte, contained in a standard mix, to 2.0 ml of water or DMEM, and then isolating the eicosanoids via the standard sample preparation method previously outlined. We also did an “add back” experiment where DMEM alone was extracted by the same method; however, instead of adding an aliquot of the standard eicosanoid mixture to the DMEM sample before extraction, the eicosanoids were added to the post-extraction methanol column effluent. Losses in the “add back” samples would indicate that materials in the media are being co-extracted with the eicosanoids, and that these contaminants affect the eicosanoid MS response. All three sets of samples were analyzed with our LC-MS/MS procedure. The eicosanoid peak intensities of these samples were compared to those of standards that had not been through the isolation procedure, but instead were directly analyzed by LC-MS/MS.

Table 3.1 reports the relative recoveries of standards that were extracted from DMEM. The mono- and di-hydroxy eicosanoids had excellent recoveries at between 75 and 100%. The leukotrienes and prostaglandins had only moderate recoveries in the range of 50%. In most cases, the recoveries of these compounds from water were in the 80 to 100% range. The “add back” experiment showed that, for the prostaglandins, most of the losses occurred in the “add back” experiment, implying that some component from the media is being extracted that decreases the MS response to the prostaglandins. However, the “add back” levels for the cysteinyl leukotrienes were 100% within experimental error, suggesting that the losses occurred during the extraction process, and that media components are not affecting leukotriene detection. Tetranor PGEM and PGFM do not bind to the Strata-X SPE columns under these conditions and could not be detected by this protocol. The PGK<sub>2</sub> had very large errors, and extraction could not be measured. Again, the yield of a given class of compounds could be improved by altering the conditions or column type, but often at the expense of other analytes.

### 3.5. Miscellany

The process of culturing cells can affect the eicosanoid levels in other ways as well. For example, PGD<sub>2</sub> can undergo dehydration to form PGJ<sub>2</sub>, 15d- $\Delta$ <sup>12,14</sup> PGJ<sub>2</sub>, and 15d- $\Delta$ <sup>12,14</sup> PGD<sub>2</sub>. This dehydration has been reported to

be accelerated in serum albumin (Fitzpatrick and Wynalda, 1983; Maxey *et al.*, 2000). This decomposition will not be compensated for by the internal standards since they are not added until after the cell incubations. We have also found that when 10% serum is present during the cell culture, no LTC<sub>4</sub> could be detected; however, LTE<sub>4</sub>, which is a breakdown product of LTC<sub>4</sub>, was detected. When the same experiments are run in serum-free media, significant levels of the LTC<sub>4</sub> were detected, but very little LTE<sub>4</sub>. Presumably, the serum is catalyzing the conversion of LTC<sub>4</sub> to LTE<sub>4</sub>. Clearly, the types of recovery experiments outlined above must be conducted whenever applying this system to a new type of sample (e.g. media, serum, or tissues) or when changing the conditions of an already-tested sample. Care must also be taken to determine the effects that the addition of any agents (e.g., inhibitors, activators, or drugs) have on the extractions and on the quantitation of any other analytes. LC-MS/MS should also be done on the agents being added to determine if they have any MRM transitions that could be mistaken for one of the standard analytes.

Traditionally, lipids solutions were routinely acidified before subjecting them to liquid extractions. We compared our recoveries with and without acidifying the media before application to the SPE columns. We found that there were no significant differences; therefore, we do not routinely acidify the media. It is possible that eicosanoids other than those we employed in our testing could benefit by acidification. In addition, some eicosanoid species are susceptible to air oxidation and/or adhere to vessels and should not be taken to dryness. To guard against these losses, 20  $\mu$ l of a 50/50 solution of glycerol/ethanol can be added to the methanol column elution just before drying down the samples on the Speedvac. The glycerol remains, and the eicosanoids are concentrated into the glycerol, which can then be taken up in the LC equilibration buffer for LC-MS/MS analysis.

### 3.6. Summary

The method outlined above is a sensitive, accurate one for identifying and quantitating a large number of eicosanoids in a single LC-MS/MS run. This method can detect 1 pg (on column) of many eicosanoids, which is similar to the sensitivity of EIA analysis. Its primary advantage is that a large number of different species can be measured in a single analysis, while EIA analysis requires specific antibodies that are often not commercially available.

### ACKNOWLEDGMENTS

We would like to thank Dr. Robert C. Murphy (University of Colorado School of Medicine, Denver, CO) for his invaluable help and advice on the use of LC-MS/MS as a quantitative tool to analyze eicosanoids. This work was supported by the LIPID

MAPS Large Scale Collaborative Grant number GM069338 from the U.S. National Institutes of Health.

## REFERENCES

- Baranowski, R., and Pacha, K. (2002). Gas chromatographic determination of prostaglandins. *Mini. Rev. Med. Chem.* **2**, 135–144.
- Buczynski, M. W., Stephens, D. L., Bowers–Gentry, R. C., Grkovich, A., Deems, R. A., and Dennis, E. A. (2007). Multiple agonist induced changes in eicosanoid metabolites correlated with gene expression in macrophages. *J. Biol. Chem.* Epub in advance of print.
- Fitzpatrick, F. A., and Wynalda, M. A. (1983). Albumin-catalyzed metabolism of prostaglandin D<sub>2</sub>: Identification of products formed *in vitro*. *J. Biol. Chem.* **258**, 11713–11718.
- Funk, C. D. (2001). Prostaglandins and leukotrienes: Advances in eicosanoid biology. *Science* **294**, 1871–1875.
- Hall, L. M., and Murphy, R. C. (1998). Electrospray mass spectrometric analysis of 5-hydroperoxy and 5-hydroxyeicosatetraenoic acids generated by lipid peroxidation of red blood cell ghost phospholipids. *J. Am. Soc. Mass Spectrom.* **9**, 527–532.
- Harkewicz, R., Fahy, E., Andreyev, A., and Dennis, E. A. (2007). Arachidonate-derived dihomoprostaglandin production observed in endotoxin-stimulated macrophage-like cells. *J. Biol. Chem.* **282**, 2899–2910.
- Kita, Y., Takahashi, T., Uozumi, N., and Shimizu, T. (2005). A multiplex quantitation method for eicosanoids and platelet-activating factor using column-switching reversed-phase liquid chromatography-tandem mass spectrometry. *Anal. Biochem.* **342**, 134–143.
- Margalit, A., Duffin, K. L., and Isakson, P. C. (1996). Rapid quantitation of a large scope of eicosanoids in two models of inflammation: Development of an electrospray and tandem mass spectrometry method and application to biological studies. *Anal. Biochem.* **235**, 73–81.
- Maxey, K. M., Hessler, E., MacDonald, J., and Hitchingham, L. (2000). The nature and composition of 15-deoxy-Delta(12,14)PGJ(2). *Prostaglandins Other Lipid Mediat.* **62**, 15–21.
- Murphy, R. C., Barkley, R. M., Zemski, B. K., Hankin, J., Harrison, K., Johnson, C., Krank, J., McAnoy, A., Uhlson, C., and Zarini, S. (2005). Electrospray ionization and tandem mass spectrometry of eicosanoids. *Anal. Biochem.* **346**, 1–42.
- Peters–Golden, M., and Brock, T. G. (2003). 5-lipoxygenase and FLAP. *Prostaglandins Leukot. Essent. Fatty Acids* **69**, 99–109.
- Reinke, M. (1992). Monitoring thromboxane in body fluids: A specific ELISA for 11-dehydrothromboxane B<sub>2</sub> using a monoclonal antibody. *Am. J. Physiol.* **262**, E658–E662.
- Sacerdoti, D., Gatta, A., and McGiff, J. C. (2003). Role of cytochrome P450-dependent arachidonic acid metabolites in liver physiology and pathophysiology. *Prostaglandins Other Lipid Mediat.* **72**, 51–71.
- Schaloske, R. H., and Dennis, E. A. (2006). The phospholipase A<sub>2</sub> superfamily and its group numbering system. *Biochim. Biophys. Acta* **1761**, 1246–1259.
- Shono, F., Yokota, K., Horie, K., Yamamoto, S., Yamashita, K., Watanabe, K., and Miyazaki, H. (1988). A heterologous enzyme immunoassay of prostaglandin E<sub>2</sub> using a stable enzyme-labeled hapten mimic. *Anal. Biochem.* **168**, 284–291.
- Simmons, D. L., Botting, R. M., and Hla, T. (2004). Cyclooxygenase isozymes: The biology of prostaglandin synthesis and inhibition. *Pharmacol. Rev.* **56**, 387–437.
- Six, D. A., and Dennis, E. A. (2000). The expanding superfamily of phospholipase A<sub>2</sub> enzymes: Classification and characterization. *Biochim. Biophys. Acta* **1488**, 1–19.

- Smith, W. L., DeWitt, D. L., and Garavito, R. M. (2000). Cyclooxygenases: Structural, cellular, and molecular biology. *Annu. Rev. Biochem.* **69**, 145–182.
- Spokas, E. G., Rokach, J., and Wong, P. Y. (1999). Leukotrienes, lipoxins, and hydroxyeicosatetraenoic acids. *Methods Mol. Biol.* **120**, 213–247.
- Takabatake, M., Hishinuma, T., Suzuki, N., Chiba, S., Tsukamoto, H., Nakamura, H., Saga, T., Tomioka, Y., Kurose, A., Sawai, T., and Mizugaki, M. (2002). Simultaneous quantification of prostaglandins in human synovial cell-cultured medium using liquid chromatography/tandem mass spectrometry. *Prostaglandins Leukot. Essent. Fatty Acids* **67**, 51–56.

# STRUCTURE-SPECIFIC, QUANTITATIVE METHODS FOR ANALYSIS OF SPHINGOLIPIDS BY LIQUID CHROMATOGRAPHY–TANDEM MASS SPECTROMETRY: “INSIDE-OUT” SPHINGOLIPIDOMICS

M. Cameron Sullards, Jeremy C. Allegood, Samuel Kelly,  
Elaine Wang, Christopher A. Haynes, Hyejung Park,  
Yanfeng Chen, *and* Alfred H. Merrill, Jr.

## Contents

1. Introduction: An Overview of Sphingolipid Structures and Nomenclature	86
2. Analysis of Sphingolipids by Mass Spectrometry	89
2.1. Electron ionization-mass spectrometry	89
2.2. Fast atom bombardment and liquid secondary ionization mass spectrometry	90
2.3. Electrospray ionization	90
2.4. Liquid chromatography, electrospray ionization, mass spectrometry and tandem mass spectrometry	91
2.5. MALDI, mass spectrometry, and tandem mass spectrometry	91
3. Analysis of Sphingolipids by “OMIC” Approaches	92
4. Materials and Methods	95
5. Materials	98
5.1. Biological samples	98
6. Extraction	98
6.1. Preparation of samples for LC-MS/MS	99
7. Identification of the Molecular Species by Tandem Mass Spectrometry	100
7.1. Materials for infusion and LC-ESI-MS/MS	100

Schools of Biology, Chemistry, and Biochemistry, and the Parker H. Petit Institute for Bioengineering and Bioscience, Georgia Institute of Technology, Atlanta, Georgia

7.2. Sphingolipid subspecies characterization prior to quantitative LC-MS/MS analysis	100
8. Quantitation by LC-ESI-MS/MS Using Multireaction Monitoring	101
8.1. Analysis of sphingoid bases and sphingoid base 1-phosphates in positive ion mode	102
9. Analysis of (Dihydro)Ceramides, (Dihydro)Sphingomyelins, and (Dihydro)Monohexosyl-Ceramides in Positive Ion Mode	104
9.1. Modifications for analysis of glucosylceramides and galactosylceramides	105
9.2. Analysis of ceramide 1-phosphates by positive and negative ion modes	106
9.3. Analytical methods for additional analytes	106
10. Other Methods	109
Acknowledgments	111
References	112

## Abstract

Due to the large number of highly bioactive subspecies, elucidation of the roles of sphingolipids in cell structure, signaling, and function is beginning to require that one perform structure-specific and quantitative (i.e., “sphingolipidomic”) analysis of all individual subspecies, or at least of those that are relevant to the biologic system of interest. As part of the LIPID MAPS Consortium, methods have been developed and validated for the extraction, liquid chromatographic (LC) separation, and identification and quantitation by electrospray ionization (ESI), tandem mass spectrometry (MS/MS) using an internal standard cocktail that encompasses the signaling metabolites (e.g., ceramides, ceramide 1-phosphates, sphingoid bases, and sphingoid base 1-phosphates) as well as more complex species (sphingomyelins, mono- and di-hexosylceramides). The number of species that can be analyzed is growing rapidly with the addition of sulfatides and other complex sphingolipids as more internal standards become available. This review describes these methods as well as summarizes others from the published literature.

Sphingolipids are an amazingly complex family of compounds that are found in all eukaryotes as well as some prokaryotes and viruses. The size of the sphingolipidome (i.e., all of the individual molecular species of sphingolipids) is not known, but must be immense considering mammals have over 400 headgroup variants (for a listing, see <http://www.sphingomap.org>), each of which is comprised of at least a few—and, in some cases, dozens—of lipid backbones. No methods have yet been developed that can encompass so many different compounds in a structurally specific and quantitative manner. Nonetheless, it is possible to analyze useful subsets of the sphingolipidome, such as the backbone sphingolipids involved in signaling (sphingoid bases, sphingoid base 1-phosphates, ceramides, and ceramide 1-phosphates) and metabolites at important branchpoints, such as the partitioning of ceramide into sphingomyelins, glucosylceramides, galactosylceramides, and ceramide 1-phosphate versus



turnover to the backbone sphingoid base. This review describes methodology that has been developed as part of the LIPID MAPS Consortium ([www.lipidmaps.org](http://www.lipidmaps.org)) as well as other methods that can be used for sphingolipidomic analysis to the extent that such is currently feasible. The focus of this review is primarily mammalian sphingolipids; hence, if readers are interested in methods to study other organisms, they should consult the excellent review by Stephen Lavery in another volume of *Methods in Enzymology* (Lavery, 2005), which covers additional species found in plants, fungi, and other organisms.

It should be noted from the start that although many analytical challenges remain in the development of methods to analyze the full “sphingolipidome,” the major impediment to progress is the limited availability of reliable internal standards for most of the compounds of interest. Because it is an intrinsic feature of mass spectrometry that ion yields tend to vary considerably among different compounds, sources, methods, and instruments, an analysis that purports to be quantitative will not be conclusive unless enough internal standards have been added to correct for these variables. Ideally, there should be some way of standardizing every compound in the unknown mixture; however, that is difficult, if not impossible, to do because the compounds are not available, and the inclusion of so many internal standards generates a spectrum that may be too complex to interpret. Therefore, a few representative internal standards are usually added, and any known differences in the ion yields of the analytes of interest versus the spiked standard are factored into the calculations. Identification of appropriate internal standards has been a major focus of the LIPID MAPS Consortium, and the methods described in this review are based on the development of a certified (i.e., compositionally and quantitatively defined by the supplier) internal standard cocktail that is now commercially available (Avanti Polar Lipids, Alabaster, AL).

For practical and philosophical reasons, an internal standard cocktail was chosen over the process of an investigator adding individual standards for only the analytes of interest. On the practical level, addition of a single cocktail minimizes pipetting errors as well as keeping track of whether each internal standard is still usable (e.g., has it degraded while in solution?). Philosophically, the internal standard cocktail was chosen because an underlying premise of systems analysis asserts that, due to the high relevancy of unexpected interrelationships involving more distant components, one can only understand a biological system when factors outside the primary focus of the experiment have also been examined. Indeed, the first payoffs of “omics” and systems approaches involve the discoveries of interesting compounds in unexpected places when a “sphingolipidomic” analytical method was being used as routine practice instead of a simpler method that would have only measured the compound initially thought to be important (Zheng *et al.*, 2006). Thus, routine addition of a broad internal standard cocktail at the outset of any analysis maximizes the opportunity for such discoveries, both at the time the original measurements are made and when one decides to return to the samples later, which can fortunately be done for many sphingolipids because they remain relatively stable in storage.

## 1. INTRODUCTION: AN OVERVIEW OF SPHINGOLIPID STRUCTURES AND NOMENCLATURE

An important first step in “omic” research is to have structurally precise (yet convenient) ways of describing the compounds that have been measured (e.g., instead of reporting the amount of unspecified “ceramides” in a biological sample, report the individual subspecies). For sphingolipids, this means specifying the nature of the sphingoid base backbones (sometimes also called “long-chain bases”), the amide-linked fatty acids (found in most complex sphingolipids), headgroups, and any other modifications. A proposed nomenclature (Fahy *et al.*, 2005) is described below, but it should always be borne in mind that it is often not possible to unassailably prove some aspects of the structure of a compound (i.e., the stereochemistry, positions of double bonds, etc.) using MS alone. Nonetheless, in cases where nature has biased the structures toward specific species, it is appropriate to propose structures based on prior experience (as has been done for genes, proteins, glycans, etc.), while ever mindful of these assumptions.

A substantial number of compounds in nature have sphingolipid-like structures (such as fumonisins and myriocin); however, those that are formally regarded to be sphingolipids have a lipid backbone comprised of a 1,3-dihydroxy, 2-amino alkane, or alkene as summarized in Fig. 4.1. The most prevalent sphingoid base in mammalian cells is *D*-erythro-sphingosine, (2*S*,3*R*,4*E*)-2-amino-octadec-4-ene-1,3-diol, which is also called *E*-sphing-4-enine. A convenient abbreviation for sphingoid bases is to assign a letter reflecting the number of hydroxyls (“d” referring to the two (di-) hydroxyl groups and “t” for three, tri-) followed by numbers reflecting the length of the alkyl chain (18 carbons for sphingosine) and the presence of double bonds. If the location and stereochemistry of the double bond are known, it can be depicted in various ways (e.g., 4*E*-18:1, 4-*trans*-d18:1, or d18:1<sup>*trans*Δ<sup>4</sup></sup> for sphingosine), although this is usually implicit for mammalian sphingolipids, and the usual abbreviation for sphingosine is “d18:1.” This scheme can quite easily depict other sphingoid bases that vary in alkyl chain length (e.g., the d20:1 found in brain gangliosides) and the number and positions of double bonds (e.g., the 4-*trans*-,14-*cis*-d18:2 found in brain and plasma), the presence of additional hydroxyl groups (e.g., t18:0 for 4-hydroxysphinganine, which is sometimes called phytosphingosine or the full chemical name [2*S*,3*R*,4*R*]-2-amino-octadecane-1,3,4-triol), and other features.

Derivatives of sphingoid bases that retain the free amino group include the sphingoid base 1-phosphates, sphingosylphosphocholine (lysosphingomyelin), sphingosyl-hexoses (such as galactosylsphingosine, which is also called psychosine), and *N*-methyl- derivatives (Zheng *et al.*, 2006). *N*-acyl-derivatives are often categorically called “ceramides,” although this name has begun to

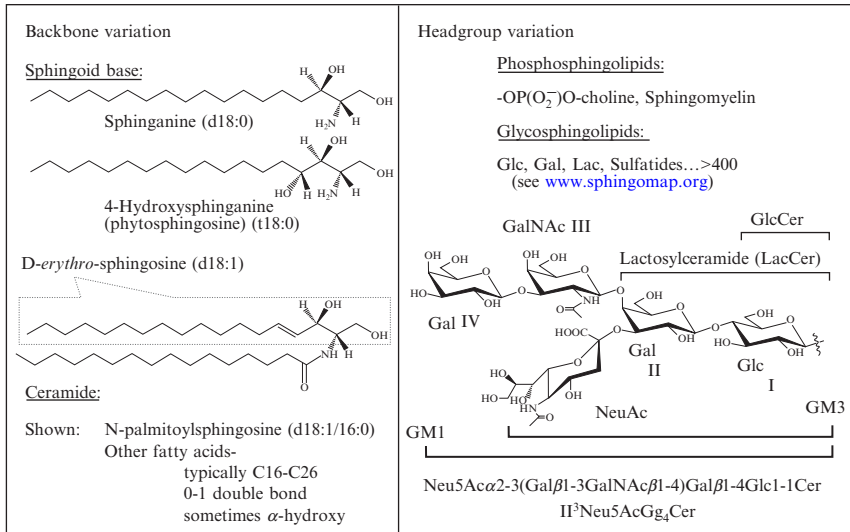


**Figure 4.1** Examples of structures of sphingolipids and nomenclature and abbreviations used.

specify N-acylsphingosines, so N-acylsphinganines are called dihydroceramides, and N-acyl-4D-hydroxysphinganines are often called “phytoceramides” or “4-hydroxydihydroceramides” (with the hydroxyl specified to distinguish them from  $\alpha$ -hydroxyceramides, where the hydroxyl group is on the fatty acid). These are the major species in most mammalian sphingolipids, and, in instances where other sphingoid bases are present, the names connote the added features of the backbone, if they have been determined (which is often not the case). The amide-linked fatty acids are typically saturated or monounsaturated with chain lengths from 14 to 26 carbon atoms (or even longer in the special case of skin), and sometimes have a hydroxyl group on the  $\alpha$ - or  $\omega$ -carbon atom. The abbreviated nomenclature for ceramides lists the features of the fatty acid after those of the sphingoid base; for example, N-palmitoylsphingosine can be abbreviated d18:1;16:0 or d18:1/16:0, and N- $\alpha$ -hydroxypalmitoylsphingosine is d18:1;h16:0 or d18:1/h16:0.

The so-called “complex” sphingolipids are comprised of a “ceramide” backbone with a headgroup in phospho- or glycosyl-linkage to the 1-hydroxyl (an enzyme that adds a fatty acid to the 1-hydroxyl has also been found, but its physiologic function is not yet clear) (Shayman and Abe, 2000). The major phosphosphingolipids of mammals are ceramide phosphates and sphingomyelins (ceramide phosphocholines); however, since other organisms have additional categories of phosphosphingolipids (e.g., ceramide

phosphoethanolamines and phosphoinositols), these broader categories are nonetheless encountered by mammals in food, and thus some microflora might be detected in some tissues if the methods are sufficiently sensitive. The major glycosphingolipids of mammalian organisms have glucose (Glc) or galactose (Gal) attached in  $\beta$ -glycosidic linkage, to which additional carbohydrates and functional groups may be attached. Glycosphingolipids are classified several ways, with the most general being to subdivide them into neutral glycosphingolipids, which contain one or more uncharged sugars such as Glc, Gal, N-acetylglucosamine (GlcNAc), N-acetylgalactosamine (GalNAc), and fucose (Fuc) versus acidic glycosphingolipids, which additionally contain ionized functional groups, phosphate, sulfate, or charged sugar residues such as sialic acid—a generic term that encompasses N-acetylneuraminic acid, NeuAc, and a large family of structurally related compounds that vary with the species (e.g., mice also have N-glycolyl-neuraminic acid, NeuGc).

The galactosylceramide (GalCer) branch is relatively small—about a half-dozen headgroup species—of which the sulfatides (sulfated GalCer and Gal-GalCer) are the most prevalent. In contrast, hundreds of glycolipids exist downstream from glucosylceramide (GlcCer), and additional information about their structures can be obtained from websites such as [www.glycoforum.gr.jp](http://www.glycoforum.gr.jp) and [www.sphingomap.org](http://www.sphingomap.org). The nomenclature for these compounds has been systematized (Chester, 1998), and is based on five major “root” glycans from which most of the more complex glycosphingolipids derive (ganglio-, Gg; globo-, Gb, and isoglobo-, iGb; lacto-,

Nomenclature for classification of glycosphingolipids					
Root name (Abbrev)	Carbohydrate in the “root” structure				Other subcategories
	IV	III	II	I	
Ganglio (Gg)	Gal $\beta$ 1-3GalNAc $\beta$ 1-4Gal $\beta$ 1-4Glc $\beta$ 1-Cer				
Lacto (Lc)	Gal $\beta$ 1-3GlcNAc $\beta$ 1-3Gal $\beta$ 1-4Glc $\beta$ 1-Cer				
Neolacto (nLc)	Gal $\beta$ 1-4GlcNAc $\beta$ 1-3Gal $\beta$ 1-4Glc $\beta$ 1-Cer				
Globo (Gb)	GalNAc $\beta$ 1-3Gal $\alpha$ 1-4Gal $\beta$ 1-4Glc $\beta$ 1-Cer				
Isoglobo (iGb)	GalNAc $\beta$ 1-3Gal $\alpha$ 1-3Gal $\beta$ 1-4Glc $\beta$ 1-Cer				
Mollu (Mu)	GalNAc $\beta$ 1-2Man $\alpha$ 1-3Man $\beta$ 1-4Glc $\beta$ 1-Cer				
Arthro (At)	GalNAc $\beta$ 1-4GlcNAc $\beta$ 1-3Man $\beta$ 1-4Glc $\beta$ 1-Cer				
Ganglioside (Gn)					Contain N-acetyl (NeuAc) or N-glycolyl- (NeuGc) neuraminic acid (Sialic acid)
(n = # of neuraminic acids; M(ono), D(di-), T(ri-), etc.)					
Galactose series					Gal $\beta$ -1Cer
Sulfatide					contain sulfate

**Figure 4.2** Classification of glycosphingolipids.

Lc, and neolacto-, nLc), as shown in Fig. 4.2. Use of these root names helps simplify the nomenclature somewhat. For example, the compound shown in Fig. 4.1 can be described as Neu5Ac $\alpha$ 2-3(Gal $\beta$ 1-3GalNAc $\beta$ 1-4)Gal $\beta$ 1-4Glc1-1Cer or as II<sup>3</sup>Neu5AcGg<sub>4</sub>Cer; however, in many cases, this is still so cumbersome that historic names for some of the more common compounds are often used (i.e., the same compound in Fig. 4.1 is called ganglioside GM1a). The Svennerhold system uses G to depict that the compound is a ganglioside, with the number of sialic acid residues denoted with a capital letter (i.e., *Mono*-, *Di*- or *Tri*-) plus a number reflecting the subspecies within that category, such as ganglioside GM1 versus GM3, etc. For a few glycosphingolipids, historically assigned names as antigens and blood group structures are also in common usage (e.g., Lexis x and sialyl Lewis x). It does not appear that a nomenclature has yet been chosen for sphingolipids that are covalently attached to protein (e.g.,  $\omega$ -hydroxy-ceramides and -glucosylceramides are attached to surface proteins of skin; inositol-phosphoceramides are used as membrane anchors for some fungal proteins).

## 2. ANALYSIS OF SPHINGOLIPIDS BY MASS SPECTROMETRY

Due to the structural complexity of sphingolipids, MS has been used for their analysis for decades; however, extension of the technology to quantitative analysis is a newer development.

### 2.1. Electron ionization-mass spectrometry

Electron ionization MS (EI-MS) was initially used to elucidate the structures of ceramides (Samuelsson and Samuelsson, 1968, 1969a) and neutral glycosphingolipids (Samuelsson and Samuelsson, 1969b; Sweeley and Dawson, 1969). These early experiments permitted the analysis of sphingolipids as intact molecular species and yielded diagnostic fragmentations that could distinguish isomeric structures (Hammarstrom and Samuelsson, 1970; Samuelsson and Samuelsson, 1970). Because these molecules were either relatively large or polar, they required derivatization to trimethylsilyl (64) or permethyl ethers to reduce the polarity and increase volatility for efficient transfer to the gas phase. However, EI induced extensive fragmentation owing to its relatively high-energy imparted during ionization, which in some cases prevented observation of intact higher mass molecular ions. Additionally, resolution of complex mixtures with varying headgroups, sphingoid bases, and N-acyl combinations was particularly challenging using these methods, as resulting spectra displayed multiple fragments from multiple precursors.

## 2.2. Fast atom bombardment and liquid secondary ionization mass spectrometry

Fast atom bombardment (FAB) and lipid secondary ionization mass spectrometry (LSIMS) are ionization techniques in which nonvolatile liquids are ionized off a probe tip by bombardment with a beam of either accelerated atoms or ions. FAB and LSIMS are considered to be much “softer” ionization techniques than EI because they eliminate the need for derivatization and yield intact molecular ions with less fragmentation, thus making them more amenable to analysis of somewhat complex mixtures of monohexosylceramides (Hamanaka *et al.*, 1989), sphingoid bases (Hara and Taketomi, 1983), and sphingomyelins (Hayashi *et al.*, 1989).

Structural information can also be obtained from these methods of MS analysis, especially if MS/MS analyses are employed to select an ion of interest, collisionally dissociate it, and detect the resultant product ions. When either  $(M + H)^+$  or  $(M - H)^-$  precursor ions fragment, they do so at specific positions to yield product ions distinctive for sphingolipid head-groups, sphingoid bases, and N-acyl fatty acids (Adams and Ann, 1993). These pathways of fragmentation can be influenced by the inclusion of alkali metal ions as  $(M + Me^+)^+$  where  $Me^+ = Li^+, Na^+, K^+, Rb^+,$  or  $Cs^+$  (Ann and Adams, 1992).

A limitation of FAB and LSIMS is that both require a matrix to ionize the analyte. These matrices induce a significant amount of background chemical noise, which can limit sensitivity, especially for lower molecular mass species, such as the free sphingoid bases. Methods such as Dynamic FAB (Suzuki *et al.*, 1989, 1990) partially solved this problem with continuous application of solvent and matrix to the probe tip; however, the  $\sim 100$ -fold reduction in background noise was not enough to completely eliminate background chemical noise from the matrix at low analyte concentrations.

## 2.3. Electrospray ionization

The electrospray ionization method allows solutions containing sphingolipids to be infused directly into the ion source of a mass spectrometer through a hollow metal needle that is held at a high positive or negative potential. At the ending tip of the needle, highly charged droplets form and are drawn into the orifice of the MS by both a potential and an atmospheric pressure difference. During transition from atmospheric pressure to vacuum, the solvent evaporates, whereas the analyte of interest remains as an ionized species in the gas phase. ESI is a much softer ionization technique, and yields primarily intact ions with little or no fragmentation when the ionization conditions have been optimized.

## 2.4. Liquid chromatography, electrospray ionization, mass spectrometry and tandem mass spectrometry

Since ESI already involves infusion of liquids into the MS, it is a logical extension to use ESI-MS to analyze the eluates from liquid chromatography. From the MS perspective, this has the advantage that the LC can be used for desalting of the compounds of interest as well as to enhance the sensitivity by chromatographic focusing of the sample in a small volume, in addition to whatever desirable separations have been achieved as a result of the LC (e.g., to separate isomers that might not be distinguished by MS alone). LC also reduces the complexity of the eluent at any given elution time, which greatly decreases ionization suppression effects from other species, further improving quantitative accuracy and sensitivity.

LC-MS/MS has been used to identify, quantify, and determine the structures of free sphingoid bases, free sphingoid base phosphates, ceramides, monohexosylceramides (both galactosylceramides and glucosylceramides), lactosylceramides, sphingomyelins (Merrill *et al.*, 2005; Sullards, 2000; Sullards and Merrill, 2001), and more complex glycosphingolipids (Kushi *et al.*, 1989; Suzuki *et al.*, 1991). Complete chromatographic resolution of all individual species is not required in LC-MS/MS because the mass spectrometer is able to differentiate between many components present in a mixture by their mass and structure (e.g., all of the N-acyl chain-length variants of Cer) (Bielawski *et al.*, 2006; Merrill *et al.*, 2005; Pettus *et al.*, 2003; Sullards and Merrill, 2001). Sphingolipid separations have mainly been distributed between two types of LC: reversed phase (Kaga *et al.*, 2005; Lee *et al.*, 2003; Merrill *et al.*, 2005) for separations based on the length and saturation of N-acyl chains (e.g., to separate sphingosine and sphinganine) and normal phase (Merrill *et al.*, 2005; Pacetti *et al.*, 2005; Pettus *et al.*, 2004) to separate compounds primarily by their headgroup constituents (e.g., resolving ceramide from sphingomyelin, etc.). The advantages that are derived from LC separation prior to MS may not be immediately obvious. For example, sphingosine and sphinganine have easily resolved precursor and product ions and can be analyzed without LC; however, sphingosine is typically much more abundant in biological samples than sphinganine, and the  $(M + 2)$  isotope of sphingosine, which has the same precursor mass-to-charge ratio ( $m/z$ ) as sphinganine, interferes with the quantitation of sphinganine unless the sphingoid bases have been separated by LC (Merrill *et al.*, 2005).

## 2.5. MALDI, mass spectrometry, and tandem mass spectrometry

Matrix-assisted laser desorption/ionization (MALDI) has been used to identify ceramides, monohexosylceramides, and sphingomyelins (Fujiwaki *et al.*, 1999) as well as complex glycosphingolipids such as lactosylceramides

and gangliosides (Suzuki *et al.*, 2006). Samples are prepared for MALDI by mixing a solution containing the analyte with a solution containing a MALDI matrix compound, which is typically a small substituted organic acid that contains a moiety that can absorb the photonic energy of the laser. Absorption of the laser energy causes the matrix to become vibrationally excited and volatilize, taking analyte molecules with it into the gas phase and inducing charge exchange reactions between the excited matrix compound and the analyte. This causes the analyte to become ionized, typically as a singly charged species even if the analyte has multiple potentially ionizable moieties. Therefore, one advantage of MALDI ionization is that compounds that might otherwise give complex spectra due to multiple ionization states will show fewer peaks in MALDI. Choice of the matrix is key to successful generation of intact molecular species with minimal fragmentation and has been thoroughly reviewed (David, 2006). A complication in MALDI is that the matrix produces background chemical noise at lower  $m/z$  values that can preclude analysis of smaller compounds. MALDI ionization is typically used in conjunction with time-of-flight (TOF) mass analyzers because the laser pulse and resulting ion plume provide a discreet event that is compatible with TOF mass analysis.

### 3. ANALYSIS OF SPHINGOLIPIDS BY “OMIC” APPROACHES

The large numbers of compounds and the wide range of chemical properties—from essentially water-insoluble for ceramides to highly water-soluble sphingosine 1-phosphate and some glycosphingolipids—pose special challenges in the development of methods that can analyze a significant fraction of the sphingolipidome. First, one must have a method that extracts all of the compounds from the biological sample of interest. Then, the compounds must be detected in ways that distinguish even compounds that are closely related structurally (and in some cases, are isobars or isomers, such as GlcCer and GalCer). Ultimately, the methods should be able to establish the amounts of each compound, or at least to be able to detect changes or differences.

Some laboratories have approached this by so-called “shotgun” methodologies where mixtures of compounds in relatively crude extracts are ionized by ESI or MALDI, and the identities of the compounds of interest in the complex mass spectra are discerned by methods such as fragmentation followed by subsequent MS/MS (see “Other Methods” section). This approach is a sensible one for an initial survey of an extract from a biological material; however, many dangers are inherent in “shotgun” lipidomics, not the least of which is its inability to discern differences between isomeric species (such as GlcCer and GalCer); the frequent occurrence of other compounds in



crude extracts may affect ionization and, hence, not only complicate quantitative analysis but also lead to the impression that some compounds are not present when they actually are. Modifications of the shotgun approach that use a pre-MS fractionation method such as LC greatly improve its reliability.

An alternative approach is to develop LC-MS/MS methods for a more modest number of compounds in which the structural identification and quantitation are more robust from the outset, then add more species as experience (and the availability of the appropriate internal standards) allows. This approach was taken by the Sphingolipid Core of the LIPID MAPS Consortium under the descriptor “inside-out sphingolipidomics,” which refers to a focus on methodologies that establish the nature and amounts of the lipid backbones (sphingoid bases and ceramides) followed by the more complex derivatives. Thus, the categories of compounds that are currently covered by these methods follow the *de novo* biosynthetic pathway (as well as turnover of the lipid backbones), as summarized in Fig. 4.3.

LC-MS/MS was chosen because it provides: (1) a high level of specificity with regard to differentiation of complex molecular species via retention time, molecular mass, and structure; (2) levels of sensitivity that are orders of magnitude higher than that of classical techniques—often  $\sim 1$  fmole or less, as is needed for analysis of small samples ( $\sim 10^3$  to  $10^6$  cells); and (3) signal responses that can be more readily correlated with the amounts of the analytes across a wide dynamic range, which is important for the “omics” analysis to be useful for systems biology studies. In spite of all these positive attributes, one still needs to be careful in the choice of sample handling and extraction protocols, validation of the internal standards, and other aspects for LC-MS/MS to fulfill its promise as a quantitative MS analysis technique. The separation that is achieved by LC can have the desired effect of removing ionization-suppressing contaminants, and possibly resolving isomeric species that could compromise the analysis; however, it might also make it difficult to obtain uniform ionization of unknowns and standards if they elute from the LC under different solvent conditions. Thus, in the selection of an LC method, it is desirable to have as many as possible of the analytes elute in the same fraction as the standards and, when this is not possible, to have enough internal standards to assess any variation in ion yield that might be affected by the solvent composition where the analytes elute.

Fortunately, sphingolipids tend to be readily ionized, and many fragment to produce abundant and distinctive product ions that are indicative of the headgroup, sphingoid base, or fatty acid moieties (Fig. 4.4). Free sphingoid bases and most complex sphingolipids ionize readily via ESI in the positive ion mode to form  $(M + H)^+$  ions, and sphingoid base-1-phosphates, ceramide-1-phosphates, sphingomyelins, sulfatides, and gangliosides form abundant  $(M - H)^-$ ,  $(M - 15)^-$ , and  $(M - nH)^{n-}$  species, respectively, when ionized in the negative ion mode. Each also undergoes structure-specific fragmentation that can be used for identification in MS/MS mode as a precursor-product pair or by neutral loss.

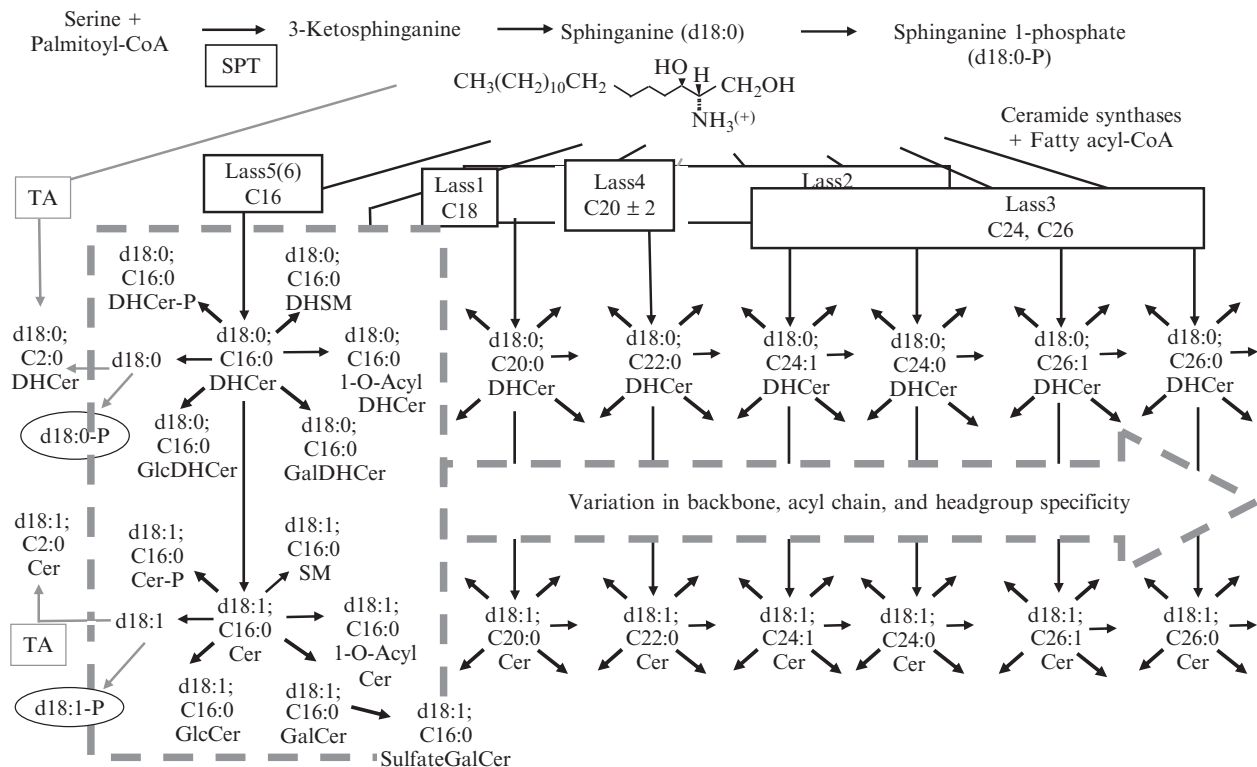


**Figure 4.3** Partial metabolic pathway for sphingolipid biosynthesis (and turnover of ceramide) summarizing the compounds analyzed by the sphingolipidomic method described in this review, with structures of selected species and numerically designated enzymatic reactions. CerS/Lass refers to the gene family for ceramide synthases that have the shown selectivity for fatty acyl-CoAs to produce the compounds shown. Also shown is the transacylase that can form N-acetyl-sphingoid bases (C2-ceramide); a separate enzyme produces the 1-O-acylceramides. For simplicity, the downstream metabolites are only shown for the C16:0 subspecies; however, the same complexity will be found for the other subspecies. For other abbreviations, see Fig. 4.1.

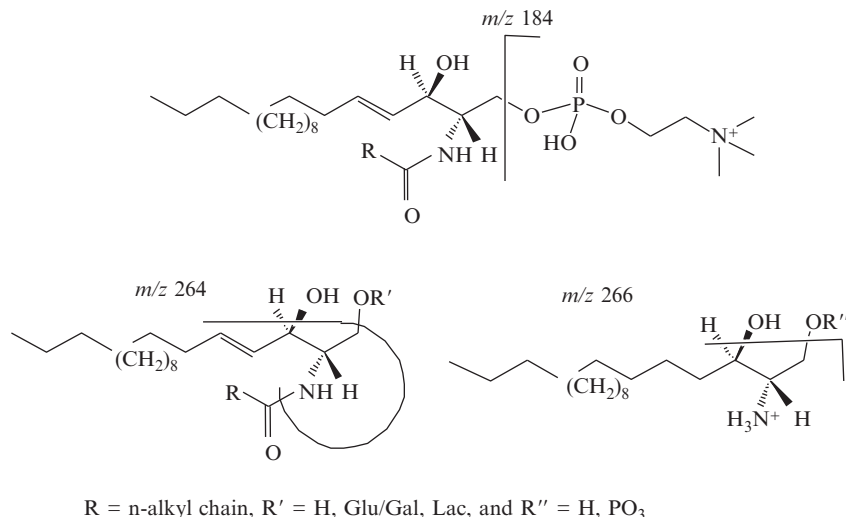


**Figure 4.4** Fragmentation of sphingolipids observed in the positive ion mode. Fragmentation of long-chain bases, long-chain base phosphates, ceramides, and monohexosylceramides involves dehydration at the 3-position, dehydration at the 1-position, or cleavage of the 1-position moiety with charge retention on the sphingoid base. Sphingomyelin similarly cleaves at the 1-position; however, the charge is retained on the phosphoryl choline headgroup yielding the  $m/z$  184 ion.

Much of the power of LC-MS/MS lies in the improbability that many biomolecules will have the same characteristics on LC, ionize to yield the same precursor  $m/z$ , and give the same fragment ion(s). This said, in LC-MS/MS, there is a trade-off in the amount of time that one can spend resolving the categories of compounds of interest by LC (i.e., one tries to keep the time for the LC as short as possible to allow more samples to be run) versus the multireaction monitoring (MRM) pairs that can be monitored during the time when compounds of interest are eluting from the column.

The sphingolipidomic method developed for the LIPID MAPS Consortium uses LC-MS/MS and has been used to identify and quantify a wide range of sphingolipids by optimizing the extraction yields (Fig. 4.5), LC, and MS parameters (Fig. 4.6), as described below for the published methods (Merrill *et al.*, 2005; Sullards and Merrill, 2001) with minor modifications, along with a brief description of the newer methods that are in development for sulfatides and other species.

## 4. MATERIALS AND METHODS

Many methods have been developed for analysis of sphingolipids from the first intermediates of the *de novo* biosynthetic pathway (i.e., 3-ketosphinganine, sphinganine and sphinganine 1-phosphate, and

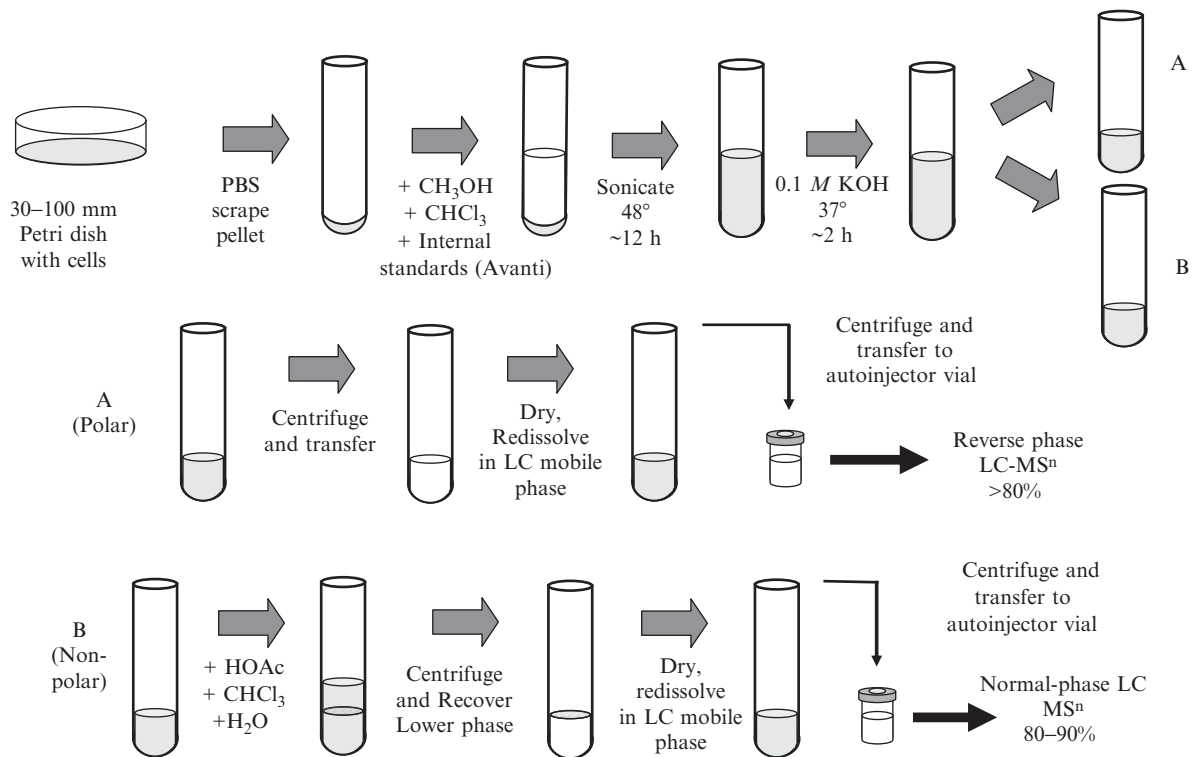


**Figure 4.5** Summary of the extraction scheme used for these methods.



dihydroceramides) through the metabolites of ceramide (ceramide phosphate, sphingomyelin, GlcCer, GalCer, and sphingosine and sphingosine 1-phosphate).

## 5. MATERIALS

### 5.1. Biological samples

The biological sample can range from cells in culture (typically  $1 \times 10^6$  cells, but depending on the analyte of interest, several orders of magnitude fewer cells might be sufficient). The same protocol is also effective with many other biological samples, such as 1 to 10 mg of tissue homogenates at 10% wet weight per volume in phosphate-buffered saline (PBS), small volumes (1 to 10  $\mu\text{l}$ ) of blood, urine, and the like. However, the recovery and optimization of the extraction volume, time, and other aspects should be tested for each new sample type. Tissue culture medium (typically 0.1 to 0.5 ml) can also be analyzed, but should be lyophilized first (in the test tubes described in the next paragraph) before extraction to reduce the aqueous volume. When the samples are prepared, aliquots or duplicate samples should be assayed for the normalizing parameter ( $\mu\text{g}$  DNA, mg protein, cell count, etc.) to be used. In our experience, it is best to do these assays first because, if they fail, the effort invested in the lipid analysis will be wasted.

The samples should be placed in Pyrex  $13 \times 100$ -mm borosilicate, screw-capped glass test tubes with Teflon caps (the Corning number for these tubes with Teflon-lined caps is 9826-13). It is vital that these specific tubes be used because transfer of samples from one container to another is often a source of variability and frustration. The samples should be stored frozen at  $-80^\circ$  until extracted. If it is necessary to ship the samples, this should be done in a shipping container that keeps the vials frozen, separated, and “right-side-up,” such as Exakt-Pak containers (catalog number for containers holding up to 20 vials, MD8000V20; for 40 vials, MD8010V40) (<http://www.exaktpak.com/>).

## 6. EXTRACTION

The steps of this extraction scheme have been summarized in [Fig. 4.5](#).

1. Start with the samples in  $13 \times 100$ -mm screw-capped glass test tubes with Teflon caps. Most samples (washed cells, tissue homogenates, etc.) will already have an approximate aqueous volume of  $\sim 0.1$  ml; if not (e.g., if the sample has been lyophilized), bring to this volume with water.

2. Add 0.5 ml of methanol, then 0.25 ml of chloroform and the internal standard cocktail (which contains 0.5 nmol each of the C12:0 fatty acid homologs of SM, Cer, GlcCer, LacCer, and ceramide 1-phosphate; C25-ceramide; and d17:1 sphingosine, d17:0 sphinganine, d17:1 sphingosine 1-phosphate, and d17:0 sphinganine-1-phosphate) (Avanti Polar Lipids, Alabaster, AL).
3. Sonicate as needed to disperse the sample, then incubate overnight at 48° in a heating block.
4. Cool and add 75  $\mu$ l of 1 M KOH in methanol, sonicate, and incubate 2 hr at 37°. (This step reduces clogging of the LC columns, but can be eliminated for some samples, if desired.)
5. Transfer half of the extract (which will be used for analysis of the more polar sphingolipids, such as sphingoid bases and sphingoid base 1-phosphates, by reverse phase LC-ESI-MS/MS) (0.4 ml) to a new test tube (this will be used in the next section).
6. To the half of the extract that remains in the original test tube(s), add 3  $\mu$ l of glacial acetic acid to bring the pH to  $\sim$  neutral, then add 1 ml of chloroform and 2 ml of distilled, deionized water, and mix with a rocking motion to avoid formation of an emulsion.
7. Centrifuge in a tabletop centrifuge to separate the layers, then carefully remove the upper layer with a Pasteur pipette, leaving the interface (with some water).
8. Evaporate the lower phase to dryness under reduced pressure (using a stream of N<sub>2</sub> or a speed vac) and save this fraction for normal phase LC-ESI-MS/MS of the complex sphingolipids.

### 6.1. Preparation of samples for LC-MS/MS

For the sphingoid base fraction (Step 5 in “Extraction” section), use a tabletop centrifuge to remove insoluble material, then transfer to a new glass test tube and evaporate the solvent under N<sub>2</sub> or reduced pressure (speed vac). Add 300  $\mu$ l of the appropriate mobile phase (as shown later) for reverse-phase LC-ESI-MS/MS, sonicate, then transfer to 1.5-ml micro-fuge tubes (organic solvent resistant) and centrifuge for several minutes or until clear. Transfer 100  $\mu$ l of the clear supernatant into a 200- $\mu$ l glass autoinjector sample vial for LC-ESI-MS/MS analysis.

Prepare the extract for normal-phase LC-ESI-MS/MS (Step 8 in “Extraction” section) in the same manner, but using the appropriate mobile phase.

**Note:** For some samples, slightly higher recoveries and/or more uniform recoveries across different sphingolipid subspecies are obtained if the residue from these redissolving steps are treated again and the extracts pooled.

## 7. IDENTIFICATION OF THE MOLECULAR SPECIES BY TANDEM MASS SPECTROMETRY

The first step of the analysis is to identify the molecular subspecies of each category of sphingolipid that is present by analysis of their unique fragmentation products using precursor ion or neutral loss scans. Once these subspecies have been identified, the investigator can build an MRM protocol for quantitative analysis of those analytes for which both the ionization and dissociation (collision energy) conditions have been optimized for individual molecular species. These parameters will vary from instrument to instrument, and thus are left to the investigator to perform based on their own circumstances (examples of parameters have been given in [Merrill \*et al.\*, 2005](#)). A general scheme for the instrumentation is given in [Fig. 4.6](#).

### 7.1. Materials for infusion and LC-ESI-MS/MS

Positive-ion infusion spray solution: CH<sub>3</sub>OH/HCOOH (99:1) (v:v) containing 5-mM ammonium formate.

Reverse-phase LC:

1. The recommended reverse-phase LC column is a Supelco 2.1 mm i.d. × 5 cm Discovery C18 column (Supelco, Bellefont, PA).
2. The following are solvents for reverse phase LC:
  - a. Reverse-phase LC solution A: CH<sub>3</sub>OH/H<sub>2</sub>O/HCOOH (74:25:1) (v:v:v) with 5-mM ammonium formate
  - b. Reverse-phase LC solution B: CH<sub>3</sub>OH/HCOOH (99:1) (v:v) with 5-mM ammonium formate

Normal-phase LC:

1. The recommended normal-phase column is a Supelco 2.1 mm i.d. × 5 cm LC-NH<sub>2</sub> column, with the exception for the LC method for separation of GlcCer and GalCer, which uses a Supelco 2.1 mm i.d. × 25 cm LC-Si column.
2. The following are solvents for normal-phase LC:

Normal-phase solvent A: CH<sub>3</sub>CN/CH<sub>3</sub>OH/CH<sub>3</sub>COOH (97:2:1) (v:v:v) with 5-mM ammonium acetate

Normal-phase solvent B: CH<sub>3</sub>OH:CH<sub>3</sub>COOH (99:1) (v:v) with 5-mM ammonium acetate

### 7.2. Sphingolipid subspecies characterization prior to quantitative LC-MS/MS analysis

1. Dilute a 50- $\mu$ l aliquot (one-sixth of complex fraction) of the reconstituted sample for complex sphingolipid analysis (as described in Section 6.1) to a final volume of 1 ml with positive ion infusion spray solution.



2. Infuse this solution into the ion source with a 1-ml syringe at 0.6 ml/hr.
3. Perform precursor ion scan(s) for predetermined unique molecular decomposition products (e.g., fragment ions of  $m/z$  264 and 266 for the d18:1 and d18:0 sphingoid base backbones, respectively, and  $m/z$  184 for SM, etc.).
4. Identify the sphingolipid precursor and product ion pairs for species present, noting potential isobaric combinations of sphingoid base and N-acyl fatty acids.

Note: At this point, it is usually most time-efficient to reanalyze the sample by LC-ESI-MS/MS using the LC method described below since the final optimization of the ionization parameters will need to be done with the same solvent composition as the compounds of interest elute from LC.

5. Using the “parts list” of species (Fig. 4.4) for each observed subspecies, determine the optimal ionization conditions and collision energy for each species. Typically, collision energy will need to be increased within each sphingolipid class as the N-acyl chain or sphingoid base increases in length.

## 8. QUANTITATION BY LC-ESI-MS/MS USING MULTIREACTION MONITORING

The optimized ionization and fragmentation conditions for each analyte of interest, combined with the LC elution position, are used to construct the MRM analysis protocols. In MRM, the mass spectrometer is programmed to monitor specific, individually optimized precursor and product ion pairs (with respect to instrument parameters for highest yield of the precursor and product ions of interest) in specific LC timeframes. The signal generated by each ion transition in most cases uniquely identifies a particular molecular species by retention time, mass, and structure, although there are still rare occasions where another compound adds to the signal; hence, whenever possible, samples should be examined for this possibility by another technique, such as further analysis of the ions of interest by tandem MS or by an orthogonal technique, such as comparing the results of other types of chromatographic separation, ionization (e.g., positive versus negative ion mode), and fragmentation. To determine the relationships between the signal response for the spiked internal standard (which can be very close to 1:1 for some instruments, such as the ABI 4000 QTrap when the MRM parameters have been optimized) and a correction factor (if needed), one typically compares the internal standard with the analyte of interest (e.g., the 17 carbon homolog of sphingosine [d17:1] versus naturally occurring sphingosine [d18:1]; in the case of more complex sphingolipids, C12-chain-length internal standard vs at least two chain length variants,

such as the C16- and C24-chain-length versions of the analyte, which are usually available commercially [from Avanti Polar Lipids, Alabaster, AL, Matreya, Pleasant Gap, PA, among others]). This comparison has been performed for all of the species covered by the standard cocktail mix, and a very high equivalence exists between the ion yields of most of the naturally occurring analytes and the selected standard when analyzed using the ABI 4000 QTrap; however, some categories show more deviation using the API 3000 triple quadrupole instrument, which illustrates the need to determine these relationships for the particular instrument being used for the analysis.

### 8.1. Analysis of sphingoid bases and sphingoid base 1-phosphates in positive ion mode

1. Portions of the reconstituted samples (prepared above) are diluted with reverse-phase LC solutions A and B for a final A:B ratio of 80:20 (v:v). (If it is desirable to concentrate the sample, the solvent can be removed by evaporation and then the residue redissolved in this solvent mixture.) The samples are centrifuged to remove any precipitate, and then placed in autosampler vials and loaded into the autosampler.
2. The LC column (reverse-phase C18) is equilibrated with reverse-phase LC solution A and B (80:20) for 0.5 min at flow rate of 1.0 ml/min.
3. The sample (typically 10 to 50  $\mu$ l) is injected (then the needle is programmed to wash with at least 5 ml of reverse-phase solution A to prevent potential sample carryover) and the following elution protocol is followed (at a flow rate of 1.0 ml per minute):
  - a. Wash the column for 0.6 min with reverse-phase solutions A and B (80:20, v:v).
  - b. Apply a linear gradient to 100% of reverse-phase solution B over 0.6 min.
  - c. Wash with 100% reverse-phase solution B for 0.3 min.
  - d. Apply a linear gradient to reverse-phase solution A:B (80:20) over 0.3 min.
  - e. Re-equilibrate the column with a 80:20 mix of reverse-phase solutions A and B for 0.5 min.
4. Determine the areas under the peaks for internal standards and analytes of interest using extracted ion chromatograms.
5. Quantify analytes relative to internal standard spike.

During the LC run, the ions of interest are followed as described by [Merrill \*et al.\* \(2005\)](#), with the salient points summarized here with comparisons between two types of mass analyzers, a triple quadrupole MS/MS (the API 3000), and a hybrid quadrupole-linear ion trap (ABI 4000 QTrap, Applied Biosystems, Foster City, CA). Positive mode analysis of the  $(M + H)^+$  ions of

long-chain bases such as sphingosine (d18:1), sphinganine (d18:0), 4-D-hydroxysphinganine (t18:0), the 17-carbon homologs (d17:1 and d17:0), and the 20-carbon homologs (d20:1 and d20:0) by MS/MS reveals that they fragment via single and double dehydration to product ions of  $m/z$  282/264, 284/266 (sphinganine also fragments to a headgroup ion with  $m/z$  60 that can be followed to avoid overlap with sphingosine isotopes), 300/282/264, 268/250, 270/252, 310/292, and 312/294, respectively. The ratios between single- and double-dehydration products varies by collision energy and type of mass spectrometer. Signal response for the single-dehydration products is greater than double-dehydration products in the ABI 4000 QTrap (even given higher collision energies), whereas in the API 3000 triple quadrupole, the ratio is reversed, with a much stronger double-dehydration signal than for single dehydration. Sphingoid base 1-phosphates derivatives undergo a similar dehydration and cleavage of the headgroup to yield the same  $m/z$  product ions as the double-dehydrated product ions described above; however, this does not interfere with their analysis in the same run because they are distinguished both by their precursor ion mass and retention times on LC.

Ionization parameters for sphingoid bases and sphingoid base 1-phosphates are similar for sphingoid bases containing 17 to 20 carbons. (In the API 3000 triple quadrupole ionization, settings are identical; however small eV differences are required in the ABI 4000 QTrap to achieve optimal signal response.) The main variable in these analyses is collision energy, which increases with sphingoid base chain length. Modifications to sphingoid bases such as N-methylation, additional sites of unsaturation, and hydroxyl addition will also require increasing collision energy and can be detected by shifts in precursor and product ion  $m/z$  as well as alteration of reverse-phase LC retention. Although one must check if there are changes in ion yield due to differences in the elution solvent, possible ion suppressing compounds in crude extracts, or other changes when compounds in a subspecies series elute slightly differently from the LC, small shifts in retention provide a useful verification of the identities of the species when product ions are otherwise identical.

Notes on 3-ketosphingoid base analysis: 3-Ketosphinganine (3kSa) can be analyzed by reverse-phase LC with the other sphingoid bases. It has the same precursor  $m/z$  as sphingosine, and, although there are differences in the degree of dehydration in the fragments (sphingosine fragments primarily to  $m/z$  264 whereas 3-ketosphinganine fragments to  $m/z$  282), the most reliable way to differentiate these compounds is by examining the differences in elution on reverse-phase LC (3-ketosphinganine elutes after sphingosine). Interestingly, one also finds 3-keto-sphingoid bases as part of 3-ketodihydroceramides, which are identifiable by earlier elution on normal-phase LC as peak pairs with normal ceramide (with 3-ketodihydroceramide eluting first).

## 9. ANALYSIS OF (DIHYDRO)CERAMIDES, (DIHYDRO)SPHINGOMYELINS, AND (DIHYDRO)MONOHEXOSYL-CERAMIDES IN POSITIVE ION MODE

1. Portions of the reconstituted samples (as prepared in a previous section) are diluted with normal-phase solution A. (If it is desirable to concentrate the sample, the solvent can be removed by evaporation and the residue redissolved in this solvent mixture.) The samples are centrifuged to remove any precipitate and then placed in autosampler vials and loaded into the autosampler.
2. The normal-phase LC-NH<sub>2</sub> column (Supelco 2.1 mm i.d. × 5 cm LC-NH<sub>2</sub>) is equilibrated for 0.5 min with normal-phase solution A (98:2, v:v) at 1.5 ml/min.
3. The sample (typically 10 to 50 μl) is injected (then the needle is programmed to wash with at least 5 ml of normal-phase solution A to prevent potential sample carryover), and the following elution protocol is followed (at a flow rate of 1.5 ml/min):
  - a. Wash the column 0.5 min with normal-phase solution A.
  - b. Apply a linear gradient to 10% normal-phase solution B over 0.2 min.
  - c. Hold at A:B (90:10, v:v) for 0.5 min.
  - d. Gradient over 0.4 min to normal-phase solutions A and B (82:18, v:v).
  - e. Hold at A:B (82:18, v:v) for 0.6 min.
  - f. Apply a linear gradient to 100% normal-phase solution B over 0.4 min.
  - g. Re-equilibrate the column with normal-phase solution A for 0.5 min.

**Note:** By this protocol, one monitors the specific precursor and product ion transitions for ceramides for the first 0.8 min, followed by monohexosylceramides for 1.15 min and then sphingomyelins for 1.05 min; however, due to age or brand of column, the elution of monohexosylceramides may shift, requiring time adjustment as needed.

Note regarding chromatography in general: It is useful to bear in mind that, when converting methods between two different size columns, it is advisable to convert flow rates, hold times, and gradients based on column volume. Pre-gradient holds should be at least five to six column volumes worth of solvent; for maximum resolution during a gradient, solvent change per column volume should be 2 to 4%. For the columns described in this review, the lengths described correspond to the column volumes in parentheses: 2.1 × 50 mm (0.11 ml), 2.1 × 150 mm (0.33 ml), and 2.1 × 250 mm (0.55 ml). Also, as columns are changed, check the recommended flow rates for that column length.

4. Determine the areas under the peaks for internal standards and analytes of interest using extracted ion chromatograms.
5. Quantify analytes relative to internal standard spike.

Product ion analysis of the  $(M + H)^+$  ions of ceramides reveals cleavage of the amide bond and dehydration of the sphingoid base to form highly abundant, structurally specific fragment ions. These product ions yield information regarding the number of carbon atoms in the chain, degree of hydroxylation, unsaturation, or other structural modifications of the long-chain base (e.g., sphingosine,  $m/z$  264; sphinganine,  $m/z$  266; and 4-hydroxysphinganine,  $m/z$  264—which is the same as for sphingosine-based ceramides, but these can be distinguished by differences in LC elution times). With this knowledge about the sphingoid base composition and the original precursor  $m/z$ , the identity of the fatty acids can be deduced.

Ionization parameters for complex sphingolipids are linked to their headgroup classes with size and charge of headgroup playing key roles. Accordingly, differences in N-acyl chain length somewhat shift the required collision energy (in our experience,  $\sim 2.5$  eV every two to four carbons).

Product ion scans of the  $(M + H)^+$  ions of GlcCer, LacCer, and more complex glycolipids reveal that these ions undergo dissociation by two pathways: cleavage at the glycosidic linkage(s) at low collision energies with loss of the carbohydrate headgroup as a neutral species with charge remaining on the ceramide moiety and cleavage of both the sugar headgroup and the fatty acid acyl chain at higher energies with charge retention on the dehydrated sphingoid base.

Low energy dissociation to remove the headgroup can be useful for analyzing glycosidic linkages in neutral glycolipids and gangliosides; however, for quantitation of individual sphingoid base and N-acyl fatty acid combinations of monohexosylceramides, high energy dissociations to the sphingoid base-specific product ion are preferable. Choosing this fragmentation pathway allows distinction of isobaric d18:1/C18:0 versus d20:1/C16:0 glucosylceramides, which would have the same low energy deglycosylated fragment  $m/z$  566 but high-energy conjugated carbocation fragments that differ ( $m/z$  264 versus  $m/z$  292, respectively).

Sphingolipids containing phosphodiester-linked headgroups, such as in sphingomyelin (SM), fragment very differently: the  $(M + H)^+$  species fragments at the phosphate-ceramide bond, with charge retention on the phospho-headgroup to yield highly abundant ions of  $m/z$  184. Ceramide phosphoethanolamines (CPE) also fragment at the phosphate-ceramide bond, but the headgroup is lost as a neutral species of mass 141 u.

### 9.1. Modifications for analysis of glucosylceramides and galactosylceramides

Because GlcCer and GalCer elute in the same fractions by the above method, biological samples that contain both of these monohexosylceramides must be analyzed by a separate method.

1. Reconstitute the samples in normal-phase solution A and load into the autosampler.
2. Pre-equilibrate a normal phase LC-Si column (Supelco 2.1 mm i.d.  $\times$  25 cm LC-Si) for 1.0 min with a normal-phase solution A at 1.5 ml per min.
3. Inject 50  $\mu$ l of each reconstituted extract and continue to elute with normal-phase solution A at 1.5 ml/min for 8 min. GlcCer elutes at 2.56 min and GalCer at 3.12 min using this isocratic normal-phase system.  
Note: GlcCer and GalCer are isobaric species, so only one MRM transition is needed per shared sphingoid base and fatty acid combination.
4. Determine the areas under the peaks for internal standards and analytes of interest using extracted ion chromatograms and quantify analytes relative to internal standard spike.

## 9.2. Analysis of ceramide 1-phosphates by positive and negative ion modes

Ceramide 1-phosphates may be examined by the reverse-phase LC method described above for sphingoid bases and sphingoid base 1-phosphates by extending the final wash with 100% reverse-phase LC solution B until the ceramide 1-phosphates elute (C12-ceramide phosphate elutes at the beginning of the change to this solvent, followed by longer chain-length species).

An orthogonal approach (normal-phase LC negative mode following phosphate as the product ion in the MRM) can also be employed using either silica (LC-Si) or diol (LC-Diol) columns (Supelco) in conjunction with elution solvents that contain triethylammonium acetate (TEAA) and begin with acetonitrile and gradient to methanol and water (formic acid and ammonium formate buffer systems can also be used because they allow CerP to ionize well in negative mode).

In positive mode, the major fragments from ceramide 1-phosphate arise from cleavage of the amide bond and dehydration of the sphingoid base to form  $m/z$  264 (for sphingosines), 266 (for sphinganine), and so on. As with the other complex sphingolipids, to maintain ionization efficiency, collision energy should be increased slightly with chain length. In negative mode, the major product ion from the precursor  $(M - H)^-$  ions is phosphate. This can be used for quantitation; however, the fidelity of the MRM pair for ceramide 1-phosphate should be confirmed since the product is no longer structure-specific for the sphingoid base and N-acyl chain combinations.

## 9.3. Analytical methods for additional analytes

Methods for more complex glycosphingolipids are still under development. Sulfatides are readily analyzed in negative ion mode and yield primarily  $(M - H)^-$  ions that fragment to the sulfate group ( $m/z$  96.9)

(lower-abundance fragment ions representing the lipid backbone can also be observed). For LC, either reverse- (C18) or normal- (LC-Si or LC-Diol) phase columns can be used, with methanol/water gradients to methanol (with 5 mM ammonium acetate and 0.01% ammonium hydroxide to promote ionization) for reverse phase. For normal phase, acetonitrile, methanol, and water combinations (with the same mobile phase modifiers or triethylammonium acetate) achieve satisfactory LC resolution.

Gangliosides also ionize readily in the negative ion mode in methanol. For gangliosides analyzed by the triple quadrupole MS/MS, the  $(M - 2H)^{2-}$  ions fragment to yield highly abundant  $C1\beta-H_2O$  ions of  $m/z$  290, which reflect the N-acetyl neuraminic acid moiety (Figs. 4.7 and 4.8). The enhanced product ion scan feature that is available using the ion trapping function of the 4000 QTrap provides more structural information because it yields better sensitivity and more abundant high mass product ions (Fig. 4.8). Additionally, cleavage at the glycosidic bonds produces characteristic  $Y_n$ -type ions and through ring cleavages, such as  $^{2,4}X_{2\alpha}$  and  $^{2,4}X_{3\alpha}$  ( $m/z$  1351.9 and 1512.8, respectively), which are useful for determination of glycosidic bond linkage.

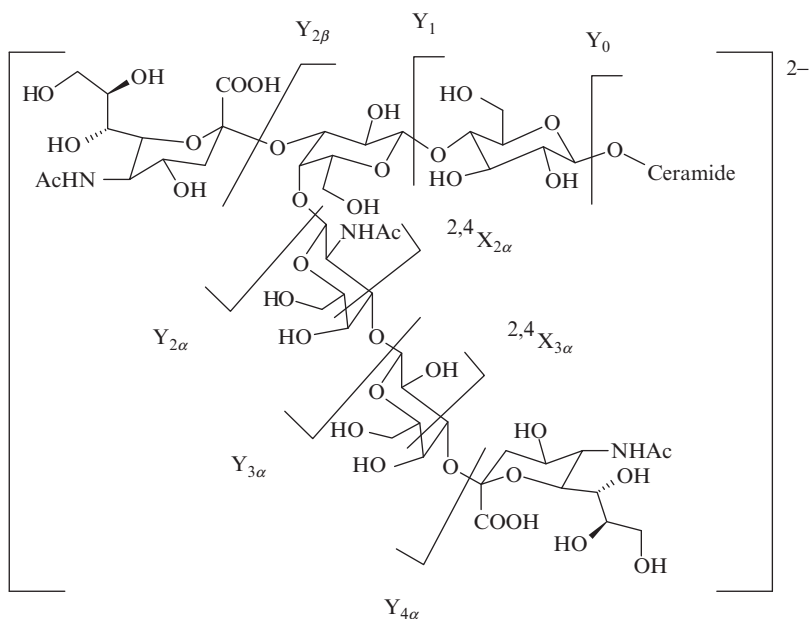


**Figure 4.7** Structure of ganglioside GD1a and major cleavage sites and nomenclature.

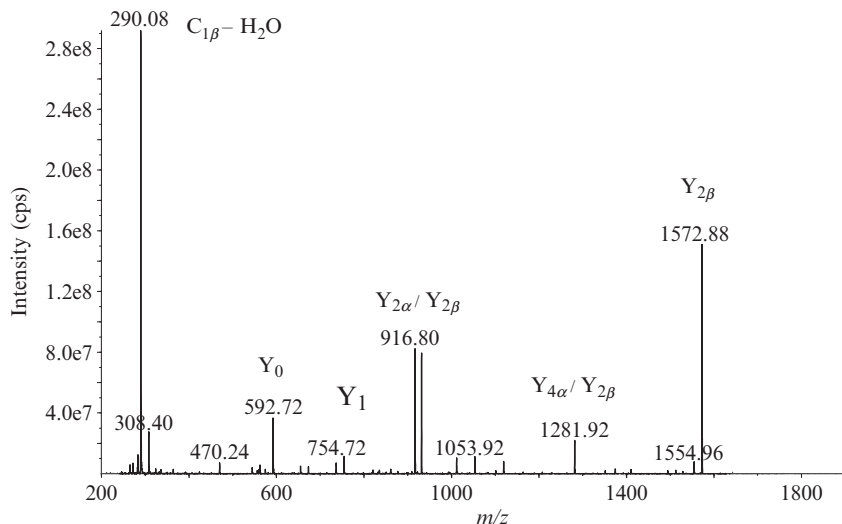


**Figure 4.8** Tandem mass spectrometry analysis of ganglioside GD1a using the 4000 QTrap in enhanced product-ion scanning (EPI) mode (~55 fmol consumed). See Fig. 4.7 for the cleavages represented by these labels.

An MS/MS/MS ( $MS^3$ ) analysis is performed much the same manner as a product ion scan. In this case the first mass analyzer (Q1) is set to pass the precursor ion of interest, which is transmitted to Q2, where it collides with a neutral gas ( $N_2$  or Ar) and dissociates to various fragment ions. Rather than mass analyzing the resulting product ions, the linear ion trap (LIT) is set to trap and hold a 2- $m/z$ -unit-wide window centered on the product ion of interest. The selected  $m/z$  is irradiated with a single wavelength amplitude frequency to induce further fragmentation to secondary product ions, which are then scanned out of the LIT to the detector. The resulting  $MS^3$  spectrum shows the fragmentation pattern of the selected product ion, and yields additional structural details regarding the primary product ion.

$MS^3$  analysis provides critical structural information about higher order sphingolipids (such as gangliosides) that is not provided in the MS/MS spectrum. Typically, MS/MS data of these ions do not reveal any information about the components of the ceramide backbone.  $MS^3$  analyses of the  $Y_0$  product ions ( $m/z$  592.6), which comprise the core lipid part of the molecule, will determine the composition of the ceramide. In the example shown in Fig. 4.9, the highly abundant S, T, U, and V + 16 ions ( $m/z$  324, 308, 282, and 283, respectively) reveal that the fatty acid is C18:0, and the complementary P and Q ions ( $m/z$  265 and 291, respectively) are characteristic of a d20:1 sphingoid base. Thus,



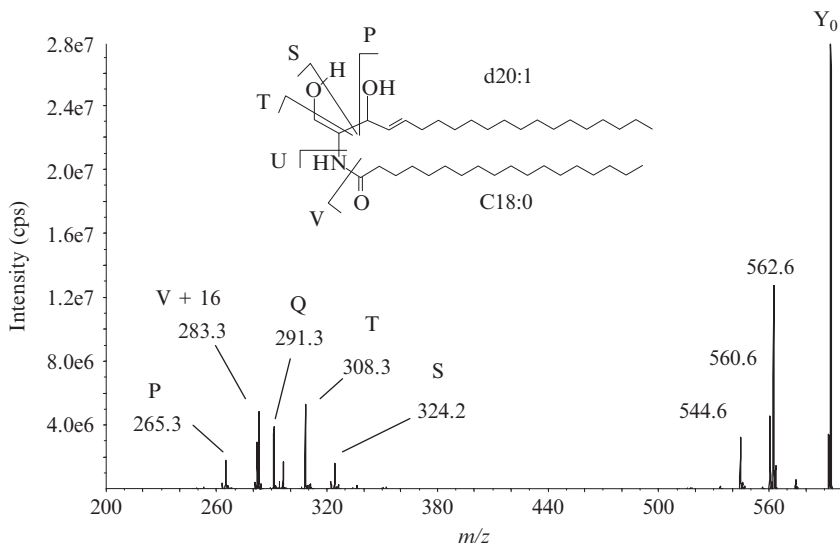


**Figure 4.9** MS/MS/MS ( $MS^3$ ) analysis of the  $Y_0$  product ions ( $m/z$  592.7) from Fig. 4.8 to reveal the highly abundant S, T, U, and V + 16 ions ( $m/z$  324, 308, 282, and 283, respectively) that establish that the fatty acid is C18:0, and the complementary P and Q ions ( $m/z$  265 and 291, respectively) that are characteristic of a d20:1 sphingoid base.

$MS^3$  scans provide an additional level of structural analysis yielding critical information regarding sphingoid base, fatty acid, and headgroups in glycosphingolipids.

## 10. OTHER METHODS

Two-dimensional (2D) ESI-MS has been introduced for the identification and quantitation of large families of sphingolipids using a triple quadrupole instrument (Han and Gross, 2003; Han *et al.*, 2004). Samples are infused and analyzed by MS and MS/MS in both positive and negative ESI conditions with the addition of aqueous LiOH and/or LiCl to aid formation of charged molecular adducts. As noted earlier in this chapter, limitations of this approach include the possibility of ionization suppression and the inability, in many instances, to distinguish isomeric and isobaric species; nonetheless, it is a relatively easy and rapid way to profile many species, including phosphatidylserines, phosphatidylethanolamines, diacyl- and triacylglycerols, phosphatidylinositols, phosphatidylcholines, sphingomyelins, some cerebrosides, cardiolipins, ceramides, free fatty acids, and phosphatidic acids (Han *et al.*, 2004).

Nanospray in conjunction with high-resolution MS and MS/MS is an extension of the 2D lipid profiling technique (Ejsing *et al.*, 2006; Ekroos *et al.*, 2002; Schwudke *et al.*, 2006) wherein very small volumes of sample are infused into a Q-TOF MS/MS via a chip containing a high-density array of nanospray nozzles. This allows data collection for extended periods of time during which numerous product ion scans across a chosen mass range can be conducted. The resulting product ion data are then queried for structure-specific fragment ions or neutral losses corresponding to the head-group, fatty acid, or sphingoid base combinations of the sphingolipid species, similar to the 2D technique. The detection of spurious peaks is reduced by using a smaller product ion selection window, which is possible using a high-resolution mass analyzer (TOF instead of quadrupole).

Chip-based nanospray techniques have several additional advantages (Ekroos *et al.*, 2002; Schwudke *et al.*, 2006). Since flow rates are on the order of nl/min, very little sample is consumed and background chemical noise is greatly reduced, which enhances overall sensitivity so that minor lipid species are more readily detected. Each chip contains a high-density array of nanospray nozzles that allows automation for higher reproducibility and sample throughput; furthermore, if the nature of the samples causes problems of carry-over and cross contamination, this can be solved by allocation of one spray nozzle per sample. Newer chip-based nanospray systems can be connected directly to LC columns as well as arranged so there is both analysis of a portion of the eluate and simultaneous fraction-collection of the remainder. When used in this manner, one gains the advantages of LC discussed earlier.

Accurate mass and ultra-high-resolution MS of sphingolipids has been performed by Fourier transform MS (FTMS) coupled to nanoESI (McFarland *et al.*, 2005; Vukelic *et al.*, 2005) or MALDI (Ivleva *et al.*, 2004; O'Connor and Costello, 2001). The former was primarily applied to the identification and structure determination of glycosphingolipids; however, the study introduced some interesting new alternative fragmentation techniques for lipids such as infrared multiphoton dissociation (IRMPD), electron capture dissociation (ECD), and electron detachment dissociation that may also be applicable to “omics” studies. MALDI FTMS has been used to analyze glycolipids directly from TLC plates (Ivleva *et al.*, 2004), and profile lipid species present in intact cells (Jones *et al.*, 2004) and plant tissues (Jones *et al.*, 2005). Ultra-high-resolution and accurate mass measurement enables the grouping of various classes of phospholipids (Jones *et al.*, 2004) and lipid or carbohydrate fragment ions using mass defect plots (McFarland *et al.*, 2005).

Ion mobility MS is another method that can separate lipids (Jackson *et al.*, 2005) with the same  $m/z$  based on differences in their mobility through a gas buffer and applied electric field. Since the mobility of a given ion is affected

by its three-dimensional shape (ions with a greater cross-section migrate more slowly than do more compact ions) in ion mobility MS, this has been able to distinguish glycans (Clowers *et al.*, 2005) and may be useful for some glycolipids.

Direct tissue imaging MS is rapidly emerging as a useful technology for lipid analysis in tissue sphingolipidomics because one does not need to extract the lipids from the sample, and one also obtains information about where the lipid is localized in the tissue. Ionization of the lipids in the sample is either achieved by MALDI (after MALDI matrix material has been deposited on the sample) or secondary ion MS (SIMS). For MALDI, the laser beam is rastered across the tissue sample, collecting spectra at discrete points; SIMS is analogous, but utilizes a tightly focused beam of primary ions to impinge on the surface and generate a secondary stream of ions (Borner *et al.*, 2006; Jackson *et al.*, 2007; Roy *et al.*, 2006; Sjovall *et al.*, 2004; Woods and Jackson, 2006). Two additional techniques, desorption ESI (DESI) and nanoSIMS, may also be used for cellular and subcellular imaging. The former uses charged droplets of solvent from an electrospray to generate intact secondary molecular ions (Wiseman *et al.*, 2006), and the latter uses a tightly focused beam of Cs<sup>+</sup> ions to scan the sample and produces primarily mono and diatomic secondary ions (Kraft *et al.*, 2006). Examples exist for the use of these technologies: MALDI-TOF has detected sphingomyelins, monohexosylceramides, sulfatides, and gangliosides (Jackson *et al.*, 2007; Woods and Jackson, 2006) in different brain regions; and SIMS TOF analysis of brain slices (Borner *et al.*, 2006) revealed that chain-length variants of galactosylceramide are differentially localized in white matter, with C18-subspecies being associated with cholesterol-rich regions, whereas C24-subspecies are found primarily in areas that are also enriched in Na<sup>+</sup> and K<sup>+</sup>. The limitations of these approaches to date include: (1) difficulties in obtaining ions from all of the analytes of interest (and in some cases, the energetics of the ionization process make it difficult to obtain parent ions for all of the compounds that are ionized); (2) variable ionization that compromises quantitative comparisons; and (3) the inability to distinguish isomeric and isobaric compounds. Nonetheless, since in many cases the location of lipids is vital to their function, the development of MS methods that provide quantitative and positional information is an important direction for new methods development.

## ACKNOWLEDGMENTS

The work that has been described in this review was supported primarily by funds from the LIPID MAPS Consortium grant (U54 GM069338) and in part from an NIH Integrated Technology Resource grant for Medical Glycomics (PA-02-132).

## REFERENCES

- Adams, J., and Ann, Q. (1993). Structure determination of sphingolipids by mass spectrometry. *Mass Spectrom. Rev.* **12**, 51–85.
- Ann, Q., and Adams, J. (1992). Structure-specific collision-induced fragmentation of ceramides cationized with alkali-metal ions. *Anal. Chem.* **65**, 7–13.
- Bielawski, J., Szulc, Z. M., Hannun, Y. A., and Bielawska, A. (2006). Simultaneous quantitative analysis of bioactive sphingolipids by high-performance liquid chromatography-tandem mass spectrometry. *Methods* **39**, 82–91.
- Borner, K., Nygren, H., Hagenhoff, B., Malmberg, P., Tallarek, E., and Mansson, J. E. (2006). Distribution of cholesterol and galactosylceramide in rat cerebellar white matter. *Biochem. Biophys. Acta* **1761**, 335–344.
- Chester, M. A. (1998). IUPAC-IUB Joint Commission on Biochemical Nomenclature (JCBN). Nomenclature of glycolipids—recommendations, 1997. *Eur. J. Biochem.* **257**, 293–298.
- Clowers, B. H., Dwivedi, P., Steiner, W. E., Hill, H. H., Jr., and Bendiak, B. (2005). Separation of sodiated isobaric disaccharides and trisaccharides using electrospray ionization-atmospheric pressure ion mobility-time of flight mass spectrometry. *J. Am. Soc. Mass Spectrom.* **16**, 660–669.
- David, J. H. (2006). Analysis of carbohydrates and glycoconjugates by matrix-assisted laser desorption/ionization mass spectrometry: An update covering the period 1999–2000. *Mass Spectrom. Rev.* **25**, 595–662.
- Ejsing, C. S., Moehring, T., Bahr, U., Duchoslav, E., Karas, M., Simons, K., and Shevchenko, A. (2006). Collision-induced dissociation pathways of yeast sphingolipids and their molecular profiling in total lipid extracts: A study by quadrupole TOF and linear ion trap-orbitrap mass spectrometry. *J. Mass Spectrom.* **41**, 372–389.
- Ekroos, K., Chernushevich, I. V., Simons, K., and Shevchenko, A. (2002). Quantitative profiling of phospholipids by multiple precursor ion scanning on a hybrid quadrupole time-of-flight mass spectrometer. *Anal. Chem.* **74**, 941–949.
- Fahy, E., Subramaniam, S., Brown, H. A., Glass, C. K., Merrill, A. H., Jr., Murphy, R. C., Raetz, C. R., Russell, D. W., Seyama, Y., Shaw, W., Shimizu, T., Spener, F., *et al.* (2005). A comprehensive classification system for lipids. *J. Lipid Res.* **46**, 839–861.
- Fujiwaki, T., Yamaguchi, S., Sukegawa, K., and Taketomi, T. (1999). Application of delayed extraction matrix-assisted laser desorption ionization time-of-flight mass spectrometry for analysis of sphingolipids in tissues from sphingolipidosis patients. *J. Chromatogr. B Biomed. Sci. Appl.* **731**, 45–52.
- Hamanaka, S., Asagami, C., Suzuki, M., Inagaki, F., and Suzuki, A. (1989). Structure determination of glucosyl beta 1-N-(omega-O-linoleoyl)-acylsphingosines of human epidermis. *J. Biochem. (Tokyo)* **105**, 684–690.
- Hammarstrom, S., and Samuelsson, B. (1970). On the biosynthesis of cerebrosides from 2-hydroxy acid ceramides: Use of deuterium labeled substrate and multiple ion detector. *Biochim. Biophys. Res. Commun.* **41**, 1027–1035.
- Han, X., and Gross, R. W. (2003). Global analyses of cellular lipidomes directly from crude extracts of biological samples by ESI mass spectrometry: A bridge to lipidomics. *J. Lipid Res.* **44**, 1071–1079.
- Han, X., Yang, J., Cheng, H., Ye, H., and Gross, R. W. (2004). Toward fingerprinting cellular lipidomes directly from biological samples by two-dimensional electrospray ionization mass spectrometry. *Anal. Biochem.* **330**, 317–331.
- Hara, A., and Taketomi, T. (1983). Detection of D-erythro and L-threo sphingosine bases in preparative sphingosylphosphorylcholine and its N-acylated derivatives and some evidence of their different chemical configurations. *J. Biochem. (Tokyo)* **94**, 1715–1718.

- Hayashi, A., Matsubara, T., Morita, M., Kinoshita, T., and Nakamura, T. (1989). Structural analysis of choline phospholipids by fast atom bombardment mass spectrometry and tandem mass spectrometry. *J. Biochem. (Tokyo)* **106**, 264–269.
- Ivleva, V. B., Elkin, Y. N., Budnik, B. A., Moyer, S. C., O'Connor, P. B., and Costello, C. E. (2004). Coupling thin-layer chromatography with vibrational cooling matrix-assisted laser desorption/ionization Fourier transform mass spectrometry for the analysis of ganglioside mixtures. *Anal. Chem.* **76**, 6484–6491.
- Jackson, S. N., Wang, H. Y., and Woods, A. S. (2007). *In situ* structural characterization of glycerophospholipids and sulfatides in brain tissue using MALDI-MS/MS. *J. Am. Soc. Mass Spectrom.* **18**, 17–26.
- Jackson, S. N., Wang, H. Y., Woods, A. S., Ugarov, M., Egan, T., and Schultz, J. A. (2005). Direct tissue analysis of phospholipids in rat brain using MALDI-TOFMS and MALDI-ion mobility-TOFMS. *J. Am. Soc. Mass Spectrom.* **16**, 133–138.
- Jones, J. J., Batoy, S. M., and Wilkins, C. L. (2005). A comprehensive and comparative analysis for MALDI FTMS lipid and phospholipid profiles from biological samples. *Comput. Biol. Chem.* **29**, 294–302.
- Jones, J. J., Stump, M. J., Fleming, R. C., Lay, J. O., Jr., and Wilkins, C. L. (2004). Strategies and data analysis techniques for lipid and phospholipid chemistry elucidation by intact cell MALDI-FTMS. *J. Am. Soc. Mass Spectrom.* **15**, 1665–1674.
- Kaga, N., Kazuno, S., Taka, H., Iwabuchi, K., and Murayama, K. (2005). Isolation and mass spectrometry characterization of molecular species of lactosylceramides using liquid chromatography-electrospray ion trap mass spectrometry. *Anal. Biochem.* **337**, 316–324.
- Kraft, M. L., Weber, P. K., Longo, M. L., Hutcheon, I. D., and Boxer, S. G. (2006). Phase separation of lipid membranes analyzed with high-resolution secondary ion mass spectrometry. *Science* **313**, 1948–1951.
- Kushi, Y., Rokukawa, C., Numajir, Y., Kato, Y., and Handa, S. (1989). Analysis of underivatized glycosphingolipids by high-performance liquid chromatography/atmospheric pressure ionization mass spectrometry. *Anal. Biochem.* **182**, 405–410.
- Lee, M. H., Lee, G. H., and Yoo, J. S. (2003). Analysis of ceramides in cosmetics by reversed-phase liquid chromatography/electrospray ionization mass spectrometry with collision-induced dissociation. *Rapid Commun. Mass Spectrom.* **17**, 64–75.
- Leverly, S. B. (2005). Glycosphingolipid structural analysis and glycosphingolipidomics. *Methods Enzymol.* **405**, 300–369.
- McFarland, M. A., Marshall, A. G., Hendrickson, C. L., Nilsson, C. L., Fredman, P., and Mansson, J. E. (2005). Structural characterization of the GM1 ganglioside by infrared multiphoton dissociation, electron capture dissociation, and electron detachment dissociation electrospray ionization FT-ICR MS/MS. *J. Am. Soc. Mass Spectrom.* **16**, 752–762.
- Merrill, A. H., Jr., Sullards, M. C., Allegood, J. C., Kelly, S., and Wang, E. (2005). Sphingolipidomics: High-throughput, structure-specific, and quantitative analysis of sphingolipids by liquid chromatography tandem mass spectrometry. *Methods* **36**, 207–224.
- O'Connor, P. B., and Costello, C. E. (2001). A high pressure matrix-assisted laser desorption/ionization Fourier transform mass spectrometry ion source for thermal stabilization of labile biomolecules. *Rapid Commun. Mass Spectrom.* **15**, 1862–1868.
- Pacetti, D., Boselli, E., Hulan, H. W., and Frega, N. G. (2005). High performance liquid chromatography-tandem mass spectrometry of phospholipid molecular species in eggs from hens fed diets enriched in seal blubber oil. *J. Chromatogr. A* **1097**, 66–73.
- Pettus, B. J., Bielawska, A., Kroesen, B. J., Moeller, P. D., Szulc, Z. M., Hannun, Y. A., and Busman, M. (2003). Observation of different ceramide species from crude cellular extracts by normal-phase high-performance liquid chromatography coupled to atmospheric pressure chemical ionization mass spectrometry. *Rapid Commun. Mass Spectrom.* **17**, 1203–1211.

- Pettus, B. J., Kroesen, B. J., Szulc, Z. M., Bielawska, A., Bielawski, J., Hannun, Y. A., and Busman, M. (2004). Quantitative measurement of different ceramide species from crude cellular extracts by normal-phase high-performance liquid chromatography coupled to atmospheric pressure ionization mass spectrometry. *Rapid Commun. Mass Spectrom.* **18**, 577–583.
- Roy, S., Touboul, D., Brunelle, A., Germain, D. P., Prognon, P., Laprevote, O., and Chaminade, P. (2006). [Imaging mass spectrometry: A new tool for the analysis of skin biopsy. Application in Fabry's disease]. *Ann. Pharm. Fr.* **64**, 328–334.
- Samuelsson, B., and Samuelsson, K. (1968). Gas-liquid chromatographic separation of ceramides as di-O-trimethylsilyl ether derivatives. *Biochim. Biophys. Acta.* **164**, 421–423.
- Samuelsson, B., and Samuelsson, K. (1969a). Gas-liquid chromatography-mass spectrometry of synthetic ceramides. *J. Lipid Res.* **10**, 41–46.
- Samuelsson, K., and Samuelsson, B. (1969b). Gas-liquid chromatography-mass spectrometry of cerebrosides as trimethylsilyl ether derivatives. *Biochem. Biophys. Res. Commun.* **37**, 15–21.
- Samuelsson, K., and Samuelsson, B. (1970). Gas chromatographic and mass spectrometric studies of synthetic and naturally occurring ceramides. *Chem. Phys. Lipids* **5**, 44–79.
- Schwudke, D., Oegema, J., Burton, L., Entchev, E., Hannich, J. T., Ejsing, C. S., Kurzchalia, T., and Shevchenko, A. (2006). Lipid profiling by multiple precursor and neutral loss scanning driven by the data-dependent acquisition. *Anal. Chem.* **78**, 585–595.
- Shayman, J. A., and Abe, A. (2000). 1-O-acylceramide synthase. *Methods Enzymol.* **311**, 105–117.
- Sjovall, P., Lausmaa, J., and Johansson, B. (2004). Mass spectrometric imaging of lipids in brain tissue. *Anal. Chem.* **76**, 4271–4278.
- Sullards, M. C. (2000). Analysis of sphingomyelin, glucosylceramide, ceramide, sphingosine, and sphingosine 1-phosphate by tandem mass spectrometry. *Methods Enzymol.* **312**, 32–45.
- Sullards, M. C., and Merrill, A. H., Jr. (2001). Analysis of sphingosine 1-phosphate, ceramides, and other bioactive sphingolipids by high-performance liquid chromatography-tandem mass spectrometry. *Sci. STKE* **2001**, PL1.
- Suzuki, M., Sekine, M., Yamakawa, T., and Suzuki, A. (1989). High-performance liquid chromatography-mass spectrometry of glycosphingolipids: I. Structural characterization of molecular species of GlcCer and IV3 beta Gal-Gb4Cer. *J. Biochem. (Tokyo)* **105**, 829–833.
- Suzuki, Y., Suzuki, M., Ito, E., Goto-Inoue, N., Miseki, K., Iida, J., Yamazaki, Y., Yamada, M., and Suzuki, A. (2006). Convenient structural analysis of glycosphingolipids using MALDI-QIT-TOF mass spectrometry with increased laser power and cooling gas flow. *J. Biochem. (Tokyo)* **139**, 771–777.
- Suzuki, M., Yamakawa, T., and Suzuki, A. (1990). High-performance liquid chromatography-mass spectrometry of glycosphingolipids: II. Application to neutral glycolipids and monosialogangliosides. *J. Biochem. (Tokyo)* **108**, 92–98.
- Suzuki, M., Yamakawa, T., and Suzuki, A. (1991). A micro method involving micro high-performance liquid chromatography-mass spectrometry for the structural characterization of neutral glycosphingolipids and monosialogangliosides. *J. Biochem. (Tokyo)* **109**, 503–506.
- Sweeley, C. C., and Dawson, G. (1969). Determination of glycosphingolipid structures by mass spectrometry. *Biochem. Biophys. Res. Commun.* **37**, 6–14.
- Vukelic, Z., Zamfir, A. D., Bindila, L., Froesch, M., Peter-Katalinic, J., Usuki, S., and Yu, R. K. (2005). Screening and sequencing of complex sialylated and sulfated glycosphingolipid mixtures by negative ion electrospray Fourier transform ion cyclotron resonance mass spectrometry. *J. Am. Soc. Mass Spectrom.* **16**, 571–580.

- Wiseman, J. M., Ifa, D. R., Song, Q., and Cooks, R. G. (2006). Tissue imaging at atmospheric pressure using desorption electrospray ionization (DESI) mass spectrometry. *Angew. Chem. Int. Ed. Engl.* **45**, 7188–7192.
- Woods, A. S., and Jackson, S. N. (2006). Brain tissue lipidomics: Direct probing using matrix-assisted laser desorption/ionization mass spectrometry. *AAPS J.* **8**, E391–E395.
- Zheng, W., Kollmeyer, J., Symolon, H., Momin, A., Munter, E., Wang, E., Kelly, S., Allegood, J. C., Liu, Y., Peng, Q., Ramaraju, H., Sullards, M. C., *et al.* (2006). Ceramides and other bioactive sphingolipid backbones in health and disease: Lipidomic analysis, metabolism and roles in membrane structure, dynamics, signaling and autophagy. *Biochim. Biophys. Acta* **1758**, 1864–1884.

# ANALYSIS OF UBIQUINONES, DOLICHOLS, AND DOLICHOL DIPHOSPHATE-OLIGOSACCHARIDES BY LIQUID CHROMATOGRAPHY-ELECTROSPRAY IONIZATION-MASS SPECTROMETRY

Teresa A. Garrett, Ziqiang Guan, and Christian R. H. Raetz

## Contents

1. Introduction	118
2. Materials	121
3. Liquid Chromatography-Mass Spectrometry	122
4. Preparation of Lipid Extracts	122
5. LC-MS Detection and Quantification of Coenzyme Q	123
6. LC-MS Detection and Quantification of Dolichol	130
7. LC-MS and LC-MS/MS Characterization of Dolichol Diphosphate-Linked Oligosaccharides	136
Acknowledgment	140
References	140

## Abstract

Prenols, a class of lipids formed by the condensation of five carbon isoprenoids, have important roles in numerous metabolic pathways of the eukaryotic cell. Prenols are found in the cell as free alcohols, such as dolichol, or can be attached to vitamins, as with the fat soluble vitamins. In addition, prenols such as farnesyl- and geranylgeranyl-diphosphate are substrates for the transfer of farnesyl and geranylgeranyl units to proteins with important implications for signal transduction within the cell. Dolichol phosphate- and dolichol diphosphate-linked sugars are central to the formation of the lipid-linked branched oligosaccharide, Dol-PP-(GlcNAc)<sub>2</sub>(Man)<sub>9</sub>(Glc)<sub>3</sub>, used for co-translational *en bloc* protein *N*-glycosylation in the lumen of the endoplasmic reticulum. Toward furthering our understanding of the role of prenoilipids in the cell, we have developed a method for the detection and quantification of dolichol and coenzyme

Department of Biochemistry, Duke University Medical Center, Durham, North Carolina

*Methods in Enzymology*, Volume 432  
ISSN 0076-6879, DOI: 10.1016/S0076-6879(07)32005-3

© 2007 Elsevier Inc.  
All rights reserved.



Q by liquid chromatography-electrospray ionization-mass spectrometry (LC-ESI-MS). These methods, developed using the mouse macrophage RAW 264.7 tumor cells, are broadly applicable to other cell lines, tissues, bacteria, and yeast. We also present a new MS-based method for the detection and structural characterization of the intact dolichol diphosphate oligosaccharide Dol-PP-(GlcNAc)<sub>2</sub>(Man)<sub>9</sub>(Glc)<sub>3</sub> from porcine pancreas.

## 1. INTRODUCTION

Prenols are a class of lipids formed by carbocation-based condensations of the five carbon isoprenoids, isopentenyl diphosphate, and dimethylallyl diphosphate (Fahy *et al.*, 2005) (Fig. 5.1). These substances are derived from mevalonate (Kuzuyama and Seto, 2003) in animals or from methylerythritol phosphate in plants (Rodriguez-Concepcion, 2004). Bacteria generate isopentenyl diphosphate and dimethylallyl diphosphate by one or the other of these pathways and, in a few instances, by both (Hedl *et al.*, 2004; Rohdich *et al.*, 2004).

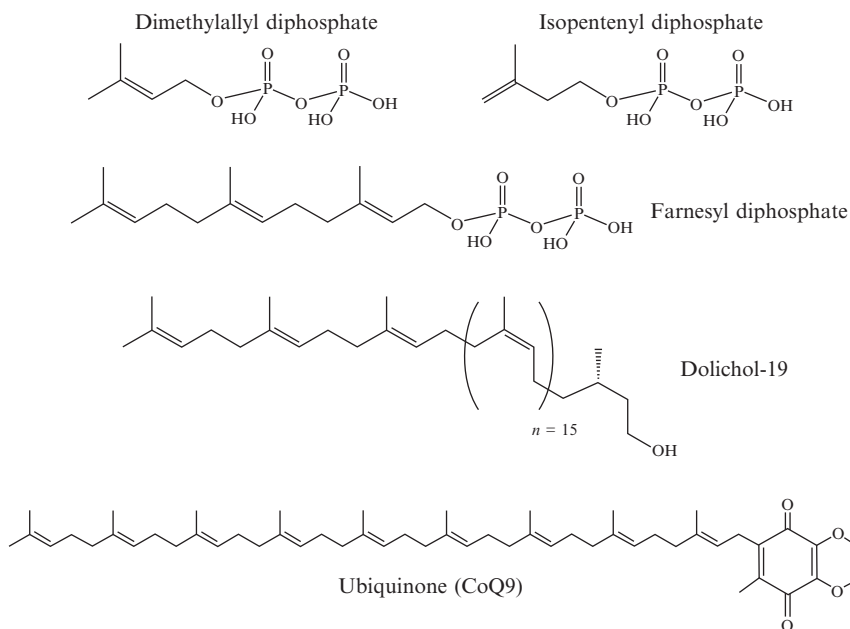


**Figure 5.1** Chemical structures of the prenyls dolichol and ubiquinone, and their biosynthetic precursors, dimethylallyl diphosphate, isopentenyl diphosphate, and farnesyl diphosphate.

In animal systems, which are the focus of LIPID MAPS, two molecules of isopentenyl diphosphate and one of dimethylallyl diphosphate are condensed by a single enzyme to generate the 15 carbon intermediate, farnesyl diphosphate (Fig. 5.1), in which the stereochemistry of the double bonds is *trans* (Kellogg and Poulter, 1997; Leyes *et al.*, 1999). A separate enzyme elongates farnesyl diphosphate to the 20-carbon geranylgeranyl diphosphate (Ericsson *et al.*, 1998). Subsequently, farnesyl- or geranylgeranyl-diphosphate may be further elongated by other prenyl transferases (Kellogg and Poulter, 1997), which incorporate additional isopentenyl units to form the dolichols (Swiezewskaa and Danikiewicz, 2005), the side chains of the ubiquinones (Turunen *et al.*, 2004), and other substances (Fig. 5.1). Both farnesyl- or geranylgeranyl-diphosphate can also function directly as donor substrates for the addition of farnesyl- or geranylgeranyl- units to proteins, many of which are involved in signal transduction (Gelb *et al.*, 2006).

Mammalian dolichol is a mixture that consists mainly of 17, 18, 19, or 20 isoprene units (Figs. 5.1 and 5.7) (Chojnacki and Dallner, 1988). Small amounts of shorter or longer species may also be detectable. All double bonds except for those of the farnesyl diphosphate primer have the *cis* configuration (Fig. 5.1) because the prenyl transferase responsible for the elongation of farnesyl diphosphate to dolichol orients and condenses its substrates differently than does farnesyl diphosphate synthase (Kellogg and Poulter, 1997). Although free dolichol is the predominant species found in cells, it is initially generated as the diphosphate derivative (Schenk *et al.*, 2001). The diphosphate moiety is subsequently cleaved to yield dolichol phosphate and free dolichol. However, kinases exist that can convert dolichol back to dolichol phosphate (Schenk *et al.*, 2001).

In our experience, dolichol phosphate is much less abundant in animal cells than is dolichol (as shown later). Dolichol phosphate is also rapidly converted to various dolichol phosphate sugars or dolichol diphosphate sugars (Chojnacki and Dallner, 1988; Schenk *et al.*, 2001). In the latter case, dolichol phosphate reacts with UDP-*N*-acetylglucosamine (UDP-GlcNAc) to form dolichol diphosphate-GlcNAc (Kean *et al.*, 1999) to which 13 additional sugars are then added by an important system of glycosyltransferases found in the endoplasmic reticulum (Schenk *et al.*, 2001). The final product is the lipid-linked, branched oligosaccharide Dol-PP-(GlcNAc)<sub>2</sub>(Man)<sub>9</sub>(Glc)<sub>3</sub> (Fig. 5.2) (Schenk *et al.*, 2001). This conserved intermediate is used for cotranslational *en bloc* protein *N*-glycosylation in the lumen of the endoplasmic reticulum (Hubbard and Ivatt, 1981; Kornfeld and Kornfeld, 1985; Rosner *et al.*, 1982). The sugar composition and glycosidic linkages of Dol-PP-(GlcNAc)<sub>2</sub>(Man)<sub>9</sub>(Glc)<sub>3</sub> (Fig. 5.2) were determined by classical biochemical and enzymatic methods. However, to our knowledge, the structure of intact Dol-PP-(GlcNAc)<sub>2</sub>(Man)<sub>9</sub>(Glc)<sub>3</sub> has not been validated by MS or nuclear magnetic resonance (NMR) spectroscopy.

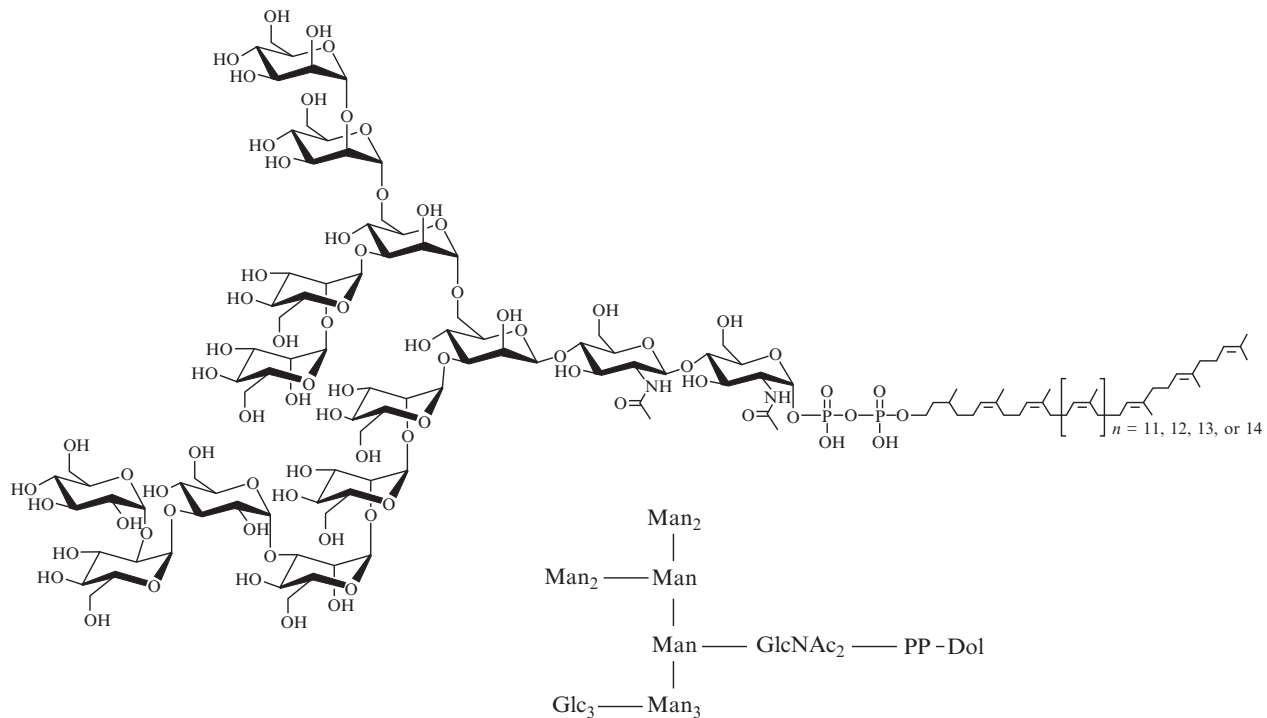


**Figure 5.2** Chemical structure of the lipid-linked, branched oligosaccharide, Dol-PP-(GlcNAc)<sub>2</sub>(Man)<sub>9</sub>(Glc)<sub>3</sub>. The inset shows a schematic of the composition and arrangement of the sugars, where GlcNAc is *N*-acetyl glucosamine, Man is mannose, and Glc is glucose.

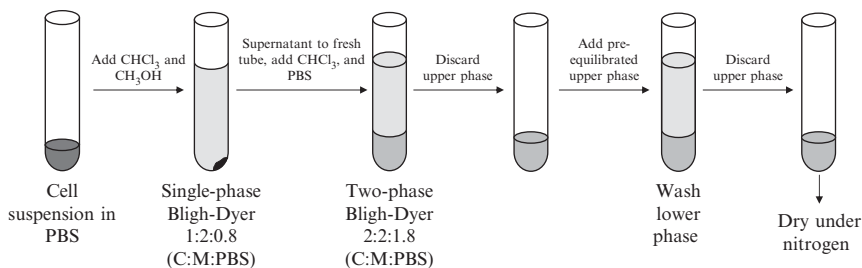


**Figure 5.3** Lipid extraction procedure.

Polyprenol chains are also found attached to other small organic molecules in the cell, such as the fat-soluble vitamins A, E, and K (Meganathan, 2001a; Olson, 1964), and the electron transport cofactor, ubiquinone, also called coenzyme Q (Fig. 5.1) (Meganathan, 2001b; Szkopinska, 2000). In the latter case, farnesyl diphosphate is elongated by a different prenyl transferase that incorporates three to seven additional isopentenyl units, depending on the system. In contrast to dolichol, all the double bonds formed during ubiquinone side-chain elongation have the *trans* stereochemistry (Fig. 5.1).

Herein we present new methods for the detection and quantification of dolichol and coenzyme Q in mouse macrophage RAW 264.7 tumor cells (Raetz *et al.*, 2006) using LC-ESI-MS. While the methods reported here were developed using cultured macrophages, we have found that they are broadly applicable to other cell lines and tissues, as well as to yeast and bacteria. We also present a new method for the detection and structural characterization of dolichol diphosphate oligosaccharides, including the first analysis by LC-ESI-MS/MS of intact Dol-PP-(GlcNAc)<sub>2</sub>(Man)<sub>9</sub>(Glc)<sub>3</sub> from porcine pancreas (Kelleher *et al.*, 2001).

## 2. MATERIALS

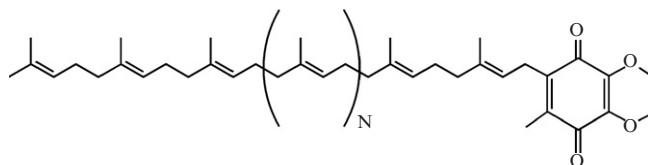
High performance liquid chromatography (HPLC)-grade solvents were from VWR (International Leicestershire, England). Ammonium acetate was from Mallinckrodt (Hazelwood, MO). Zorbax SB-C8 (2.1 × 50 mm, 5 μm) reverse-phase column was from Agilent (Palo Alto, CA). Coenzyme Q6 and Q10 standards were from Sigma-Aldrich (St. Louis, MO). Synthetic nor-dolichol was from Avanti Polar Lipids (Alabaster, AL). Dolichol-diphosphate-oligosaccharide purified from pig pancreas was a gift from Dr. R. Gilmore (University of Massachusetts Medical School, Worcester, MA). All extractions were done in glass tubes equipped with Teflon-lined screw caps using disposable glass pipettes.

### 3. LIQUID CHROMATOGRAPHY-MASS SPECTROMETRY

LC-MS analysis was performed using a Shimadzu LC system (comprising a solvent degasser, two LC-10A pumps, and a SCL-10A system controller) coupled to a QSTAR XL quadrupole time-of-flight (TOF), tandem mass spectrometer (Applied Biosystems/MDS Sciex). A Zorbax SB-C8 reversed-phase column (5  $\mu\text{m}$ , 2.1  $\times$  50 mm) was used for all LC-MS analyses. LC was operated at a flow rate of 200  $\mu\text{l}/\text{min}$  with a linear gradient as follows: 100% mobile phase A (methanol:acetonitrile:aqueous 1 mM ammonium acetate; 60:20:20) was held for 2 min, then linearly increased to 100% mobile phase B (100% ethanol containing 1 mM ammonium acetate) over 14 min and held at 100% mobile phase B for 4 min. The column was re-equilibrated to 100% mobile-phase A for 2 min prior to the next injection. The post-column split diverted 10% of the LC flow to the ESI source. All MS data were analyzed using Analyst QS software (Applied Biosystems/MDS Sciex). The mass spectrometer was calibrated in both the negative and positive mode using PPG3000 (Applied Biosystems).

### 4. PREPARATION OF LIPID EXTRACTS

RAW cells, cultured according to (Raetz *et al.*, 2006), were extracted using the method of Bligh and Dyer (1959), as shown in Fig. 5.3. A 150-mm tissue culture plate at about 90% confluence was washed with 10 ml phosphate buffered saline (PBS) and then scraped into 5 ml PBS (137 mM NaCl, 0.027 mM KCl, 0.01 mM  $\text{Na}_2\text{HPO}_4$ , 0.0018 mM  $\text{KH}_2\text{PO}_4$ ). The cell suspension was centrifuged at  $400\times g$  to harvest the cells. This culture plate size typically yields about  $100 \times 10^6$  cells or  $\sim 0.1$  g of cells (wet weight). The cell pellet is resuspended in 1 ml of PBS and transferred to a  $16 \times 150$ -mm-glass centrifuge tube with a Teflon-lined cap.



N	CoQ species	Formula [M]	[M+H] <sup>+</sup>		[M+NH <sub>4</sub> ] <sup>+</sup>		[M+Na] <sup>+</sup>	
			Observed	Exact	Observed	Exact	Observed	Exact
1	CoQ6	C <sub>39</sub> H <sub>58</sub> O <sub>4</sub>	591.434	591.441	608.469	608.467	613.423	613.423
4	CoQ9	C <sub>54</sub> H <sub>82</sub> O <sub>4</sub>	795.647	795.629	812.678	812.655	817.640	817.611
5	CoQ10	C <sub>59</sub> H <sub>90</sub> O <sub>4</sub>	863.713	863.691	880.734	880.718	885.689	885.673

**Figure 5.4** Structures and masses of coenzyme Q6, Q9, and Q10.

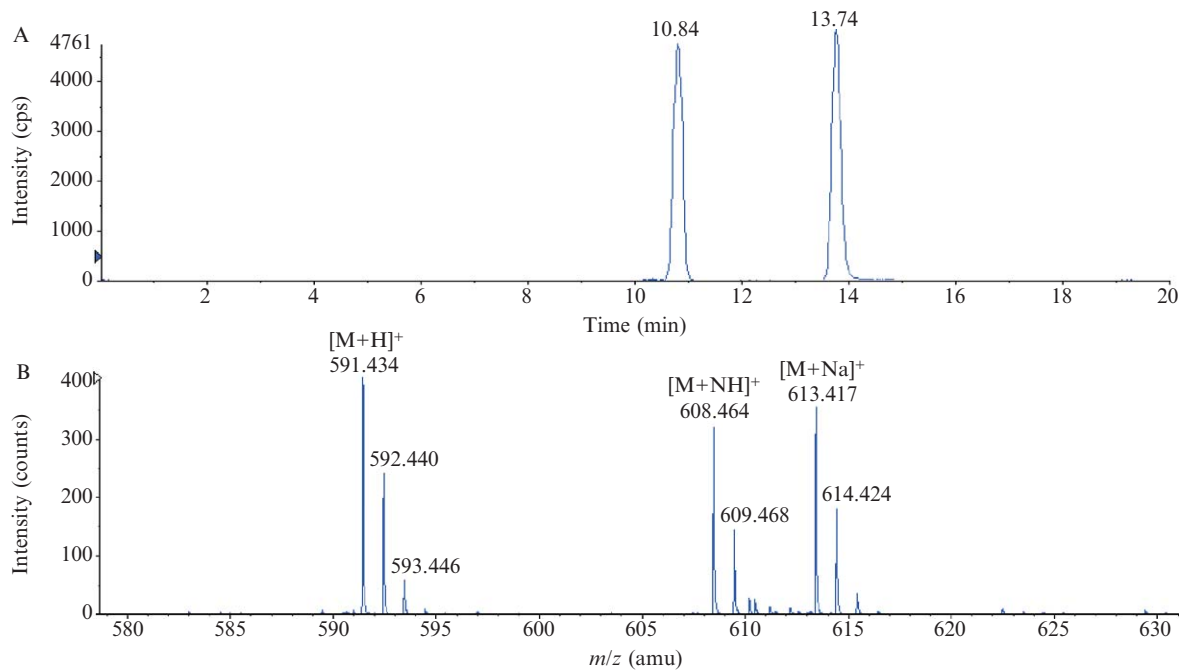
Next, 1.25 ml of chloroform and 2.5 ml of methanol are added to generate a single-phase Bligh-Dyer mixture (final ratio: 1:2:0.8, C:M:PBS). This mixture is vigorously mixed with a vortex and, if necessary, subjected to sonic irradiation in a bath apparatus for 2 min to break up any chunks of cells. The single-phase extraction mixture is incubated at room temperature for 15 min, then centrifuged at  $\sim 500\times g$  for 10 min in a clinical centrifuge to pellet the cell debris (Fig. 5.3). The supernatant is transferred to a fresh tube; 1.25 ml chloroform and 1.25 ml PBS are added to generate a two-phase system (final ratio; 2:2:1.8, C:M:PBS). After vigorous mixing, the tubes are centrifuged as previously stated to resolve the phases. The upper phase and any interface that may be present is removed and discarded. The interface is generally minimal. Next, the lower phase is washed with 4.75 ml pre-equilibrated neutral upper phase, vortexed, and centrifuged as previously stated to resolve the phases. After removal of the upper phase, the lower phase is dried under a stream of nitrogen, and the dried lipids are stored at  $-20^\circ$  until analysis. Generally, from 0.1 g of cells or tissue, about 10 mg of dried lipid is obtained.

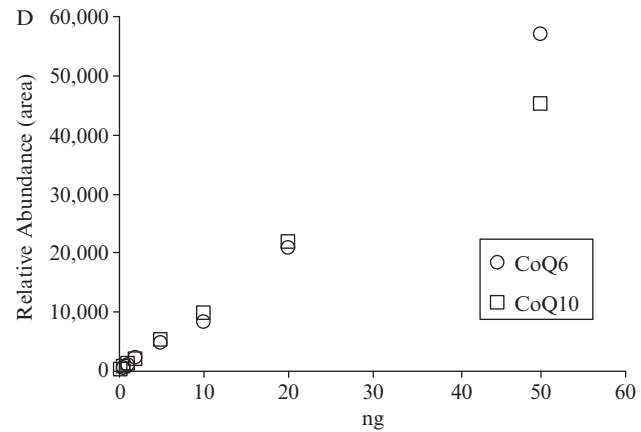
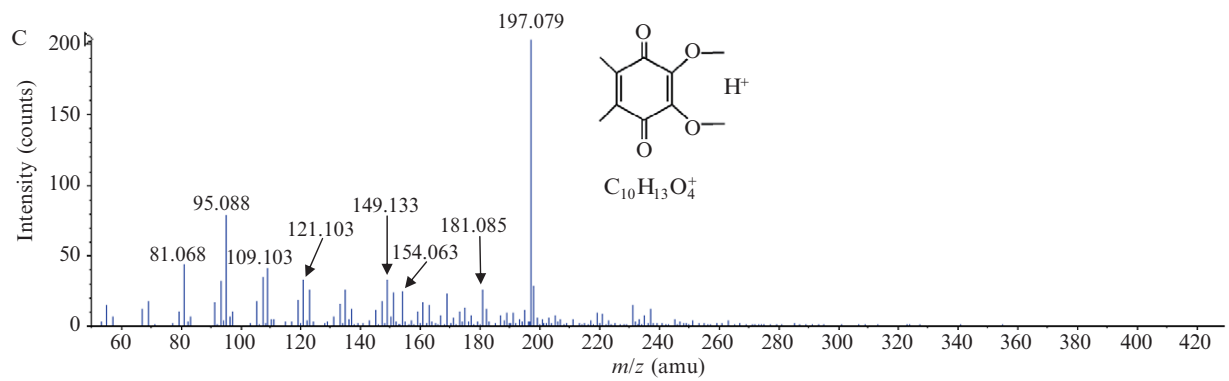
Note on scaling up: This method of extraction can be used with larger quantities of cells or tissues. Volumes should be scaled accordingly; however, a three- to five-fold concentration of the initial PBS suspension of cells or tissue should not affect extraction efficiency. With larger volumes, 250 ml Teflon-lined centrifuge bottles (VWR) are useful for centrifugation and separation of the phases.

## 5. LC-MS DETECTION AND QUANTIFICATION OF COENZYME Q

Coenzyme Q (CoQ), also known as ubiquinone, is involved in the transport of electrons from complex I (NADH:ubiquinone oxidoreductase) and II (succinate:ubiquinone reductase) to complex III (ubiquinone:cytochrome c oxidoreductase) in the electron transport chain of aerobic organisms (Saraste, 1999). The structure of CoQ is shown in Figs. 5.1 and 5.4. It is a quinone derivative with a long polyprenoid chain that can be 7 to 11 units long depending on the organism (Szkopinska, 2000). In humans, the most abundant CoQ has 10 isoprenoid units. In murine RAW cells, the most abundant CoQ has a side chain consisting of nine units (Olgun *et al.*, 2003).

In order to develop LC-MS methods for the detection of CoQ in total lipid extracts, we needed to (1) determine the linear range for MS response with respect to the amount of standard analyzed; (2) establish that this linear range applied to the MS response when analyzing the standard in total lipid extracts; (3) show that the number of isoprene units on the CoQ did not alter the MS response; and (4) determine the amount of standard to add to our sample to get approximately the same peak area of the extracted ion







current for the standard and the analyte. We found that we could use a CoQ with a different number of isoprene units as a standard instead of using deuterated CoQ (Gould *et al.*, 2006; Haroldsen *et al.*, 1987).

We obtained two CoQ standards, one with 6 isoprenoid units, CoQ6, and the other with 10 isoprenoid units, CoQ10 (Sigma) (Fig. 5.4). For LC-MS analysis, the standard was re-dissolved in  $\text{CHCl}_3$  and diluted into DMSO:MeOH (9:1 v/v) at a concentration of 0.1, 0.2, 0.5, 1, 2, or 5 ng/ $\mu\text{l}$ . Next, 10  $\mu\text{l}$  of each dilution were injected, in turn, onto a Zorbax SB-C8 ( $2.1 \times 50$  mm, 5 mm) column at 200  $\mu\text{l}/\text{min}$  and eluted as described above. CoQs were detected in the positive ion mode as  $[\text{M}+\text{H}]^+$ ,  $[\text{M}+\text{NH}_4]^+$ , and  $[\text{M}+\text{Na}]^+$  ions using the following mass spectrometer settings: ESI voltage, +5500 V; declustering potential, 60 V; and focusing potential, 265 V; and nebulizer gas, 20 psi.

Figure 5.5A shows the extracted ion current (EIC) for the  $[\text{M}+\text{H}]^+$  ion of CoQ6 and CoQ10. Each standard was analyzed in separate LC-MS runs, and the spectra were overlaid. The CoQ6 elutes from the reverse phase column at about 11.1 min, and the CoQ10 elutes at about 13.7 min, consistent with the difference in the polyprenol chain length. Figure 5.5B and C show the positive ion MS and collision-induced dissociation MS (CID-MS) for the  $[\text{M}+\text{H}]^+$  CoQ6 standard. The collision energy was set at 52 V (laboratory frame of reference), and nitrogen was used as the collision gas. The major fragment ion is  $m/z$  197.079, which corresponds by exact mass to a proton adduct of the quinone ring and is formed by the elimination of the isoprenoid chain (Teshima and Kondo, 2005). The CID-MS of the CoQ10 standard produces a similar fragment ion pattern (data not shown). As shown in Fig. 5.5D, the peak area of the EICs of the CoQ6 and CoQ10 standards are linear for 1 ng to 50 ng injected onto the column. This also shows that, for CoQs, the number of isoprenoid repeats does not alter the ionization efficiency, as is sometimes seen with other lipids analyzed by MS (Callender *et al.*, 2007). In addition, the peak area of the EIC of the CoQ6 standard increased linearly when increasing amounts of the standard were co-extracted with the RAW cells (data not shown).

---

**Figure 5.5** Positive-ion liquid chromatography-mass spectrometry (LC-MS) analysis of CoQ6 and CoQ10 standards. (A) The extracted ion current (EIC) for the  $[\text{M}+\text{NH}_4]^+$  ions of CoQ6 (608.464  $m/z$ ) and CoQ10 (880.734  $m/z$ ) standards. Under these liquid chromatography conditions, the CoQ6 elutes at about 10 minutes while the CoQ10 elutes at about 14 minutes. (B) The mass spectrum of the material eluting from minutes 10.6 to 11.1, representing the CoQ6 standard. The CoQ6 form  $[\text{M}+\text{H}]^+$ ,  $[\text{M}+\text{NH}_4]^+$ , and  $[\text{M}+\text{Na}]^+$  adduct ions. (C) The collision-induced mass spectrometry (CID-MS) of the  $[\text{M}+\text{H}]^+$  ion of the CoQ6 standard. The major fragment ion ( $m/z$  197.079) corresponds to the quinone ring and is formed by the elimination of the isoprenoid chain (Teshima and Kondo, 2005). (D) The plot of the peak area of the extracted ion current of the  $[\text{M}+\text{H}]^+$  ion of CoQ6 and CoQ10 versus the nanogram (ng) of standard injected onto the Zorbax C-8 reverse phase column. The peak areas of the CoQ6 and the CoQ10 were similar when equivalent amounts of standard were analyzed.

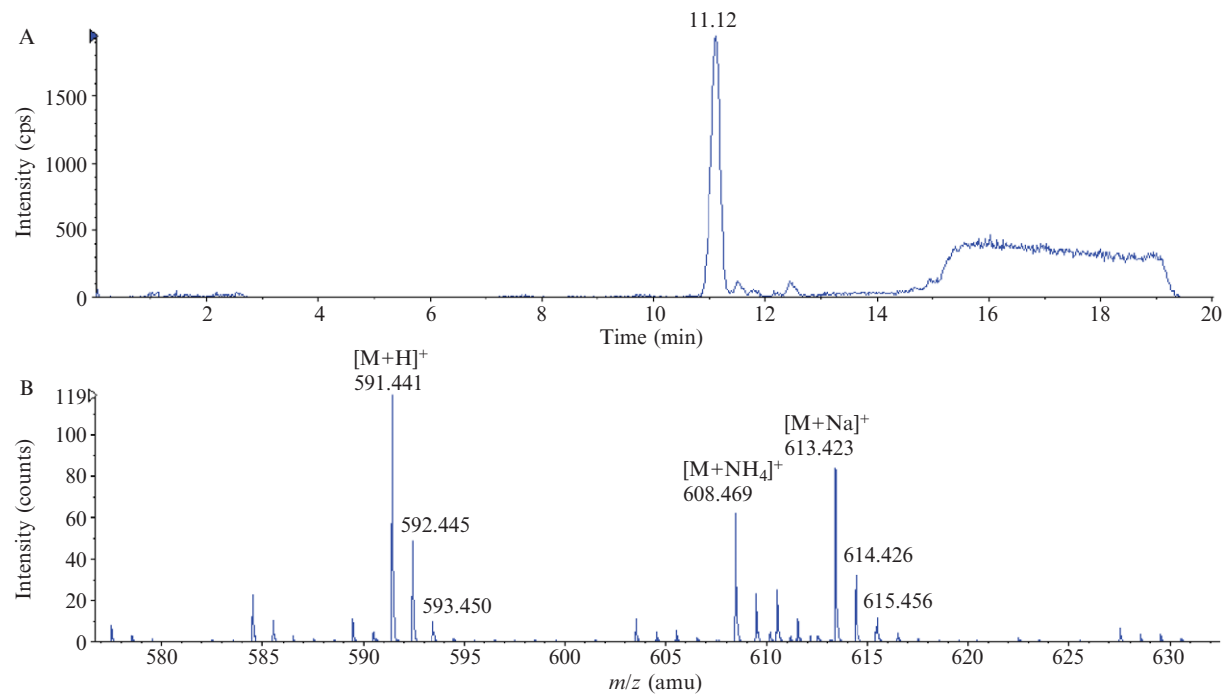


**Figure 5.6** (continued)

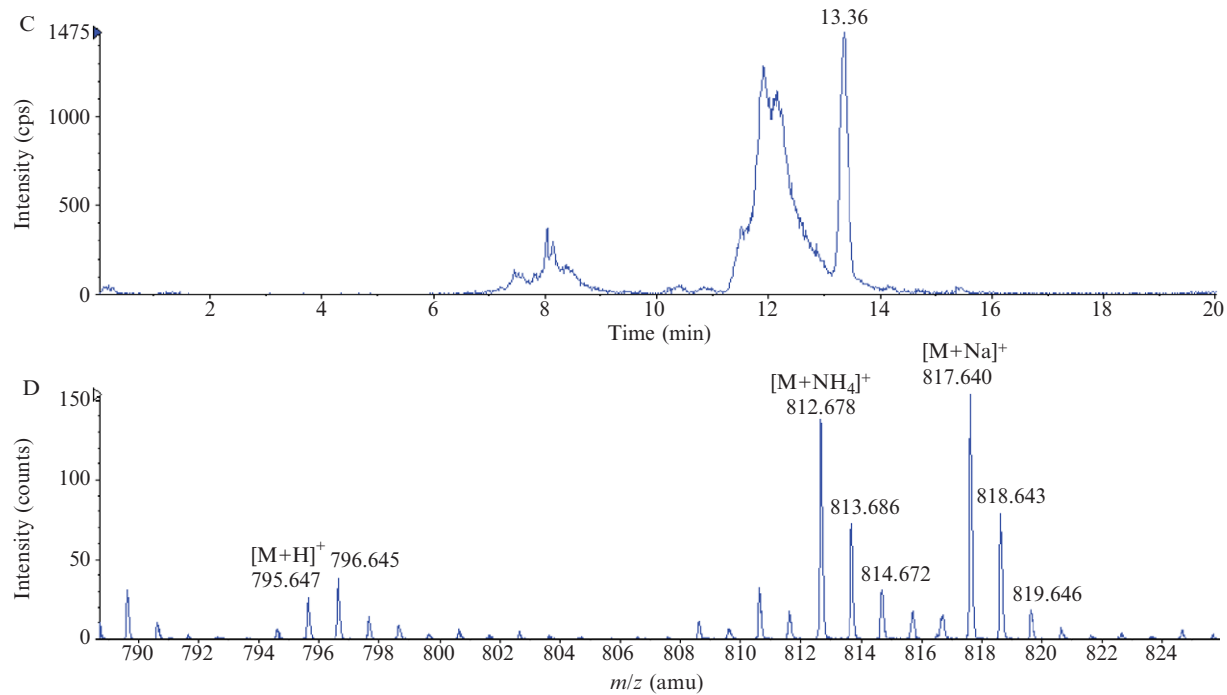


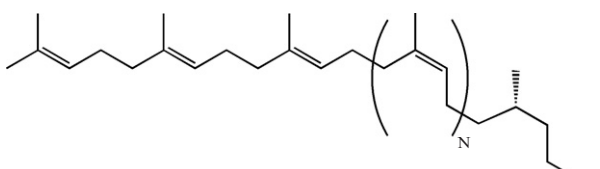
**Figure 5.6** Positive ion liquid chromatography-mass spectrometry (LC-MS) analysis of CoQs in RAW lipid extracts. (A) The extracted ion current (EIC) for the  $[M+NH_4]^+$  ion of CoQ6 standard after 1  $\mu\text{g}$  of standard is co-extracted in the presence of RAW cells from one 150-mm plate. The retention time (11.12 min) is consistent with the retention time seen when the standard is injected alone (Fig. 5.5A). (B) The mass spectrum of the material eluting between 10.9 and 11.3 min. The  $[M+H]^+$ ,  $[M+NH_4]^+$ , and  $[M+Na]^+$  ions of the CoQ6 standard are easily resolved. (C) The extracted ion current of the  $[M+NH_4]^+$  ion of the major CoQ of RAW cells, CoQ9. The CoQ9 elutes at approximately 13.3 min under these liquid chromatography conditions. The peaks at approximately 8 and 12 min are due to isobaric lipids found in the lipid extract and are not due to CoQ9. (D) The mass spectrum of the material eluting between 13.3 and 14.3 min. The  $[M+H]^+$ ,  $[M+NH_4]^+$ , and  $[M+Na]^+$  ions of the CoQ9 standard are detected.

Therefore, the linear range established using the standard also applies to the analysis of CoQs from total lipid extracts.

Because the major CoQs found in mouse tissue are CoQ9 and CoQ10, we chose to use CoQ6 as the internal standard for our quantitative analysis (Olgun *et al.*, 2003). CoQ6 is not found in RAW cells and is not isobaric with other ions eluting at a similar retention time.

In addition to establishing the linear range of the MS response, we needed to determine the amount of CoQ6 standard to add to the extraction mixture in order for the peak area of the EIC for the standard to be about equal to the peak area of the EIC for the CoQs being quantified in the sample. By varying the amount of CoQ6 added during the co-extraction, we determined that, for a 150-mm culture dish grown to ~90% confluence, 5  $\mu\text{g}$  of CoQ6 standard gave an EIC peak area about equal to the EIC peak of the major coenzyme species of the cell, CoQ9.

Overall, our quantification procedure for CoQs in RAW cells is as follows: 5  $\mu\text{g}$  of CoQ6 (dissolved in  $\text{CHCl}_3$  at 1 mg/ml) standard is added to the cell suspension (1 ml) prior to the addition of chloroform (1.25 ml) and methanol (2.5 ml) to form the single-phase extraction mixture; the lipids are extracted as previously described, dried under a stream of nitrogen, and stored at  $-20^\circ$  until analysis; the dried lipids are redissolved in 0.2 ml of chloroform:methanol (1:1, v:v) and diluted twofold into chromatography solvent A; 10  $\mu\text{l}$  is injected onto the reverse-phase column and analyzed using the LC-MS procedure previously shown. The extracted ion current and mass spectra for the CoQ6 standard and endogenous CoQ9 are shown in Figs. 5.6A–D. For CoQ9, the major ion species are observed as  $[\text{M}+\text{H}]^+$  at  $m/z$  795.647,  $[\text{M}+\text{NH}_4]^+$  at  $m/z$  812.678, and  $[\text{M}+\text{Na}]^+$  at  $m/z$  817.640 (Fig. 7D). For CoQ10, the major ion species are observed as  $[\text{M}+\text{H}]^+$  at  $m/z$  863.713,  $[\text{M}+\text{NH}_4]^+$  at  $m/z$  880.734, and  $[\text{M}+\text{Na}]^+$  at  $m/z$  885.673 (data not shown). The peak area of the EIC for the  $[\text{M}+\text{NH}_4]^+$  is used



<i>n</i>	Dol species	Formula [M]	[M+Ac] <sup>-</sup>	
			Observed	Exact
13	Dol-17	C <sub>85</sub> H <sub>140</sub> O	1236.076	1236.104
14	Dol-18	C <sub>90</sub> H <sub>148</sub> O	1304.133	1304.166
15	Dol-19	C <sub>95</sub> H <sub>156</sub> O	1372.178	1372.229
16	Dol-20	C <sub>100</sub> H <sub>164</sub> O	1440.239	1440.292

**Figure 5.7** Structures and masses of the acetate adducts of dolichols-17, -18, -19, and -20.

to quantify the total content of CoQ9 and CoQ10 in the RAW cells. For example, the quantification of the CoQ9 is accomplished using the following equation:

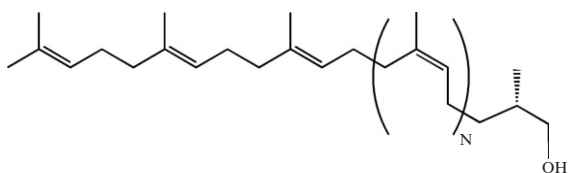
$$\begin{aligned} &[(\text{CoQ9 peak area}/\text{CoQ6 standard peak area}) \times 5 \mu\text{g}]/\text{MW of CoQ9} \\ &= \mu\text{mol CoQ9} \end{aligned}$$

in the sample. Using this method, we have been able to detect CoQs in all cells and tissues we have analyzed.

## 6. LC-MS DETECTION AND QUANTIFICATION OF DOLICHOL

Dolichols are linear polymers of five carbon isoprenoid units ranging in length from mostly 17 to 20 units in animals and up to 40 units in some plants (Figs. 5.1 and 5.7) (Burda and Aebi, 1999; Krag, 1998). Dolichol is found predominantly as the free alcohol in animal tissues, but it may also be esterified to fatty acids or derivatized with sugar phosphates (Chojnacki and Dallner, 1988; Elmberger *et al.*, 1989). The form and distribution of dolichol are tissues and species dependent (Elmberger *et al.*, 1989; Krag, 1998). Whether or not dolichols have functions other than their role in membrane-associated glycosylation reactions is unclear (Lai and Schutzbach, 1986; Rip *et al.*, 1981; Rugar *et al.*, 1982; Valtersson *et al.*, 1985).

Quantitative, chemically defined standards of dolichol are not commercially available. In order to quantify the dolichol content of the RAW cells, a nor-dolichol standard with 17 to 20 isoprene units, which differs from dolichol (Figs. 5.1, 5.7, and 5.8) by the absence of one CH<sub>2</sub> unit at the hydroxyl end of the molecule, was prepared by modification of natural dolichol at Avanti Polar Lipids.



<i>n</i>	nor-Dol species	Formula [M]	[M+Ac] <sup>-</sup>	
			Observed	Exact
13	nor-Dol-17	C <sub>84</sub> H <sub>138</sub> O	1222.137	1222.086
14	nor-Dol-18	C <sub>89</sub> H <sub>146</sub> O	1290.196	1290.151
15	nor-Dol-19	C <sub>94</sub> H <sub>154</sub> O	1358.255	1358.214
16	nor-Dol-20	C <sub>99</sub> H <sub>162</sub> O	1426.316	1426.276

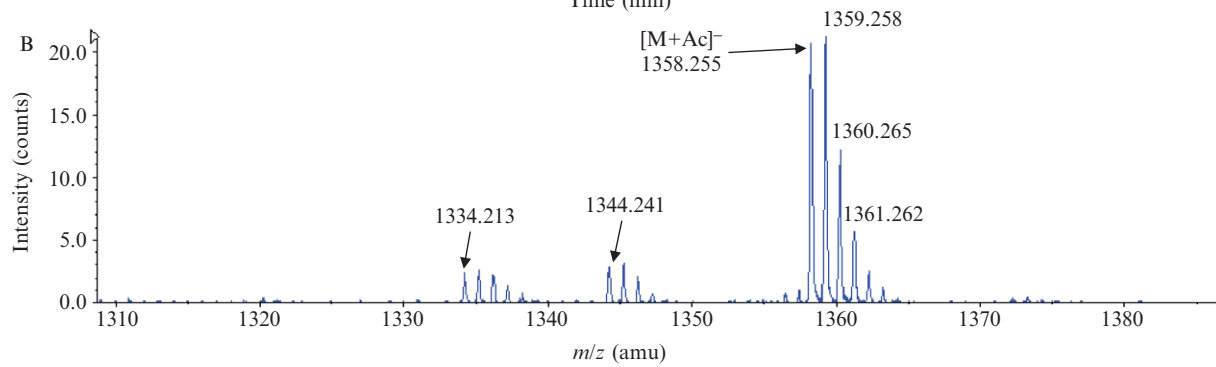
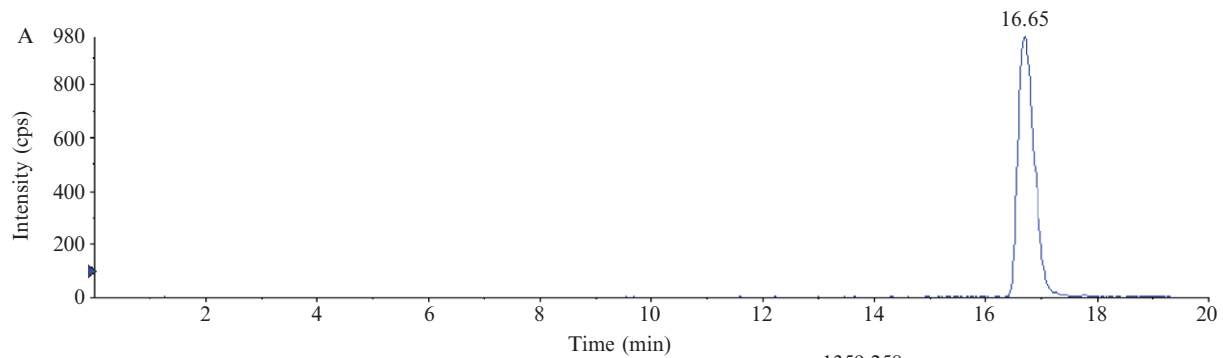
**Figure 5.8** Structures and masses of the acetate adducts of nor-dolichols-17, -18, -19, and -20.

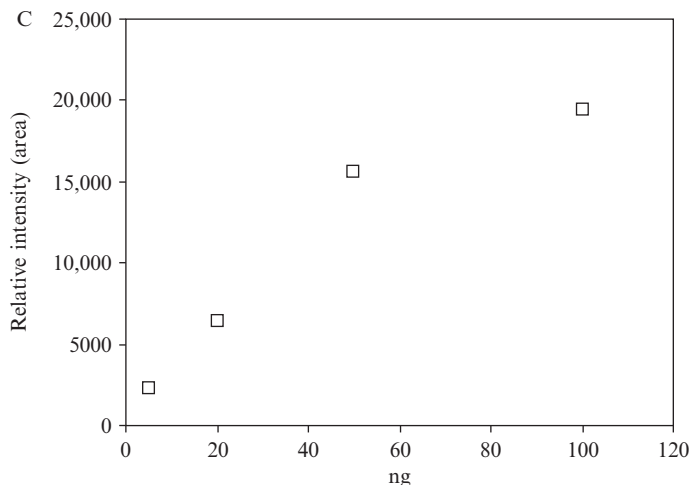
For the LC-MS analysis, we established, as with the coenzyme Q, the linear range of the MS response with respect to the amount of nor-dolichol injected onto the column. Using the same LC-MS system as previously shown and detecting in the negative ion mode, 5, 20, 50, or 100 ng in 10  $\mu$ l of chromatography solvent A were injected onto the Zorbax SB-C8 (2.1  $\times$  50 mm, 5  $\mu$ m) reverse-phase column and eluted using the same scheme as previously described. The mass spectrometer settings are as follows: ESI voltage,  $-4400$  V; declustering potential,  $-55$  V; focusing potential,  $-265$  V; nebulizer gas, 18 psi. The semisynthetic nor-dolichol is a mixture of species with the number of isoprene units ranging from mainly 16 to 21 (Fig. 5.8). The smaller nor-dolichols, such as nor-dolichol with 17 isoprene units, eluted from the column first, followed by the larger nor-dolichol species. The nor-dolichols are detected as the acetate adduct  $[M+Ac]^-$  ions in the negative ion mode using the LC-MS method as previously described. Figure 5.9A shows the EIC for the predominant nor-dolichol-19. The MS of 16.3 to 17.3 min when the nor-dolichol-19 acetate adduct  $[M + Ac]^-$  elutes from the column is shown (Fig. 5.9B). Small amounts of contaminants at  $m/z$  1334.213 and 1344.241 may correspond to oxidative loss of additional carbon atoms from the dolichol during the preparation of the nor-dolichol. Similar to the CoQ standard, the peak area of the EIC for the dolichol standard was linear for 5 ng to 50 ng injected on the column (Fig. 5.9C).

We determined the amount of nor-dolichol standard to add to the extraction mixture in order to have the peak area of the EIC for the standard be about equal to the peak area of the EIC for the dolichols being quantified in the sample. By varying the amount of nor-dolichol added during the co-extraction, we determined that, for a 150-mm culture dish grown to  $\sim 90\%$  confluence, 1  $\mu$ g of the nor-dolichol standard gave an EIC peak area of the nor-dolichol-18 about equal to the EIC peak of the major dolichol species of the cell, dolichol-18.

The ion intensities of dolichol species present in RAW cell lipid extracts are relatively low compared to those of CoQs. Dolichol cannot be detected by direct injection of total lipid extracts without prior chromatography. In addition, while CoQ ions can be readily detected when approximately 5% of the total lipid extract is analyzed using the above LC-MS system, endogenous dolichol ions are only effectively detected when 15% of the total lipid extract is injected onto the reverse-phase column.

Overall, our method for quantifying dolichol is as follows: 1  $\mu$ g of nor-dolichol (dissolved in  $CHCl_3$  at 1 mg/ml) is added to the cell suspension (1 ml) just prior to the addition of chloroform (1.25 ml) and methanol (2.5 ml) to form the single-phase extraction mixture; the lipids are extracted as previously described, dried under a stream of nitrogen, and stored at  $-20^\circ$  until analysis; the dried lipids are redissolved in 0.2 ml of chloroform/methanol (2:1, v/v), and 30  $\mu$ l is injected onto the reverse-phase column and analyzed using the LC-MS procedure previously described.



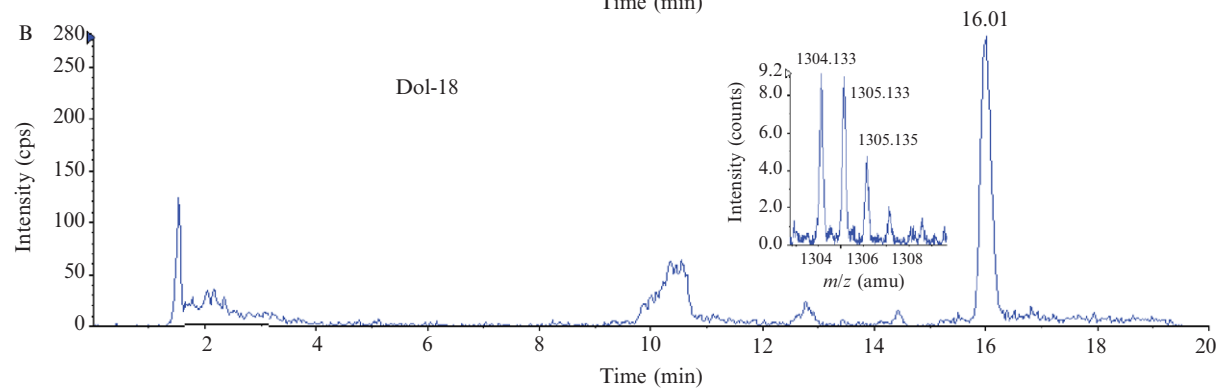
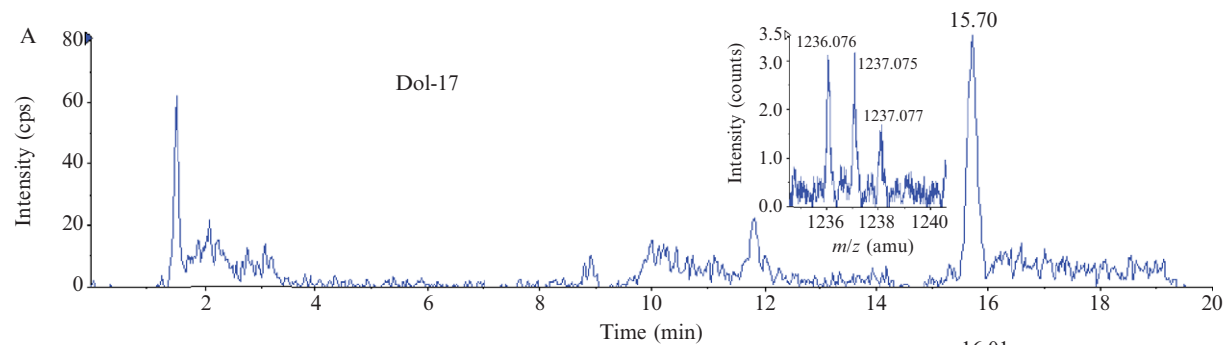


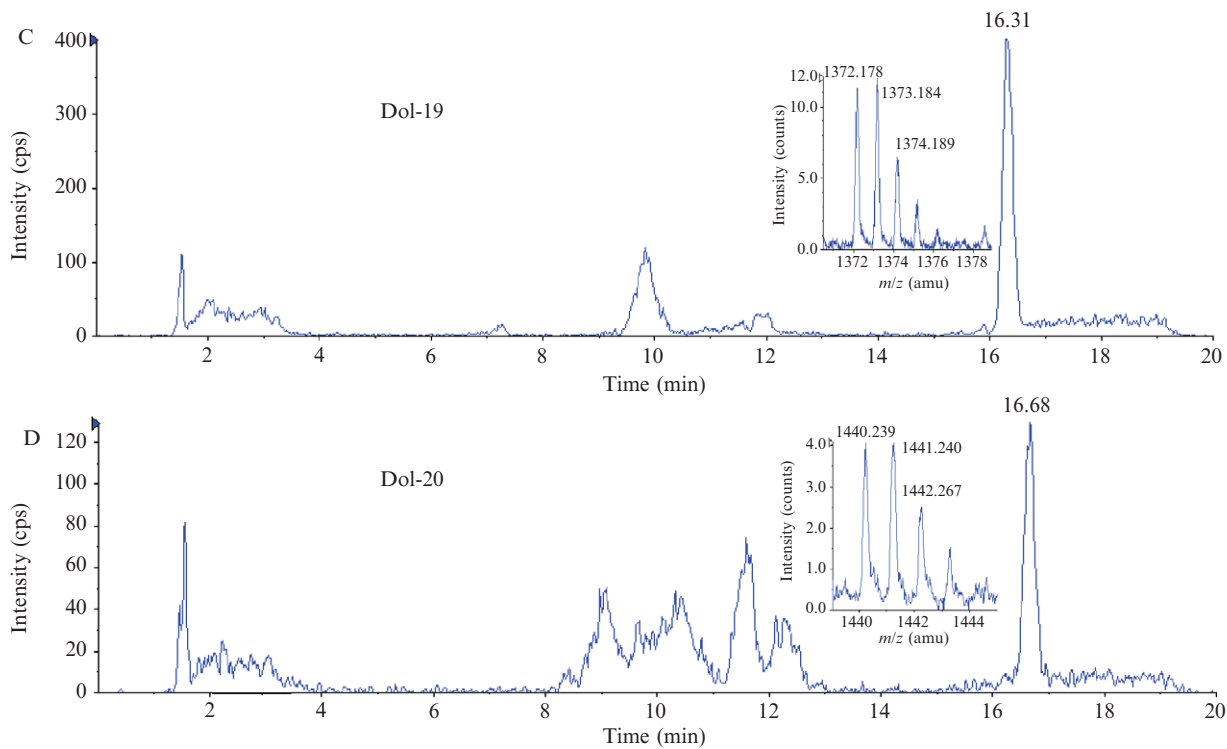
**Figure 5.9** Negative-ion liquid chromatography-mass spectrometry (LC-MS) analysis of nor-dolichol standard. (A) The extracted ion current (EIC) for the  $[M+Ac]^-$  ions of the nor-dolichol-19 (1358.255  $m/z$ ) standard. Under these liquid chromatography conditions, the nor-dolichol-19 elutes at approximately 16.7 min. The shorter nor-dolichols, nor-dolichol-17 and 18, elute slightly earlier, while the nor-dolichol-20 elutes slightly later. (B) The mass spectrum of material eluting between 16.3 to 17.3 min, representing mainly nor-dolichol-19. The small peaks at  $m/z$  1334.213 and 1344.241 are likely due to loss of additional carbons from the dolichol during the preparation of the nor-dolichol standard. (C) The plot of the peak area of the extracted ion current of the  $[M+Ac]^-$  ion of nor-dolichol-19 versus the nanogram (ng) of standard injected onto the Zorbax C-8 reverse-phase column.

Figure 5.10A to D shows the EIC and MS for the endogenous dolichol with 17, 18, 19, and 20 isoprene units. The peak area of the EIC for the  $[M + Ac]^-$  ion of the nor-dolichol-17 was used to quantify dolichol-17; nor-dolichol-18 was used to quantify dolichol 18 and so forth. Because the nor-dolichol standard is a mixture, we needed to determine which fraction of the standard was nor-dolichol-17, nor-dolichol-18, etc. To do this, we summed the peak area of the EIC of nor-dolichol-16 to nor-dolichol-21 to obtain the total peak area when 1  $\mu\text{g}$  of standard was injected onto the column. The total amount of nor-dolichol-18, for example, was then calculated by dividing the peak area of the EIC for nor-dolichol-18 by the summed peak areas. Using this method, we determined the total amount of dolichol in the sample using the following equation:

$$\left[ \frac{\text{Dol-18 peak area}}{\text{nor-Dol-18 standard peak area}} \right] \times 1 \mu\text{g} / \text{MW of Dol-18} = \mu\text{mol Dol-18}$$







**Figure 5.10** Negative ion liquid chromatography-mass spectrometry (LC-MS) analysis of dolichols in RAW lipid extracts. (A–D) The extracted ion current (EIC) of the acetate adducts of dolichol-17, -18, -19, and -20, respectively. For each, the peak labeled with a retention time corresponds to the relevant extracted ion current peak for a given dolichol. The inset on each panel shows the mass spectra of each of the dolichols detected in the RAW lipid extract.

in the sample. Because large amounts of total lipid extract are being injected onto the column, a blank is run between each sample being analyzed to prevent carry-over between samples.

Note: Separate cell suspensions are not necessary for the quantification of the CoQs and dolichols. Routinely, a single cell suspension is co-extracted with both the nor-dolichol and CoQ6 standard. After extraction, the sample is divided in two and analyzed using positive-ion LC-MS for quantification of the CoQs and negative-ion LC-MS for quantification of the dolichols.

## 7. LC-MS AND LC-MS/MS CHARACTERIZATION OF DOLICHOL DIPHOSPHATE-LINKED OLIGOSACCHARIDES

Dolichols play a central role in the *N*-glycosylation and *O*-glycosylation of eucaryotic proteins (Imperiali and O'Connor, 1999; Schenk *et al.*, 2001; Weerapana and Imperiali, 2006). Dol-PP-(GlcNAc)<sub>2</sub>(Man)<sub>9</sub>(Glc)<sub>3</sub> (Fig. 5.3) serves as the donor for *en bloc* transfer to select asparagine residues during the co-translational processing of secretory proteins in the lumen of the endoplasmic reticulum (Burda and Aebi, 1999; Helenius and Aebi, 2004). Removal and addition of sugars to this oligosaccharide occur as the protein moves through the secretory pathway and is involved, in part, in the targeting of proteins to their proper locations in cells (Burda and Aebi, 1999; Huet *et al.*, 2003). Previously, the structure and biosynthesis of the 14-sugar oligosaccharide donor had been proposed based on the studies using a combination of radio-labeling, enzymatic digestion, chemical derivatization, thin layer chromatography, and gas-liquid chromatography (Kornfeld *et al.*, 1978; Li and Kornfeld, 1979; Li *et al.*, 1978). However, none of the structural characterization was performed on the intact donor molecule.

We wanted to develop a MS-based technique to detect and confirm the structure of the intact Dol-PP-(GlcNAc)<sub>2</sub>(Man)<sub>9</sub>(Glc)<sub>3</sub>. A sample of Dol-PP-(GlcNAc)<sub>2</sub>(Man)<sub>9</sub>(Glc)<sub>3</sub>, purified from porcine pancreas, was kindly provided by Dr. R. Gilmore. Due to the amphiphatic nature of this molecule, we modified the LC-MS method previously described. Specifically, a new solvent mixture was used as chromatography solvent B (chloroform:methanol:1 mM ammonium acetate [2:3:1 v/v/v], supplemented with 0.1% piperidine). With this modification, we were able to detect the Dol-PP-(GlcNAc)<sub>2</sub>(Man)<sub>9</sub>(Glc)<sub>3</sub> eluting between 9 and 12 min, depending on the length of the dolichol to which the 14-sugar oligosaccharide was attached. Figures 5.11A–D shows the EIC and MS for the [M–2H]<sup>2–</sup> ion for the oligosaccharide attached to Dol-17, 18, 19, and 20. The exact mass predicted from the proposed structure matches the mass of the major [M–2H]<sup>2–</sup> (Fig. 5.3 and Table 5.1) and [M–3H]<sup>3–</sup> ions (not shown) within experimental error.

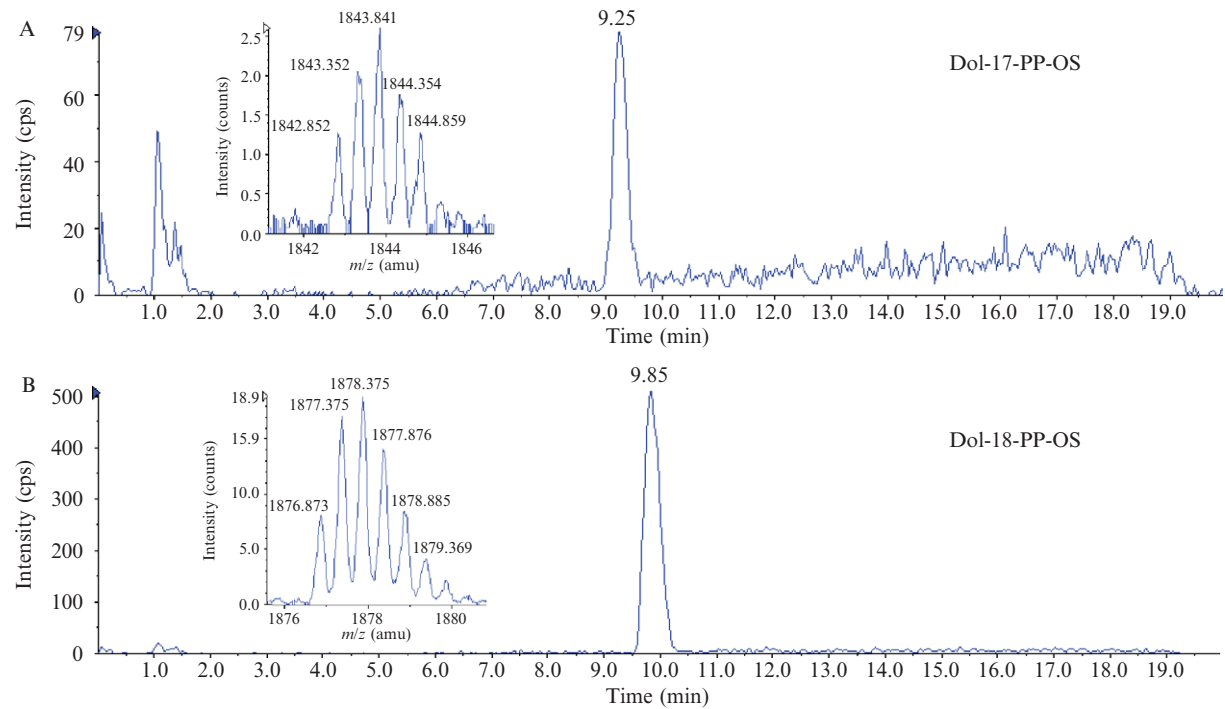
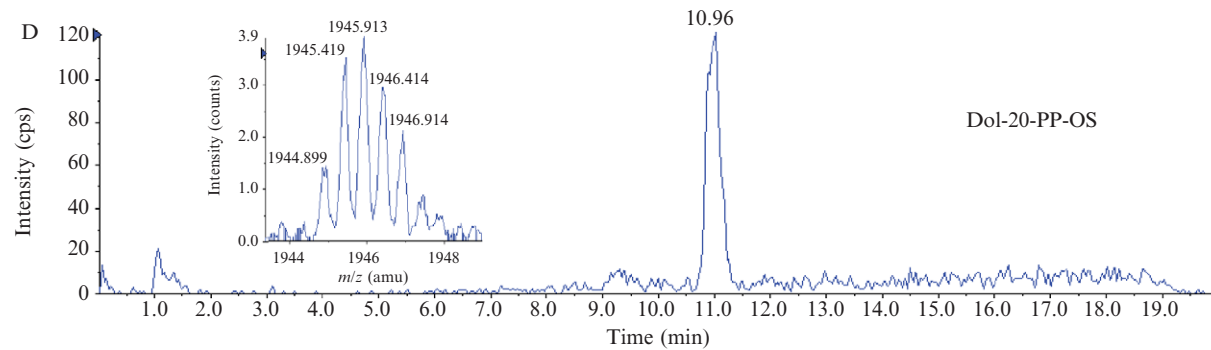
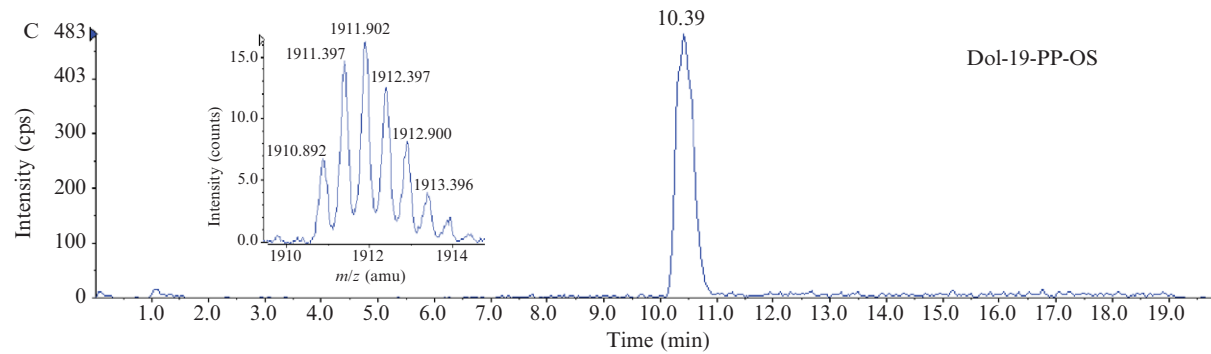
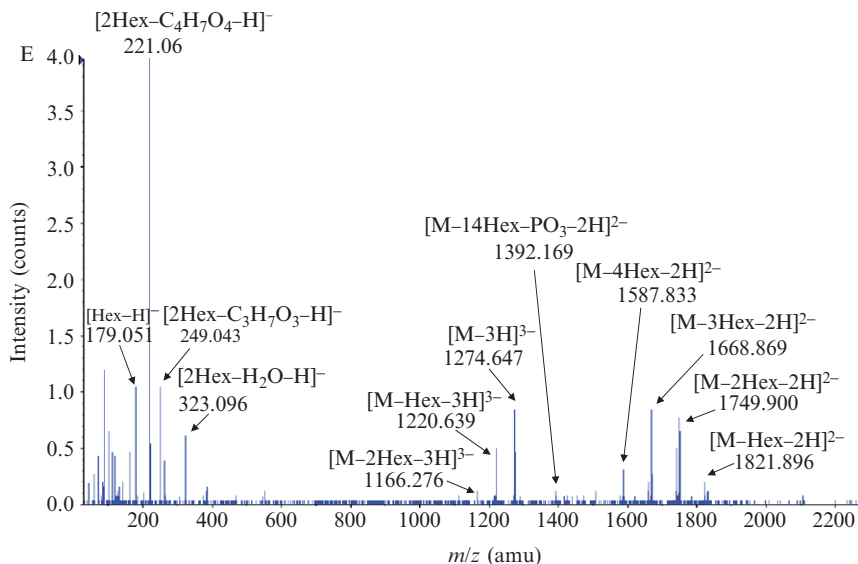


Figure 5.11 (continued)





**Figure 5.11** Negative-ion liquid chromatography-mass spectrometry (LC-MS) analysis of purified Dol-PP-(GlcNAc)<sub>2</sub>(Man)<sub>9</sub>(Glc)<sub>3</sub>. (A–D) The extracted ion current (EIC) of Dol-PP-(GlcNAc)<sub>2</sub>(Man)<sub>9</sub>(Glc)<sub>3</sub> with 17, 18, 19, and 20 isoprenoid units on the dolichol, respectively. The inset shows the mass spectrum of the [M–2H]<sup>2–</sup> ion for the Dol-PP-(GlcNAc)<sub>2</sub>(Man)<sub>9</sub>(Glc)<sub>3</sub> detected in the purified sample. (E) The collision-induced mass spectrometry (CID-MS) of the most abundant isotope of the [M–3H]<sup>3–</sup> ion of the Dol-19-PP-(GlcNAc)<sub>2</sub>(Man)<sub>9</sub>(Glc)<sub>3</sub> (*m/z* 1274.647). Sequential loss of 162 u, which corresponds to the loss of one, two, three, or four hexoses, is observed. A fragment ion corresponding to Dol-19-P is also detected as a singly charged ion at *m/z* 1392.169. Fragment ions corresponding to a single hexose (*m/z* 179.051) and two hexoses (*m/z* 323.096) are detected in the low mass region. The remaining low mass fragment ions are most likely due to cross-ring cleavage as described by [Sheeley and Reinhold \(1998\)](#).

**Table 5.1** Masses of the [M–2H]<sup>2–</sup> Ions of Dol-PP-(GlcNAc)<sub>2</sub>(Man)<sub>9</sub>(Glc)<sub>3</sub>

<i>n</i>	Dol-PP-OS species	Formula [M]	[M–2H] <sup>2–</sup>	
			Observed ( <i>m/z</i> )	Exact ( <i>m/z</i> )
11	Dol-17-PP-OS	C <sub>173</sub> H <sub>288</sub> N <sub>2</sub> O <sub>77</sub> P <sub>2</sub>	1842.852	1484.908
12	Dol-18-PP-OS	C <sub>178</sub> H <sub>296</sub> N <sub>2</sub> O <sub>77</sub> P <sub>2</sub>	1876.873	1876.939
13	Dol-19-PP-OS	C <sub>183</sub> H <sub>304</sub> N <sub>2</sub> O <sub>77</sub> P <sub>2</sub>	1910.892	1910.971
14	Dol-20-PP-OS	C <sub>188</sub> H <sub>312</sub> N <sub>2</sub> O <sub>77</sub> P <sub>2</sub>	1944.899	1445.002

Using this technique, we also performed CID-MS on the most abundant isotope of the triply charged ion of the Dol-19-PP-(GlcNAc)<sub>2</sub>(Man)<sub>9</sub>(Glc)<sub>3</sub> to verify the structure proposed by (Kornfeld *et al.*, 1978; Li and Kornfeld, 1979; Li *et al.*, 1978). This spectrum, shown in Fig. 5.11E, shows the sequential loss of 162 u, which corresponds to the loss of one, two, three, or four hexoses. A fragment ion corresponding to Dol-19-P is also detected as a singly charged ion at  $m/z$  1392.169. In the lower mass region, fragment ions corresponding to a single hexose ( $m/z$  179.051) and two hexoses ( $m/z$  323.096) are also detected. The remaining low-mass fragment ions are most likely due to cross-ring cleavage as described by Sheeley and Reinhold (1998). Our data are consistent with the proposed structure shown in Fig. 5.2, but cannot be used to confirm the positions of the glycosidic linkages, the anomeric stereochemistry, or the actual sugar composition. These issues will have to be evaluated via NMR spectroscopy and other procedures.

We were unable to detect Dol-PP-(GlcNAc)<sub>2</sub>(Man)<sub>9</sub>(Glc)<sub>3</sub> in lipid extracts of RAW cells grown at the scale described above. The Bligh-Dyer extraction procedure that we use (Fig. 5.3) is not likely to extract this material, as it differs significantly from the procedure used by Kelleher *et al.* (2001). However, one would expect that dolichol phosphate, dolichol diphosphate, and dolichol phosphates derivatized with one or two sugars would be efficiently extracted by our procedure. Using a similar extraction, one does in fact readily detect undecaprenol phosphate in a total *Escherichia coli* lipid extract (Z. Guan and C. R. H. Raetz, unpublished), and both dodecaprenol phosphate and dodecaprenol phosphate-galacturonic acid in *Rhizobium leguminosarum* (Kanjilal-Kolar and Raetz, 2006). While we have been able to detect purified dolichol-phosphate and dolichol phosphate mannose (provided by Charles J. Waechter at University of Kentucky College of Medicine) using the LC-MS conditions described above (data not shown), our inability to detect dolichol phosphate, dolichol diphosphate, dolichol phosphate-hexose, or dolichol diphosphate-N-acetylglucosamine in the total lipids of RAW cells suggests that the endogenous levels of these compounds are extremely low.

## ACKNOWLEDGMENT

We thank Dr. Robert Murphy for many stimulating discussions and advice with LC-MS conditions.

## REFERENCES

- Bligh, E. G., and Dyer, W. J. (1959). A rapid method of total lipid extraction and purification. *Can. J. Biochem. Phys.* **37**, 911–917.

- Burda, P., and Aebi, M. (1999). The dolichol pathway of N-linked glycosylation. *Biochim. Biophys. Acta* **1426**, 239–257.
- Callender, H. L., Forrester, J. S., Ivanova, P., Preininger, A., Milne, S., and Brown, H. A. (2007). Quantification of diacylglycerol species from cellular extracts by electrospray ionization mass spectrometry using a linear regression algorithm. *Anal. Chem.* **79**, 263–272.
- Chojnacki, T., and Dallner, G. (1988). The biological role of dolichol. *Biochem. J.* **251**, 1–9.
- Elmberger, P. G., Eggens, I., and Dallner, G. (1989). Conditions for quantitation of dolichyl phosphate, dolichol, ubiquinone and cholesterol by HPLC. *Biomed. Chromatogr.* **3**, 20–28.
- Ericsson, J., Greene, J. M., Carter, K. C., Shell, B. K., Duan, D. R., Florence, C., and Edwards, P. A. (1998). Human geranylgeranyl diphosphate synthase: Isolation of the cDNA, chromosomal mapping and tissue expression. *J. Lipid Res.* **39**, 1731–1739.
- Fahy, E., Subramaniam, S., Brown, H. A., Glass, C. K., Merrill, A. H. J., Murphy, R. C., Raetz, C. R., Russell, D. W., Seyama, Y., Shaw, W., Shimizu, T., Spener, F., et al. (2005). A comprehensive classification system for lipids. *J. Lipid Res.* **46**, 839–861.
- Gelb, M. H., Brunsfeld, L., Hrycyna, C. A., Michaelis, S., Tamanoi, F., Van Voorhis, W. C., and Waldmann, H. (2006). Therapeutic intervention based on protein prenylation and associated modifications. *Nat. Chem. Biol.* **2**, 518–528.
- Gould, T. A., Herman, J., Krank, J., Murphy, R. C., and Churchill, M. E. (2006). Specificity of acyl-homoserine lactone synthases examined by mass spectrometry. *J. Bacteriol.* **188**, 773–783.
- Haroldsen, P. E., Clay, K. L., and Murphy, R. C. (1987). Quantitation of lyso-platelet activating factor molecular species from human neutrophils by mass spectrometry. *J. Lipid Res.* **28**, 42–49.
- Hedl, M., Tabernero, L., Stauffacher, C. V., and Rodwell, V. W. (2004). Class II 3-hydroxy-3-methylglutaryl coenzyme A reductases. *J. Bacteriol.* **186**, 1927–1932.
- Helenius, A., and Aebi, M. (2004). Roles of N-linked glycans in the endoplasmic reticulum. *Annu. Rev. Biochem.* **73**, 1019–1049.
- Hubbard, S. C., and Ivatt, R. J. (1981). Synthesis and processing of asparagine-linked oligosaccharides. *Annu. Rev. Biochem.* **50**, 555–593.
- Huet, G., Gouyer, V., Delacour, D., Richet, C., Zanetta, J. P., Delannoy, P., and Degand, P. (2003). Involvement of glycosylation in the intracellular trafficking of glycoproteins in polarized epithelial cells. *Biochimie* **85**, 323–330.
- Imperiali, B., and O'Connor, S. E. (1999). Effect of N-linked glycosylation on glycopeptide and glycoprotein structure. *Curr. Opin. Chem. Biol.* **3**, 643–649.
- Kanjilal-Kolar, S., and Raetz, C. R. (2006). Dodecaprenyl phosphate-galacturonic acid as a donor substrate for lipopolysaccharide core glycosylation in *Rhizobium leguminosarum*. *J. Biol. Chem.* **281**, 12879–12887.
- Kean, E. L., Wei, Z., Anderson, V. E., Zhang, N., and Sayre, L. M. (1999). Regulation of the biosynthesis of N-acetylglucosaminylpyrophosphoryldolichol, feedback and product inhibition. *J. Biol. Chem.* **274**, 34072–34082.
- Kelleher, D. J., Karaoglu, D., and Gilmore, R. (2001). Large-scale isolation of dolichol-linked oligosaccharides with homogeneous oligosaccharide structures: Determination of steady-state dolichol-linked oligosaccharide compositions. *Glycobiology* **11**, 321–333.
- Kellogg, B. A., and Poulter, C. D. (1997). Chain elongation in the isoprenoid biosynthetic pathway. *Curr. Opin. Chem. Biol.* **1**, 570–578.
- Kornfeld, R., and Kornfeld, S. (1985). Assembly of asparagine-linked oligosaccharides. *Annu. Rev. Biochem.* **54**, 631–664.
- Kornfeld, S., Li, E., and Tabas, I. (1978). The synthesis of complex-type oligosaccharides. II. Characterization of the processing intermediates in the synthesis of the complex oligosaccharide units of the vesicular stomatitis virus G protein. *J. Biol. Chem.* **253**, 7771–7778.



- Krag, S. S. (1998). The importance of being dolichol. *Biochem. Biophys. Res. Comm.* **243**, 1–5.
- Kuzuyama, T., and Seto, H. (2003). Diversity of the biosynthesis of the isoprene units. *Nat. Prod. Rep.* **20**, 171–183.
- Lai, C. S., and Schutzbach, J. S. (1986). Localization of dolichols in phospholipid membranes. An ESR spin label study. *FEBS Lett.* **203**, 153–156.
- Leyes, A. E., Baker, J. A., and Poulter, C. D. (1999). Biosynthesis of isoprenoids in *Escherichia coli*: Stereochemistry of the reaction catalyzed by farnesyl diphosphate synthase. *Org. Lett.* **1**, 1071–1073.
- Li, E., and Kornfeld, S. (1979). Structural studies of the major high mannose oligosaccharide units from Chinese hamster ovary cell glycoproteins. *J. Biol. Chem.* **254**, 1600–1605.
- Li, E., Tabas, I., and Kornfeld, S. (1978). The synthesis of complex-type oligosaccharides. I. Structure of the lipid-linked oligosaccharide precursor of the complex-type oligosaccharides of the vesicular stomatitis virus G protein. *J. Biol. Chem.* **253**, 7762–7770.
- Meganathan, R. (2001a). Biosynthesis of menaquinone (vitamin K<sub>2</sub>) and ubiquinone (coenzyme Q): A perspective on enzymatic mechanisms. *Vitam. Horm.* **61**, 173–218.
- Meganathan, R. (2001b). Ubiquinone biosynthesis in microorganisms. *FEMS Microbiol. Lett.* **203**, 131–139.
- Olgun, A., Serif, A., Tezcan, S., and Kutluay, T. (2003). The effect of isoprenoid side chain length on ubiquinone on life span. *Med. Hypotheses* **60**, 325–327.
- Olson, J. A. (1964). The biosynthesis and metabolism of carotenoids and retinol (vitamin A). *J. Lipid Res.* **5**, 281–299.
- Raetz, C. R. H., Garrett, T. A., Reynolds, C. M., Shaw, W. A., Moore, J. D., Smith, D. C., Jr., Ribeiro, A. A., Murphy, R. C., Ulevitch, R. J., Fearn, C., Reichart, D., *et al.* (2006). Kdo<sub>2</sub>-lipid A of *Escherichia coli*, a defined endotoxin that activates macrophages via TLR-4. *J. Lipid Res.* **47**, 1097–1111.
- Rip, J. W., Rugar, C. A., Chaudhary, N., and Carroll, K. K. (1981). Localization of a dolichyl phosphate phosphatase in plasma membranes of rat liver. *J. Biol. Chem.* **256**, 1929–1934.
- Rodriguez-Concepcion, M. (2004). The MEP pathway: A new target for the development of herbicides, antibiotics, and antimalarial drugs. *Curr. Pharm. Des.* **10**, 2391–2400.
- Rohdich, F., Bacher, A., and Eisenreich, W. (2004). Perspectives in anti-infective drug design. The late steps in the biosynthesis of the universal terpenoid precursors, isopentenyl diphosphate and dimethylallyl diphosphate. *Bioorg. Chem.* **32**, 292–308.
- Rosner, M. R., Hubbard, S. C., Ivatt, R. J., and Robbins, P. W. (1982). N-asparagine-linked oligosaccharides: Biosynthesis of the lipid-linked oligosaccharides. *Methods Enzymol.* **83**, 399–408.
- Rugar, C. A., Rip, J. W., Chaudhary, N., and Carroll, K. K. (1982). The subcellular localization of enzymes of dolichol metabolism in rat liver. *J. Biol. Chem.* **257**, 3090–3094.
- Saraste, M. (1999). Oxidative phosphorylation at the fin de siecle. *Science* **283**, 1488–1493.
- Schenk, B., Fernandez, F., and Waechter, C. J. (2001). The ins(ide) and outs(ide) of dolichyl phosphate biosynthesis and recycling in the endoplasmic reticulum. *Glycobiology* **11**, 61R–70R.
- Sheeley, D. M., and Reinhold, V. N. (1998). Structural characterization of carbohydrate sequence, linkage, and branching in a quadrupole ion trap mass spectrometer: Neutral oligosaccharides and N-linked glycans. *Anal. Chem.* **70**, 3053–3059.
- Swiezewska, E., and Danikiewicz, W. (2005). Polyisoprenoids: Structure, biosynthesis and function. *Prog. Lipid Res.* **44**, 235–258.
- Szkopinska, A. (2000). Ubiquinone. Biosynthesis of quinone ring and its isoprenoid side chain. Intracellular localization. *Acta Biochim. Pol.* **47**, 469–480.

- Teshima, K., and Kondo, T. (2005). Analytical method for ubiquinone-9 and ubiquinone-10 in rat tissues by liquid chromatography/turbo ion spray tandem mass spectrometry with 1-alkylamine as an additive to the mobile phase. *Anal. Biochem.* **338**, 12–19.
- Turunen, M., Olsson, J., and Dallner, G. (2004). Metabolism and function of coenzyme Q. *Biochim. Biophys. Acta* **1660**, 171–199.
- Valtersson, C., van Duyn, G., Verkleij, A. J., Chojnacki, T., de Kruijff, B., and Dallner, G. (1985). The influence of dolichol, dolichol esters, and dolichyl phosphate on phospholipid polymorphism and fluidity in model membranes. *J. Biol. Chem.* **260**, 2742–2751.
- Weerapana, E., and Imperiali, B. (2006). Asparagine-linked protein glycosylation: From eukaryotic to prokaryotic systems. *Glycobiology* **16**, 91R–101R.

# EXTRACTION AND ANALYSIS OF STEROLS IN BIOLOGICAL MATRICES BY HIGH PERFORMANCE LIQUID CHROMATOGRAPHY ELECTROSPRAY IONIZATION MASS SPECTROMETRY

Jeffrey G. McDonald, Bonne M. Thompson,  
Erin C. McCrum, *and* David W. Russell

---

## Contents

1. Introduction	146
2. Supplies and Reagents	148
3. Extraction of Lipids from Cultured Cells and Tissues	149
4. Saponification of Lipid Extracts	151
5. Solid-Phase Extraction	152
6. Analysis by HPLC-ESI-MS	153
6.1. High performance liquid chromatography	153
6.2. Electrospray ionization mass spectrometry	153
7. Quantitation	156
8. Data	157
9. Discussion, Nuances, Caveats, and Pitfalls	162
9.1. Quantitation	162
9.2. Availability and purity of primary and deuterated standards	163
9.3. Resolving related sterols by HPLC	164
9.4. Acetonitrile and signal intensity	165
9.5. Auto-oxidation and use of SPE columns	165
9.6. Sample clean-up	166
9.7. Residual insoluble material	167
9.8. Comparing relative peak areas	168
9.9. Electrospray using other instrumental platforms	168
Acknowledgments	168
References	169

Department of Molecular Genetics, University of Texas Southwestern Medical Center at Dallas, Dallas, Texas

*Methods in Enzymology*, Volume 432  
ISSN 0076-6879, DOI: 10.1016/S0076-6879(07)32006-5

© 2007 Elsevier Inc.  
All rights reserved.

## Abstract

We describe the development of a high performance liquid chromatography mass spectrometry (HPLC-MS) method that allows the identification and quantitation of sterols in mammalian cells and tissues. Bulk lipids are extracted from biological samples by a modified Bligh/Dyer procedure in the presence of eight deuterated sterol standards to allow subsequent quantitation and determination of extraction efficiency. Sterols and other lipids are resolved by HPLC on a reverse-phase C<sub>18</sub> column using a binary gradient of methanol and water, both containing 5 mM ammonium acetate. Sterol identification is performed using an Applied Biosystems (Foster City, CA) 4000 QTRAP<sup>®</sup> mass spectrometer equipped with a TurboV electrospray ionization source and operated in the positive (+) selected reaction monitoring (SRM) mode. The total run time of the analysis is 30 min. Sterols are quantitated by comparison of the areas under the elution curves derived from the detection of endogenous compounds and isotopically labeled standards. The sensitivity of the method for sterol detection ranges between 10 and 2000 fmol on-column. Cultured RAW 264.7 mouse macrophages contain many different sterols, including the liver X receptor (LXR) ligand 24,25-epoxycholesterol. Tissues such as mouse brain also contain large numbers of sterols, including 24(s)-hydroxycholesterol, which is involved in cholesterol turnover in the brain. The extraction procedure described is flexible and can be tailored to sample type or information sought. The instrumental analysis method is similarly adaptable and offers high selectivity and sensitivity.

## 1. INTRODUCTION

Sterols play fundamental roles in many physiological processes in virtually all living organisms. Sterols have regulatory functions, are involved in cellular signaling, and are an integral building block of cell membranes in which they modulate fluidity. The most abundant sterol in mammals is cholesterol, which is a precursor to a host of important end-products including steroid hormones, bile acids, vitamin D, and others (Myant, 1981; Russell, 2003). Cholesterol has gained a certain amount of notoriety due to its negative impact on health when present in high levels, while other sterols, such as the phytosterols derived from plants, offer health benefits by lowering plasma cholesterol levels (Moruise *et al.*, 2006; Ostlund *et al.*, 2003). In most mammalian tissues, sterols are both synthesized and absorbed through the diet, while in the brain they result exclusively from *de novo* synthesis (Dietschy and Turley, 2004).

Few advances have been made in the area of instrumental analysis of sterols. Many sterols are not well suited for analysis in their native state by modern instrumental analytical techniques due to their chemical structures and functional groups. Sterols have historically been analyzed by gas

chromatographic MS (GC-MS) (Lund and Diczfalusy, 2003; Wilund *et al.*, 2004). GC offers high temporal resolution, allowing for the separation of sterols of similar composition such as positional isomers and diastereomers. Analysis by GC-MS relies upon vaporization of the sample, and the polarity imparted to a sterol by functional groups decreases its ability to transition to the gas phase. This decrease is largely due to hydrogen bonding and analyte interactions with the glass liner of the injection port, which can interfere with vaporization and cause thermal degradation. These issues can be overcome by reducing the polarity of the molecule by derivatization with trimethylsilanes or methyl groups to achieve reasonable signal intensity and good chromatographic separation (Abidi, 2001; Isobe *et al.*, 2002); however, derivatization adds additional steps to sample preparation, increases instrument maintenance requirements, and can increase the complexity of the resulting chromatogram. GCs are typically coupled to electron impact mass spectrometers, which offer the ability to compare acquired mass spectra to reference libraries for possible identification of unknowns. The almost exclusive use of single quadrupole electron impact mass spectrometers with GC systems does not offer the ability to perform advanced mass spectral investigations like tandem MS (MS/MS) or precursor/product ion scans.

Sterols are more amenable in their native state to separation by high performance liquid chromatography (HPLC), although few suitable detectors are available. Most sterols lack a chromophore, which prevents their detection by ultraviolet (UV)/visible or fluorescence spectroscopy. Sterols can be modified to better absorb light by derivatization or by oxidation of alcohol substituents to oxo-groups; however, these modifications add complexity and additional steps to the analysis. Evaporative light-scattering detection (ELSD) was developed for use with HPLC and has good sensitivity. An ELSD device generates particles from the eluent of the HPLC column via heated nebulization and produces a signal based on light scattered from an analyte. The ELSD responds only to the number of particles present, and thus does not discriminate based on the physical characteristics of the molecule being measured. Note that ELSD produces a nonlinear response, which should be considered when interpreting data. These features allow for relative comparisons to be made between chromatographic peaks, especially when the compounds of interest are present in similar amounts; however, ELSD does not provide selectivity in terms of mass or other compound-specific information, which renders the analysis dependent on the chromatographic performance of the HPLC system.

Historically, MS has been challenging to couple with HPLC, in part because taking microliter to milliliter quantities of HPLC eluent from atmospheric pressure to the high-vacuum environment of MS is difficult. Until recently, the eluent was thermally vaporized prior to MS analysis; however, this approach did not allow detection of thermally labile compounds.

Atmospheric Pressure Chemical Ionization (APCI) is a different ionization source that has been successfully employed for sterol analysis by HPLC-MS (Burkard *et al.*, 2004; Palmgren *et al.*, 2005; Tian *et al.*, 2006).

The efficient generation of ions and their transport into the mass spectrometer was another technological hurdle. A variety of techniques were used to ionize analytes; however, no one technique proved to be broadly applicable. The advent of electrospray ionization (ESI) (Fenn *et al.*, 1989) overcame these hurdles and made HPLC-ESI-MS a broadly applicable method for small molecule analysis. The electrospray interface can be used independently or to couple HPLC to most types of mass spectrometers, further diversifying the utility of this approach.

Although numerous biological functions of sterols have been described, many more are yet to be discovered. The elucidation of new functions will require not only advances in biology but also more sophisticated and sensitive analytical techniques to identify quantitative behaviors of sterols *in situ*. An increasing number of methods in the literature report on the extraction and analysis of sterol subclasses, such as oxysterols (Pulfer *et al.*, 2005; Shan *et al.*, 2003) and plant sterols (Abidi, 2001), using HPLC-MS; however, no comprehensive method exists for HPLC-MS of all sterols. We report here a method for the extraction and analysis of sterols from tissue and other biological matrices using HPLC-ESI-MS. The extraction procedure is flexible and can be tailored to sample type and information sought. The instrumental analysis offers excellent selectivity and sensitivity and is adaptable to virtually all sterols with a run time of 30 min per sample.

## 2. SUPPLIES AND REAGENTS

Phosphate Buffered Saline (PBS)

Cell lifters

Glass culture tubes with Teflon<sup>TM</sup>-lined caps (7-, 11-, 14-, 18-ml)

Wheaton Science Products

7-ml 358640

11-ml 358646

14-ml 358647

18-ml 358648

10-ml glass pipettes

Pasteur pipettes

Mechanical pipette pump

Glass vials with Teflon<sup>TM</sup>-lined caps (2-, 4-, 8-ml)

Wheaton Science Products

2-ml W224581

4-ml W224582

8-ml W224584

Solid-phase extraction (SPE) cartridges (100-mg silica, Isolute)  
Vacuum apparatus for SPE  
0.5% (v/v) isopropanol in hexane  
30% (v/v) isopropanol in hexane  
HPLC-grade methanol, ethanol, chloroform, hexane, and H<sub>2</sub>O  
Potassium hydroxide (10 N)  
Ammonium acetate  
Saponification solution  
Hyrolysis solution (6 ml of 10 N KOH diluted to 100 ml with ethanol)  
Bligh/Dyer solvent (1:2 [v/v] chloroform:methanol)  
Primary and deuterated sterol standards  
Luna C<sub>18</sub> reverse-phase HPLC column (250 × 2 mm; 3 μm-particle size)

### 3. EXTRACTION OF LIPIDS FROM CULTURED CELLS AND TISSUES

Extraction of cultured cells begins by placing the culture dishes (6-cm dishes seeded with  $2 \times 10^6$  cells) on ice. The medium is removed with a glass pipette to a screw-cap glass culture tube and stored for extraction later. Cells are gently washed twice with 3 ml of cold PBS, which is removed and discarded. An additional 1.6 ml of cold PBS are added to the cells, which are then gently scraped from the surface of the dish using a cell lifter. Cells are transferred to a 14-ml screw-cap glass culture tube. Depending on the desired information, aliquots of the medium or cells may be taken at this stage for assays to determine levels of cytokines, DNA, or protein. Lipids are extracted from the cells using a Bligh/Dyer procedure (Bligh and Dyer, 1959) in which 6 ml of chloroform:methanol (1:2 v/v) is added to the resuspended cells in 14-ml screw-cap glass culture tubes. At this point, deuterated surrogate sterol standards are added for quantitative analysis, as indicated in Table 6.1 (see “Quantitation” section for definition of surrogate standards). Samples are vortexed at high speed for 10 s, then centrifuged at 2600 rpm (1360 rcf) for 5 min to pellet insoluble material. The supernatant is decanted to a fresh 14-ml glass culture tubes and 2 ml each of chloroform and PBS is added. Samples are again vortexed for 10 s and centrifuged at room temperature for 5 min at 2600 rpm. Two liquid phases should now be observed. The organic lower phase is removed using a Pasteur pipette and transferred to a 4-ml glass vial with a Teflon-lined cap. The upper aqueous phase is discarded. We recommend the use of a mechanical pipette pump (e.g., Scienceware Pipette Pump) versus a pipette bulb for better control when removing liquid near the aqueous-organic interface.

The organic phase is evaporated under a gentle stream of dry nitrogen while heating at approximately 35° to counter the evaporative

**Table 6.1** Deuterated and primary sterols and the masses and volumes used for quantitative analysis

Compound <sup>a</sup>	Parts per million (PPM)
<b>Surrogate mix 1 (10 <math>\mu</math>l)</b>	
25-Hydroxycholesterol (D3)	4
27-Hydroxycholesterol-(25R) (D7)	4
24,25-Epoxycholesterol (D6) (R+S)	3
7 $\alpha$ -Hydroxycholesterol (D7)	4
7-Ketocholesterol (D7)	4
4 $\beta$ -Hydroxycholesterol (D7)	2
<b>Surrogate mix 2 (10 <math>\mu</math>l)</b>	
Cholesterol (D7)	150
Desmosterol (D6)	80
<b>Internal standard (10 <math>\mu</math>l)</b>	
6 $\alpha$ -Hydroxycholestanol (D7)	4
<b>Sterol mix (10 <math>\mu</math>l)</b>	
22R-Hydroxycholesterol	4
25-Hydroxycholesterol	4
27-Hydroxycholesterol-(25R)	4
24,25-Epoxycholesterol	3
7 $\alpha$ -Hydroxycholesterol	4
7-Ketocholesterol	4
4 $\beta$ -Hydroxycholesterol	2
Desmosterol	80
7-Dehydrocholesterol	100
Cholestenone	15
Cholesterol	150
Lanosterol	100

<sup>a</sup> See Table 6.3 for systematic sterol names and Table 6.4 for deuterium positions.

cooling effect. The dried extracts are reconstituted in approximately 200  $\mu$ l of 95% (v/v) methanol, shaken gently, and transferred to an auto-sampler vial containing the appropriate deuterated internal standard based on the amount given in Table 6.1 (see “Quantitation” section for definition of internal standard). An additional 200  $\mu$ l of 95% methanol is added, the sample is gently shaken, and the solution is transferred to the same auto-sampler vial. This additional rinse ensures maximum transfer of sterols from the sample vial to the auto-sampler vial. Vortexing or sonicating the sample should not be done, as these treatments can disperse any residual insoluble material into the solution, which in turn adversely affects subsequent HPLC or MS analyses of the extracts. Occasionally, even gently shaking the extract can cause resuspension of insoluble material. If insoluble material is inadvertently resuspended, centrifugation and decanting the supernatant are usually



sufficient to clarify the extract. If the final extract is not colorless and free of solid material, then the Bligh/Dyer extraction should be repeated. The auto-sampler vial should be equipped with an appropriate volume-reducing insert if the final volume is less than 500  $\mu\text{l}$ .

This extraction method is also suitable for animal tissues (brain, liver, etc.), plasma, and medium from tissue culture. Adjustments to the volumes of extraction solvents must be made to maintain the water:chloroform:methanol ratio of 1:2:0.8 for the azeotrope and a 2:2:1.8 ratio for formation of the two-phase system (Bligh and Dyer, 1959). Exact volumes must be determined empirically for each sample type; however, we have found the following information useful as a guide: when extracting lipids from liquid solutions, the entire volume should be treated as the aqueous component; for tissues, the endogenous water content will contribute to the aqueous component in the azeotrope, and different tissues have different water contents. For example, an adult mouse brain ( $\sim 400$  mg) will typically contribute 0.4 ml of water, meaning that 1.2 ml of PBS would be added instead of the 1.6 ml suggested above. Final volumes must also be adjusted depending on initial mass of the sample and lipid content. Tissues often require homogenization in PBS using a Potter-Elvehjem device or a polytron prior to addition of chloroform and methanol, and again after addition of these organic solvents. The deuterated sterol standards surrogates should be added after homogenization to avoid nonspecific adsorption (Lund and Diczfalusy, 2003).

## 4. SAPONIFICATION OF LIPID EXTRACTS

Sterols can exist in biological matrices in free and esterified forms (Myant, 1981). The amount of total sterols or the ratio of free to esterified sterols may be of interest, in which case steryl conjugates, typically esters in most mammalian cells, must be saponified to remove fatty acyl groups and free the sterols. Cholesteryl esters require different chromatographic and mass spectral methods to measure their abundance compared to those used to measure free sterols. Saponifying steryl esters to free sterols requires additional steps in the extraction and purification scheme, but is a more judicious use of time and resources compared to employing two HPLC-ESI-MS methods, which can more than double instrument time.

Our saponification procedure is derived from those previously described by Lund and Diczfalusy (2003) and Yang *et al.* (2006). Hydrolysis reagents should be prepared immediately prior to use according to the prescribed method already listed. The lipid extract is dried under nitrogen at approximately 35° in a glass vial with a Teflon-lined cap, and 1 ml of hydrolysis solution is added. The vial is capped, vortexed for 10 s at maximum speed,

heated to 90° for 2 h, and then allowed to cool to room temperature. Lipids are extracted from the solution using a modified Bligh/Dyer extraction in which ethanol is substituted for methanol as follows. The hydrolyzed lipid solution is transferred to a 14-ml screw-cap glass culture tube using a Pasteur pipette, and the glass vial is rinsed once with 1 ml of ethanol. To the 2-ml volume of hydrolyzed extract in ethanol, 2 ml of chloroform and 1.8 ml of PBS are added. Samples are vortexed for 10 s at maximum speed and centrifuged at 2600 rpm for 5 min. Two phases should be observed, and the organic phase (lower) is removed using a Pasteur pipette and placed in a fresh 4-ml glass vial with a Teflon-lined cap, dried down, and reconstituted in 95% methanol.

## 5. SOLID-PHASE EXTRACTION

Bulk-lipid extracts made with the Bligh/Dyer procedure contain many nonpolar species such as steryl esters, monoacylglycerols, diacylglycerols, and triacylglycerols, which are all strongly retained on reverse phase HPLC columns. Accumulation of these compounds on the column can lead to changes in retention time, decreased resolution, and increased back pressure. For these reasons, it is often advisable to resolve the major lipid classes by SPE prior to HPLC-MS analysis. Sterols can be isolated from other classes of lipids by sequential development of a single SPE column and, with the appropriate solvents, oxysterols, or sterols containing additional hydroxy-, oxo-, or epoxy-groups, can be separated from cholesterol and other sterols that contain a single hydroxyl functional group.

For routine SPE (Lund and Diczfalusy, 2003), a 100-mg Isolute silica cartridge (Biotage, Charlottesville, VA) is prewashed by passing 2 ml of hexane through the column. A dried lipid extract prepared as previously described (with or without saponification) is dissolved in 1 ml of toluene and passed through the cartridge. Nonpolar compounds such as cholesteryl esters are eluted first with 1 ml of hexane. Cholesterol and other related sterols are eluted next with 8 ml of 30% isopropanol in hexane. The eluted sterols are dried down and then resuspended in 95% methanol prior to analysis by HPLC-MS.

To resolve sterols containing a single hydroxyl group from those containing more than one hydroxyl group (e.g., cholesterol from oxysterols), the SPE column is pre-washed and loaded with lipids from the extraction procedure as described above. Steryl esters are again eluted from the column with 1 ml of hexane. Cholesterol and other mono-hydroxysterols are then eluted with 8 ml of 0.5% isopropanol in hexane. Oxysterols are eluted next with 5 ml of 30% isopropanol in hexane. Eluates from the individual chromatographic steps are dried under nitrogen and resuspended in 95% (v/v) methanol/water.

Our laboratory has determined that, in general, a 400- $\mu\text{l}$  final volume for 5 to  $10 \times 10^6$  cells is suitable for the instrumental analysis described in the “Analysis by HPLC-ESI-MS” section. The final volume-to-cell number ratio can be scaled to accommodate varying amounts of cells.

## 6. ANALYSIS BY HPLC-ESI-MS

### 6.1. High performance liquid chromatography

Sterols are resolved using reverse-phase HPLC (RP-HPLC). A 10- $\mu\text{l}$  aliquot of lipid extract (in 95% methanol) is loaded onto a RP-HPLC column (Luna C<sub>18</sub> 2  $\times$  250 mm, 3- $\mu\text{m}$  particle; Phenomenex, Torrance, CA) equipped with a guard column (C<sub>18</sub>, 4  $\times$  2 mm). From this point on, lipids are resolved by gradient elution. The gradient program begins with 100% Solvent B (85% methanol, 5 mM ammonium acetate) for 2 min, and is thereafter ramped to Solvent A (100% methanol, 5 mM ammonium acetate) over a 13-min period and held for 10 min. Solvent B is then passed through the column for 5 min to re-equilibrate the column prior to the next run. The flow rate is 0.25 ml/min, and the column is maintained at 30° using a column oven.

### 6.2. Electrospray ionization mass spectrometry

The HPLC is coupled to a 4000 QTrap triple quadrupole mass spectrometer (Applied Biosystems, Foster City, CA) through a Turbo V<sup>TM</sup> ESI source. The source is operated in the positive (+) mode with a spray voltage of 5500 V, a curtain gas of 15 psi (nitrogen), and ion Source Gas 1 and 2 set to 60 and 20 psi, respectively (both nitrogen). Gas 2 is maintained at 50°. The mass spectrometer is operated in standard reaction monitoring (SRM) mode to achieve maximum selectivity. To increase signal intensity, the first quadrupole is set to low resolution and the third quadrupole is set to unit resolution. These settings allow ions of wider mass distribution to pass through quadrupole 1 into the collision cell where ions are fragmented and resolved by quadrupole 3. Individual transitions, optimal declustering potentials, collision energies, limits of detection, and linear ranges are given in Table 6.2. SRM pairs are chosen by infusing individual sterols into the MS and generating product ion MS/MS from which these values are selected and optimized. Examples of product-ion spectra from several different types of sterols are shown in Fig. 6.1. A more comprehensive list of sterol product-ion MS can be found at <http://www.lipidmaps.org>. Common ions formed for most sterols by electrospray include  $[\text{M}+\text{NH}_4]^+$ ,  $[\text{M}+\text{H}]^+$ ,  $[\text{M}+\text{H}-\text{H}_2\text{O}]^+$ , and  $[\text{M}+\text{H}-2\text{H}_2\text{O}]^+$  (Pulfer *et al.*, 2005). Note that the  $[\text{M}+\text{H}]^+$  ion does not result from gaining a proton during electrospray, but is likely the result of losing gaseous ammonia (NH<sub>3</sub>) from the NH<sub>4</sub> adduct (Murphy, 2006).

**Table 6.2** Molecular weight, instrumental parameters, and figures of merit for representative sterols

Common name	Peak # (Fig. 6.3)	MW <sup>a</sup>	SRM ions	DP (v)	CE (v)	Dwell time (msec)	RT (min)	LOD (fmol on- column)	Linear range (fmol on-column)
22 <i>R</i> -Hydroxycholesterol	1	402.7	420/385	50	15	110	10.5	50	5.00e1–1.25e5
24-Hydroxycholesterol ( <i>R+S</i> )	2/4	402.7	420/385	50	15	110	12.2	60	6.50e1–1.50e5
25-Hydroxycholesterol	3	402.7	420/367	50	15	110	13.3	25	2.50e1–2.50e5
27-Hydroxycholesterol- (25 <i>R</i> )	5	402.7	420/385	50	15	110	13.9	55	5.50e1–1.25e5
24,25-Epoxycholesterol	6	400.4	418/383	45	12	80	14.5	20	2.00e1–1.25e5
7 $\alpha$ -Hydroxycholesterol	7	402.7	385/367	50	15	110	16.5	60	6.00e1–1.25e5
7-Ketocholesterol	8	400.6	401/383	80	35	70	17.3	85	9.00e1–6.30e4
5,6 $\beta$ -Epoxycholesterol	9	402.7	420/385	50	15	110	18.7	5	5.00e0–8.70e4
5,6 $\alpha$ -Epoxycholesterol	10	402.7	420/385	50	15	110	19.5	5	6.00e0–8.70e4
4 $\beta$ -Hydroxycholesterol	11	402.7	420/385	50	15	110	20.2	25	2.50e1–6.20e4
Zymosterol	<i>a</i>	384.6	385/367	85	20	70	N/A	N/A	N/A
Desmosterol	12	384.6	402/367	55	20	110	21.9	2000	6.50e4–3.20e6
7-Dehydrocholesterol	13	384.6	385/367	85	20	70	22.6	520	5.20e2–3.30e6
Cholest-4-en-3-one	14	384.6	385/367	85	20	70	23.4	390	3.90e2–1.60e6
Lathosterol	15	386.7	404/369	110	13	70	24	1300	9.00e3–2.50e6
Cholesterol	16	386.7	404/369	110	13	70	24.3	1000	2.60e4–3.20e6
Lanosterol	17	426.7	444/409	80	15	100	24.9	175	2.30e3–3.00e6
Cholestanol	18	388.7	404/369	110	13	70		<i>b</i>	<i>b</i>
24-Dihydrolanosterol	19	428.7	429/411	100	17	70		<i>b</i>	<i>b</i>

<sup>a</sup> Compound no longer commercially available. Existing material is limited and impure; thus, LOD and linear ranges are not measured.

<sup>b</sup> Standards are of questionable purity; thus, LOD and linear range were not measured.

Key to abbreviations: CE, collision energy; DP, declustering potential; LOD, limit of detection; MW, molecular weight; N/A, not applicable; RT, retention time; SRM, selected reaction monitoring.

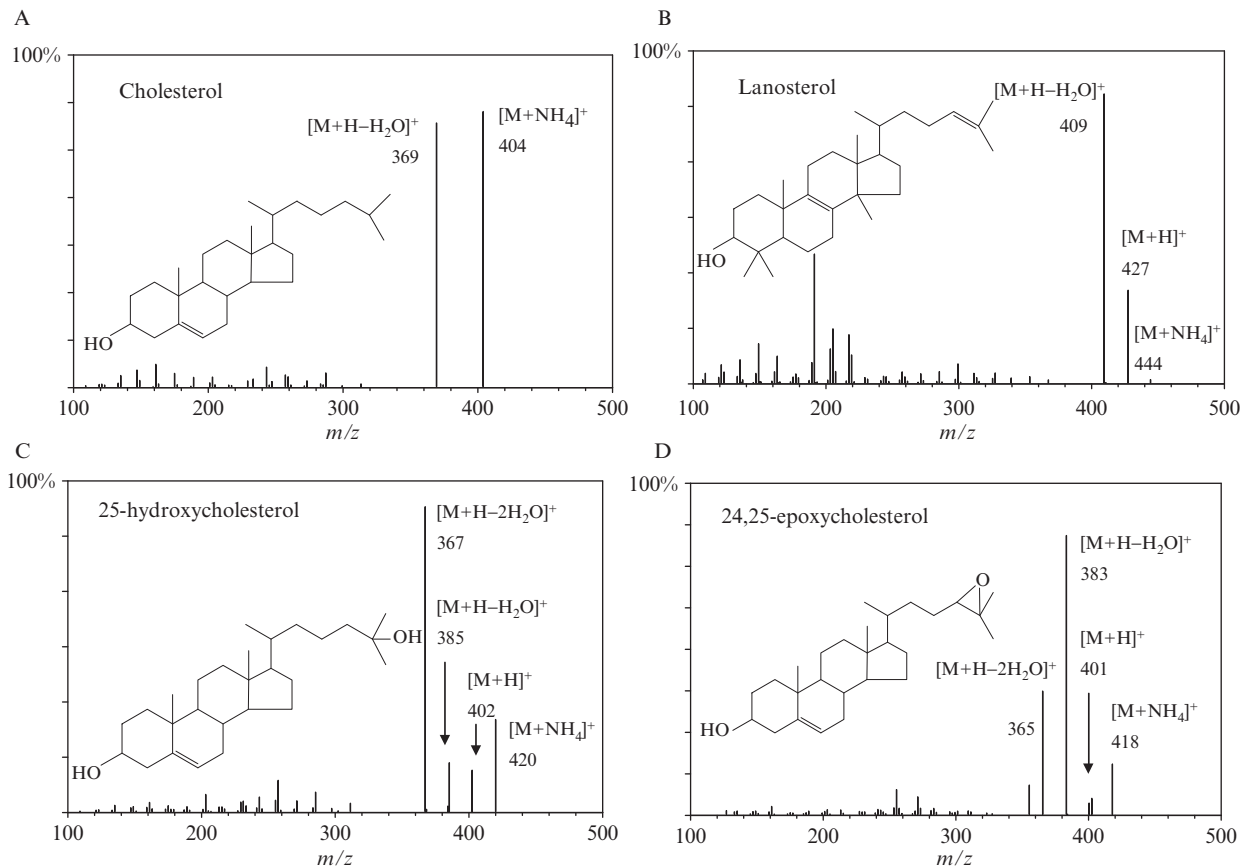


**Figure 6.1** Product-ion mass spectra for selected sterols. See <http://www.lipidmaps.org> for additional spectra.

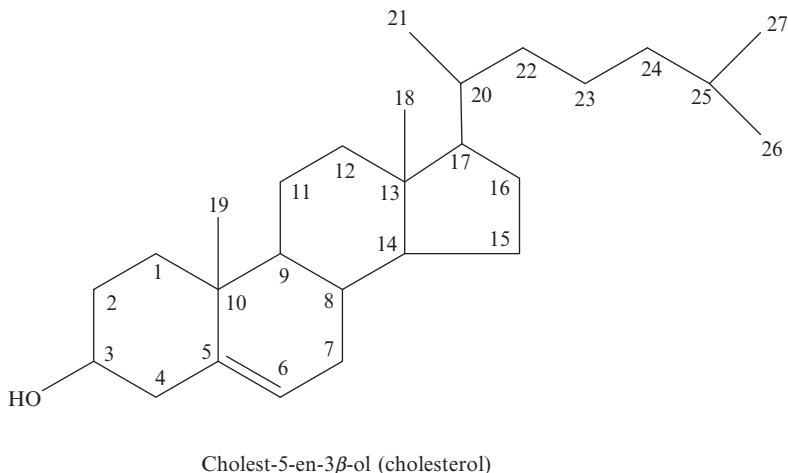


**Figure 6.2** Structure of cholesterol with positional numbering system.

## 7. QUANTITATION

Deuterated analogs of sterols are used for quantitation because they have similar physical properties as non-isotopically labeled (i.e., endogenous) sterols, but can be resolved from the latter by MS due to their increased mass. Quantitation relies on the principle of isotope dilution MS in which known amounts of deuterated sterol standards are added to the biological sample at the beginning of the extraction and are thereafter carried through the extraction procedure with endogenous sterols. The amount of endogenous sterol in the cell or tissue extract is then calculated using a predetermined relative response factor (RRF) between peak areas and masses of the deuterated versus endogenous sterols. To obtain RRFs, a standard mixture of deuterated surrogates and internal standard is prepared as indicated in [Table 6.1](#) prior to instrumental analysis. An autosampler vial is fitted with a 500- $\mu$ l insert, and  $\sim$ 400  $\mu$ l of 95% methanol is added. Deuterated surrogates and internal standards are then added to the solution in the exact manner in which they were added to the sample as previously described (same volume, pipette, stock mixtures, etc.). Corresponding primary sterols are added to the mixture as well. The masses and volumes for all compounds are given in [Table 6.1](#).

The quantitation mixture is analyzed at the beginning and end of the instrument sequence, and after every 8 to 10 samples. Using the masses of standard added to the quantitation mixture and the areas under the elution curves generated by HPLC-ESI-MS, a response factor can be generated using [Equation 1](#).

$$RRF = \frac{(Area_{Analyte} \times Mass_{std})}{(Area_{std} \times Mass_{analyte})} \quad (1)$$

The response factors are averaged over the course of the sequence to account for any instrumental drift. Should the response factor drift excessively between two standard analyses, specific response factors should be used only for the samples they bracket. This approach establishes the relationship between mass and peak area, which can be used to quantitate the amount of each sterol present in individual samples. Equation 2 takes into account the area under the elution curve for the sterol of interest ( $Area_{analyte}$ ), the deuterated analog ( $Area_{std}$ ), the mass of the deuterated analog ( $Mass_{std}$ ) added to the sample, and the RRF generated with Equation 1.

$$Mass_{analyte} = \frac{(Area_{Analyte} \times Mass_{std})}{(Area_{std} \times RRF)} \quad (2)$$

Equation 2 can be seen as a rearrangement of Equation 1 in which the RRF established for each sterol and deuterated analog in Table 6.1 is incorporated.

Deuterated analogs are not available for all sterols. To overcome this problem, an alternate deuterated analog of similar chemical composition to that of the analyte to be measured can be substituted. For example, quantitative analysis of 22-hydroxycholesterol can be performed using (d3) 25-hydroxycholesterol as an alternative surrogate. Common primary and deuterated sterol standards and their sources are given in Tables 6.3 and 6.4.

## 8. DATA

An HPLC-ESI-MS chromatogram of a mixture of sterols is shown in Fig. 6.3A. Using our standard gradient elution program, sterols elute from the column between 10 and 28 min, and, in general, more hydrophilic oxysterols elute before cholesterol and other more hydrophobic sterols. Experience has shown that the earliest eluting sterols (i.e., the most hydrophilic) extracted from cultured mammalian cells are trihydroxy compounds, which elute several minutes before a 22-hydroxycholesterol standard. The latest eluting sterol (i.e., most hydrophobic) is 24-dihydrolanosterol. All other sterols detected in this laboratory elute between these two extremes. Peak widths are generally less than 20 s at the full-width, half maximum setting,

**Table 6.3** Sources of representative sterol standards

Systematic name <sup>a</sup>	Common name <sup>d</sup>	MW	Source
Cholest-5-en-3 $\beta$ ,22-diol (22 <i>R</i> )	22 <i>R</i> -Hydroxycholesterol	402.7	Sigma Aldrich <sup>b</sup>
Cholest-5-en-3 $\beta$ ,24-diol	24-Hydroxycholesterol( <i>R+S</i> )	402.7	Avanti Polar Lipids <sup>c</sup>
Cholest-5-en-3 $\beta$ ,25-diol	25-Hydroxycholesterol	402.7	Avanti Polar Lipids
Cholest-(25 <i>R</i> )-5-en-3 $\beta$ ,27-diol	27-Hydroxycholesterol-(25 <i>R</i> )	402.7	Avanti Polar Lipids
24,25-Epoxycholest-5-en-3 $\beta$ -ol	24,25-Epoxycholesterol	400.6	Avanti Polar Lipids
Cholest-5-en-3 $\beta$ ,7 $\alpha$ -diol	7 $\alpha$ -Hydroxycholesterol	402.7	Avanti Polar Lipids
7-Keto-5-cholesten-3 $\beta$ -ol	7-Ketocholesterol	400.6	Avanti Polar Lipids
5,6 $\beta$ -Epoxy-5 $\beta$ -cholestan-3 $\beta$ -ol	5,6 $\beta$ -Epoxycholesterol	402.7	Avanti Polar Lipids
5,6 $\alpha$ -Epoxy-5 $\alpha$ -cholestan-3 $\beta$ -ol	5,6 $\alpha$ -Epoxycholesterol	402.7	Avanti Polar Lipids
Cholest-5-en-3 $\beta$ ,4 $\beta$ -diol	4 $\beta$ -Hydroxycholesterol	402.7	Avanti Polar Lipids
8,24(5 $\alpha$ )-Cholestadien-3 $\beta$ -ol	Zymosterol	384.7	<i>a</i>
Cholest-5,24-dien-3 $\beta$ -ol	Desmosterol	384.7	Avanti Polar Lipids
Cholesta-5,7-dien-3 $\beta$ -ol	7-Dehydrocholesterol	384.7	Sigma Aldrich
Cholest-4-en-3-one	Cholestenone	384.7	Sigma Aldrich
Cholest-7-en-3 $\beta$ -ol	Lathosterol	386.7	Steraloids <sup>e</sup>
Cholest-5-en-3 $\beta$ -ol	Cholesterol	386.7	Avanti Polar Lipids
Lanosta-8,24-dien-3 $\beta$ -ol	Lanosterol	426.7	Steraloids
Cholestan-3 $\beta$ -ol	Cholestanol	388.7	Sigma Aldrich
5 $\alpha$ -Lanost-8-en-3 $\beta$ -ol	24-Dihydrolanosterol	428.7	Steraloids

<sup>a</sup> Compound no longer commercially available.

<sup>b</sup> St. Louis, MO.

<sup>c</sup> Alabaster, AL.

<sup>d</sup> See [Fahy et al. \(2005\)](#) for systematic nomenclature of sterols.

<sup>e</sup> Newport, RI.



**Table 6.4** Sources of deuterated sterol standards

Common name (deuterium positions) <sup>a</sup>	MW	Source
24-Hydroxycholesterol(D6) (26,26,26,27,27,27-D6)	408.7	Avanti Polar Lipids <sup>b</sup>
25-Hydroxycholesterol (D3) (26,26,26-D3)	405.7	Avanti Polar Lipids
27-Hydroxycholesterol-(25 <i>R</i> )(D5) (26,26,26,27,27-D5)	407.7	Medical Isotopes, Inc. <sup>c</sup>
24,25-Epoxycholesterol (D6) ( <i>R</i> + <i>S</i> ) (26,26,26,27,27,27-D6)	406.6	Avanti Polar Lipids
6 $\alpha$ -Hydroxycholestanol(D7) (25,26,26,26,27,27,27-D7)	411.7	Avanti Polar Lipids
7 $\alpha$ -Hydroxycholesterol(D7) (25,26,26,26,27,27,27-D7)	409.7	Avanti Polar Lipids
7 $\beta$ -Hydroxycholesterol(D7) (25,26,26,26,27,27,27-D7)	409.7	Avanti Polar Lipids
7-ketocholesterol(D7) (25,26,26,26,27,27,27-D7)	407.6	Avanti Polar Lipids
5,6 $\alpha$ -Epoxycholesterol (D7) (25,26,26,26,27,27,27-D7)	409.7	Avanti Polar Lipids
4 $\beta$ -Hydroxycholesterol(D7) (25,26,26,26,27,27,27-D7)	409.7	Avanti Polar Lipids
Desmosterol (D6) (26,26,26,27,27,27-D6)	390.7	Avanti Polar Lipids
Cholesterol (D7) (25,26,26,26,27,27,27-D7)	393.7	Avanti Polar Lipids

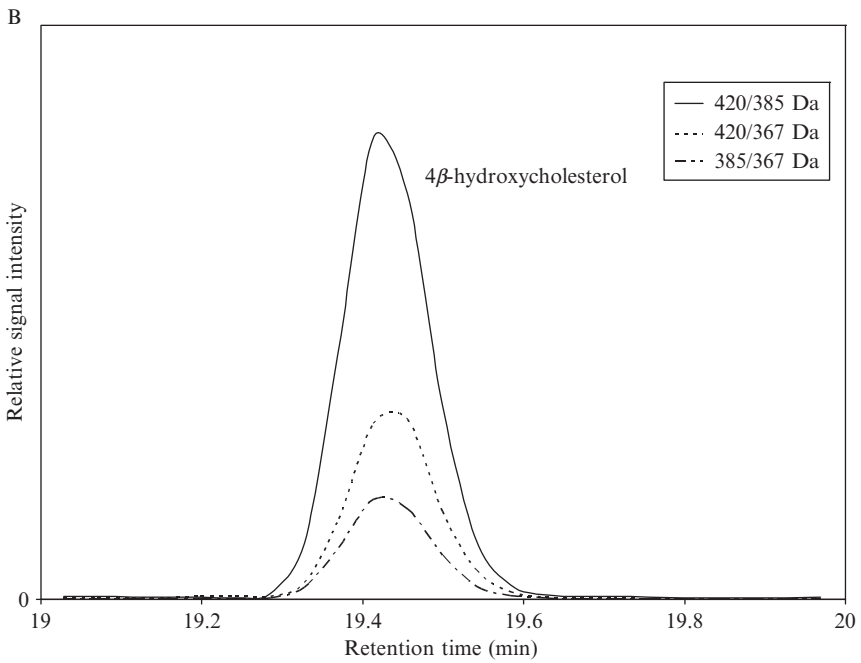
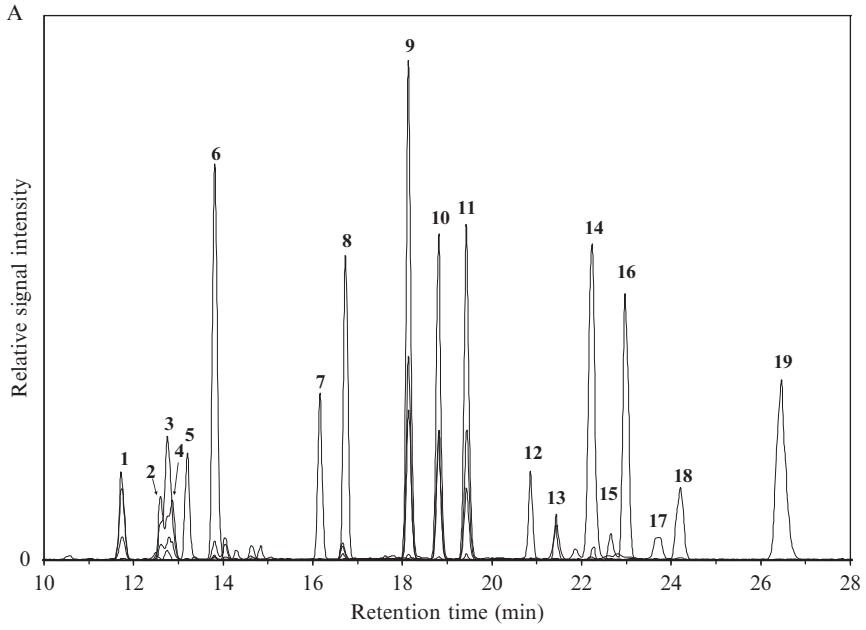
<sup>a</sup> See Table 6.3 for systematic sterol names.

<sup>b</sup> Alabaster, AL.

<sup>c</sup> Pelham, NH.

which gives excellent resolution. Note that some sterols show multiple SRM pairs for a single compound. For example, 4 $\beta$ -hydroxycholesterol (peak 11, Fig. 6.3B) shows an SRM signal of 420/385, 420/367, and 385/367 u. These additional SRM pairs add confidence to the identification of a specific sterol and can provide further information regarding compound identification based on their relative intensities.

An HPLC-ESI-MS chromatogram derived from analysis of a Bligh/Dyer extract from wild-type mouse brain is shown in Fig. 6.4. Early in the chromatogram, a group of compounds was observed that was not retained by the stationary phase and eluted with the solvent front. This observation is common in biological extracts, especially when no additional pre-purification



or separation is performed. Multiple compounds are observed eluting in the sterol region, some of which can be identified based on SRM pairs and retention times. For example, 24-hydroxycholesterol eluting at 12.8 min is abundant in the brain and readily observed in the chromatogram. Other sterols identified in the brain extract include 24,25-epoxycholesterol (13.5 min), 4 $\beta$ -hydroxycholesterol (19.7 min), desmosterol (21.3 min), cholesterol (23.7 min), and lanosterol (24.3 min). Note that the region around the cholesterol peak is shown at one-tenth scale. The chromatographic peak resulting from cholesterol is typically an order of magnitude or larger than any other sterol, which reflects the large abundance of this sterol in most mammalian tissues and cells. In this example, the cholesterol peak has a split top indicative of poor chromatographic performance due to column overloading. Injecting a smaller volume or a more dilute sample will improve peak shape. Additional sterols are present in the extract as shown by

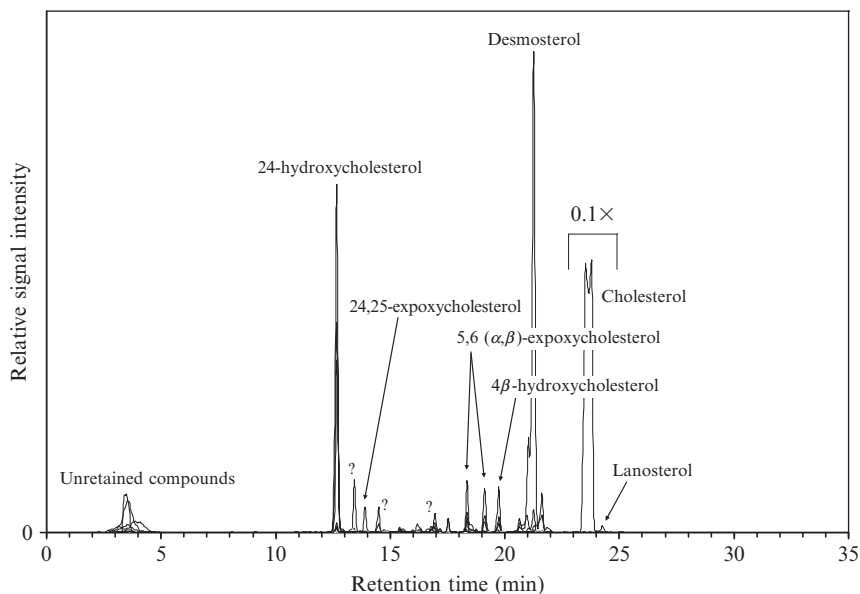


**Figure 6.4** Reconstructed SRM chromatogram of a Bligh/Dyer extract of wild-type mouse brain. Known sterols are identified by name, and unknown compounds with sterol-like signatures are indicated with a “?” Note the reduced scale ( $\times 0.1$  between 23 and 25 min).

**Figure 6.3** (A) Reconstructed SRM ion chromatogram derived from the analysis of a mixture of common sterols. Corresponding peak numbers are given in Table 6.2. The baseline is truncated for clarity to show only 10 to 28 minutes. (B) Expanded view of multiple SRM pairs for peak 11 (4 $\beta$ -hydroxycholesterol).

signals from other SRM pairs. These represent known or unidentified sterols, or non-sterol compounds that happen to produce a signal identical to one or more of the SRM pairs but do not match the retention time of any of the sterol standards.

## 9. DISCUSSION, NUANCES, CAVEATS, AND PITFALLS

### 9.1. Quantitation

A practical description and discussion of quantitative MS by isotope dilution are provided here. For additional information, see [Duncan \*et al.\* \(2006\)](#) or [USEPA \(2003\)](#). Surrogate standards are deuterated analogs added to the sample prior to extraction and carried through the extraction process with the endogenous compounds. Theoretically, deuterated analogs will behave identically to their non-isotopically labeled and endogenous counterparts during the extraction process, including any losses due to incomplete transfer, oxidation, degradation, or others. When surrogates are used for quantitation, losses are accounted for and corrected automatically. In contrast, internal standards are those added to the sample after extraction but immediately prior to HPLC-ESI-MS analysis. As internal standards are added after the extraction, they cannot account for losses during extraction.

A combination of surrogate and internal standards provides additional information, allowing for the measure of extraction efficiency. The amount of surrogate recovered at the end of an extraction can be calculated providing extraction efficiency using the mass and peak areas of a surrogate and an internal standard. While there is no specified level of recovery necessary for a suitable extraction, a minimum of 50% recovery is our internal target. Values that are consistently lower than 50% recovery indicate the need for evaluation and modification of the extraction procedure. Occasional recovery values below 50% are typically not of concern, but should be evaluated on a case-by-case basis. Extraction efficiency is especially important in sterol analysis as many are present in trace quantities within cells and tissues. The extraction procedure previously described for cells typically yields between 70 and 80% average recovery using (d<sub>6</sub>) 27-hydroxycholesterol as an internal standard.

When measuring the response factor of a sterol and its deuterated analog, the ratio should ideally be unity; however, due to impurities in the primary standards and to potential deuterium exchange during the ESI process, this ratio may be higher or lower than one. The ratio should be determined empirically for each sterol and deuterated analog. The RRF between a sterol and a related, but non-ideal deuterated surrogate may be very different from unity and must be determined empirically. The linear working ranges of response factors (i.e., calibration curves) must also be determined

empirically, but generally reflect the linear ranges of the individual sterols themselves.

Deuterated analogs are not available for all sterols. In this situation, we use (d3) 25-hydroxycholesterol as an alternate deuterated analog of 22-hydroxycholesterol and (d7) cholesterol as the deuterated surrogate for 7-dehydrocholesterol, cholestenone, and lathosterol. Other common primary and deuterated sterol standards and their sources are given in [Tables 6.3 and 6.4](#).

Isotope dilution has the benefit of alleviating the analyst from having to know the volumes of the extract, including the final volume. Because the calculations are based on ratios between peak area and mass, no knowledge of extract volume is necessary. The calculated value will have the units (mass/extract) that allow the end user to normalize the mass of sterol to a variety of standard measures, including DNA, protein, cell number, or tissue weight.

## 9.2. Availability and purity of primary and deuterated standards

Primary sterol standards are available from several commercial sources. Some standards are prepared synthetically while others are extracted from biological matrices and purified. It has been our experience that the purity of individual sterols varies greatly depending on the specific sterol and the supplier. For example, cholesterol is available from multiple sources as a highly pure compound (>99%), but 24-dihydrolanosterol has limited availability and typically contains many impurities. Some stereochemically pure compounds are available, such as 22*R*-hydroxycholesterol, 27-hydroxycholesterol-(25*R*), and 24(*S*)-hydroxycholesterol. Others are currently only available as the racemic mixture. Suppliers generally offer limited analytical data to demonstrate purity, which ranges from a basic thin layer chromatographic (TLC) analysis, to an HPLC-UV/vis analysis and nuclear magnetic resonance (NMR) analysis.

Evaluating the purity of primary and deuterated sterol standards can be complex and time-consuming and may be beyond the scope of many research laboratories. As described in the introductory section, sterols are not well suited for analysis in their native state by most modern analytical techniques. Even when detected, the response between two similar sterols can differ by more than an order of magnitude, which makes it difficult to ascertain relative percent purity without having standards for each impurity detected. HPLC-ELSD is currently the most widely used and nondiscriminatory technique for evaluation of sterol purity. HPLC-ELSD is optimal for evaluation of standards but, because it does not provide mass information, has limited applicability with complex extracts. Finally, NMR is often considered a definitive technique for identifying purity and structure of organic

compounds; however, access to NMR is not always readily available to those studying sterols.

A collection of deuterated sterol standards and an increasing number of primary sterol standards has become available from Avanti Polar Lipids (Alabaster, AL) as part of the LIPID MAPS consortium. The deuterated sterols available at the time of this writing are listed in Table 6.4, and many of the primary sterol standards available are listed in Table 6.3. Each standard from Avanti has been prepared with a full complement of available analytical data, including HPLC-ESI-MS, ESI-MS, HPLC-ELSD, and NMR. This characterization far exceeds the QA/QC data offered by other commercial vendors of sterol standards at this time. Additionally, Avanti performs routine stability testing of stocked compounds and will notify users should the purity of a given standard fail their specified compliance of  $\pm 5\%$ .

### 9.3. Resolving related sterols by HPLC

Many sterols are fully resolved by the chromatographic method previously described; however, some, such as 24-hydroxycholesterol (*R+S*) and 25-hydroxycholesterol, co-elute. Mass spectrometry can offer an additional level of resolution by differentiating co-eluting compounds by mass but, because many sterols are isobaric, this dimension is of variable worth. 24-Hydroxycholesterol (*R+S*) and 25-hydroxycholesterol share three SRM pairs, but they vary in relative intensities between 24- and 25-hydroxycholesterol. 24-Hydroxycholesterol shows 420/385 u as the most abundant transition, whereas 25-hydroxycholesterol shows 420/367 u as the most abundant transition. In some cases, a difference in the tissue-specific distribution of two closely related sterols obviates the need for HPLC separation. In this example, a variety of tissues contain 25-hydroxycholesterol, but 24-hydroxycholesterol is selectively present in the brain.

We have made an extensive effort to develop a single gradient elution method that resolves all closely related sterols present in a typical mammalian cell, and this effort has largely succeeded. To date, our most favorable results allow for a qualitative identification of the known co-eluting sterols; however, resolution is still inadequate for quantitation. Should resolution of two co-eluting sterols be necessary, various isocratic elution methods can be employed. This approach, however, usually produces broader peaks and lower signal intensity (Uomori *et al.*, 1987). Also, more hydrophobic sterols, such as cholesterol and lanosterol, will have long isocratic elution times that fall outside of optimal chromatographic conditions. GC-MS remains a viable alternative for the quantitation of 24- and 25-hydroxycholesterol (Lund and Diczfalusy, 2003).

#### 9.4. Acetonitrile and signal intensity

Some methods describing the analysis of sterols by HPLC-MS utilize acetonitrile as a component of the mobile phase (Burkard *et al.*, 2004; Pulfer *et al.*, 2005; Shan *et al.*, 2003). When we incorporated acetonitrile into the gradient mobile phases, a modest to significant decrease in signal intensity was observed for all sterols analyzed by LC-ESI-MS. Oxysterols suffered the largest reduction in signal intensity in the presence of acetonitrile, whereas the reduction observed for other mono-hydroxylated sterols was not as severe. Chromatographic parameters were similar in terms of peak-width and retention time. Thus, reductions in signal intensity are not likely explained by changes in chromatographic performance. We have no clear explanation for this phenomenon at this time, but it appears that acetonitrile has a detrimental effect on the electrospray process and adduct formation, which in turn causes decreased signal intensity for oxysterols. Recent research by Lawrence and Brenna (2006) and Van Pelt *et al.* (1999) has described acetonitrile as a reactive gas-phase reagent with atmospheric pressure ionization methods that may be related to the decreased signal intensity observed here. For this reason, and because no increase is observed in chromatographic resolution when using acetonitrile, the methanol/water gradient previously described was implemented.

#### 9.5. Auto-oxidation and use of SPE columns

It has been shown that cholesterol is subject to autooxidation, forming oxidized end-products such as 22-, 24-, 25-, and 27-hydroxycholesterol, and 5/6( $\alpha/\beta$ )-epoxycholesterol (Breuer and Björkhem, 1995; Kudo *et al.*, 1989). In our experience, the most readily formed oxidation product is 5/6( $\alpha/\beta$ )-epoxycholesterol, which has been shown to be physiologically irrelevant (Breuer and Björkhem, 1995; Kudo *et al.*, 1989). Other oxidation end-products are formed in negligible amounts. We have found that extraction of biological samples using the Bligh/Dyer approach above described typically results in minimal oxidation. When further purification steps are conducted on SPE silica columns, the abundance of 5/6( $\alpha/\beta$ )-epoxycholesterol increases. A pilot study using deuterated compounds to allow quantitation and the full extraction/SPE procedure previously described showed that as much as 1 to 3% of cholesterol can be oxidized to 5/6( $\alpha/\beta$ )-epoxycholesterol. No other autooxidation products of cholesterol were detected. Addition of the antioxidant butylhydroxy toluene (BHT) to the sample prior to extraction produced only a modest decrease in oxidation. In most experiments, we do not consider these oxidation products problematic. Minimizing oxidation by using good lab practices is

important, but to eliminate oxidation would require processing the samples in an inert environment, which is not logistically possible for most laboratories. It should be noted that 5/6 $\alpha$ - and 5/6 $\beta$ -epoxycholesterol are among the most sensitive sterols analyzed by this instrumental method (Table 6.2), which can result in large signals being observed in the SRM chromatograms relative to other signals. This imbalance in relative signal strength adds complexity and, possibly, confusion to the interpretation of the data.

## 9.6. Sample clean-up

Depending on sample type and desired information, additional sample processing may be desirable; however, in addition to the increased formation of oxidation products already described, we find that typical clean-up steps such as saponification and SPE require additional time and resources and produce only limited benefit. While we have described here a comprehensive extraction procedure involving extraction, saponification, and solid-phase purification, the last two steps are not always required for successful analysis of sterols. In specific cases, such as plasma, oxysterols are found as free and esterified compounds (Bodin *et al.*, 2001; Dzeletovic *et al.*, 1995; Smith *et al.*, 1981). Saponifying the extracts will increase the amount of free oxysterols present in the extract, resulting in stronger signal intensities for these compounds. Otherwise, unless knowledge of free-to-esterified sterol ratios is required or the final extracts are not suitable for analysis after multiple Bligh/Dyer extractions, we do not recommend performing additional separation and purification steps beyond the Bligh/Dyer extraction. Use of a guard column with the primary HPLC column will trap many highly retained compounds and can be replaced with minimal expense relative to the HPLC column. Should diminished chromatographic performance be observed, back-flushing the column with a strong reverse-phase solvent such as chloroform or isooctane will often remove most retained compounds and extend the life of the column. Alternatively, HPLC columns are consumable items, and the cost of replacing a column with greater frequency is usually smaller than that associated with the increased equipment and time required for additional separation and purification steps. The chromatographic method outlined above adequately separates a majority of sterols in mammalian cells, and SPE cannot itself resolve problems associated with the analysis of co-eluting sterols or diastereomers. Lastly, with every new step in processing comes the possibility of additional sample loss and, although surrogate standards can account for these losses, if the sterol of interest exists at trace levels, excess processing may reduce its signal below the limits of detection. Figure 6.5 shows various work-flows for the extraction of sterols that can be tailored to individual user's requirements.



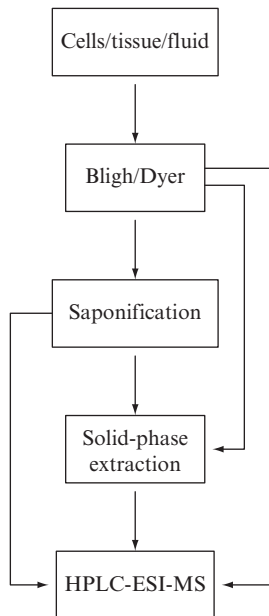


**Figure 6.5** Flow chart of various procedures for the extraction and preparation of sterols from biological extracts.

### 9.7. Residual insoluble material

Regardless of how extensively an extract is separated and purified, residual insoluble material is often present in the final dried extract. When this situation is encountered, we redissolve lipids in 95% methanol and make every effort to minimize resuspension of insoluble material. We investigated the composition of this insoluble material by performing additional extractions with both methanol and chloroform followed by ESI-MS analysis. Methanol extraction of particulates showed only small amounts of cholesterol, which may represent residual compound remaining after the extract was transferred to the auto-sampler vial. Chloroform extraction showed no additional sterols, but did dissolve some of the residual material. It would appear that the minor amounts of insoluble material that sometimes form using the above methods is of little concern for subsequent sterol analyses.

Recent experiments (unpublished work) demonstrate that the majority of residual insoluble material previously described is due to the use of plastics in conjunction with organic solvents. We recommend using only glass and Teflon when contact with any organic solvents will occur. The only steps where plastics and organic solvents should come into contact are during the addition of the surrogate and internal standards (when using positive

displacement pipettes with disposable tips) or during pre-purification of extracts with SPE columns (the columns are made of plastic). Completely eliminating plastics in these steps would add considerable effort and cost.

## 9.8. Comparing relative peak areas

Individual sterols have varying responses to ESI. The more polar oxysterols (e.g., 24,25-epoxycholesterol) are generally more amenable to ESI ionization compared to less polar compounds (e.g., lanosterol). This difference is reflected in [Table 6.2](#), which shows that limits of detection span several orders of magnitude. Also, later eluting sterols are subject to longitudinal diffusion, which causes peak-broadening and results in a less-intense signal compared to the narrower peaks eluting early in the elution profile. Both of these phenomena prevent interpretation of the relative amounts of sterols in an extract solely by evaluation of their signal intensities. Equivalent signals for two sterols may be the result of very different amounts. Interpretation of relative amounts can only be evaluated by assessing the instrumental response of primary standards for the compounds of interest.

## 9.9. Electrospray using other instrumental platforms

Electrospray ionization and adduct formation of sterols is dependent on the mass spectrometer and, more importantly, the ionization source used. Two laboratories analyzing cholesterol by ESI-MS using the previously mentioned parameters but with instruments and/or ionization sources from other manufacturers or other models from the same manufacturer, may obtain different mass spectra or have varying optimal SRM pairs. The method described here is developed and optimized for an Applied Biosystems 4000 QTrap<sup>®</sup> equipped with a Turbo V<sup>™</sup> ionization source. Through discussions with other mass spectrometrists, it is clear that, with some instruments, sterol-ammonium adducts are not observed, but in-source decay products (e.g., loss of NH<sub>3</sub>, H<sub>2</sub>O, etc.) are. Furthermore, some instruments ionize and transfer sterols to the MS so inefficiently that atmospheric pressure chemical ionization (APCI) is employed in place of ESI ([Burkard \*et al.\*, 2004](#); [Palmgren \*et al.\*, 2005](#); [Tian \*et al.\*, 2006](#)). The parameters and results described here are specific to the 4000 QTrap triple quadrupole system, although, on other platforms, they can serve as a foundation from which a suitable HPLC-MS method can be developed, including those for single quadrupole systems.

## ACKNOWLEDGMENTS

This work was supported by the National Institutes of Health (NIH) Glue Grant 1 U54 GM69338. We thank Carolyn Cummins for reviewing this manuscript.

## REFERENCES

- Abidi, S. L. (2001). Chromatographic analysis of plant sterols in foods and vegetable oils. *J. Chrom. A* **935**, 173–201.
- Bligh, E. G., and Dyer, W. J. (1959). A rapid method of total lipide extraction and purification. *Can. J. Biochem. Physiol.* **37**, 911–917.
- Bodin, K., Bretillon, L., Aden, Y., Bertilsson, L., Broome, U., Einarsson, C., and Diczfalusy, U. (2001). Antiepileptic drugs increase plasma levels of 4 $\beta$ -hydroxycholesterolin humans. Evidence for involvement of cytochrome P450 3A4. *J. Biol. Chem.* **276**, 38685–38689.
- Breuer, O., and Björkhem, I. (1995). Use of an <sup>18</sup>O<sub>2</sub> inhalation technique and mass isotopomer distribution analysis to study oxygenation of cholesterol in rat. *J. Biol. Chem.* **270**, 20278–20284.
- Burkard, I., Rentsch, K. M., and von Eckardstein, A. (2004). Determination of 24S- and 27-hydroxycholesterol in plasma by high-performance liquid chromatography-mass spectrometry. *J. Lipid Res.* **45**, 776–781.
- Dietschy, J. M., and Turley, S. D. (2004). Thematic review series: Brain lipids. Cholesterol metabolism in the central nervous system during early development and in the mature animal. *J. Lipid Res.* **45**, 1375–1397.
- Duncan, M. W., Gale, P. J., and Yergey, A. L. (2006). “The Principles of Quantitative Mass Spectrometry.” Rockpool Productions, LLC., Denver, CO.
- Dzeletovic, S., Breuer, O., Lund, E., and Diczfalusy, U. (1995). Determination of cholesterol oxidation products in human plasma by isotope dilution-mass spectrometry. *Anal. Biochem.* **225**, 73–80.
- Fahy, E., Subramaniam, S., Brown, H. A., Glass, C. K., Merrill, A. H., Jr., Murphy, R. C., Raetz, C. R. H., Russell, D. W., Seyama, Y., Shaw, W., Shimizu, T., Spener, F., *et al.* (2005). A comprehensive classification system for lipids. *J. Lipid Res.* **46**, 839–862.
- Fenn, J. B., Mann, M., Meng, C. K., Wong, S. F., and Whitehouse, C. M. (1989). Electrospray ionization for mass spectrometry of large biomolecules. *Science* **246**, 64–71.
- Isobe, K. O., Tarao, M., Zakaria, M. P., Chiem, N. H., Minh, L. Y., and Takada, H. (2002). Quantitative application of fecal sterols using gas chromatography-mass spectrometry to investigate fecal pollution in tropical waters: Western Malaysia and Mekong Delta, Vietnam. *Environ. Sci. Technol.* **36**, 4497–4507.
- Kudo, K., Emmons, G. T., Casserly, E. W., Via, D. P., Smith, L. C., St. Pyrek, J., and Schroepfer, G. J., Jr. (1989). Inhibitors of sterol synthesis. Chromatography of acetate derivatives of oxygenated sterols. *J. Lipid Res.* **30**, 1097–1111.
- Lawrence, P., and Brenna, J. T. (2006). Acetonitrile covalent adduct chemical ionization mass spectrometry for double bond localization in non-methylene-interrupted polyene fatty acid methyl esters. *Anal. Chem.* **78**, 1312–1317.
- Lund, E. G., and Diczfalusy, U. Quantitation of receptor ligands by mass spectrometry. *Methods Enzymol.* **364**, 24–37.
- Moruisi, K. G., Oosthuizen, W., and Opperman, A. M. (2006). Phytosterols/stanols lower cholesterol concentrations in familial hypercholesterolemic subjects: A systematic review with meta-analysis. *J. Am. Coll. Nutr.* **25**, 41–48.
- Murphy, R. C. (2006). Personal Communication.
- Myant, N. B. (1981). “The Biology of Cholesterol and Related Steroids.” Heinemann Medical Books, London, England.
- Ostlund, R. E., Jr., Racette, S. B., and Stenson, W. F. (2003). Inhibition of cholesterol absorption by phytosterol-replete wheat germ compared with phytosterol-depleted wheat germ. *Am. J. Clin. Nutr.* **77**, 1385–1389.
- Palmgren, J. J., Toyras, A., Mauriala, T., Monkkonen, J., and Auriola, S. (2005). Quantitative determination of cholesterol, sitosterol, and sitostanol in cultured Caco-2 cells

- by liquid chromatography-atmospheric pressure chemical ionization mass spectrometry. *J. Chrom. B.* **821**, 144–152.
- Pulfer, M. K., Taube, C., Gelfand, E., and Murphy, R. C. (2005). Ozone exposure *in vivo* and formation of biologically active oxysterols in the lung. *J. Pharmacol. Exp. Ther.* **312**, 256–264.
- Russell, D. W. (2003). The enzymes, regulation, and genetics of bile acid synthesis. *Annu. Rev. Biochem.* **72**, 137–174.
- Shan, H., Pang, J., Li, S., Chiang, T. B., Wilson, W. K., and Schroepfer, J. G. J. (2003). Chromatographic behavior of oxygenated derivatives of cholesterol. *Steroids* **68**, 221–233.
- Smith, L. L., Teng, J. I., Yong Yeng, L., Seitz, P. K., and McGehee, M. F. (1981). Sterol metabolism—XLVII. Oxidized cholesterol esters in human tissues. *J. Steroid Biochem.* **14**, 889–900.
- Tian, Q., Failla, M. L., Bohn, T., and Schwartz, S. J. (2006). High-performance liquid chromatography/ atmospheric pressure chemical ionization tandem mass spectrometry determination of cholesterol uptake by Caco-2 cells. *Rapid Commun. Mass Spectrom.* **20**, 3056–3060.
- United States Environmental Protection Agency (USEPA) (2003). EPA, SWA-846 Method 8000C. Determinative chromatographic separations. Available at: <http://nlquery.epa.gov>.
- Uomori, A., Seo, S., Sato, T., Youshimura, Y., and Takeda, K. J. (1987). Synthesis of (25R)-[26-2H]cholesterol and <sup>1</sup>H n.m.r. and h.p.l.c. resolution of (25R)- and (25S)-26-hydroxycholesterol. *J. Chem. Soc. Perkin. Trans. I.* **33**, 1713–1718.
- Van Pelt, C. K., Carpenter, B. K., and Brenna, J. T. (1999). Studies of structure and mechanism in acetonitrile chemical ionization tandem mass spectrometry of polyunsaturated fatty acid methyl esters. *J. Am. Soc. Mass Spectrom.* **10**, 1253–1262.
- Wilund, K. R., Yu, L., Xu, F., Vega, G. L., Grundy, S. M., Cohen, J. C., and Hobbs, H. H. (2004). No association between plasma levels of plant sterols and atherosclerosis in mice and men. *Arterioscler. Thromb. Vasc. Biol.* **24**, 2326–2332.
- Yang, C., McDonald, J. G., Patel, A., Zhang, Y., Umetani, M., Xu, F., Westover, E. J., Covey, D. F., Mangelsdorf, D. J., Cohen, J. C., and Hobbs, H. H. (2006). Sterol intermediates from cholesterol biosynthetic pathway as liver X receptor ligands. *J. Biol. Chem.* **281**, 27816–27826.

## THE LIPID MAPS INITIATIVE IN LIPIDOMICS

Kara Schmelzer,<sup>\*,†</sup> Eoin Fahy,<sup>‡</sup> Shankar Subramaniam,<sup>\*,‡,§</sup>  
and Edward A. Dennis<sup>\*,†</sup>

### Contents

1. Introduction	172
2. Building Infrastructure in Lipidomics	173
3. Classification, Nomenclature, and Structural Representation of Lipids	174
4. Mass Spectrometry as a Platform for Lipid Molecular Species	177
5. Future Plans	180
Acknowledgments	182
References	182

### Abstract

The Lipid Metabolites and Pathways Strategy (LIPID MAPS) initiative constitutes the first broad scale national exploration of lipidomics and is supported by a U.S. National Institute of General Medical Sciences Large Scale Collaborative “Glue” Grant. The emerging field of lipidomics faces many obstacles to become a true systems biology approach on par with the other “omics” disciplines. With a goal to overcome these hurdles, LIPID MAPS has been developing the necessary infrastructure and techniques to ensure success. This review introduces a few of the challenges and solutions implemented by LIPID MAPS. Among these solutions is the new comprehensive classification system for lipids, along with a recommended nomenclature and structural drawing representation. This classification system was developed by the International Lipids Classification and Nomenclature Committee (ILCNC) in collaboration with LIPID MAPS and representatives from Europe and Asia. The latest changes implemented by the committee are summarized. In addition, we discuss the adoption of mass spectrometry (MS) as the instrumental platform to investigate lipidomics. This platform has the versatility to quantify known individual lipid molecular species and search for novel lipids affecting biological systems.

\* Department of Chemistry and Biochemistry, University of California, San Diego, La Jolla, California

† Department of Pharmacology, University of California, San Diego, La Jolla, California

‡ San Diego Supercomputer Center, University of California, San Diego, La Jolla, California

§ Department of Bioengineering, University of California, San Diego, La Jolla, California

## 1. INTRODUCTION

Remarkable technological advances in the biological sciences have forged a new era of research in the field of systems biology. These comprehensive investigations of living organisms at the molecular system level can be classified into different fields: genomics, transcriptomics, proteomics, and metabolomics, otherwise known as the “omics cascade.” The integrative analysis of an organism’s response to a perturbation on the “omics” levels will lead to a more complete understanding of the biochemical and biological mechanisms in complex systems.

An explosion of information has occurred in the fields of genomics, transcriptomics, and proteomics because each field was able to adopt a single instrumental methodology to analyze all of their respective components in a given sample. However, whereas genomics, transcriptomics, and proteomics have made significant strides in technological development, the tools for the comprehensive examination of the metabolome are still emerging. Although metabolomics is the endpoint of the “omics cascade” and the closest to phenotype, no single instrument can currently analyze all metabolites (Bino *et al.*, 2004).

Comprehensive investigation of the metabolome is hindered by its enormous complexity and dynamics. The metabolome represents a vast number of components that belong to a wide variety of compound classes, including nucleic acids, amino acids, sugars, and lipids. These compounds are diverse in their physical and chemical properties and occur in vastly different concentration ranges. Additionally, metabolite concentrations can vary spatially and temporally. Furthermore, diet- and/or nutrient-dependent biological variability confounds such analysis (Vigneau-Callahan *et al.*, 2001). For example, within the lipid classes, highly abundant compounds exist, such as fatty acids, triglycerides, and phospholipids, and trace level components, such as eicosanoids, which have important regulatory effects on homeostasis and disease states.

In addition to analyzing a vast number of metabolites, a comprehensive lipidomic investigation includes studying the metabolizing enzymes and lipid transporters. Together, these components play a role in cell signaling, metabolism, physiology, and disease, making them excellent targets for systematic measurements. The LIPID MAPS initiative is a result of our quest to characterize the mammalian lipidome to an extent similar to that of the genome and proteome (Dennis *et al.*, 2005). To accomplish this goal, we have formed a consortium of twelve independent laboratories from seven academic institutions and one company. We have six lipidomics cores that are charged with identifying, quantifying, and becoming experts in six major categories of lipids: fatty acyls, glycerolipids, glycerophospholipids,

sphingolipids, sterol lipids, and prenol lipids. This division of labor is essential, as there are hundreds of thousands of individual molecular species of metabolites in each category of lipids, presenting a challenge for routine quantification. Additionally, the Lipid Synthesis/Characterization Core is charged with generating quantitative lipid standards and the synthesis and characterization of novel lipids. We also have a Bioinformatics Core, a Cell Biology Core, and a MS Development Core. Finally, five independent sections explore more specific aspects of lipidomics as related to future core methodologies and the medical field.

The following text will discuss each of the LIPID MAPS contributions to lipidomics. The “[Building Infrastructure in Lipidomics](#)” section discusses the development of critical infrastructure for lipidomics to become a true systems biology approach. “Classification, Nomenclature, and Structural Representation of Lipids” describes the standardization of the lipid classification scheme, lipid nomenclature, and structural representation (Fahy *et al.*, 2005). “Mass Spectrometry as a Platform for Lipid Molecular Species” describes the adoption of MS as the major platform to investigate lipidomics and the challenges in quantifying the complex lipid metabolites in a biological system. This section addresses the complications associated with integrating the molecular species lipidomic data and the need for analyte standards. After the first 3 years of the project, we have implemented most of the infrastructure and have evolved our future plans to expand lipidomics, as described in the “[Future Plans](#)” section.



## 2. BUILDING INFRASTRUCTURE IN LIPIDOMICS

In 2003, the consortium identified several important challenges that any lipidomics effort would face. These obstacles included developing a robust and versatile platform to quantify the lipidome, specific reagents and experimental protocols, high throughput methods, data export standardization, computer algorithms for automated data analysis, visualization tools, libraries, and databases for integration of lipidomics with the other omic cascades.

Because no single quantization platform is capable of measuring the entire lipidome, the first goal of the initiative was to develop the requisite quantitation technology. In order for different laboratories to minimize instrument variability and to ensure interoperability and method sharing capabilities, LIPID MAPS chose for all cores to use the same ABI-4000 Q-trap mass spectrometers (Foster City, CA) for quantitative comparisons. We have and will continue to design stringent sets of isotopic-labeled reference compounds that will allow the accurate quantification of a wide range of lipid metabolites. The reference standards are intended to be commercially

available to all researchers worldwide, both within and beyond the lipid field, which will facilitate inter-laboratory comparison.

Once a requisite quantitation technology was established, we realized that, to successfully conduct bioinformatic analysis of data collected from six different laboratories, a significant level of reproducibility between experiments and between laboratories would be required. To achieve this reproducibility, we have employed a rigorously maintained set of common biological, biochemical, and analytical technologies in each of the consortium laboratories. To this end, we have tried to standardize all reagents. We purchased a large lot of fetal calf serum, which is being employed by all consortium laboratories for the duration of this project. We also prepared a large batch of RAW 264.7 cells obtained from ATCC (Manassas, VA) and froze enough stabs to supply fresh cells from this one batch to all laboratories for the duration of the project. Thus, all cells in these experiments were similarly passaged and treated. For example, to investigate changes associated with the binding of the Toll-like receptor 4 (TLR-4), we developed the methodology to prepare highly purified 3-deoxy-D-manno-octulosonic acid Kdo<sub>2</sub>-Lipid A, and then evaluated it by electrospray ionization (ESI)-MS (ESI-MS), liquid chromatography (LC)-MS (LC-MS), and <sup>1</sup>H-NMR (nuclear magnetic resonance). Finally, we compared its bioactivity with laser plasma spectrometry (LPS) in RAW 264.7 cells and bone marrow macrophages from wild-type and TLR-4-deficient mice. Now, standardized Kdo<sub>2</sub>-Lipid A ensures a crucial intra-laboratory quality control agonist for TLR-4 (Raetz *et al.*, 2006).

No universal classification system for lipids was suitable for modern informatics and experimental investigations. Unlike existing lipid legacy databases, such as Lipid Bank and Lipidat, our new system plans to integrate all the omic cascades associated with lipidomics. Integrating the MS data on lipidomics with the genomic data will lead to a more complete understanding of how complex lipidomic networks function, from biosynthesis to the removal of cellular lipids and the important roles of metabolites as second messengers. With thorough and extensive experimental planning, we are able to integrate and analyze large amounts of data that will be developed into “road maps.”

### **3. CLASSIFICATION, NOMENCLATURE, AND STRUCTURAL REPRESENTATION OF LIPIDS**

With the emergence of lipidomics as a rapidly expanding field came an urgent need for an internationally accepted method of describing and classifying lipid molecules. The first step toward classification of lipids was



the establishment of an ontology that was extensible, flexible, and scalable. One must be able to classify, name, and represent these molecules in a logical manner that is amenable to databasing and computational manipulation. Lipids have been loosely defined as biological substances that are generally hydrophobic in nature and, in many cases, soluble in organic solvents (Smith, 2000). These chemical features are present in a broad range of molecules, such as fatty acids, phospholipids, sterols, sphingolipids, and terpenes (Christie, 2003). The LIPID MAPS consortium has taken a chemistry-based approach by defining lipids as hydrophobic or amphipathic small molecules that may originate entirely or in part by carbanion-based condensations of thioesters such as fatty acids and polyketides (Fig. 7.1A) and/or by carbocation-based condensations of isoprene units such as prenols and sterols (Fig. 7.1B) (Fahy *et al.*, 2005).

The classification scheme shown in Table 7.1 organizes lipids into well-defined categories that cover eukaryotic and prokaryotic lipid origins, and is equally applicable to archaea and synthetic (manufactured) lipids (Fahy *et al.*, 2005). Biosynthetically related compounds that are not technically lipids due to their water solubility are included for completeness in this classification scheme.

Lipids are divided into eight categories (fatty acyls, glycerolipids, glycerophospholipids, sphingolipids, sterol lipids, prenol lipids, saccharolipids, and polyketides) containing distinct classes and subclasses of molecules, and a 12-digit unique identifier is associated with each distinct lipid molecule.

For each lipid, the unique 12-character identifier based on this classification scheme is an important database field in the Lipids Database (Sud *et al.*, 2007). The format of the LIPID ID, outlined in Table 7.2, provides a systematic means of assigning a unique identification to each lipid molecule and allows for the addition of large numbers of new categories, classes, and subclasses in the future. The last four characters of the ID comprise a unique identifier within a particular subclass and are randomly assigned. Initially using numeric characters allows 9999 unique IDs per subclass; however, with the additional use of 26 uppercase alphabetic characters, a total of 1.68 million possible combinations can be generated, providing ample scalability within each subclass.

The classification system is under the guidance of the ILCNC, which meets periodically to propose changes and updates to classification, nomenclature, and structural representation. The ILCNC currently consists of Dr. Edward A. Dennis (chair), Dr. Robert C. Murphy, Dr. Masahiro Nishijima, Dr. Christian R.H. Raetz, Dr. Takao Shimizu, Dr. Friedrich Spener, Dr. Gerrit van Meer, and Dr. Michael Wakelam. The most recent meeting was on July 7, 2006 in La Jolla, CA, during which a number of recommendations were implemented to extend the original system (Fahy *et al.*, 2005). Some key changes can be seen in Table 7.3.

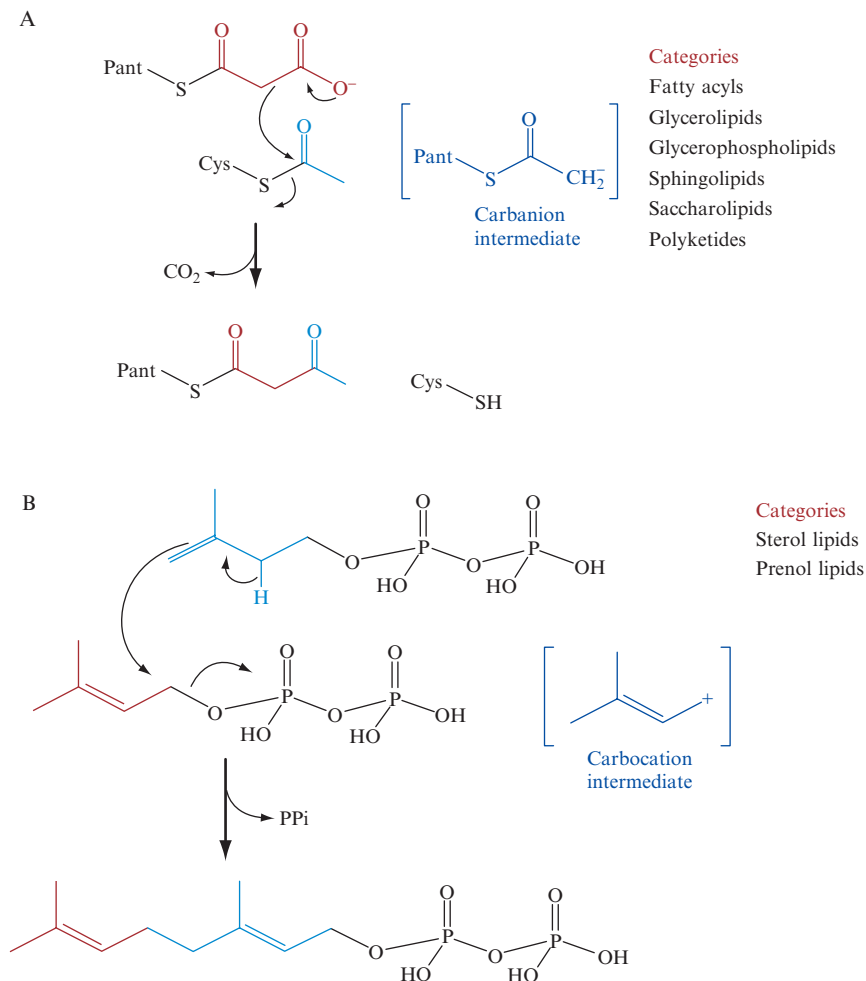


**Figure 7.1** The LIPID MAPS chemistry-based approach defines lipids as molecules that may originate entirely or in part by carbanion-based condensations of (A) thioesters and/or by (B) carbocation-based condensations of isoprene units.

The ILCNC has been greatly assisted by many experts throughout the world who have given helpful advice and comments on enhancing the scope and utility of the lipid classification scheme. The scheme can be conveniently browsed on the LIPID MAPS website (<http://www.lipidmaps.org>), in which the various classes and subclasses are linked to the LIPID MAPS structure database (Fahy and Subramaniam, 2007).

The LIPID MAPS classification scheme has now gained widespread international acceptance and has recently been adopted by KEGG (Kyoto

**Table 7.1** LIPID MAPS lipid categories and examples

Category	Abbreviation	Example
Fatty acyls	FA	Dodecanoic acid
Glycerolipids	GL	1-Hexadecanoyl-2-(9Z-octadecenoyl)- <i>sn</i> -glycerol
Glycerophospholipids	GP	1-Hexadecanoyl-2-(9Z-octadecenoyl)- <i>sn</i> -glycero-3-phosphocholine
Sphingolipids	SP	N-(tetradecanoyl)-sphing-4-enine
Sterol lipids	ST	Cholest-5-en-3 $\beta$ -ol
Prenol lipids	PR	2E,6E-farnesol
Saccharolipids	SL	UDP-3-O-(3R-hydroxy-tetradecanoyl)- $\beta$ D-N-acetylglucosamine
Polyketides	PK	Aflatoxin B1

**Table 7.2** Format of 12-character LIPID ID

Characters	Description	Example
1–2	Fixed database designation	LM
3–4	Two-letter category code	FA
5–6	Two-digit class code	03
7–8	Two-digit subclass code	02
9–12	Unique four-character identifier within subclass	AG12

Encyclopedia of Genes and Genomes), where functional hierarchies involving lipids, reactions, and pathways have been constructed (<http://www.genome.ad.jp/brite/>). In addition, LIPID MAPS lipid structures are now available on NCBI's PubChem website (<http://pubchem.ncbi.nlm.nih.gov/>), where entries are hyperlinked to the LIPID MAPS classification system.

## 4. MASS SPECTROMETRY AS A PLATFORM FOR LIPID MOLECULAR SPECIES

Mass spectrometry is an established and invaluable tool for the characterization of changes in lipidomics and lipid-mediated signaling processes resulting from disease, toxicant exposure, genetic modifications, or drug therapy

**Table 7.3** Updates to LIPID MAPS classification system

1. Under the fatty acyls category, the hydroxyeicosatrienoic acids, hydroxyeicosatetraenoic acids, and hydroxyeicosapentaenoic acids subclasses have been expanded to include the corresponding hydroperoxy and keto analogues. The N-acyl amide and N-acyl ethanolamide subclasses have been renamed to N-acyl amines and N-acyl ethanolamines.
2. In order to improve representation of plant lipids in the classification scheme, the glycosylmonoradyl and glycosyldiradylglycerol classes were created within the glycerolipid category.
3. Several new bile acids (C22, C23, C25, and C29 bile acids, alcohols, and derivatives) and secosteroids (vitamin D4, D5, D6, and D7 and derivatives) have been added to the sterol lipids category.
4. It was decided not to rely on phylum- or species-based references in the classification scheme, but rather to use structural core units where possible. Accordingly, the phytosterol, marine sterol, and fungal sterol subclasses were removed from the sterol lipids category and replaced with a more extensive, structurally based list (ergosterols, stigmasterols, C24-propyl sterols, gorgosterols, furostanols, spirostanols, furospirostanols, calysterols, cardenolides, bufanolides, brassinolides, and solanidines/alkaloids) of sterols.
5. The retinoids subclass was added to the prenol lipids category. The hopanoids class was also moved to this category (from sterol lipids).
6. In the case of lipids with multiple functional groups (especially fatty acyls) where it may be difficult to objectively classify a structure, the Cahn-Ingold-Prelog rules are applied to place the lipid in the subclass with the highest Cahn-Ingold-Prelog "score." However, to ensure that lipids containing a particular functional group (e.g., a hydroxyl-fatty acid) can be located in a database that uses this classification system, an ontology-based system has been implemented, where a user may locate all lipids with the specified functionality, regardless of their subclass designation.
7. The LIPID MAPS glycerophospholipid abbreviations (GPCho, GPEtn, etc.) are used to refer to species with one or two radyl side-chains, where the structures of the side chains are indicated within parentheses, such as GPCho(16:0/18:1(9Z)).

(Watkins and German, 2002). MS provides a wide dynamic range to quantify lipids. In addition, it offers excellent selectivity for examining compounds using parameters such as ionization mode (positive/negative), mass selection, MS/MS characterization, and numerous MS<sup>n</sup> techniques for structural elucidation. MS-based lipidomics can deliver detailed, quantitative information about the cellular lipidome constitution and provide insights into biochemical mechanisms of lipid metabolism, lipid-lipid, and lipid-protein interactions.

Traditionally, lipids have been analyzed using gas chromatographic (GC) separation, electron impact ionization MS (EI-MS), and flame ionization

detection (FID). GC is limiting because compounds must be thermally stable with high enough vapor pressure to volatilize during injection. Therefore, extensive sample manipulation is required on complex lipid samples to produce accurate data. Sample preparation can include pre-separation of lipid classes, hydrolysis, derivatization, or pyrolysis. Although highly quantitative, these labor-intensive preparations destroy structural information regarding lipid composition. One of the LIPID MAPS goals is to improve the ability to quantify discrete molecular species, utilizing MS.

Detection of the specific molecular species was made possible by the development of solid state ion sources (e.g., fast atom bombardment [FAB] or matrix-assisted laser desorption/ionization [MALDI]) and liquid-phase ion sources (e.g., electrospray ionization [ESI], atmospheric pressure chemical ionization [APCI], or atmospheric pressure photo ionization [APPI]) (Griffiths, 2003). Although MALDI and other laser-based ionization methods have great potential for nonpolar species, our initial work has focused on ESI ion sources, as they are efficient for a wide variety of metabolites and are easily mated to high performance liquid chromatography (HPLC). ESI in positive mode allows for the detection of phosphatidylcholine, lysophosphatidylcholine, phosphatidylethanolamine, and sphingomyelins. ESI in negative mode allows for the detection of phosphatidic acid, phosphatidylserine, phosphatidylinositol, phosphatidylglycerol, phosphotidylethanolamine, free fatty acids, and eicosanoids. Finally, compounds that are not readily ionized by ESI, such as neutral lipids (e.g., triacylglycerols), can be detected by examining ammonium, lithium, or sodium adducts with ESI in positive mode (Duffin *et al.*, 1991; Han and Gross, 2005; Hsu and Turk, 1999).

Ionized lipids are further studied by tandem MS (MS/MS) to identify lipid species within specific classes. For example, the specific headgroups of phospholipids produce characteristic fragmentation patterns that are used for their identification (Griffiths, 2003; Pulfer and Murphy, 2003; Merrill *et al.* 2005) used both neutral loss and precursor-ion methods to identify sphingolipids. Precursor-ion scans for  $m/z$  184 in positive mode are used to identify sphingomyelin while scans for  $m/z$  264 are used to identify ceramide. More complex lipids, such as gangliosides, require advanced MS<sup>n</sup> experiments for elucidation.

Certain lipid classes lend themselves to automated computational lipidomic approaches because of structural similarities and differentiation only in their headgroups and acyl groups. Forrester *et al.* (2004) developed methods to automate spectral interpretation and quantification of multiple phospholipid species utilizing direct injection ESI-MS/MS analysis. Han and Gross (2003, 2005) have also attempted to eliminate the need for HPLC by developing a “shotgun lipidomic” approach. They utilized the traditional Bligh/Dyer extraction to produce tissue extracts, and then directly injected the sample onto the mass spectrometer in both positive and negative mode ESI. Hermansson *et al.* (2005), using LC-ESI-MS/MS, quantified

more than 100 polar lipids using a fully automated method from sample handling to computer algorithms analysis of the spectra produced. In most cases, only semiquantitative data were reported.

The current goal of LIPID MAPS focuses on the complete quantitative analysis of the exact molecular species. Accurate quantitative data require a known standard for each molecular species, as well as internal standards to mimic analytes in these biological samples. Internal standards are most commonly deuterated analogues or lipids containing odd chain fatty acids. LIPID MAPS has collaborated with suppliers who provide analytical, chemically pure standards for precise quantization. In some categories, such identification of discrete molecular species is extremely labor-intensive. While it would be labor- and cost-prohibitive to develop the standards for quantifying all of the known molecular species, we continue to develop as many standards as possible. Moreover, when unknown species are detected and characterized, their final identification requires chemically synthesized standards (Harkewicz *et al.*, 2007)

Progress to date in developing standards is shown in Table 7.4.

## 5. FUTURE PLANS

Signaling through lipid metabolism constitutes key cellular events that participate in innate immunity, inflammation, and a host of other physiological phenomena. The complexity of lipid metabolites in biological

**Table 7.4** Mass spectrometry standards

Core	Library MS/MS SPECTRA <sup>a</sup>	Internal standard <sup>b</sup>	Primary standard <sup>c</sup>	LIPID MAPS standard <sup>d</sup>
Fatty acyls eicosanoids	74	16	16	0
Glycerolipids	21	15		15
Glycerophospholipids	182	24	40	24
Sphingolipids	5	15		15
Sterols	23	13	13	11
Prenols/other	13	1		7
<b>Total</b>	<b>318</b>	<b>84</b>	<b>69</b>	<b>72</b>

<sup>a</sup> MS/MS spectra of chemically pure analytes, which are located in the LIPID MAPS library on [www.lipidmaps.org](http://www.lipidmaps.org).

<sup>b</sup> Analyte analog (e.g., stable isotope, odd carbon fatty acid).

<sup>c</sup> Chemically pure, accurately quantitated analyte.

<sup>d</sup> Internal or primary standard that is a certified, chemically pure analyte, quantitated, and stability-tested for shelf life.

samples has presented a great challenge. As stated previously, the different subclasses of lipids are affected by various stimuli and produce both temporal and spatial metabolites in a biological system. Therefore, the true goal of “lipidomics,” namely the quantitative analysis of all lipid metabolites in a biological system, requires different tools to probe the lipidome for dynamic changes. Two complementary approaches are lipid fingerprinting and lipid profiling.

Lipid fingerprinting identifies patterns, or “fingerprints,” of lipid metabolites that change in response to various stimuli. These methods, which are not intended to quantify compounds, cast a wide net and generate and test hypotheses. Specifically, LIPID MAPS–collected lipid extracts will be subjected to a general lipid fingerprinting analysis using LC–time-of-flight (TOF)–MS. This technique is used to screen for differences in lipid expression among treatment groups and identify important lipid metabolites and potential biomarkers. The bioinformatics team will process the data and, when significant changes are detected, further efforts will be taken to identify and quantify these compounds. This approach allows for the discovery of novel lipids that change in response to a given stimulus as well as interpretation of the role in biochemical processes.

Lipid profiling uses analytical methods for quantifying metabolites in a pathway or for a class of compounds. LIPID MAPS has developed infrastructure for quantifying analytes in each lipid class using this approach. The quantitative lipid analysis information has allowed us to produce information that can be applied to known biochemical pathways and physiological interactions. Profiling methods are used to test specific hypotheses and investigate mechanisms of action within the biological systems. Individual analyte data comprise a platform-independent legacy database, while the collection of lipid profiles provide temporal snapshots that lead to identification of different response stages among the different various groups. In combination with fingerprinting, various biomarkers can potentially be discerned from each stage.

In future work, we will use both approaches to comprehensively investigate lipid changes resulting from a genetic modification, toxicant exposure, diet, disease, or drug therapy. LIPID MAPS plans to carry out systematic and quantitative measurements of lipid changes in an effort to reconstruct normal and pathological networks associated with inflammation. Our vehicle for these experiments will be primary macrophages and macrophage cell lines as well as mouse plasma and various tissues. We will continue to develop novel MS techniques, as well as methods for integrating lipidomic and genomic technologies. We anticipate that our efforts will provide the foundation for building a bridge to translational medicine and serve as a paradigm for interdisciplinary systems medicine projects.

## ACKNOWLEDGMENTS

We wish to thank our LIPID MAPS colleagues, including H. Alex Brown, Christopher Glass, Alfred Merrill, Jr., Robert C. Murphy, Christian R. H. Raetz, David Russell, Walter Shaw, Michael VanNieuwenhze, Stephen H. White, and Joseph Witztum, and their laboratories for their contributions to this work. Financial support of the National Institute of General Medical Science U54 GM069338-3 is gratefully acknowledged, as is the advice of NIGMS Program Officer Jean Chin.

## REFERENCES

- Bino, R. J., Hall, R. D., Fiehn, O., Kopka, J., Saito, K., Draper, J., Nikolau, B. J., Mendes, P., Roessner-Tunali, U., Beale, M. H., Trethewey, R. N., Lange, B. M., *et al.* (2004). Potential of metabolomics as a functional genomics tool. *Trends Plant. Sci.* **9**, 418–425.
- Christie, W. (2003). “Lipid analysis, 3rd ed.” Oily Press, Bridgewater, UK.
- Dennis, E. A., Brown, H. A., Deems, R., Glass, C. K., Merrill, A. H., Murphy, R. C., Raetz, C. R. H., Shaw, W., Subramaniam, S., and Russell, D. W. (2005). The LIPID MAPS approach to lipidomics. In “Functional Lipidomics” (L. Feng and G. D. Prestwich, eds.), pp. 1–15. CRC Press/Taylor and Francis Group, Boca Raton, FL.
- Duffin, K. L., Henion, J. D., and Shieh, J. J. (1991). Electrospray and tandem mass spectrometric characterization of acylglycerol mixtures that are dissolved in nonpolar solvents. *Anal. Chem.* **63**, 1781–1788.
- Fahy, E., Subramaniam, S., Brown, H. A., Glass, C. K., Merrill, A. H., Jr., Murphy, R. C., Raetz, C. R. H., Russell, D. W., Seyama, Y., Shaw, W., Shimizu, T., Spener, F., *et al.* (2005). A comprehensive classification system for lipids. *J. Lipid Res.* **46**, 839–862.
- Fahy, E., and Subramaniam, S. (2007). New resources in lipid classification and databases. *Meth. Enzymol.* In press.
- Forrester, J. S., Milne, S. B., Ivanova, P. T., and Brown, H. A. (2004). Computational lipidomics: A multiplexed analysis of dynamic changes in membrane lipid composition during signal transduction. *Mol. Pharmacol.* **65**, 813–821.
- Griffiths, W. J. (2003). Tandem mass spectrometry in the study of fatty acids, bile acids, and steroids. *Mass Spectrom. Rev.* **22**, 81–152.
- Han, X., and Gross, R. W. (2003). Global analyses of cellular lipidomes directly from crude extracts of biological samples by ESI mass spectrometry: A bridge to lipidomics. *J. Lipid Res.* **44**, 1071–1079.
- Han, X., and Gross, R. W. (2005). Shotgun lipidomics: Electrospray ionization mass spectrometric analysis and quantitation of cellular lipidomes directly from crude extracts of biological samples. *Mass Spectrom. Rev.* **24**, 367–412.
- Harkewicz, R., Fahy, E., Andreeyev, A., and Dennis, E. A. (2007). Arachidonate-derived dihomoprostaglandin production observed in endotoxin-stimulated macrophage-like cells. *J. Biol. Chem.* **282**, 2899–2910.
- Hermansson, M., Uphoff, A., Käkälä, R., and Somerharju, P. (2005). Automated quantitative analysis of complex lipidomes by liquid chromatography/mass spectrometry. *Anal. Chem.* **77**, 2166–2175.
- Hsu, F. F., and Turk, J. (1999). Structural characterization of triacylglycerols as lithiated adducts by electrospray ionization mass spectrometry using low-energy collisionally activated dissociation on a triple stage quadrupole instrument. *J. Am. Soc. Mass Spectrom.* **10**, 587–599.



- Merrill, A. H., Jr., Sullards, M. C., Allegood, J. C., Kelly, S., and Wang, E. (2005). Sphingolipidomics: High-throughput, structure-specific, and quantitative analysis of sphingolipids by liquid chromatography tandem mass spectrometry. *Methods* **36**, 207–224.
- Pulfer, M., and Murphy, R. C. (2003). Electrospray mass spectrometry of phospholipids. *Mass Spectrom. Rev.* **22**, 332–364.
- Raetz, C. R., Garrett, T. A., Reynolds, C. M., Shaw, W. A., Moore, J. D., Smith, D. C., Jr., Ribeiro, A. A., Murphy, R. C., Ulevitch, R. J., Fearn, C., Reichart, D., Glass, C. K., et al. (2006). *Kdo2-Lipid A* of *Escherichia coli*, a defined endotoxin that activates macrophages via TLR-4. *J. Lipid Res.* **47**, 1097–1111.
- Smith, A. (2000). “Oxford Dictionary of Biochemistry and Molecular Biology,” 2nd ed. Oxford University Press, New York.
- Sud, M., Fahy, E., Cotter, D., Brown, A., Dennis, E. A., Glass, C. K., Merrill, A. H., Jr., Murphy, R. C., Raetz, C. R., Russell, D. W., and Subramaniam, S. (2007). LMSD: LIPID MAPS structure database. *Nucleic Acids Res.* **35**(Database issue), D527–D532.
- Vigneau-Callahan, K. E., Shestopalov, A. I., Milbury, P. E., Matson, W. R., and Kristal, B. S. (2001). Characterization of diet-dependent metabolic serotypes: Analytical and biological variability issues in rats. *J. Nutr.* **131**, 924S–932S.
- Watkins, S. M., and German, J. B. (2002). Toward the implementation of metabolomic assessments of human health and nutrition. *Curr. Opin. Biotechnol.* **13**, 512–516.

## BIOINFORMATICS FOR LIPIDOMICS

Eoin Fahy,<sup>\*</sup> Dawn Cotter,<sup>\*</sup> Robert Byrnes,<sup>\*</sup> Manish Sud,<sup>\*</sup>  
 Andrea Maer,<sup>\*</sup> Joshua Li,<sup>\*</sup> David Nadeau,<sup>\*</sup> Yihua Zhou,<sup>\*</sup> and  
 Shankar Subramaniam<sup>\*,†,‡</sup>

### Contents

1. Introduction	248
2. Lipid Structure Databases	249
2.1. Ontology, classification, and nomenclature	249
2.2. Lipid structure databases	251
2.3. Lipid structure representation	253
3. Lipid-Associated Protein/Gene Databases	254
3.1. LIPID MAPS genome/proteome database	254
3.2. Extracting lipid genes and proteins from databases and legacy knowledge	255
4. Tools for Lipidomics	256
4.1. LIPID MAPS website and user interface	256
4.2. Tools for automated drawing and naming of lipids	260
4.3. Tools for prediction of lipid mass spectra	262
4.4. Tools for managing lipidomic metadata	263
4.5. Tools for collection, display, and analysis of experimental lipidomic data	264
4.6. Tools for lipid profiling	267
5. Lipid Pathways	268
5.1. Bioinformatics resources for lipid-related pathways	268
5.2. Tools for drawing pathways	269
6. Challenges for Future Lipid Informatics	270
Acknowledgments	272
References	272

<sup>\*</sup> San Diego Supercomputer Center, University of California, San Diego, La Jolla, California

<sup>†</sup> Departments of Bioengineering and Chemistry and Biochemistry, University of California, San Diego, La Jolla, California

<sup>‡</sup> Graduate Program in Bioinformatics and Systems Biology, University of California, San Diego, La Jolla, California

## Abstract

Lipids are recognized as key participants in the regulation and control of cellular function, having important roles in signal transduction processes. The diversity in lipid chemical structure presents a challenge for establishing practical methods to generate and manage high volumes of complex data that translate into a snapshot of cellular lipid changes. The need for high-quality bioinformatics to manage and integrate experimental data becomes imperative at several levels: (1) definition of lipid classification and ontologies, (2) relational database design, (3) capture and automated pipelining of experimental data, (4) efficient management of metadata, (5) development of lipid-centric search tools, (6) analysis and visual display of results, and (7) integration of the lipid knowledge base into biochemical pathways and interactive maps. This chapter describes the recent contributions of the bioinformatics core of the LIPID MAPS consortium toward achieving these objectives.

## 1. INTRODUCTION

The LIPID MAPS consortium is an exemplary systems biology project that quantitatively measures cell-wide lipid changes upon stimulus and attempts to reconstruct biochemical pathways associated with lipid processing and signaling. The cell-wide measurements of components of these pathways include mass spectrometric measurements of lipid changes in response to stimulus in mammalian cells, changes in transcription profiles in response to stimulus, and, in select cases, proteomic changes in response to stimulus. Reconstruction efforts will rely on organization, analysis, and integration of these data, and this warrants a strong bioinformatics effort. The UCSD Bioinformatics Laboratory is involved in the creation of the infrastructure of LIPID MAPS and in the methodology needed to carry out systematic reconstruction leading to new biological hypotheses. This infrastructure involved the development of the following:

- A completely systematic and universal classification and nomenclature system
- A LIPID MAPS website that provides a comprehensive introduction, description of the project, and reports of developments in the project
- A series of databases pertinent to lipids
- Web interfaces that provide easy navigation and query capabilities for LIPID MAPS
- Analysis tools for lipid-related molecules
- A laboratory information management system
- A pathway representation and visualization system

The following sections provide a comprehensive, albeit synoptic, description of these facets of the LIPID MAPS bioinformatics infrastructure for lipidomics.

## 2. LIPID STRUCTURE DATABASES

### 2.1. Ontology, classification, and nomenclature

The first step toward classification of lipids is the establishment of an ontology that is extensible, flexible, and scalable. When efforts to sequence genomes and to measure proteomes were initiated, significant investments were made in bioinformatics infrastructures that could accommodate the huge amounts of data. Structured vocabularies were developed to classify these macromolecules, database schemas were developed to house the data in relational tables, and numerous algorithms were developed to carry out extensive gene and protein sequence analysis (Jorde *et al.*, 2005). Similarly, in the case of lipids, one must first be able to classify, name, and represent these molecules in a logical manner that is amenable to databasing and computational manipulation. A number of online resources (Table 11.1) outline comprehensive classification schemes for lipids. In view of the fact that lipids comprise an extremely heterogeneous collection of molecules from a structural and functional standpoint, it is not surprising that significant differences exist with regard to the scope and organization of current classification schemes. The Lipid Library (<http://www.lipidlibrary.co.uk>) site defines lipids as “fatty acids and their derivatives, and substances related biosynthetically or functionally to these compounds.” The Cyberlipids (<http://www.cyberlipid.org>) website has a broader approach and includes isoprenoid-derived molecules such as steroids and terpenes. Both of these resources classify lipids into “simple” and “complex” groups, with simple lipids being those yielding at most two types of distinct entities upon hydrolysis (e.g., acylglycerols: fatty acids and glycerol) and complex lipids (e.g., glycerophospholipids: fatty acids, glycerol, and headgroup) yielding three or more products upon hydrolysis. The LipidBank (<http://lipidbank.jp>) database in Japan defines 17 top-level categories in their classification scheme, covering a wide variety of animal and plant sources. The LIPID MAPS group (<http://www.lipidmaps.org>) has taken a more chemistry-based approach and defines lipids as hydrophobic or amphipathic small molecules that may originate entirely or in part by carbanion-based condensations of thioesters (fatty acids, polyketides, etc.) and/or by carbocation-based condensations of isoprene units (prenols, sterols, etc.). Lipids are divided into eight categories (fatty acyls, glycerolipids, glycerophospholipids, sphingolipids, sterol lipids, prenol lipids, saccharolipids,

**Table 11.1** Online resources for lipid classification and databasing

Resource	URL	Country	Comments
Lipid Library	<a href="http://www.lipidlibrary.co.uk">http://www.lipidlibrary.co.uk</a>	U.K.	Multiple reference topics and examples, mass spectrometry (MS) and nuclear magnetic resonance (NMR) libraries, literature service
Cyberlipid Center	<a href="http://www.cyberlipid.org">http://www.cyberlipid.org</a>	France	Descriptions of lipid classes with examples and literature references
LipidBank	<a href="http://lipidbank.jp">http://lipidbank.jp</a>	Japan	Lipid database with a wide variety of categories, including plant lipids
LIPIDAT	<a href="http://www.lipidat.chemistry.ohio-state.edu">http://www.lipidat.chemistry.ohio-state.edu</a>	U.S.	Database composed mostly of phospholipids and associated thermodynamic data
LIPID MAPS	<a href="http://www.lipidmaps.org">http://www.lipidmaps.org</a>	U.S.	Classification scheme, lipid and protein databases, MS libraries, search tools

and polyketides) containing distinct classes and subclasses of molecules. A 12-digit unique identifier is associated with each distinct lipid molecule.

For each lipid, the unique 12-character identifier based on this classification scheme (Fahy *et al.*, 2005) is an important database field in the Lipids Database. The format of the LIPID ID provides a systematic means of assigning a unique identification to each lipid molecule and allows for the addition of large numbers of new categories, classes, and subclasses in the future. The last four characters of the ID comprise a unique identifier within a particular subclass and are randomly assigned. By initially using numeric characters, this allows 9999 unique IDs per subclass; however, with the additional use of 26 uppercase alphabetic characters, a total of 1.68 million possible combinations can be generated, providing ample scalability within

each subclass. In cases where lipid structures were obtained from other sources, such as LipidBank or LIPIDAT, the corresponding IDs for those databases are included to enable cross-referencing. The LIPID MAPS classification scheme has been adopted by KEGG (Kyoto Encyclopedia of Genes and Genomes), where functional hierarchies involving lipids, reactions, and pathways have been constructed (<http://www.genome.ad.jp/brite/>). The classification system may conveniently be browsed online from the LIPID MAPS website (<http://www.lipidmaps.org>), in which the various classes and subclasses are linked to the LIPID MAPS structure database (LMSD).

Nomenclature of lipids falls into two main categories: systematic names and common, or trivial, names. The latter includes abbreviations, which are a convenient way to define acyl/alkyl chains in acylglycerols, sphingolipids, and glycerophospholipids. The generally accepted guidelines for systematic names have been defined by the International Union of Pure and Applied Chemists and the International Union of Biochemistry and Molecular Biology (IUPAC-IUBMB) Commission on Biochemical Nomenclature (<http://www.chem.qmul.ac.uk/iupac/>). The use of core structures such as prostanic acid, cholestane, or phosphocholine is strongly recommended as a way of simplifying systematic nomenclature; commercially available software packages that perform structure-to-name conversions generally create overly complicated names for several categories of lipids.

Many lipids, in particular the glycerolipids, glycerophospholipids, and sphingolipids, may be conveniently described in terms of a shorthand name, where abbreviations are used to define backbones, headgroups, and sugar units, and the radyl substituents are defined by a descriptor indicating carbon chain length and number of double bonds. These shorthand names lend themselves to fast, efficient, text-based searches and are used widely in lipid research as compact alternatives to systematic names. The use of a shorthand notation for selected lipid categories that incorporates a condensed text nomenclature for glycan substituents has also been deployed by LIPID MAPS. The abbreviations for the sugar units follow the current IUPAC-IUBMB recommendations (Chester, 1998).

## 2.2. Lipid structure databases

Modern bioinformatics has become increasingly sophisticated, permitting complex database schemas and approaches that enable efficient data accrual, storage, and dissemination. A large number of repositories, such as GenBank, SwissProt, and ENSEMBL (<http://www.ensembl.org>), support nucleic acid and protein databases; however, only a few specialized databases (e.g., LIPIDAT [Caffrey and Hogan, 1992] and LipidBank [Watanabe *et al.*, 2000]) are dedicated to cataloging lipids. The LIPIDAT database, developed by Martin Caffrey's group at Ohio State University, focuses on the biophysical properties

of glycerolipids and sphingolipids and contains over 12,000 unique molecular structures. The LipidBank online database in Japan contains over 6000 structures across a broad range of lipid classes and is a rich resource for associated spectral data, biological properties, and literature references.

Given the importance of these molecules in cellular function and pathology, it is essential to have a well-organized database of lipids with a defined ontology that is extensible, flexible, and scalable. The ontology of lipids must incorporate classification, nomenclature, structure representations, definitions, related biological/biophysical properties, cross-references, and structural features (formula, molecular weight, number of carbon atoms, number of various functional groups, etc.) of all objects stored in the database. This ontology is then transformed into a well-defined schema that forms the foundation for a relational database of lipids. An object-relational database of lipids, based on the previously mentioned classification scheme and containing structural, biophysical, and biochemical characteristics, is available on the LIPID MAPS website with browsing and searching capabilities. The database (Sud *et al.*, 2007) currently contains over 10,000 structures, which are obtained from these four sources: the LIPID MAPS consortium's core laboratories and partners; lipids identified by LIPID MAPS experiments; computationally generated structures for appropriate lipid classes; and biologically relevant lipids manually curated from LipidBank, LIPIDAT, and other public sources. All structures have been classified and redrawn according to LIPID MAPS guidelines. After lipids have been selected for inclusion into LMSD, they are classified following the LIPID MAPS classification scheme as explained earlier under the "[Ontology, Classification, and Nomenclature](#)" section. Structures of the lipids are drawn either manually or generated automatically by computational structure drawing tools developed by the LIPID MAPS consortium; the structure representation is consistent and adheres to the rules proposed by the LIPID MAPS consortium. LMSD implements storage of lipid structure representations using the following three formats: Binary Large Object (BLOB), ChemDraw Exchange (CDX) format ([www.cambridgesoft.com/services/documentation/sdk/chemdraw/cdx/](http://www.cambridgesoft.com/services/documentation/sdk/chemdraw/cdx/)), and Graphics Interchange Format (GIF). LMSD uses BLOB format to store MDL MOL file structural representation via the Accord Chemical Cartridge. CDX format, a richer and more flexible format with support for not only structure data but also for visual characteristics and annotations, is stored in LMSD as Character Large Object (CLOB) data; CDX format objects are used to support viewing of structures via ChemDraw viewer. GIF images representing structures are stored in the database table as BLOB objects. The structures are either drawn manually using ChemDraw or generated automatically by structure drawing tools developed by the LIPID MAPS consortium. Based on its classification, each lipid structure in LMSD is assigned a unique 12-character LIPID MAPS identifier (LM ID). The format of the LM ID not only maintains uniqueness of ID, but also provides the capability to add new categories, classes, and

subclasses as the need arises. In addition to manual curation of biologically relevant lipids from LIPIDAT and LipidBank according to LIPID MAPS classification and structure representation schemes, LMSD also maintains their original IDs to enable cross-referencing.

### 2.3. Lipid structure representation

In addition to having rules for lipid classification and nomenclature, it is important to establish clear guidelines for drawing lipid structures. These guidelines are a prerequisite for any useful lipid molecular database in terms of consistent molecular structure presentation. Large and complex lipids are difficult to draw, which leads to the use of shorthand and unique formats that often generate more confusion than clarity among lipid researchers. The LIPID MAPS consortium has chosen a consistent format for representing lipid structures where, in the simplest case of the fatty acid derivatives, the acid group (or equivalent) is drawn on the right and the hydrophobic hydrocarbon chain is on the left (Fig. 11.1). For fatty acids and derivatives, the acid group or its equivalent is drawn on the right side and the

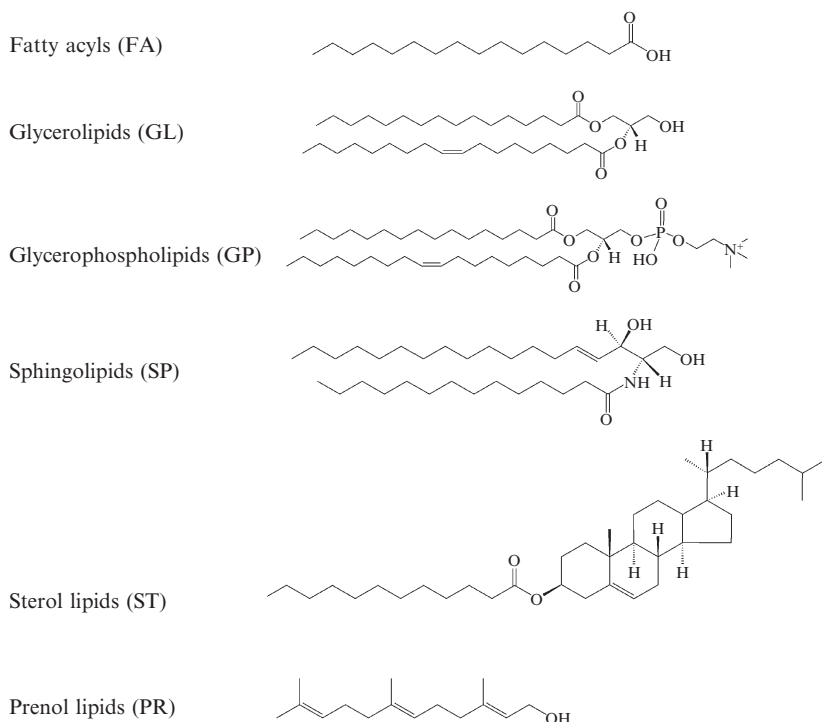


**Figure 11.1** Consistent format for representing lipid structures.



hydrophobic chain on the left, except for the eicosanoid class, in which the hydrocarbon chain wraps around in a counter clockwise fashion to produce a more compact structure. For glycerolipids and glycerophospholipids, the radyl hydrocarbon chains are drawn to the left; the glycerol group is drawn horizontally with stereochemistry defined at *sn* carbons; the headgroups for glycerophospholipids are depicted on the right. For sphingolipids, the C1 hydroxyl group of the long-chain base is placed on the right and the alkyl portion on the left; the headgroup of sphingolipids ends up on the right. The linear prenols and isoprenoids are drawn like fatty acids, with the terminal functional groups on the right. Several structurally complex lipids—acylamino sugar glycans, polycyclic isoprenoids, and polyketides—cannot be drawn using these simple rules. Rather, these structures are drawn using commonly accepted representations. This approach, adopted by the LIPID MAPS consortium, has the potential to standardize drawings of lipids and eliminate ambiguity in structural representations to a reasonable extent.

### 3. LIPID-ASSOCIATED PROTEIN/GENE DATABASES

#### 3.1. LIPID MAPS genome/proteome database

Although the public domain EntrezGene and UniProt databases contain sequences and annotations for most of the known lipid-associated genes and proteins, no unique gene and protein database of lipid-associated proteins contains comprehensive summary- and context-dependent annotation of these molecules. In order to fill this void, the LIPID MAPS Proteome Database (LMPD) was developed to provide a catalog of genes and proteins involved in lipid metabolism and signaling. The initial release of LMPD establishes a framework for creating a lipid-associated protein list, collecting relevant annotations, databasing this information, and providing a user interface. The LMPD is an object-relational database of lipid-associated protein sequences and annotations (Cotter *et al.*, 2006). The current version contains approximately 3000 records, representing human and mouse proteins involved in lipid metabolism and signaling. A new release, which is currently undergoing extensive curation, is planned for spring of 2007 with substantially more records. Users may search LMPD by database ID or keyword, and filter by species and/or lipid class associations. From the search results, one can then access a compilation of data relevant to each protein of interest, cross-linked to external databases. LMPD is publicly available from the LIPID MAPS consortium website (<http://www.lipidmaps.org/data/proteome/index.cgi>).

### 3.2. Extracting lipid genes and proteins from databases and legacy knowledge

In order to populate the LMPD, a list of lipid-related GO (Gene Ontology, <http://www.geneontology.org>) (Harris *et al.*, 2004) terms and KEGG (Kanehisa and Goto, 2000) pathway data was compiled, using lipid-specific keywords, such as trivial names of classes, subclasses, and individual lipid compounds (Fig. 11.2). In the new release, the list of lipid-specific keywords was expanded, and, in addition to GO and KEGG terms, the description field of UniProt records and the EntrezGene names were scanned (for human and mouse species). The UniProt (Apweiler *et al.*, 2004) proteins annotated with those terms were then collected, and these proteins were classified (based on their substrates/products or interactions) according to the lipid classification scheme previously described. Annotations are organized by category: record overview, Gene/GO/KEGG Information, UniProt annotations, related proteins, and experimental data. The record overview contains LMPD\_ID, species, description, gene symbols, lipid categories, EC number, molecular weight, sequence length, and protein sequence. Gene information includes EntrezGene ID, chromosome, map location, primary name, primary symbol, and alternate names and symbols; GO IDs and descriptions; and KEGG pathway IDs and descriptions. UniProt annotations include primary accession number, entry name, and comments, such as catalytic activity, enzyme

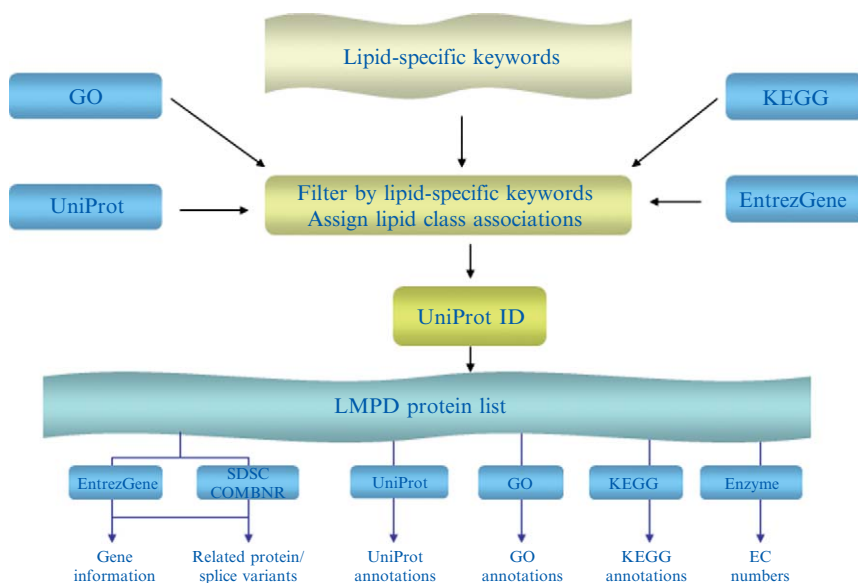


**Figure 11.2** Overview of the LIPID MAPS Proteome Database (LMPD).

regulation, function, and similarity. Efforts are underway to curate the current database of lipid-associated genes/proteins by (1) selecting entries with annotations from multiple sources (GO, UniProt, KEGG, EntrezGene), (2) ruling out entries whose annotations consist only of similarity-based terms (“like,” “similar to,” “hypothetical,” etc.), (3) conducting PubMed and other literature searches, and (4) consulting with experts in the lipidomics field. The resulting “high-confidence” set of lipid-associated genes/proteins will be useful as sources of information for interfacing with studies on lipid-related pathways and networks.

## 4. TOOLS FOR LIPIDOMICS

### 4.1. LIPID MAPS website and user interface

In an effort to increase public awareness of lipidomics research and resources, the LIPID MAPS consortium has developed a website (<http://www.lipidmaps.org>) that provides a comprehensive introduction and description of the project, a set of databases and online query interfaces pertinent to lipids, access to a wide range of experimental data relating to lipids, and a collection of analysis tools for lipid-related molecules. In addition to providing background information about the goals of the LIPID MAPS project, participants, and literature references, the website (Fig. 11.3) is divided into three main sections:

1. **Data:** Interfaces to lipid and gene/protein databases, lipid classification system, lipid standards, experimental lipid time-course data, and gene-array data.
2. **Tools:** Interfaces to lipidomics tools, such as drawing programs and mass spectrometry (MS) prediction tools
3. **Protocols:** Information on procedures and protocols relating to lipidomic research

A good example of the type of online browsing and querying capability of the website is provided by the interface to the LMSD. The LMSD browsing page provides multiple search formats, including the capability to retrieve lipids based on the LIPID MAPS classification scheme. After the user selects one of the main categories of lipids, a listing of all lipids present in the selected category, along with a link to the set of lipids in each main class and subclass, is provided. The user may then select all lipids that belong to either a main class or a subclass and display the results as a result summary page. In the case of lipids containing multiple functional groups, assignment of a structure to a particular subclass may be somewhat subjective. For example, a fatty acid containing both epoxy and hydroxy groups could be assigned to either epoxy or hydroxy

The screenshot shows the LIPID MAPS website interface. The main header includes the site logo and navigation links: Contact, News, Publications, Site Map. Below this is a secondary navigation bar with About, Data, Tools, Protocols, and Home. The page is divided into several sections:

- Lipid Classification Scheme:** Lists categories such as Fatty Acyls, Glycerolipids, Glycerophospholipids, Sphingolipids, Sterol Lipids, Prenol Lipids, Saccharolipids, and Polyketides.
- Publications:** Features two articles, including one on arachidonate-derived dihomoprostaglandin production and another on quantification of diacylglycerol species.
- LIPID MAPS Highlights:** The central section, titled "LIPID MAPS Structure Database (LMSD)", states it contains over 10,000 records. It features a "Sample record" for PGD2, showing its chemical structure and a table of properties:
 


LM ID	LMFA03010004
Common Name	PGD2
Systematic Name	9S,15S-dihydroxy-11-oxo-5Z,13E-prostadienoic acid
Exact Mass	352.22
Formula	C <sub>20</sub> H <sub>32</sub> O <sub>2</sub>
Category	Fatty Acyls [FA]
Main Class	Eicosanoids [FA03]
Sub Class	Prostaglandins [FA0301]
LIPIDBANK ID	XPR1301
Synonyms	-
- Lipid Search:** A search box with a "Submit" button and a link to "Advanced Search".
- News:** A section with RSS and XML feeds, containing three news items dated 01/11/07 and 01/10/07 regarding LMSD updates and interface improvements.

Figure 11.3 LIPID MAPS public website (<http://www.lipidmaps.org>).

fatty acids subclass. To address this situation, an ontology-based search is also provided. The user may choose to search for lipids containing similar functionality, and all the lipids with the specified functionality, irrespective of their subclass designation, will be retrieved.

The text-based query page (Fig. 11.4) allows the user to search LMSD by any combination of the following data fields: LM ID, common or systematic name, mass along with a tolerance value, formula, category, main class, and subclass. Selecting a category from the category drop-down menu causes the corresponding set of main classes to appear in the main class drop-down menu. Selecting a main class then shows the corresponding set of subclasses in the subclass menu.

The structure-based query page provides the capability to search LMSD by performing a substructure or exact match using the structure drawn by the user. Supported structure drawing tools are Chemdraw, MarvinSketch


**LIPID Metabolites And Pathways Strategy**

[About](#) | [Data](#) | [Tools](#) | [Protocols](#) | [Home](#)  
[Lipid Classification Scheme](#) | [Component Databases](#) | [Experimental Results](#)

### Structure Database (LMSD)

#### Browse

By [Lipid Classification](#)

- [Fatty Acyls](#)
- [Glycerolipids](#)
- [Glycerophospholipids](#)
- [Sphingolipids](#)
- [Sterol Lipids](#)
- [Prenol Lipids](#)
- [Saccharolipids](#)
- [Polyketides](#)

[All Lipids](#)

#### Search

[Text-based Search](#)

Search by LIPID MAPS ID, Systematic Common Name, Mass, Formula, Class, and Sub Class

[Structure-based Search](#)

Search by substructure or exact one of these structure drawing

- [MarvinSketch Applet](#)
- [JME Applet](#)

#### Text-Based Search

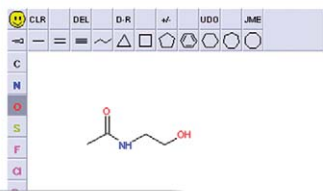
LM ID:

Name (Common or Systematic):

Mass:

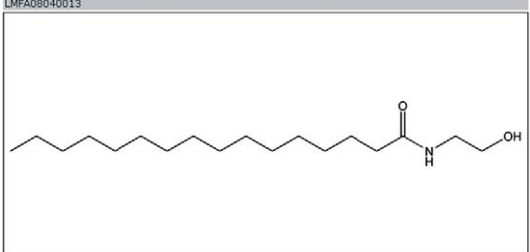
Formula:

#### Structure-Based Search using JME



Category: Fatty Acyls [FA]  
 --> Main class: Fatty amides [FA08] --> Sub class: N-acyl ethanol. [Search for other lipids in different subclasses with this functional](#)

LM_ID	Common Name	Systematic Name
<a href="#">LMFA08040001</a>	Arachidonoyl-EA	N-(5Z,8Z,11Z,14Z-eicosatetraenoyl)-ethanolamine
<a href="#">LMFA08040002</a>		
<a href="#">LMFA08040003</a>		
<a href="#">LMFA08040004</a>		
<a href="#">LMFA08040005</a>		
<a href="#">LMFA08040006</a>		
<a href="#">LMFA08040007</a>		
<a href="#">LMFA08040008</a>		
<a href="#">LMFA08040009</a>		
<a href="#">LMFA08040010</a>		



LM ID: LMFA08040013  
 Common Name: Anandamide (16:0)  
 Systematic Name: N-hexadecyl-ethanolamine  
 Exact Mass: 299.28  
 Formula: C<sub>16</sub>H<sub>37</sub>NO<sub>2</sub>  
 Formula: C<sub>16</sub>H<sub>37</sub>NO<sub>2</sub>  
 Category: [Fatty Acyls \[FA\]](#) [View lipid standards](#)  
 Main Class: [Fatty amides \[FA08\]](#)  
 Sub Class: [N-acyl ethanolamides \(endocannabinoids\) \[FA0804\]](#)  
 LIPIDBANK ID: [XPR7013](#)  
 Synonyms: Palmitoyl ethanolamide; palmitoylethanolamide  
 PubChem Substance ID (SID): [7850592](#)  
 Status: Active  
 SphingoMap ID: (n.a.)  
 View Structure using [MarvinView Applet](#) [JmolApplet](#) [ChemDraw](#) (?)

**Figure 11.4** Online interfaces for searching the LIPID MAPS Structure Database (LMSD).

([www.chemaxon.com/marvin/](http://www.chemaxon.com/marvin/)), and JME ([www.molinspiration.com/jme/index.html](http://www.molinspiration.com/jme/index.html)). The latter two structure drawing tools are Java applets and require only applet support in the browser. In addition to structure, the user can also specify an LM ID or a common or systematic name for the search.

The results summary page displays a table containing all the lipids matching specified search criteria. The results table contains the following columns for text-based and structure-based queries: LM ID, common name, systematic name, main class, subclass, and exact mass. The record details page, in addition to displaying the structure for the selected lipid, also contains the following data fields: LM ID, common name, systematic name, formula, category, main class, subclass, synonyms, and status. Appropriate links to other external databases and collections, such as LipidBank, KEGG, LIPIDAT, PubChem, and SphingoMap, are also provided, where applicable.

The default page uses a GIF image for representing the structure of the lipid. The following additional structure viewing tools are also supported: MarvinView, ([www.chemaxon.com/products.html](http://www.chemaxon.com/products.html)), Jmol (<http://jmol.sourceforge.net/>), and ChemDraw.ActiveX/Plugin Viewer ([www.cambridgesoft.com/software/ChemDraw/](http://www.cambridgesoft.com/software/ChemDraw/)). LIPID MAPS lipid structures are now available on NCBI's PubChem website, where they have been assigned PubChem Substance ID's. LMSD lipid structures are deposited into the PubChem database (<http://pubchem.ncbi.nlm.nih.gov/>) periodically, and a link to PubChem Substance ID (SID) is also maintained within LMSD. All the deposited LIPID MAPS lipids on the PubChem website have hyperlinks back to the LIPID MAPS site. The entire LMSD dataset is now available for download in SD file format from the LIPID MAPS website at <http://www.lipidmaps.org/data/structure/index.html>.

The online interface (Fig. 11.5) to LMPD also has multiple browsing/query formats. The default query form allows the user to browse the protein list with the ability to browse by associated lipid category. The "Advanced Search" query form provides choices for conducting a more focused search, including options to search by database ID or keyword and to filter by species and/or lipid class association. Database ID fields searched include UniProt accession, UniProt entry name, gene symbols, GenBank GI, EC number, GO ID, and KEGG pathway ID. Keyword search fields include UniProt description and Swiss-Prot comments. The results summary page presents a sortable list of proteins matching the query criteria, along with selected summary information, including LMPD\_ID, accession, protein name, protein symbol, and associated lipid categories. From the summary page, the user may display complete LMPD annotations for each protein. For each record selected from the results summary, all LMPD data relevant to that protein are displayed, with external database IDs linked to their respective resources. Annotations are organized by category: record overview, Gene/GO/KEGG information, UniProt annotations, and related proteins. The record overview contains LMPD\_ID, species, description, gene symbols, lipid categories, EC number, molecular weight, sequence length, and protein sequence. Gene information includes EntrezGene ID, chromosome, map location, primary name, primary symbol, and alternate names and symbols; GO IDs and descriptions; and KEGG pathway IDs and descriptions. UniProt annotations include primary

The screenshot displays the LIPID MAPS Proteome Database (LMPD) interface. On the left, there is an 'Advanced Search' sidebar with options for searching by Database ID, Keyword, Case sensitivity, and protein inclusion (Fatty acids, glycerolipid, glycerophospholipid). The main area shows a search result for 'Dgke diacylglycerol kinase, epsilon [Mus musculus]' with a table of records. A 'Record Overview' for LMP000009 is shown, including taxonomy (Mus musculus), description (Diacylglycerol kinase), symbols (Dgke), lipid category (Glyceroacylphospholipid), EC number (2.7.1.10), molecular weight (636), sequence length (564), and sequence (MEEG...). A 'Record Overview' for LMP000009 is also visible, showing details for the gene 'Dgke diacylglycerol kinase, epsilon [Mus musculus]' with GeneID: 56077 and an official symbol 'Dgke'.

**Figure 11.5** Online interface to LIPID MAPS Proteome Database (LMPD) at the LIPID MAPS website.

accession number, entry name, and comments, such as catalytic activity, enzyme regulation, function, and similarity.

#### 4.2. Tools for automated drawing and naming of lipids

In addition to having rules for lipid classification and nomenclature, it is important to establish clear guidelines for drawing lipid structures. Large and complex lipids are difficult to draw, which leads to the use of many unique formats that often generate more confusion than clarity among the lipid research community. For example, the use of SMILES (Simplified Molecular Input Line Entry System) strings to represent lipid structures, while being very compact and accurate in terms of bond connectivity, valence, and chirality, causes problems when the structure is rendered. This is due to the fact that the SMILES format does not include two-dimensional (2D) coordinates. Therefore, the orientation of the structure is arbitrary, making

visual recognition and comparison of related structures much more difficult. Additionally, the structure drawing step is typically the most time-consuming process in creating molecular databases of lipids; however, many classes of lipids lend themselves well as targets for automated structure drawing due to their consistent 2D layout. A suite of structure-drawing tools has been developed and deployed that dramatically increases the efficiency of data entry into lipid-structure databases and permits “on-demand” structure generation in conjunction with a variety of MS-based informatics tools. Online versions of the structure drawing tools for fatty acyls, glycerolipids, glycerophospholipids, sphingolipids, and sterols are available in the “Tools” section of the LIPID MAPS website. Current versions of this software are now capable of drawing chiral centers and ring structures. In addition, a set of standalone drawing tools, written in Perl, are available for download from the LIPID MAPS website (Fig. 11.6) (<http://www.lipidmaps.org/tools/>).

Concurrently, a generalized lipid abbreviation format has been developed that enables structures, systematic names, and ontologies to be

Create a Glycerophospholipid Structure

Choose acyl chains and headgroup from menus below:

sn1-Acyl group 16:0		headgroup GPCho
------------------------	--	--------------------

Submit Reset

**Systematic Name** 1-hexadecanoyl-2-tetradecanoyl-*sn*-glycero-3-phosphocholine  
**Abbreviation** GPCho(16:0/14:0)

Display Structure using Chemdraw

Figure 11.6 Online structure-drawing tool for sphingolipids.



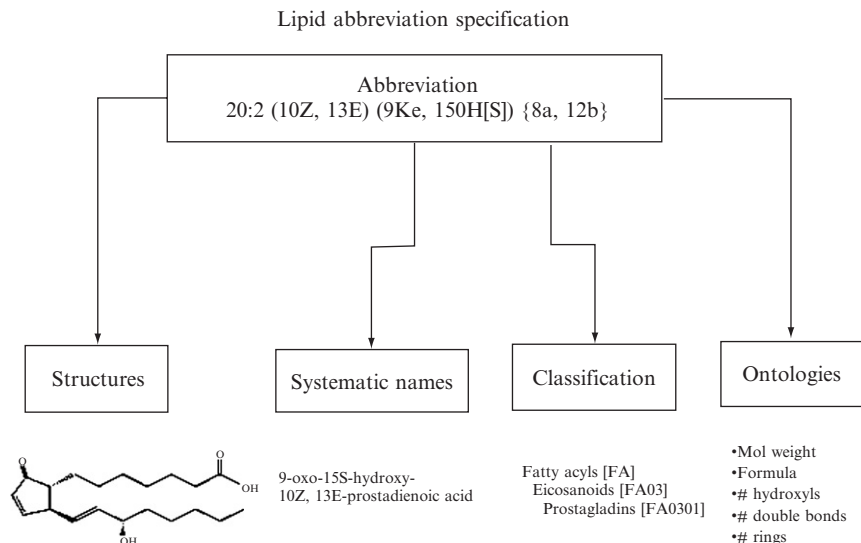


**Figure 11.7** Flowchart showing structure/name/ontology generation from abbreviation.

generated automatically from a single source format (Fig. 11.7). Lipid structure, nomenclature, classification, and ontology creation may be performed computationally, using well-defined, unique abbreviations as a starting point. Figure 11.7 demonstrates the conversion of a text abbreviation for a bile acid into a dataset containing structure (Molfile), systematic name, classification, and various molecular attributes, such as formula, molecular weight, number of functional groups, double bonds, and rings.

### 4.3. Tools for prediction of lipid mass spectra

Certain classes of lipids, such as acylglycerols and phospholipids, composed of an invariant core (glycerol and headgroups) and one or more acyl/alkyl substituents are good candidates for MS computational analysis since they fragment more predictably in electrospray ionization mass spectrometry (ESI-MS), leading to loss of acyl side-chains, neutral loss of fatty acids, and loss of water and other diagnostic ions depending on the phospholipid headgroup (Murphy *et al.*, 2001). It is possible to create a virtual database of permutations of the more common side chains for glycerolipids and glycerophospholipids and to calculate “high-probability” product ion candidates in order to compare experimental data with predicted spectra. The LIPID MAPS group has developed a suite of search tools allowing the user to

enter a mass-to-charge ( $m/z$ ) value of interest and view a list of matching structure candidates, along with a list of calculated neutral-loss ions and “high-probability” product ions. These search interfaces have been integrated with structure-drawing and isotopic-distribution tools (Fig. 11.8).

Currently, MS prediction tools (<http://www.lipidmaps.org/tools/>) for three different categories of lipids (glycerolipids, cardiolipins, and glycerophospholipids) can be found online. In each case, all possible structures corresponding to a list of likely headgroups and acyl, alkyl-ether, and vinyl-ether chains were expanded and enumerated by computational methods to generate a table containing the nominal and exact mass for each discrete structure as well as additional ontological information, such as formula, abbreviation, and numbers of chain carbons and double bonds. This tabular data was then uploaded into category-specific database tables, making it amenable for online tools.

#### 4.4. Tools for managing lipidomic metadata

To accomplish transfer, centralized storage, sharing, and integration of “metadata” (information on experimental procedures, protocols, reagents, and resources) among LIPID MAPS member laboratories, a Laboratory Information Management System (LIMS) customized for lipidomics research has been developed. The LIPID MAPS LIMS is written in the Java programming language and is implemented as a Java Web Start program that runs on a user’s desktop computer. The modules allow users to enter information and browse the LIMS data, which is connected to a central Oracle database. The LIMS also allows tracking of laboratory materials and protocols via printed labels that may be scanned into modules using barcode readers.

The LIPID MAPS LIMS is a two-tier client-server window form-based application that, at its core, enables entry and tracking of information pertinent to lipidomics experiments. It is composed of 13 modules, selectable from a main form. The LIMS is primarily devoted to cell treatments and MS experiments, and the essential process of a simplified pattern of usage is shown in Fig. 11.9.

The LIPID MAPS LIMS is a specialized, yet powerful data tracking system for lipidomics studies. It provides functions that encompass many of the goals of systems biology, where each LIMS module represents an idealized abstraction of an experimental step performed in a laboratory and records information pertinent for that step. It provides a means of accurately associating experimental conditions and protocols (metadata) with the corresponding experimental results (data) in a multi-user, multi-center research environment.

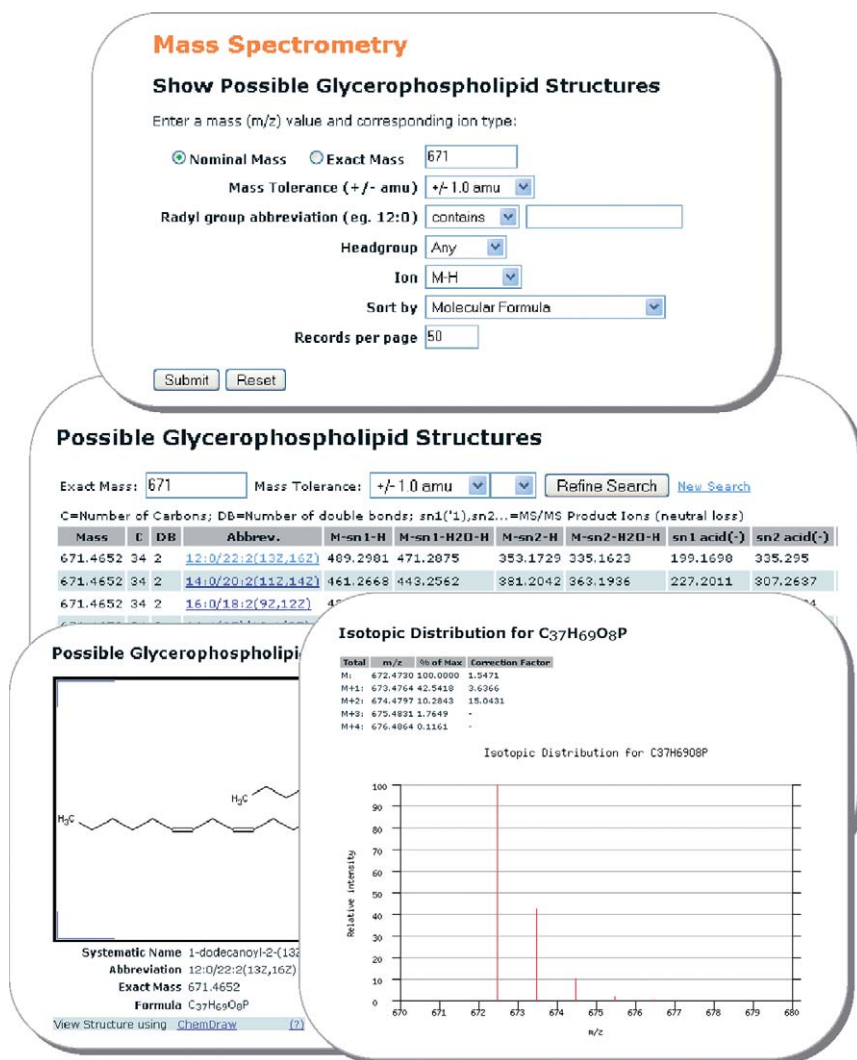


**Figure 11.8** Online utility to predict possible lipid structures from mass spectrometry (MS) data.

#### 4.5. Tools for collection, display, and analysis of experimental lipidomic data

Data analysis of lipidomics experiments represents significant challenges both in volume and complexity. Typical experiments yield component lists of lipids with quantitative content data and a catalog of interactions and networks involving lipids. A truly comprehensive “lipidomics” approach must

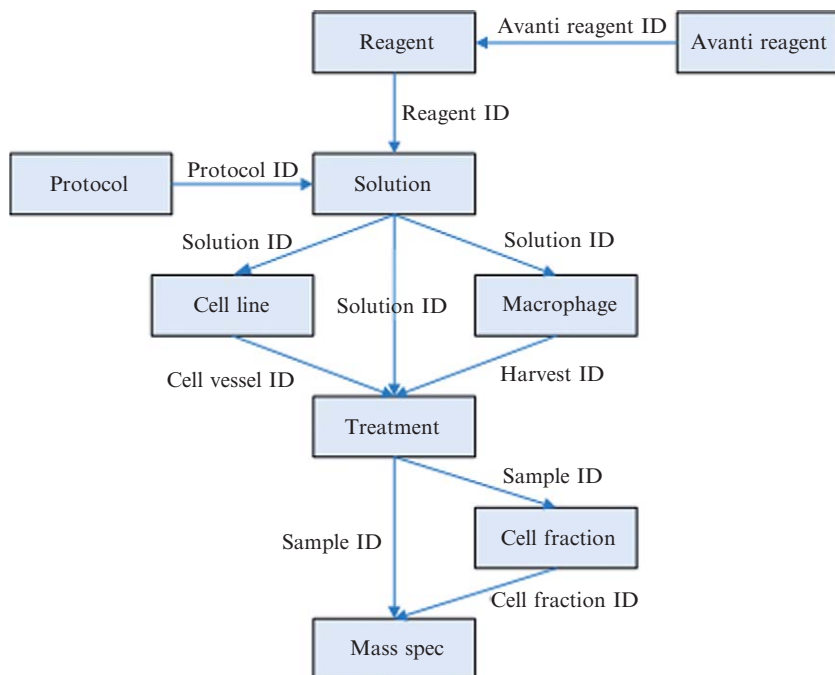


**Figure 11.9** Simplified sequential flow of Laboratory Information Management System (LIMS) usage. Rectangles represent modules of functionality as described in the text. Arrow labels indicate sets of one or more identifiers that are generated by the module at the base of the arrow and entered into the immediately following target module.

incorporate multiple separation and identification techniques, maintaining sufficient sensitivity to distinguish closely related metabolites while remaining robust enough to cope with the wide variety of heterogeneous classes of cellular lipid species. ESI-MS, with its extraordinary sensitivity and its capacity for high throughput, has become the technique of choice for the analysis of complex mixtures of lipids from biological samples. From a bioinformatics standpoint, one must record and store all the experimental conditions and protocols pertaining to a particular set of experiments (metadata) via the aforementioned LIMS, as well as the actual experimental measurements (data).

With the advent of sensitive analytical instrumentation, such as MS, it is now possible to obtain quantitative data on large numbers of lipid species under a variety of experimental conditions, allowing us to investigate time-dependent changes in lipid-associated processes in response to a variety of stimuli. For example, the LIPID MAPS consortium has embarked on a time-dependent study of a wide range of lipid classes in mouse macrophage cells in response to stimulation of the Toll-like receptor 4 (TLR4) with

Kdo<sub>2</sub>-Lipid A. This required the establishment of an informatics pipeline to convert MS experimental data into a format suitable for viewing by end-users. In this case, MS quantitative time-course measurements in heterogeneous formats on a variety of lipids over a 24-hour time-course were first converted into a common data format prior to processing and import into an Oracle database. A middleware layer composed of Apache webserver and PHP scripting was used to create a web-based user interface with the MS database data. All online data displays were integrated with the LIMS system (via sample barcodes) and the LIPID MAPS structure database, allowing seamless navigation across both data and metadata. A software drawing component was used to generate “on-demand” online graphs in response to user input. In addition, a set of online query and display tools was developed to allow the end-user to view MS time-course data in a number of different formats (Fig. 11.10). These include tabular and graphical displays of data as averages of technical and biological replicates, as well as “drill-down” links to the corresponding LIMS metadata (cell samples) and structure/classification information (analytes).

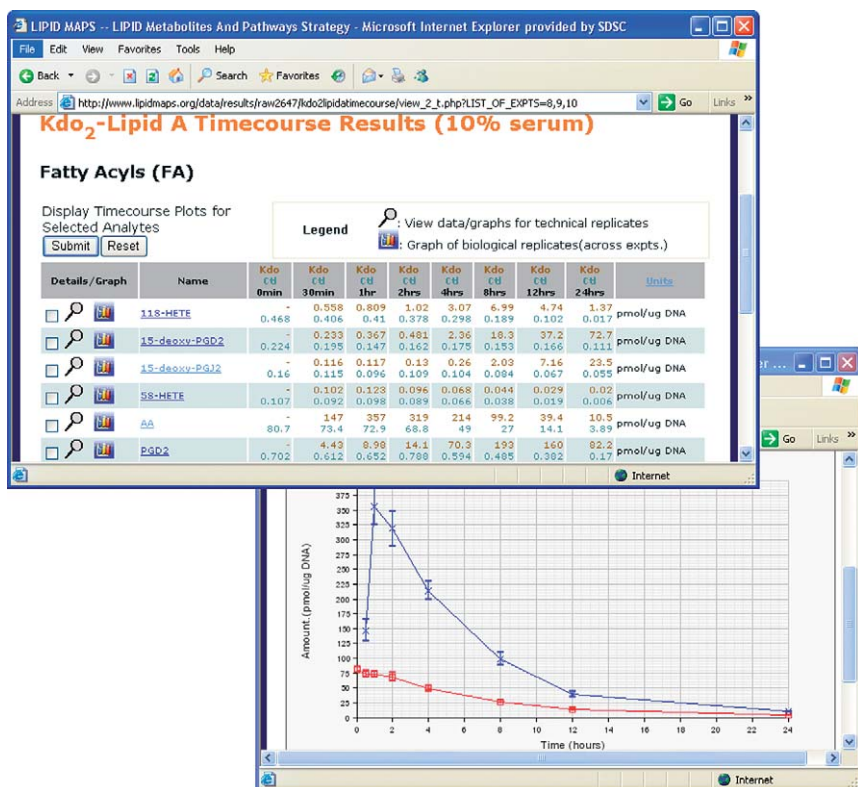


**Figure 11.10** Online interface for viewing lipidomics mass spectrometry (MS) data.

Query tools include a feature that allows the end-user to select any combination of analytes for graphing with a view to comparing time-course profiles of lipids that are part of the same biochemical or signaling pathways. Quantitative data from these experiments are being used to validate existing lipid networks and to elucidate novel interactions.

The structural heterogeneity of many classes of lipids precludes accurate and reliable prediction of MS fragmentation in tandem spectra (MS/MS) in contrast to the situation for MS interpretation of proteins, where facile cleavage of the peptide bonds has led to the development of search algorithms, which compare MS/MS fragmentation data to a list of “virtual spectra” computed from a protein database. In this situation, comparison of spectral data with libraries of lipid standards can be very informative. An online library of lipid standards, including MS/MS data generated by the LIPID MAPS core facilities, has recently been made available to the public. This database currently consists of approximately 200 analytes spanning seven lipid categories. An online search interface (Fig. 11.11) allowing end-users to search by precursor or product ion mass has also been developed.

#### 4.6. Tools for lipid profiling

With the advent of high-sensitivity liquid chromatography MS (LC-MS) systems, one increasingly utilized type of LC-MS application is differential profiling in which the extraction, LC methods, and MS instrument setup are set to provide a broad coverage of compounds in order to enable relative quantitative comparisons for individual compounds across multiple samples. The applications of such an approach can be found in domains of systems biology, functional genomics, and biomarker discovery. Within the last couple of years, a number of software packages have been developed by various companies and research groups to analyze data generated by MS profiling of metabolites, including lipids. The data processing for differential profiling usually proceeds through several stages, including input file manipulation, spectral filtering, peak detection, chromatographic alignment, normalization, visualization, and data export. Examples of metabolic profiling software are the MarkerView package (ABI) and the freely-available Java-based Mzmine (Katajamaa and Oresic, 2005) application (Turku Centre for Biotechnology, Finland). The LIPID MAPS bioinformatics group has set up the Mzmine software to run in parallel-processing, creating a high-throughput computational cluster devoted to the analysis of lipid profiling experiments of the LIPID MAPS cores.

Within the LIPID MAPS consortium, in-house software has been developed for more specific profiling tasks, such as processing and comparing control and deuterium-supplemented MS data sets from LC-MS experimental runs. This involves a stepwise process of (1) extracting data from raw MS data files, (2) integrating peaks in each scan over a user-defined mass

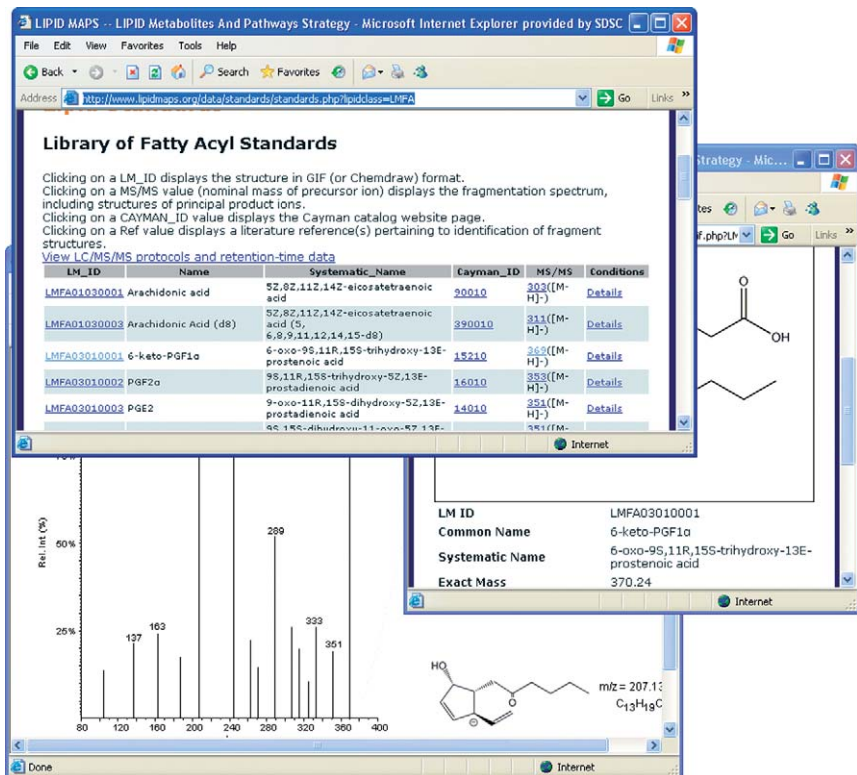


**Figure 11.11** Online interface to Lipid Standards Library and associated data.

window to generate a formatted array of quantitated data, (3) applying an algorithm to identify deuterated metabolites, (4) performing data normalization and subtractive analysis, and (5) displaying and listing peaks of interest according to user-defined criteria. This software has been utilized to investigate the biosynthesis of eicosanoids derived from arachidonic acid in RAW cells (Harkewicz *et al.*, 2007).

## 5. LIPID PATHWAYS

### 5.1. Bioinformatics resources for lipid-related pathways

Lipids play central roles in energy storage, cell membrane structure, cellular communication, and regulation of biological processes, such as inflammatory response, neuronal signal transmission, and carbohydrate metabolism.

Organizing these processes into useful, interactive pathways and networks represents a great bioinformatics challenge. The KEGG consortium maintains a collection of manually drawn pathway maps representing current knowledge on the molecular interaction and reaction networks, several of which pertain to lipids (<http://www.genome.jp/kegg/pathway.html>), including fatty acid biosynthesis and degradation, sterol metabolism, and phospholipids pathways. Additionally, the KEGG Brite (<http://www.genome.jp/kegg/brite.html>) collection of hierarchical classifications includes a section devoted to lipids where the user can select a lipid of interest and view reactions and pathways involving that molecule. A number of category-specific lipid pathways have been constructed, notably the SphinGOMAP (<http://www.sphingomap.org>), a pathway map of approximately 400 different sphingolipid and glycosphingolipid species (Sullards *et al.*, 2003), by a member of the LIPID MAPS consortium.

## 5.2. Tools for drawing pathways

LIPID MAPS has developed a comprehensive graphical pathway display, editing, and analysis program, LIPID MAPS Biopathways Workbench (LMBP), with the capability to display a variety of lipid-related entities and states, such as lipids, enzymes, genes, pathways, activation states, and experimental results. This graphical tool is tightly integrated with the underlying LIPID MAPS relational databases and will play an important role in the reconstruction of lipid networks using emerging data from LIPID MAPS core facilities and other public sources.

The central theme for LMBP data is a reaction network graph, or pathway, with chemical compounds represented as nodes, and chemical interactions represented as links, or edges, between the nodes. Numeric, text, and structured data attributes may be bound to nodes and edges, including molecule names, synonyms, locations, concentrations, charges, interaction types, molecule roles in those interactions, and so forth. For example, experimental data such as time-course measurements for a series of lipids may be displayed in graphical form in a pathway window (Fig. 11.12).

The LMBP software tools may be downloaded from the <http://www.biopathwaysworkbench.org> website. The current alpha/beta release is comprised of two components: (1) The Biopathways Workbench (BPW; a Java programming toolkit for managing pathway data) and (2) the Pathway Editor (a Java application built using the BPW). It presents a pathway drawing area, menu bar, toolbar, and operations to open, edit, and save pathways and search databases of pathways, compounds, and time-course data.

The current version contains an extensive list of metabolic pathways that have been imported from KEGG as well as tools allowing the user to create pathway diagrams from scratch.



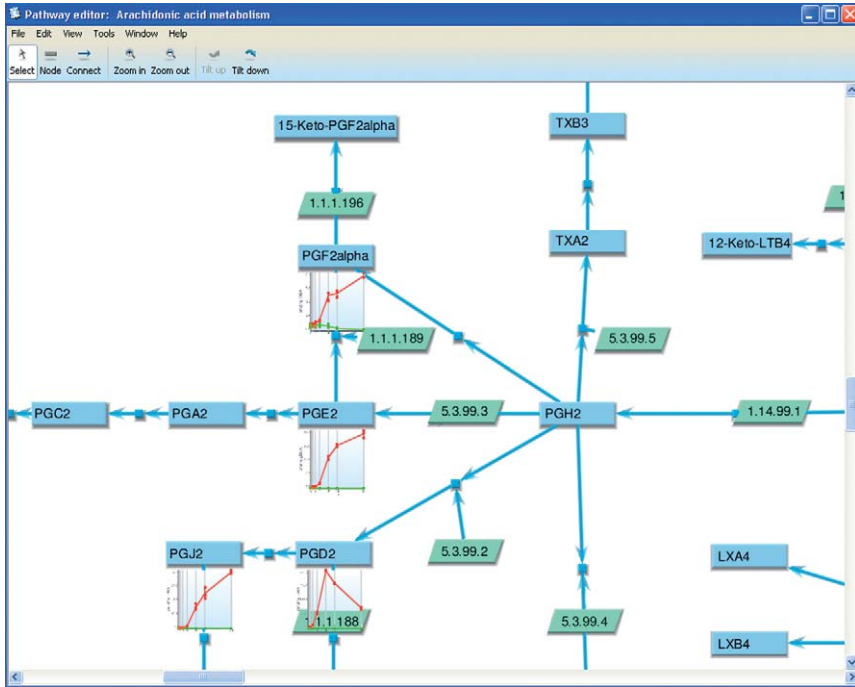


**Figure 11.12** Screenshot of the Biopathways editor showing a portion of the arachidonate pathway with overlaid timecourse data.

The freely available VANTED application (<http://vanted.ipk-gatersleben.de/>) has also been used by the bioinformatics core to import existing KEGG lipid-specific pathways, to modify and customize existing KEGG pathways, and to draw new pathways and networks. The application enables the user to import and graph experimental data from Excel templates, to store and export data-containing pathways, and to perform many types of statistical analyses on the networks.

Additionally, custom VANTED templates (Fig. 11.13) have been created in which the nodes corresponding to lipids and enzymes have been hyper-linked to the LIPID MAPS structure and protein databases, respectively, enabling a high level of integration between key bioinformatics resources.

## 6. CHALLENGES FOR FUTURE LIPID INFORMATICS

Despite the significant role of lipids in normal and disease physiology, lipidomics has not reached the same stage of advancement and knowledge as genomics and proteomics. With the advent of precise MS methods, we are

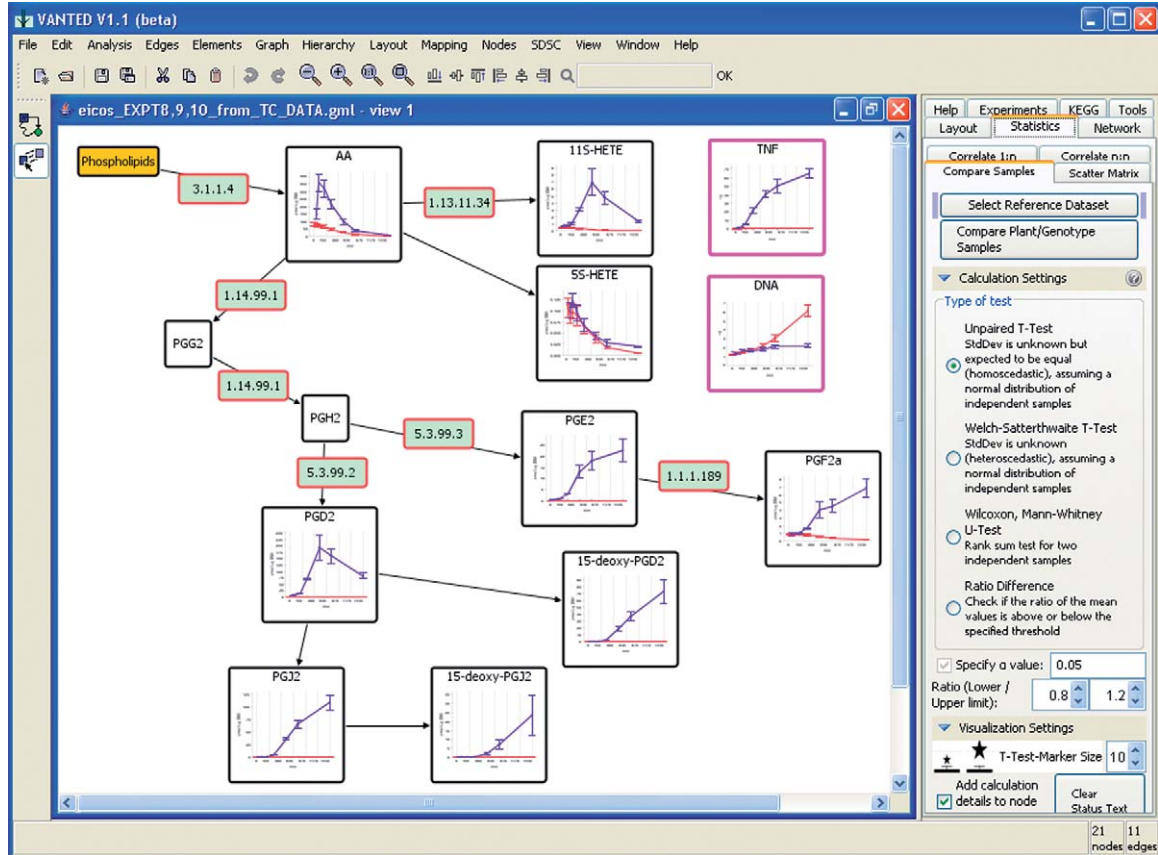


Figure 11.13 VANTED application showing arachidonate pathway and time-course data.

now in a position to measure dynamical changes in lipids in cells subject to stimulus. However, no tools are currently available that relate these changes to phenotypic changes in cellular states or physiology. The context-specific identification of lipid components, their integration with the proteome and transcriptome, and the derivation of lipid networks in normal and pathological states remain as major challenges for lipidomics. Initiatives such as LIPID MAPS are early steps in this direction.

## ACKNOWLEDGMENTS

The authors wish to express their sincere gratitude to LIPID MAPS core directors H. Alex Brown (Vanderbilt University), Christopher K. Glass (University of California, San Diego), Alfred H. Merrill Jr. (Georgia Institute of Technology), Robert C. Murphy (University of Colorado Health Sciences Center), Christian R. H. Raetz (Duke University Medical Center), David W. Russell (University of Texas Southwestern Medical Center), and LIPID MAPS principal investigator Edward A. Dennis (University of California, San Diego). This work was supported by the National Institutes of Health (NIH) National Institute of General Medical Sciences (NIGMS) Glue Grant NIH/NIGMS Grant 1 U54 GM69558.

## REFERENCES

- Apweiler, R., Bairoch, A., Wu, C. H., Barker, W. C., Boeckmann, B., Ferro, S., Gasteiger, E., Huang, H., Lopez, R., Magrane, M., Martin, M. J., Natale, D. A., *et al.* (2004). UniProt: The Universal Protein knowledgebase. *Nucleic Acids Res.* **32**, D115–D119.
- Caffrey, M., and Hogan, J. (1992). LIPIDAT: A database of lipid phase transition temperatures and enthalpy changes. DMPC data subset analysis. *Chem. Phys. Lipids* **61**, 1–109.
- Chester, M. A. (1998). IUPAC-IUB Joint Commission on Biochemical Nomenclature (JCBN). Nomenclature of glycolipids LIPIDAT: A database of lipid phase transition temperatures and enthalpy changes. *Eur. J. Biochem* **257**, 293–298. Accessed at <http://www.chem.qmul.ac.uk/iupac/misc/glylp.html>.
- Cotter, D., Maer, A., Guda, C., Saunders, B., and Subramaniam, S. (2006). LMPD: LIPID MAPS proteome database. *Nucleic Acids Res.* **34**, D507–D510.
- Fahy, E., Subramaniam, S., Brown, H. A., Glass, C. K., Merrill, A. H., Jr., Murphy, R. C., Raetz, C. R. H., Russell, D. W., Seyama, Y., Shaw, W., Shimizu, T., Spener, F., *et al.* (2005). A comprehensive classification system for lipids. *J. Lipid Res.* **46**, 839–862.
- Harkewicz, R., Fahy, E., Andreyev, A., and Dennis, E. A. (2007). Arachidonate-derived dihomoprostaglandin production observed in endotoxin-stimulated macrophage-like cells. *J. Biol. Chem.* **282**, 2899–2910.
- Harris, M. A., Clark, J., Ireland, A., Lomax, J., Ashburner, M., Foulger, R., Eilbeck, K., Lewis, S., Marshall, B., Mungall, C., *et al.* (2004). The Gene Ontology (GO) database and informatics resource. *Nucleic Acids Res.* **32**, D258–D261.
- Jorde, L. B., Little, P. F. R., Dunn, M. J., and Subramaniam, S. (2005). “Encyclopedia of Genetics, Genomics, Proteomics and Bioinformatics.” Wiley Press, Hoboken, NJ.
- Kanehisa, M., and Goto, S. (2000). KEGG: Kyoto encyclopedia of genes and genomes. *Nucleic Acids Res.* **28**, 27–30.

- Katajamaa, M., and Oresic, M. (2005). Processing methods for differential analysis of LC/MS profile data. *BMC Bioinformatics* **6**, 179.
- Murphy, R. C., Fiedler, J., and Hevko, J. (2001). Analysis of nonvolatile lipids by mass spectrometry. *Chem. Rev.* **101**, 479–526.
- Sud, M., Fahy, E., Cotter, D., Brown, A., Dennis, E. A., Glass, C. K., Merrill, A. H., Jr., Murphy, R. C., Raetz, C. R., Russell, D. W., and Subramaniam, S. (2007). LMSD: LIPID MAPS structure database. *Nucleic Acids Res.* **35**, D527–D532.
- Sullards, M. C., Wang, E., Peng, Q., and Merrill, A. H., Jr. (2003). *Cell Mol. Biol.* **49**, 789–797.
- Watanabe, K., Yasugi, E., and Ohshima, M. (2000). How to search the glycolipid data in “LipidBank for web,” the newly-developed lipid database in Japan. *Trends Glycosci. Glycotechnol.* **12**, 175–184.

# QUANTITATION AND STANDARDIZATION OF LIPID INTERNAL STANDARDS FOR MASS SPECTROSCOPY

Jeff D. Moore, William V. Caufield, *and* Walter A. Shaw

---

## Contents

1. Introduction	352
2. Lipid Handling Guidelines	352
3. Chemical Characterization of Lipid Stocks	353
4. Preparation of Working Lipid Standards	355
5. Packaging of Lipid Standards	359
6. Quality Control and Stability Testing	361
6.1. Ceramide/sphingoid base internal standard mixture	361
6.2. Triglyceride-d <sub>5</sub> internal standard mixture	363
7. Discussion	364
References	366

## Abstract

Qualification, preparation, and use of lipid compounds as analytical reference standards are daunting endeavors. The sheer vastness of the number of lipid compounds present in biological samples make it impossible to directly standardize each entity. Available lipid compounds chosen for preparation as standards are difficult to maintain as pure entities of stable concentration due to their physical and chemical interactions. The lipid chemist must understand these constraints for each chosen molecule to construct a standard material, which provides accurate measurement for a practical length of time. We provide methods and guidelines to aid the chemist in these endeavors. These aids include analytical methods for preparation and handling techniques, qualification of candidate materials, packaging, storage, and, finally, stability testing of working standard materials. All information will be provided under the purview of standardization of lipid analysis by mass spectrometry.

## 1. INTRODUCTION

Lipids function as essential and abundant building blocks of cells and their organelles, neurological second messengers, nutrients, hormones, protein modifiers, and substrates of enzymes, to name a few, and are implicated in many disease processes. They are available from numerous sources and exist in such heterogeneity of structure that they are classified according to molecular functional group similarities, degree of polarity, or biological origin. However, few sources of chemically pure and structurally characterized lipid reference standards exist. None are available for major lipid classes through certified sources, such as the United States Pharmacopoeia, National Formulary, or National Institute of Technology and Standards, nor from international agencies. This is largely due to the difficulty in purifying lipid mixtures from natural sources or synthetically manufacturing sufficient and stable quantities, which are of a single molecular entity. Of those available, they are typically of simple structure, not characterized by modern analytical methods, and generally do not represent lipid structures of current scientific interest. Chemical stability and, therefore, constant concentration is a major concern for any standard material. This is more so for reference standards of lipid molecules due to their reactivity with light, air, moisture, and active surfaces to produce oxidation, hydrolysis, and decomposition. The researcher must locate a source that provides standards for their interests or must qualify available materials as suitable for use as reference standards. The intended final use of these materials as standards for calibration of mass spectrometry techniques dictates a multiple methodology approach to ensure chemical identity and purity. Once chemically characterized, they should be packaged and stored in containers that achieve the best stability for extended use. And lastly, these packaged standards require testing over time to document their continued structural and concentration integrity. Before discussion of analytical procedures, a general overview of handling lipid materials for prevention of avoidable and commonly encountered problems is necessary.

## 2. LIPID HANDLING GUIDELINES

Lipids, by definition, are soluble in organic solvents, such as chloroform and methanol, but only sparingly soluble, if at all, in water. Ideally, lipid compounds should be stored in glass containers at relatively high concentration ( $mM$  to  $M$ ). Optimal storage conditions will include the absence of light and temperatures below  $-15^{\circ}$ . Lipid materials removed from storage should be allowed to reach room temperature before opening for use. This prevents weighing and delivery errors due to changes in

density per temperature or evaporation of solvents from solutions. Stock lipid solutions should always be prepared in high quality and fresh solvents of low water content. Organic solvent solutions of lipids should be stored in glass only, as plastics and polymers dissolve and contaminate the lipid solution (Pidgeon *et al.*, 1989). Glass closures and lids that have plastic or rubber cemented into their top should be avoided as well. Closures that have Teflon<sup>TM</sup> welded into their top are recommended. This contamination is also observed to a lesser extent when lipid solutions are transferred with plastic or polymer pipette tips commonly used in the laboratory. Lipid solutions should be transferred with glass pipettes, glass syringes, or auto-pipettors with Teflon and glass surfaces when the possibility of contamination must be completely avoided. Saturated lipids, which contain no double bonds in their structure, generally produce free-flowing powders amenable to direct handling and weighing. However, extended exposure to air will hydrate many saturated phospholipids. Phosphatidylcholine compounds are a prime example of this through addition of water to the phosphocholine headgroup to a maximum of 4 to 8% water. This hydration contributes to hydrolysis of fatty acids from the glycerol backbone producing “lyso”-phosphatidylcholine and free fatty acid. Atmospheric hydration of monounsaturated and polyunsaturated lipids produce materials that are difficult to accurately weigh. They initially become “sticky,” preventing quantitative transfer of weighed amounts, and progressively absorb moisture to a “waxy” appearance when extremely wet. If unsaturated lipids must be handled as solids, use of a dry box should be employed. This atmospheric exposure also introduces oxygen contact with the double bonds of the lipid. Oxidation of unsaturated lipids form peroxides, epoxides, and aldehydes at their double bond positions. The physical appearance of a poor quality or contaminated unsaturated lipid is a waxy yellow substance. It is for these reasons many researchers store lipid stocks with a blanket of inert gas, such as argon or nitrogen, in the head space of containers.

Standards for mass spectrometry are typically very low in final concentrations in the range of  $\mu\text{M}$  to  $\text{nM}$ . Researchers usually obtain excess materials for standard preparation, which are easily handled and weighed by conventional glassware and balances. Therefore, making concentrated stock solutions for chemical characterization and further dilution to working solutions is a practical way to handle and preserve the purity of the lipid for extended future use.

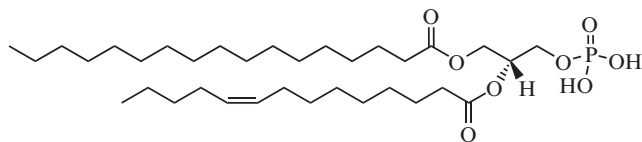
### 3. CHEMICAL CHARACTERIZATION OF LIPID STOCKS

The absence of existing reference materials for comparative analysis dictates sufficient chemical analysis to verify theoretical structure and purity. The analytical techniques to evaluate these aspects include well-established

and reported methods of lipid analysis, such as thin-layer chromatography, high performance liquid chromatography, gas chromatography, nuclear magnetic resonance, ultraviolet (UV) spectrophotometry, and atomic absorption. Stock solutions should have concentration determination by an empirical method such as phosphorus and nitrogen content or fatty acid content by gas chromatography. These techniques are essential and should not be omitted. Furthermore, focus on the use of mass spectrometry to evaluate lipids as standards should be initiated only after these techniques have provided satisfactory data.

The nonvolatile nature of most lipids requires them to be assayed by mass spectrometers, which have a liquid interface. Simply described, the lipid compound in solution must be liberated from the solvent phase into the gas phase, which is amenable to ion resolution by the mass spectrometer. Our work has been performed on an API 4000 QTRAP<sup>TM</sup> (Applied Biosystems), a hybrid, triple-quadrupole, linear ion trap mass spectrometer coupled with a Turbospray<sup>TM</sup> liquid interface. This interface introduces the lipid molecules to the mass spectrometer source and produces positive and negative ions. Initial qualitative identification is performed by infusing a dilute solution on the order of 1 to 10  $\mu\text{g}/\text{ml}$  of the compound into the mass spectrometer with a syringe pump at 5 to 20  $\mu\text{l}/\text{min}$  and scanning a molecular weight range suitable to detect the exact mass of its positive or negative ion and possible contaminants and degradants. While this is simple in principle, it is complex in practice. Different lipid classes ionize preferentially to positive or negative ions according to individual molecular structure, solvent system, and mass spectrometer instrument settings. The desired scan spectrum, which contains only simple adducts of the lipid's exact mass, is achieved through trial- and-error adjustments of the mass spectrometers ion source settings. Detection of masses that correspond to related degradation products can often be due to in-source fragmentation of the compound and should not be interpreted immediately as contaminants. Intensity comparison of these ions relative to their precursor over a range of instrument settings often helps determine the ions' origin. One must keep in mind that these scanning experiments are solely for qualitative purposes. Only subjective estimates to the degree of contamination should be assigned from mass spectral scan data. Second, the linear ion trap (LIT) is utilized to confirm the exact mass and isotopic ratios as compared to the theoretical molecular formula of the compound. The LIT's mass accuracy is not on the order of some other mass spectrometer designs, such as time of flight, but is reasonably used for this purpose to one decimal place accuracy for singly charged molecules. The LIT should be programmed to achieve full 0.5 to 1.0 u resolution and scanned over a mass range of  $M \pm 5$  to 10 u for comparison of isotopic ratios. Finally, the compound should be analyzed to provide fragmentation data that coincides to its theoretical structure. This is performed with triple quadrupole experiments through mass selection of the exact mass molecular ion and collision-activated





Chemical formula:  $C_{34}H_{65}O_8P$

Exact mass: 632.44

Molecular weight: 632.85

**Figure 14.1** Structure of 1-heptadecanoyl-2-(9Z-tetradecenoyl)-sn-glycerol-3-phosphate (17:0-14:1 GPA).

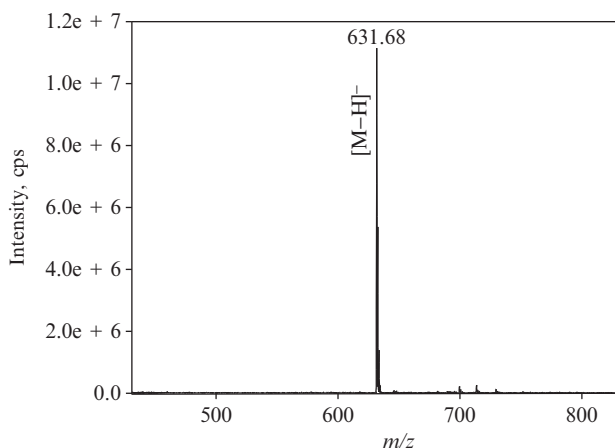


**Figure 14.2** Flow infusion of 10  $\mu\text{g}/\text{ml}$  of 17:0 to 14:1 GPA at 10  $\mu\text{l}/\text{min}$ . Scan used a linear ion trap (LIT) detector  $[M-H]^- = 631.7$  u.

dissociation with inert gas and energy to form structurally related fragment ions of the precursor molecule. This collision pattern can be interpreted and is often conformational among lipid classes. (Murphy *et al.*, 2001). Figures 14.1 to 14.4 demonstrate the qualitative mass spectrometry experiments for 1-heptadecanoyl-2-(9Z-tetradecenoyl)-sn-glycero-3-phosphate(17:0-14:1 GPA).

## 4. PREPARATION OF WORKING LIPID STANDARDS

Upon satisfactory qualification of molecular structure, purity, and concentration through requisite analytical methods and mass spectrometry, the stock molecule must be diluted to a working concentration practical for direct use in quantitative mass spectrometry methods. Here is where special

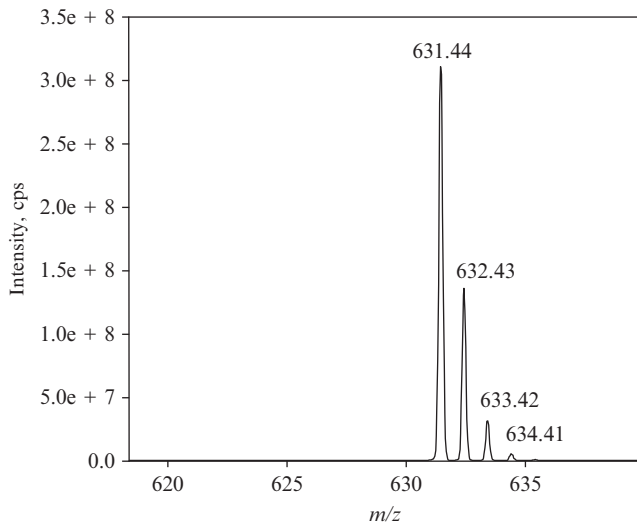


**Figure 14.3** Enhanced resolution of 10  $\mu\text{g/ml}$  of 17:0–14:1 GPA using linear ion trap (LIT). Exact mass = 632.44,  $[\text{M}-\text{H}]^- = 631.44$ . Isotopic distribution consistent with  $[\text{M}-\text{H}]^-$  formula of  $\text{C}_{34}\text{H}_{65}\text{O}_8\text{P}^-$ .

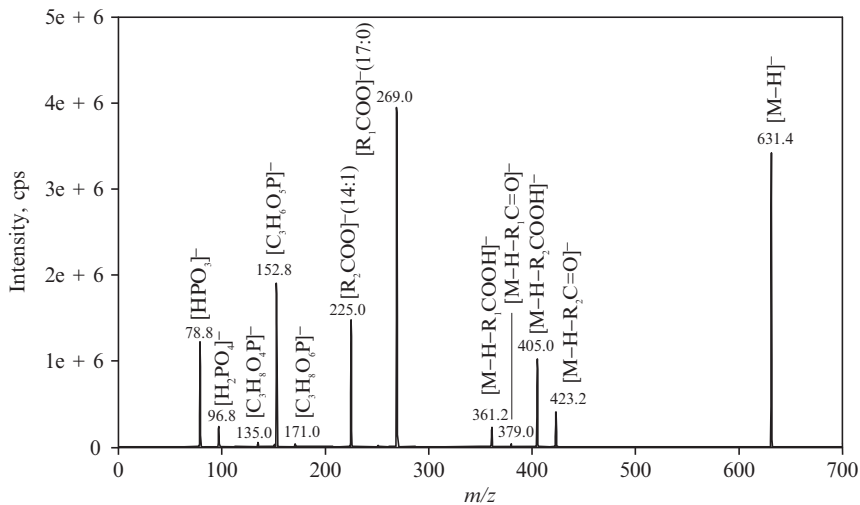


**Figure 14.4** Fragmentation of 631.56 (CE =  $-55$  eV) provides molecular structure confirmation.

attention should be given to issues of solvent integrity, solubility, and surface interactions for the working solutions. Solvents used for final preparation should be of the highest quality and recent manufacture. We routinely use high performance liquid chromatography (HPLC)–grade solvents

for all lipid standards. Decomposition of aged chloroform to phosgene and hydrochloric acid will immediately destroy lipid compounds at low concentration. We have found that minor contaminants from impure solvents form adducts with polar lipids under certain conditions. An HPLC-grade methanol containing 0.004% formaldehyde produced a corresponding Schiff's base analog in a 10  $\mu\text{g}/\text{ml}$  solution of 1-heptadecanoyl-2-(5Z,8Z,11Z,14Z-eicosatetraenoyl)-sn-glycero-3-phosphoethanolamine (17:0-20:4 GPEtn) in a packaged ampoule upon flame sealing at room temperature, as seen in Fig. 14.5. Reformulation with the same source of methanol containing 0.002% formaldehyde along with pre-cooling the solution on dry ice prior to flame sealing reduced the Schiff's base below detection. We routinely filter methanol as a lipid standard diluent through 0.45- $\mu\text{m}$  filters to remove particulates followed by helium sparging to diminish oxygen content and, thus, the extent of lipid oxidation. We discovered that filtering solvents as polar as methanol dissolved nylon filters. Nylon 6.6 was introduced into final lipid solutions, as shown in Fig. 14.6. The use of PTFE filters is recommended.

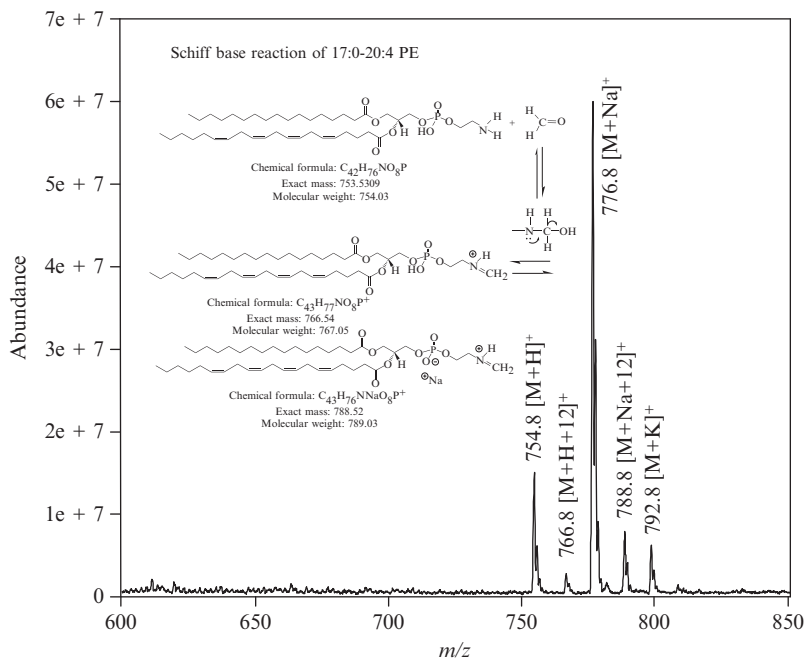


**Figure 14.5** Presence of Schiff's base adduct of 17:0 to 20:4 GPEtn at 766.8 and 788.8 u consistent with formation from formaldehyde present in high performance liquid chromatography (HPLC) methanol upon heating.

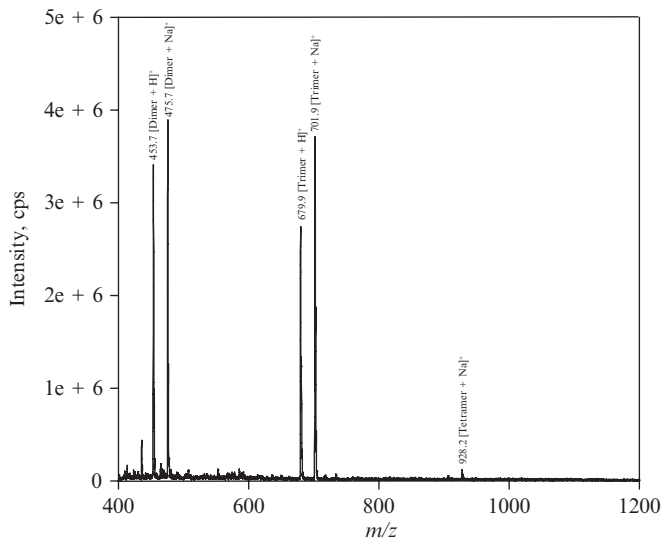


**Figure 14.6** Nylon 6.6 mass ions in positive mode from methanol filtered through a 0.45-mm nylon filter.

When possible, we use simple solvents to dissolve lipids at low concentrations. We have used methanol to make working mass spectrometry standards for the phospholipid classes; phosphatidylcholine (GPCCho), phosphatidylethanolamine (GPEtn), phosphatidylinositol (GPIIns), phosphatidylserine (GPSer), phosphatidic acid (GPA), lyso-phosphatidylcholine (lyso-GPCCho), lyso-phosphatidic acid (lyso-GPA), and cardiolipins (CL), as well as multiple sterols. Mixtures of 1:1 toluene:methanol serve as solvent for stocks and mixtures of triglycerides (TG) and diglycerides (DG) ranging in fatty acid composition from myristic acid (14:0) to eicosapentaenoic acid (20:5). In some instances, a compound will not be stable in its optimum solvent. Solvents for acidic and long chain saturated lipids typically contain water or an ionic buffer that contributes to degradation over time. In these instances, it is best to package these compounds as solids in small quantities by lyophilizing them from *t*-butanol:water or cyclohexane into their final container. This is true of polyphosphoinositides such as phosphatidylinositol-phosphate (PIP), phosphatidylinositol-bisphosphate (PIP<sub>2</sub>), and phosphatidylinositol-trisphosphate (PIP<sub>3</sub>), as well as KDO<sub>2</sub> Lipid A and dolichols. For ease of use and assay precision, a standard mixture can be formulated to contain multiple compounds within the same class or according to the focus of the mass spectrometric method. The solubility characteristics of the compounds can often be quite diverse. This is true for ceramides and sphingolipids. Sphingosine-1-phosphate, sphinganine-1-phosphate, and ceramide-1-phosphate required

addition of 2.75%/v dimethylamine in 98:2 ethanol:dimethylsulfoxide to dissolve these lipids to respective 20 mg/ml stocks. Sphingomyelin, sphingosine, sphinganine, and ceramide were directly soluble in ethanol at 20 mg/ml. Glucosylceramide and lactosylceramide were dissolved in 65:25:4 (v/v) chloroform:methanol:water. Ten compounds within these classes were added together to form an intermediate stock containing 2.5 mM of each in ethanol. This intermediate stock was further diluted to 25  $\mu$ M in ethanol as the final working solution. Table 14.1 reports the standard solutions formulated according to their respective solvent and concentration. Primary stocks, intermediate stocks, and working stocks of a compound or mixture should be stored at less than  $-15^{\circ}$  in tightly sealed aliquots of sufficient quantity and concentration whereby their purity can be preserved with constant temperature and minimal exposure to the atmosphere.

## 5. PACKAGING OF LIPID STANDARDS

The working standard solutions of known identity, purity, and concentration now require packaging for storage and reproducible daily use. The best packaging option for working standards is a quantity sufficient for a single experiment or batch sealed into an inert glass ampoule. A common glass used for pure lipid compounds is pharmaceutical type 1 borosilicate glass. Previous studies performed by us have demonstrated degradation of low concentration solutions stored in glass containers within one hour after packaging. This effect was observed with 18:1, 20:4, and 22:6 lyso-GPCho compounds, when 1 ml was stored as chloroform solutions (0.5 mg/ml) in 10-ml sodium borosilicate glass ampoules. Degradation was not observed when the volume of solution or concentration of solution was increased or when the compound was stored as a lyophilized solid. The cause of degradation was hypothesized to be surface interactions between lipid and glass and/or possible generation of HCl from chloroform vapor upon exposure in flame sealing of the glass ampoule. To rectify these issues, amber ampoules made of highly chemical-resistant glass known as Schott Fiolax<sup>TM</sup> 8414 were tested as above with flame sealing of ampoules partially suspended in a dry ice/acetone bath ( $\sim -70^{\circ}$ ). No degradation of the test compounds was detectable by HPLC or mass spectrometry.

An automated repeat pipettor with less than 0.1% variance and more than 99.5% accuracy is used to fill ampoules. This allows rapid filling of 100 to 500 ampoules for sealing and use. Upon preparing these quantities, it is advisable to place the empty ampoules on dry ice to fill. By doing so, the vapor pressure of the volatile solvent is decreased, preventing evaporation as well as thermally protecting the lipid standard awaiting sealing.

**Table 14.1** Standard solutions according to concentration and solubility

Methanol (10 $\mu\text{g/ml}$ )	Methanol (50–150 $\mu\text{g/ml}$ )	Toluene:methanol 400 $\mu\text{M}$
12:0-13:0 GPCho	19:0 Cholesterol ester	20:0-18:0 DG
17:0-20:4 GPCho	Cholesterol(d7)	17:1-18:1(C13) DG
21:0-22:6 GPCho	25-hydroxy-cholesterol(d3)	1,3-20:5 DG-d5
17:0-14:1 GPCho	4- $\beta$ -hydroxy-cholesterol(d7)	1,3-14:0 DG-d5
12:0-13:0 GPETn	7 $\alpha$ -hydroxy-cholesterol(d7)	1,3-15:0 DG-d5
17:0-20:4 GPETn	7 $\beta$ -hydroxy-cholesterol(d7)	1,3-16:0 DG-d5
21:0-22:6 GPETn	5,6 $\alpha$ -epoxy-cholesterol(d7)	1,3-17:0 DG-d5
17:0-14:1 GPETn	6 $\alpha$ -hydroxycholestanol(d7)	1,3-19:0 DG-d5
12:0-13:0 GPGro	7-oxocholesterol(d7)	1,3-20:0 DG-d5
17:0-20:4 GPGro	Desmosterol(d6)	1,3-20:2 DG-d5
21:0-22:6 GPGro	24,25-epoxy-cholesterol(d6)	1,3-20:4 DG-d5
17:0-14:1 GPGro	24-hydroxy-cholesterol(d6)	1,3-16:1 DG-d5
12:0-13:0 GPSer	<b>Lyophilized solids</b>	1,3-18:0 DG-d5
17:0-20:4 GPSer	<b>100 <math>\mu\text{g}</math></b>	1,3-18:1 DG-d5
21:0-22:6 GPSer	17:0-20:4 PI(3)P	1,3-18:2 DG-d5
17:0-14:1 GPSer	17:0-20:4 PI(4)P	16:0-16:0-18:0 TG
12:0-13:0 GPA	17:0-20:4 PI(5)P	16:0-16:0-18:1 TG
17:0-20:4 GPA	17:0-20:4 PI(3,4)P2	20:5-22:6-20:5 TG-d5
21:0-22:6 GPA	17:0-20:4 PI(3,5)P2	14:0-16:1-14:0 TG-d5
17:0-14:1 GPA	17:0-20:4 PI(4,5)P2	15:0-18:1-15:0 TG-d5
12:0-13:0 GPIns	17:0-20:4 PI(3,4,5)P3	16:0-18:0-16:0 TG-d5
17:0-20:4 GPIns	Nor-dolichol-[13-22]	17:0-17:1-17:0 TG-d5
21:0-22:6 GPIns	<b>1 mg</b>	19:0-12:0-19:0 TG-d5
17:0-14:1 GPIns	Kdo2lipid A	20:0-20:1-20:0 TG-d5
13:0 lyso-GPCho	<b>Ethanol</b>	20:2-18:3-20:2 TG-d5
17:1 lyso-GPCho	<b>2.5 mM</b>	20:4-18:2-20:4 TG-d5
13:0 lyso-GPA	Sphingosine (C17)	<b>4 <math>\mu\text{M}</math></b>
17:1 lyso-GPA	Sphinganine (C17)	18:1c9-18:1c6-18:1c9 TG
	Sphingosine-1-PO4 (C17)	18:1c6-18:1c9-18:1c6 TG
<b>100 <math>\mu\text{g/ml}</math></b>	Sphinganine-1-PO4 (C17)	d5-TG mixture of 9 cmpds
24:1(3)-14:1 CL	Ceramide (C12)	d5-DG mixture I of 9 cmpds
14:1(3)-15:1 CL	Ceramide (C25)	d5-DG mixture II of 4 cmpds
15:0(3)-16:1 CL	Ceramide-1-PO4 (C12)	
22:1(3)-14:1 CL	Sphingomyelin (C12)	
CL Mixture I of 4 cmpds	Glucosyl( $\beta$ ) C12 ceramide	
	Lactosyl ( $\beta$ ) C12 ceramide	
	<b>25 <math>\mu\text{M}</math></b>	
	Cer/Sph mixture of 10 cmpds	

## 6. QUALITY CONTROL AND STABILITY TESTING

Confidence in use requires the researcher to know that standards do not change concentration upon prolonged storage. Measurement of standard compounds' concentrations packaged at micromolar concentrations require sensitive detection afforded by liquid chromatography tandem mass spectrometry methods. The multireaction monitoring (MRM) technique routinely utilized in quantitative mass spectrometry analysis of small molecules is incorporated upon fast resolution of compounds by liquid chromatography. We provide methods of quantitative measurement for two internal standard mixtures by HPLC-MS/MS.

### 6.1. Ceramide/sphingoid base internal standard mixture

As described above, a mixture of ceramides and sphingoid bases was prepared to contain 10 lipids each at 25  $\mu\text{M}$  in ethanol and packaged in ampoules for routine use as an internal standard in sphingolipid mass spectrometry methods (Merrill *et al.*, 2005). The lipids were either odd carbon or non-endogenous 12 carbon acids on the d18 backbone of ceramide and of the sphingoid base. The mixture contained (2S,3R,4E)-2-aminoheptadec-4-ene-1,3-diol (C17 So), (2S,3R)-2-aminoheptadecane-1,3-diol (C17 Sa), heptadecaspheing-4-ene-1-phosphate (C17 So-1-P), heptadecaspheinganine-1-phosphate (C17 Sa-1-P), N-(dodecanoyl)-sphing-4-ene (C12 Cer), N-(pentacosanoyl)-sphing-4-ene (C25 Cer), N-(dodecanoyl)-sphing-4-ene-1-phosphate (C12 Cer-1-P), N-(dodecanoyl)-sphing-4-ene-1-phosphocholine (C12 SM), N-(dodecanoyl)-1- $\beta$ -glucosyl-sphing-4-ene (C12 GlucCer), and N-(dodecanoyl)-1- $\beta$ -lactosyl-sphing-4-ene (C12 LacCer). The mixed solution from the ampoules and the intermediate stock are volumetrically diluted to an equivalent concentration (25  $\mu\text{M}$ ) just prior to analysis by HPLC-MS/MS. For each experiment, three ampoules are assayed with triplicate injections of each. The %RSD for injections is routinely less than 5% for each compound. The HPLCMS/MS conditions are provided in Table 14.2. The MRM transitions for components of this mixture were assigned by experimentation with individual standards and mass spectrometer collisional settings with guidance from the work of Sullards *et al.* (2003). The  $[\text{M} + \text{H}]^+$  ion of C17 So and C17 Sa was monitored in Q1 and fragmented to selective detection of their respective characteristic fragments of 268.2 and 270.2 u for quantitation. The  $[\text{M} + \text{H}]^+$  ion of C12 SM was selectively monitored by detection of its characteristic 184 u phosphocholine fragment. The d18:1 ceramides of C12 Cer, C12 GlucCer, and C12 LacCer were monitored through the collision of their  $[\text{M} + \text{H}]^+$  ion to the characteristic ceramide base ion of 264.2 u. Unexpected was the optimum MRM for C25 ceramide as the loss of water from the parent  $[\text{M} + \text{H}]^+$  of 664.8 to

**Table 14.2** Liquid chromatography tandem mass spectrometry condition for the assay of ceramide/sphingoid base internal standard mixture**HPLC-MS/MS**

Column: Mercury C18, 20 × 2 mm, 3 μ, Temp: 30° (Phenomenon, Torrance, CA)

Mobile phase A: 60:40:0.2 (v/v) methanol:water:acetic acid + 10 mM ammonium acetate

Mobile phase B: 60:40:0.2 methanol:chloroform:acetic acid + 10 mM ammonium acetate

Total time (min)	Flow rate (μl/min)	A (%)	B (%)		
Equilibrate					
5.0	600	100	0		
3.0	600	87	13		
4.0	600	60	40		
5.5	600	50	50		
6.5	600	30	70		
10.0	600	30	70		
Mass spectrometer settings					
CUR:				10	
IS:				5500	
TEM:				550°	
GS1:				14	
GS2:				0	
ihe:				ON	
CAD:				Medium	
EP:				10	
Compound	Q1	Q3	DP	CE	CXP
C17 So	286.4	268.2	36	17	16
C17 Sa	288.4	270.2	66	21	14
C17 So-1-P	366.3	250.2	56	25	14
C17 Sa-1-P	368.4	252.3	71	19	6
C12 SM	647.7	184.1	121	35	10
C12 Cer	482.6	264.2	66	33	14
C12 GlucCer	644.7	264.5	66	45	14
C12 LacCer	806.7	264.4	96	57	16
C12 Cer-1-P	562.6	264.5	91	6	6
C25 Cer	664.8	646.7	81	23	18

CAD, collision activation; CE, collision energy; CUR, curtain gas; CXP, Q2 exit potential; DP, declustering potential; Dwell, 150 msec for each compound; EP, exit potential; GS1, nitrogen; GS2, air; ihe, interface heater; IS, ion spray voltage; Q1, quadrupole 1 ion; Q3, quadrupole 3 fragment; TEM, interface temperature.



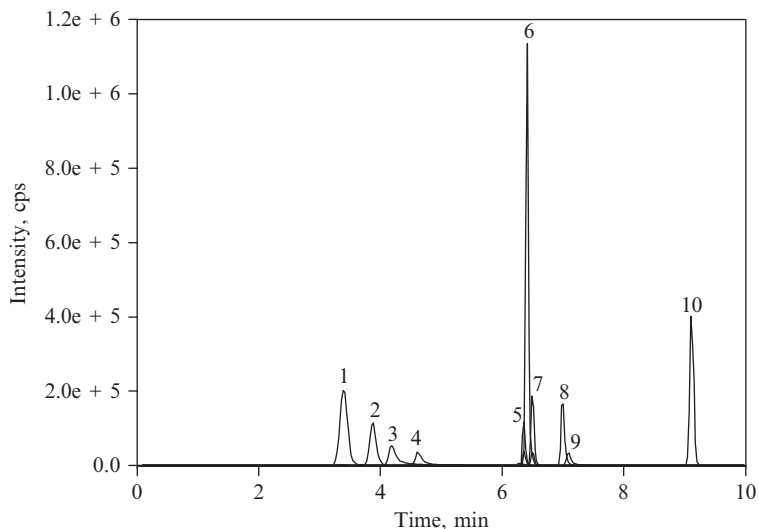


**Figure 14.7** Liquid chromatographic tandem mass spectrometry (LC-MS/MS) of Ceramide/Sphingoid base internal standard mixture. 1 = C17 So, 2 = C17 Sa, 3 = C17 So-1-P, 4 = C17 Sa-1-P, 5 = C12 LacCer, 6 = C12 SM, 7 = C12 GlucCer, 8 = C12 Cer, 9 = C12 Cer-1-P, and 10 = C25 Cer. High performance liquid chromatography (HPLC) and mass spectrometer settings are provided in [Table 14.2](#).

646.7 u rather than 264.2 u. The phosphorylated sphingoid bases of C17 So-1-P and C17 Sa-1-P were monitored through the collisional activation of their  $[M + H]^+$  ion to their respective 250.2 and 252.2 u fragments. These ampoules were assayed upon packaging and on a schedule of 0.5, 1, 3, 5, 7, 9, and 12 months of storage at  $-16$  to  $-24^\circ$ . Current analysis of ampoules stored over a 5-month period produced concentration between 22.5 and 27.5  $\mu\text{M}$  for all 10 compounds. The accurate quantitation of the long chain saturated compound C25 Ceramide requires complete re-dissolution into the solvent for both ampoules and intermediate stock when stored at freezer temperatures. This can be accomplished by allowing the solution to reach room temperature equilibrium followed by bath sonication at ambient temperature for 5 to 15 min. A representative LC-MS/MS chromatogram is provided in [Fig. 14.7](#).

## 6.2. Triglyceride-d<sub>5</sub> internal standard mixture

Another mixture containing nine triglycerides deuterated at the position of their glycerol backbone protons with positionally defined acyl groups was formulated to contain 4  $\mu\text{M}$  of each in 1:1 (v/v) toluene:methanol as a readily usable internal standard mixture for triglyceride MS ([McAnoy et al., 2005](#)). The mixture contained 1,3-di-(5Z,8Z,11Z,14Z,17Z-eicosa-pentaenoyl)-2-(4Z,7Z,10Z,13Z,16Z,19Z-docosa-hexaenoyl)-sn-glycerol-d<sub>5</sub>

(20:5(2)-22:6 TG-d5), 1,3-ditetradecanoyl-2-(9Z-hexadecenoyl)-sn-glycerol-d5 (14:0(2)-16:1TG-d5), 1,3-dipentadecanoyl-2-(9Z-octadecenoyl)-sn-glycerol-d5 (15:0(2)-18:1 TG-d5), 1,3-dihexadecanoyl-2-octadecanoyl-sn-glycerol-d5 (16:0(2)-18:0 TG-d5), 1,3-diheptadecanoyl-2-(10Z-heptadecenoyl)-sn-glycerol-d5 (17:0(2)-17:1 TG-d5), 1,3-dinonadecanoyl-2-dodecanoyl-sn-glycerol-d5 (19:0(2)-12:0 TG-d5), 1,3-dieicosanoyl-2-(11Z-eicosenoyl)-sn-glycerol-d5 (20:0(2)-20:1 TG-d5), 1,3-di-(11Z,14Z-eicosadienoyl)-2-(6Z,9Z,12Z-octadecatrienoyl)-sn-glycerol-d5 (20:2(2)-18:3 TG-d5), and 1,3-di-(5Z,8Z,11Z,14Z-eicosatetraenoyl)-2-(9Z, 12Z-octadecadienoyl)-sn-glycerol-d5 (20:4(2)-18:2 TG-d5). The mixed solution from the ampoules was assayed against the mixture's intermediate stock at 400  $\mu\text{M}$ , and manually diluted to an equivalent concentration just prior to analysis. For each experiment, three ampoules were assayed with triplicate injections of each. The %RSD for injections is routinely less than 3% for each compound. The HPLC-MS/MS conditions are provided in [Table 14.3](#). The  $[\text{M} + \text{NH}_4]^+$  ion of each d5-TG was selected in Q1 and fragmented for detection of its corresponding  $[\text{M}-\text{R}_1\text{COOH}]^+$  fragment for quantitation. Since each d5-TG was formulated to equimolar concentrations, the dwell time for each was adjusted to achieve near equivalent responses across the compounds' molecular weight distribution in the MRM experiment. A higher dwell time was required to compensate for low ionization/detection of the saturated, long-chain versus polyunsaturated lipids. These ampoules were assayed upon packaging and on a schedule of 0.5, 1, 3, 5, 7, 9, and 12 months of storage at  $-16$  to  $-24^\circ$ . Current analysis of ampoules stored over a 7-month period produced concentration between 3.6 and 4.4  $\mu\text{M}$  for all nine compounds. A representative HPLC-MS/MS chromatogram is provided in [Fig. 14.8](#).

## 7. DISCUSSION

The lipid compounds at the specified concentrations listed in [Table 14.1](#) have been prepared as 1-ml solutions packaged in ampoules as described. These compounds have been furnished to the operational cores of the LIPID MAPS glue grant. LIPID MAPS is funded by National Institutes of Health (NIH)/National Institute of Genetic Medical Sciences (NIGMS), Grant 1 U54 GM69338. Each operational core is assigned to measure all lipids within a specified class of the lipidome in the mouse tumor-derived macrophage-like RAW 246.7 cell. In general, measurement of lipids are to be assessed from RAW cell extracts pre- and post-stimulation with KDO<sub>2</sub> lipid A, also manufactured, characterized, and packaged by Avanti Polar Lipids ([Raetz et al., 2006](#)). Their work is reported in other

**Table 14.3** Liquid chromatography tandem mass spectrometry conditions for the assay of d<sub>5</sub>-TG internal standard mixture**HPLC-MS/MS Conditions**

Column: Mercury C8, 20 × 2 mm, 3 μ (Phenomenex, Torrance, CA)

Mobile phase A: 10 mM ammonium acetate in 1:9 (v/v) methanol:water

Mobile phase B: 10 mM ammonium acetate in methanol

Total time (min)	Flow rate (μl/min)	A (%)	B (%)
0	200	40	60
5	200	40	60

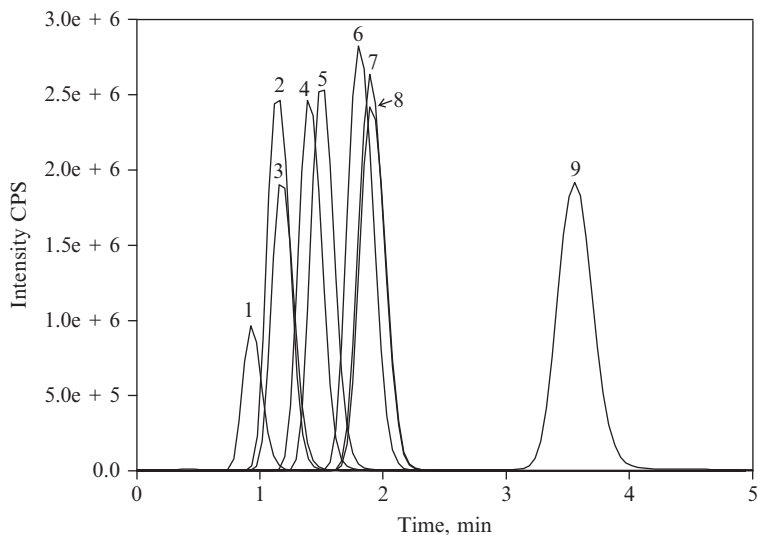
Mass spectrometer settings	
CUR:	10
IS:	5500
TEM:	550
GS1:	50
GS2:	50
ihe:	ON
CAD:	Medium
EP:	10

TG-d <sub>5</sub>	Q1 mass (amu)	Q3 mass (amu)	Dwell (msec)	Param
20:5(2)–22:6	993.8	674.4	10	CE 37
14:0(2)–16:1	771.8	526.3	100	CE 33
15:0(2)–18:1	827.8	568.3	300	CE 33
19:0(2)–12:0	857.8	542.4	400	CE 35
17:0(2)–17:1	869.8	582.4	400	CE 41
16:0(2)–18:0	857.8	584.5	450	CE 35
20:0(2)–20:1	996.0	666.5	900	CE 41
20:2(2)–18:3	955.8	630.4	150	CE 43
20:4(2)18:2	949.8	628.4	15	CE 35

CAD, collision activation; CE, collision energy; CUR, curtain gas; CXP, Q2 exit potential; DP, declustering potential; Dwell, 150 msec for each compound; EP, exit potential; GS1, nitrogen; GS2, air; ihe, interface heater; IS, ion spray voltage; Q1, quadrupole 1 ion; Q3, quadrupole 3 fragment; TEM, interface temperature.

chapters of this volume. Each core was supplied with 50 to 100 1-ml ampoules of each lipid internal standard of their respective class assignment. The principle of numerous ampoules is to provide a one-experiment use whereby the ampoule is opened and used directly or further diluted and added to cells prior to extraction. This single-use approach circumvents many, if not all, of the physical and chemical constraints of lipid degradation and interactions. Accompanying each shipment is a lot-specific certificate of



**Figure 14.8** Liquid chromatographic tandem mass spectrometry (LC-MS/MS) of triglyceride-d5 internal standard mixture. 1 = 20:5(2)-22:6 TG-d5, 2 = 14:0(2)-16:0 TG-d5, 3 = 20:4(2)-18:2 TG-d5, 4 = 20:2(2)-18:3 TG-d5, 5 = 15:0(2)-18:1 TG-d5, 6 = 17:0(2)-17:1 TG-d5, 7 = 19:0(2)-12:0 TG-d5, 8 = 16:0(2)-18:0 TG-d5, and 9 = 20:0(2)-20:1 TG-d5. High performance liquid chromatography (HPLC) and mass spectrometer settings are provided in [Table 14.3](#).

analysis reporting the methods and results for chemical characterization and concentration determination. Additionally, each lot of ampoules is assayed on a scheduled basis for concentration stability within a specification of  $100 \pm 5\%$  for individual components and  $100 \pm 10\%$  for mixtures. Should a lot of internal standard exceed these specifications, the core is notified to discontinue use and a new lot is prepared. Personal communications on the quality, utility, and consistency of the provided materials have been favorable. We have also provided these materials to the general public as a service of the grant. Continued and repeated requests suggest acceptable performance in the hands of researchers.

## REFERENCES

- McAnoy, A. M., Wu, C. C., and Murphy, R. C. (2005). Direct qualitative analysis of triacylglycerols by electrospray mass spectrometry using a linear ion trap. *J. Am. Soc. Mass Spectrom.* **16**, 1498–1509.
- Merrill, A. H., Jr., Sullards, M. C., Allegood, J. C., Kelly, S., and Wang, E. (2005). Sphingolipidomics: High-throughput, structure specific and quantitative analysis of sphingolipids by liquid chromatography tandem mass spectrometry. *Methods* **36**, 207–224.

- Murphy, R. C., Fiedler, J., and Hevko, J. (2001). Analysis of nonvolatile lipids by mass spectrometry. *Chem. Rev.* **101**, 479–526.
- Pidgeon, C., Apostol, G., and Markovich, R. (1989). Fourier transform infrared assay of liposomal lipids. *Anal. Biochem.* **181**, 28–32.
- Raetz, C. R. H., Garrett, T. A., Reynolds, C. M., Shaw, W. A., Moore, J. D., Smith, D. C., Jr., Ribeiro, A. A., Murphy, R. C., Ulevitch, R. J., Fearn, C., Reichart, D., Glass, C. K., *et al.* (2006). Kdo<sub>2</sub>-Lipid A of *Escherichia coli*, a defined endotoxin that activates macrophages via TLR-4. *J. Lipid Res.* **47**, 1097–1111.
- Sullards, M. C., Wang, E., Peng, Q., and Merrill, A. H., Jr. (2003). Metabolomic profiling of sphingolipids in human glioma cell lines by liquid chromatography tandem mass spectrometry. *Cell Mol. Biol.* **49**, 789–797.